Eau Terre Environnement Research Centre

Uncertainty and sensitivity analyses in wind resource assessment
Analyses d'incertitude et de sensibilité dans l'évaluation des ressources éoliennes

By

Olga Tsvetkova

Dissertation presented in partial fulfillment of the requirements

for the degree of

Doctor of Philosophy (Ph.D.)

In Earth Sciences

Jointly offered by INRS and Université Laval

Evaluation committee members

Commitee President and Internal Examiner	Andre St-Hillaire ETE-INRS
External Examiner	Zhanna Kapsalyamova Economics Department, Nazarbaev University
External Examiner	Marouane Temimi Department of Civil, Environmental and Ocean Engineering Stevens Institute of Technology
Internal Examiner	Andre St-Hillaire INRS-ETE
Internal Examiner	Saeid Homayouni INRS-ETE
Research Director	Taha B.M.J. Ouarda INRS-ETE

© Olga Tsvetkova, December 2022

DEDICATION

I dedicate this work to my daughter Emma, who went through thick and thin with me and often with me alone, and all the females in my ancestral lineage. I truly hope I have created a better world for you and given you a chance at a better future with this endeavour.

ACKNOWLEDGEMENTS

I cannot express the extent of the deepest gratitude and respect I feel for my supervisor, Professor Taha B.M.J. Ouarda, who believed in my success, when no one else did, including, unfortunately, myself. I would like to express my endless love and gratitude to my parents, Andrei Tsvetkov and Liudmila Tsvetkova, and my sister Nataly Tsvetkova for supporting me through my extended educational journey, which helped me learn who I am. I thank my closest friends, Sophie Larrivee, Anna Maria Farais Pereira, Laurie St-Criq, Danny Savard, Alexandra Khomitch, Iryna Komarova, Ia Revia, Natalia Scherbakova, Tatyana Kryzhanovskaya, Maya Voinarovskaya, Lilia Blades and David Pelster, for making this moment possible for me.

ABSTRACT AND KEYWORDS

This dissertation deals with the aspects of quantifying uncertainty in wind resource assessment with the practices of uncertainty and sensitivity analyses. The objectives of this dissertation are to review and assess the quality of sensitivity analysis practices in wind resource assessment, to discourage the use of one-at-a-time sensitivity analysis, encourage the use of global sensitivity analysis instead, introduce methods from other fields, and showcase how uncertainty and global sensitivity analyses adds value to the decision support process. This dissertation is organized in four articles:

I. Review article of 102 feasibility studies: a review of sensitivity analysis practices in wind resource assessment with a case study of comparison of one-at-a-time vs. global sensitivity analyses of the levelized cost of offshore wind energy;
II. Research article: Quasi-Monte Carlo technique in global sensitivity analysis in wind resource assessment with a case study on United Arab Emirates;
III. Research article: Use of the Halphen distribution family for mean wind speed estimation with a case study on Eastern Canada;
IV. Application article: Offshore wind resource assessment study of the Persian Gulf with QuikSCAT satellite data.

Articles I-III have each resulted in a peer-reviewed publication, while Article IV – in a submission. Article I offers classifications by sensitivity analysis output variable, method, application, country, and software. It reveals the lack of collective agreement on the definition of sensitivity analysis in the literature, the dominance of nonlinear models, the prevalence of one-at-a-time sensitivity analysis method, while one-at-a-time method is only valid for linear models. Article I highlights gaps in the literature, provides evidence of the pitfalls, leading to costly erroneous wind resource assessment results. Article II shows how global sensitivity analysis offers improvement by means of the quasi-Monte Carlo with its elaborate sampling designs enabling faster convergence. Article III introduces the Halphen distribution family for the purpose of wind recourse assessment. Article IV uses SeaWinds/QuikSCAT satellite data for offshore wind resource assessment of the Persian Gulf.

The main contributions to the state-of-the-art with this dissertation follow. To the best of author's knowledge, no review of sensitivity analysis in wind resource assessment is currently available in the literature, Article I offers such. Article II bridges mathematical modelling and wind resource assessment by introducing quasi-Monte Carlo technique to wind resource assessment. Article III introduces the Halphen distribution family from flood frequency analysis to wind resource assessment.

Keywords : Quasi-Monte Carlo, Wind energy, Wind resource assessment, Sensitivity analysis, Global sensitivity analysis, Uncertainty analysis, Halphen distribution family, Halphen type A distribution, Halphen type B distribution, QuickSCAT

RÉSUMÉ ET MOTS-CLÉS

Cette thèse traite des aspects de la quantification de l'incertitude dans l'évaluation des ressources éoliennes avec les pratiques d'analyses d'incertitude et de sensibilité. Les objectifs de cette thèse sont d'examiner et d'évaluer la qualité des pratiques d'analyse de sensibilité dans l'évaluation des ressources éoliennes, de décourager l'utilisation d'une analyse de sensibilité à la fois, d'encourager l'utilisation d'une analyse de sensibilité globale à la place, d'introduire des méthodes d'autres domaines., et montrer comment les analyses d'incertitude et de sensibilité globale ajoutent de la valeur au processus d'aide à la décision. Cette thèse est organisée en quatre articles :

I. Une revue des pratiques d'analyse de sensibilité dans l'évaluation des ressources éoliennes avec une étude de cas de comparaison d'analyses de sensibilité individuelles et globales du coût actualisé de l'énergie éolienne offshore ;
II. Technique Quasi-Monte Carlo dans l'analyse de sensibilité globale dans l'évaluation des ressources éoliennes avec une étude de cas sur les Émirats Arabes Unis;
III. Utilisation de la famille de distribution Halphen pour l'estimation de la vitesse moyenne du vent avec une étude de cas sur l'Est du Canada;
IV. Étude d'évaluation des ressources éoliennes offshore du golfe Persique avec les données satellitaires QuikSCAT.

Les articles I à III ont chacun donné lieu à une publication évaluée par des pairs, tandis que l'article IV - à une soumission. L'article I propose des classifications par variable de sortie d'analyse de sensibilité, méthode, application, pays et logiciel. L'article I met en évidence les lacunes de la littérature, fournit des preuves des pièges, conduisant à des résultats d'évaluation erronés et coûteux des ressources éoliennes. L'article II montre comment l'analyse de sensibilité globale offre une amélioration au moyen du quasi-Monte Carlo avec ses plans d'échantillonnage élaborés permettant une convergence plus rapide. L'article III introduit la famille de distribution Halphen pour l'évaluation des ressources éoliennes. Article IV utilise les données satellitaires SeaWinds/QuikSCAT pour l'évaluation des ressources éoliennes offshore du golfe Persique.

Les principales contributions à l'état de l'art avec cette thèse suivent. À la connaissance de l'auteur, aucune revue de l'analyse de sensibilité dans l'évaluation des ressources éoliennes n'est actuellement disponible dans la littérature, l'article I en propose une. L'article II relie la modélisation mathématique et l'évaluation des ressources éoliennes en introduisant la technique de quasi-Monte Carlo dans l'évaluation des ressources éoliennes. L'article III présente la famille de distribution de Halphen, de l'analyse de la fréquence des crues à l'évaluation des ressources éoliennes.

Mots-clés : quasi-Monte Carlo, Énergie éolienne, Évaluation des ressources éoliennes, Analyse de sensibilité, Analyse de sensibilité globale, Analyse d'incertitude, Famille de distribution Halphen, Halphen type A, Halphen type B, QuickSCAT

SOMMAIRE RECAPITULATIF

Les crises de ces dernières années appellent de toute urgence à faire face aux conséquences urgentes du changement climatique. Un changement rapide vers une énergie propre et durable n'est plus une question d'amour pour la planète, c'est devenu une question de sécurité pour la race humaine. Non seulement les crises climatiques pointent dans cette direction, mais aussi les crises de réfugiés causées par la violence des économies basées sur les combustibles fossiles comme la Russie. Gabor Mate n'aurait pas pu résumer l'essence du problème de manière plus directe et plus précise que dans son travail sur les dépendances - « Les effets néfastes à long terme de la dépendance de notre société, sinon au pétrole, puis aux commodités et au luxe que le pétrole peut apporter, sont évidentes. Ils vont de la destruction de l'environnement, du changement climatique et des effets toxiques de la pollution sur la santé humaine aux nombreuses guerres que le besoin de pétrole, ou l'attachement à la richesse pétrolière a déclenchées » (Mate, 2008). L'énergie éolienne est la source d'énergie renouvelable qui connaît la croissance la plus rapide, mais l'accord de Paris ("Accord de Paris", 2015) visant à réduire les émissions de gaz à effet de serre exige une croissance plus. Le vent est la deuxième meilleure source d'énergie renouvelable au Canada après l'hydroélectricité, il contribue à 3,5% de la production d'électricité au Canada (About Renewable Energy, s.d.).

L'analyse de sensibilité est un outil important mais sous-évalué dans la découverte scientifique. L'analyse de sensibilité en tant que composante « formelle » et « standard » du développement scientifique et du soutien aux politiques est relativement jeune affirme (Saltelli et al., 2021) dans un récent éditorial d'un numéro spécial de Environmental Modeling and Software. Bien qu'il s'agisse «historiquement, mais de manière informelle, d'un fondement de la découverte scientifique et de la prise de décision humaine » (Saltelli et al., 2021). Saltelli et al. (2021) soulignent que les avancées scientifiques et les politiques qui y sont liées ont « des racines profondes mais informelles dans l'analyse de sensibilité ». De plus, de nouveaux domaines de connaissances qui ont donné naissance aux métiers modernes, tels que la science des données et l'apprentissage automatique, bénéficient tous deux d'une analyse de sensibilité (Saltelli et al., 2021).

Razavi et al. (2020) et Saltelli et al. (2016) ont appelé à promouvoir l'analyse de sensibilité en tant que discipline indépendante en raison de son potentiel inutilisé. Saltelli et al. (2021) ont affirmé que l'analyse de sensibilité moderne évolue actuellement vers une « discipline formelle et

indépendante ». Bien que l'analyse de sensibilité globale fasse déjà partie de plusieurs lignes directrices internationales pour l'évaluation d'impact (Leinfellner et al., 1990) (Funtowicz & Ravetz, 1990) et revues disciplinaires, son adoption en est encore « à ses balbutiements » (Andrea Saltelli et al., 2019). Le terme analyse de sensibilité est largement stéréotypé comme la soi-disant analyse de sensibilité une à la fois (Andrea Saltelli et al., 2019), même dans la communauté scientifique. L'analyse de sensibilité dans l'évaluation des ressources éoliennes ne fait pas exception.

L'époque de la pandémie de COVID-19 a donné lieu à des aspects importants du fonctionnement de la modélisation, de la science et des politiques dans le monde complexe d'aujourd'hui, inondé d'informations (Saltelli et al., 2020; Saltelli et al., 2022; Saltelli, 2022; Saltelli et Sarewitz, 2022). L'essence des modèles mathématiques est qu'ils sont des « représentations simplifiées de systèmes ou de processus réels » (Saltelli, 2022). Minding the frame (Saltelli, 2022) fait référence aux différents angles, visions du monde ou « hypothèses sous-jacentes qui guident la façon dont les individus, les groupes et les sociétés perçoivent un problème particulier » (Saltelli, 2022). Tenir compte des conséquences (Saltelli, 2022) signifie que si elle est exécutée correctement, la modélisation mathématique aide la société à prendre des décisions plus intelligentes et vice versa, si elle est exécutée de manière inappropriée, les modèles peuvent conduire à des choix erronés ou simplement injustifiés. Enfin, faire attention à l'inconnu (Andrea Saltelli, 2022) signifiait que « le fait de ne pas reconnaître et communiquer les incertitudes peut limiter artificiellement les options politiques et ouvrir la porte à des conséquences imprévues » (Andrea Saltelli, 2022). Un article récent de Nature (Andrea Saltelli et al., 2020) n'a pas appelé à la fin de la quantification, ni à la production de modèles apolitiques, mais à la place, ils appellent à une divulgation complète et brutalement honnête. Selon l'article (Andrea Saltelli et al., 2020), si ces cinq points sont respectés, cela aiderait à préserver la modélisation mathématique comme un outil précieux. (Andrea Saltelli et al., 2020) concluent « Ignorez les cinq et les prédictions des modèles deviennent des chevaux de Troie pour des intérêts et des valeurs non déclarés. Modéliser de manière responsable ». Ce serait tout quant à l'importance de traiter l'incertitude dans une prédiction ou une estimation selon les mots d'un talentueux simplificateur de la modélisation mathématique et prêcheur en faveur de l'analyse de sensibilité.

Les questions que l'analyse d'incertitude et l'analyse de sensibilité traitent sont profondément différentes. L'analyse d'incertitude répond à la question « Dans quelle mesure la sortie est-elle incertaine ? », tandis que l'analyse de sensibilité répond à des questions telles que « D'où vient l'incertitude dans le système ou le modèle mathématique ? », « Quelle entrée est la

plus et/ou la moins influente en termes de de l'incertitude de la sortie ? », « Quel est le classement des intrants ? », « Comment ce niveau d'incertitude peut-il être atteint dans le système ? », etc. (Saltelli et al., 2008). Saltelli et al. (2019) rapportent que les analyses d'incertitude et de sensibilité sont parfois mal interprétées ou que les termes sont utilisés de manière interchangeable, ce qui suggère qu'il y a place à amélioration dans la façon dont nous, en tant qu'utilisateurs de la méthode scientifique, raisonnons sur l'incertitude.

Les objectifs de cette thèse sont d'examiner et d'évaluer la qualité des pratiques d'analyse de sensibilité dans l'évaluation des ressources éoliennes, de décourager l'utilisation d'une analyse de sensibilité à la fois, d'encourager l'utilisation d'une analyse de sensibilité globale à la place, d'introduire des méthodes d'autres domaines., et montrer comment les analyses d'incertitude et de sensibilité globale ajoutent de la valeur au processus d'aide à la décision. Cette thèse est organisée en quatre articles :

I. Une revue des pratiques d'analyse de sensibilité dans l'évaluation des ressources éoliennes avec une étude de cas de comparaison d'analyses de sensibilité individuelles et globales du coût actualisé de l'énergie éolienne offshore (Tsvetkova & Ouarda, 2021).

II. Technique Quasi-Monte Carlo dans l'analyse de sensibilité globale dans l'évaluation des ressources éoliennes avec une étude de cas sur les Émirats Arabes Unis (Tsvetkova & Ouarda, 2019);

III. Utilisation de la famille de distribution Halphen pour l'estimation de la vitesse moyenne du vent avec une étude de cas sur l'Est du Canada (Tsvetkova and Ouarda, 2023a);

IV. Étude d'évaluation des ressources éoliennes offshore du golfe Persique avec les données satellitaires QuikSCAT (Tsvetkova and Ouarda, 2022).

Les articles I à III ont chacun donné lieu à une publication évaluée par des pairs, tandis que l'article IV - à une soumission. L'article I propose des classifications par variable de sortie d'analyse de sensibilité, méthode, application, pays et logiciel. L'article I met en évidence les lacunes de la littérature, fournit des preuves des pièges, conduisant à des résultats d'évaluation erronés et coûteux des ressources éoliennes. L'article II montre comment l'analyse de sensibilité globale offre une amélioration au moyen du quasi-Monte Carlo avec ses plans d'échantillonnage élaborés permettant une convergence plus rapide. L'article III introduit la famille de distribution

Halphen pour l'évaluation des ressources éoliennes. Le Article IV utilise les données satellitaires SeaWinds/QuikSCAT pour l'évaluation des ressources éoliennes offshore du golfe Persique.

Une revue de l'analyse de sensibilité dans l'évaluation des ressources éoliennes est présentée dans le premier article (Tsvetkova and Ouarda, 2021), offrant des classifications par variable de sortie d'analyse de sensibilité (ou modèle), méthode, application, pays et logiciel. Aucune revue de l'analyse de sensibilité dans l'évaluation des ressources éoliennes n'est actuellement disponible dans la littérature. Le pool d'examen se compose de 102 articles avec des modèles traitant des aspects statistiques et économiques de l'évaluation des ressources éoliennes (mesures d'ajustement, énergie éolienne, énergie éolienne, la valeur actuelle nette, la période de récupération, le taux de rendement interne, le coût actualisé de l'énergie, des dépenses en capital et des dépenses d'exploitation). Les études d'analyse de sensibilité, où le vent est prédit avec des modèles de recherche et de prévision météorologiques, l'analyse de sensibilité des systèmes énergétiques hybrides avec une composante éolienne et l'analyse de sensibilité des charges de fatigue des éoliennes, dépassent la portée de cette thèse. Cette revue révèle l'absence d'accord collectif sur la définition de l'analyse de sensibilité dans la littérature, la prédominance des modèles non linéaires (100%) et la prévalence de la méthode d'analyse de sensibilité une à la fois (82%). L'examen met en évidence les lacunes existantes dans le domaine, fournit des preuves des pièges courants, pouvant conduire à des interprétations erronées coûteuses des données sur le site et donc à des évaluations de faisabilité erronées. L'examen invite à repenser la manière de mener une analyse de sensibilité dans l'évaluation des ressources éoliennes. Il comprend également la comparaison d'une analyse de sensibilité à la fois et d'une analyse de sensibilité globale pour des modèles linéaires et non linéaires.

Le deuxième article (Tsvetkova & Ouarda, 2019) fait le pont entre la modélisation mathématique et l'évaluation des ressources éoliennes. L'analyse de sensibilité relie des parties de la variance de sortie à la variance de chaque variable d'entrée. L'analyse de sensibilité globale explore les entrées à l'échelle mondiale. L'analyse de sensibilité un par un domine dans l'évaluation des ressources éoliennes, tandis que l'analyse de sensibilité globale est souvent négligée. Par rapport aux méthodes traditionnelles, l'analyse de sensibilité globale offre une amélioration potentielle au moyen de la technique de quasi-Monte Carlo avec ses plans d'échantillonnage élaborés permettant une convergence plus rapide. La principale nouveauté de ce travail est double: l'utilisation du quasi-Monte Carlo dans l'évaluation des ressources éoliennes et de la méthode Sobol comme méthode d'analyse de sensibilité globale basée sur la variance dans l'évaluation des ressources éoliennes. Cet article est parmi quelques-uns utilisant l'analyse

de sensibilité globale dans l'évaluation des ressources éoliennes. Deux études de cas ont été réalisées. La première étude de cas montre que le quasi-Monte Carlo avec un échantillonnage basé sur l'échantillonnage Sobol surpasse l'échantillonnage latin hyper cubé et l'échantillonnage pseudo-aléatoire. Il montre également qu'en termes de précision des résultats, le calcul par force brute des indices de sensibilité de Sobol doit être utilisé chaque fois que le modèle le permet, sinon les indices de sensibilité peuvent être estimés. Le deuxième étude de cas démontre une étude d'analyse de sensibilité globale valide pour l'évaluation des ressources éoliennes à Masdar City, aux Émirats arabes unis. Les résultats suggèrent que l'influence de la variance des paramètres de Weibull sur la production d'énergie annuelle pourrait être surestimée, alors qu'elle est responsable de 2 % de l'incertitude de la production d'énergie annuelle, et l'influence de la variance de la densité de l'air pourrait être négligée, tandis que trouvé pour représenter 94% de la variance de la production annuelle d'énergie à Masdar City. Les études d'évaluation des ressources éoliennes bénéficieraient grandement de l'utilisation du quasi-Monte Carlo et de la méthode Sobol. La méthode Sobol est une méthode d'analyse de sensibilité globale universelle fournissant des résultats valides pour les modèles non linéaires typiques pour l'évaluation des ressources éoliennes et le quasi-Monte Carlo fournit une évolutivité globale, une indépendance du modèle et une flexibilité dans la quantification de l'incertitude.

La famille de distribution Halphen (HDF) pour modéliser la vitesse moyenne du vent est présentée dans le troisième article (Tsvetkova and Ouarda, 2023a). La famille est flexible et est utilisée pour s'adapter à une grande variété de données. La famille est composée de trois distributions à trois paramètres (un paramètre d'échelle et deux paramètres de forme): Halphen type A (HA), Halphen type B (HB) et Halphen inverse type B (HIB). HA est une généralisation de la distribution harmonique à deux paramètres, HB a la distribution gamma comme cas limite, et HIB est basé sur la fonction factorielle exponentielle et la distribution Gamma inverse comme cas limite. Le HDF possède un certain nombre de propriétés favorables à la modélisation des données de vent, telles que la limite inférieure à zéro (absence de paramètre de localisation), la flexibilité pour couvrir une large gamme de formes et la forme explicite des fonctions génératrices de moment. Les propriétés du HDF garantissent l'optimalité et la cohérence des estimateurs du maximum de vraisemblance utilisés pour l'estimation des paramètres de distribution. Nous avons examiné 126 stations dans l'Est du Canada. Nous avons constaté que HDF fournit un ajustement supérieur à la distribution la plus couramment utilisée à cette fin, la distribution de Weibull à deux paramètres, dans 98 % des stations selon le critère d'information d'Akaike (AIC) et dans 99 % des stations selon le critère bayésien. Critère d'information (BIC). La distribution là mieux ajustée

la plus courante pour les stations de l'étude de cas de l'Est du Canada est le HDF (84 % selon l'AIC et le BIC). Les résultats de l'étude de cas montrent que les observations de vent ne peuvent pas être ajustées par le HIB, mais peuvent être très bien modélisées par HA (meilleur ajustement pour 38 % des stations selon AIC et BIC) ou HB (meilleur ajustement pour 46 % des stations selon AIC et BIC). Nous encourageons l'utilisation de HDF dans les études d'estimation des ressources éoliennes basées sur l'estimation de la vitesse moyenne du vent.

Les données de vitesse du vent SeaWinds/QuikSCAT sont utilisées pour l'évaluation des ressources éoliennes offshore du golfe Persique dans le quatrième article (Tsvetkova and Ouarda, 2022). Les données ont été collectées du 07.1999 au 11.2009. La vitesse du vent est extrapolée à une hauteur de moyeu de 100 m. La distribution de Weibull à deux paramètres est ajustée à la vitesse du vent extrapolée, et les paramètres de forme et d'échelle de Weibull sont estimés avec la méthode du maximum de vraisemblance. La région d'intérêt est une grille 11 x 20 délimitée par (51,8° E, 24° N ; 56,3° E, 26,5° N) ou 220 quadrants de taille 25,45 km x 24 km. La production annuelle d'énergie et le coût de production d'électricité éolienne sont calculés pour chaque quadrant. La production annuelle d'énergie avec une éolienne de 3MW est de 1050 - 1265 W/m2 et 17,5 - 19 GWh/a. La vitesse moyenne du vent à 100 m de hauteur est de 10,4 à 11 m/s. La vitesse du vent la plus probable à 100 m de hauteur est de 14,4 à 15,8 m/s, et la vitesse du vent avec une énergie maximale à 100 m de hauteur est de 7,2 à 12,9 m/s. L'électricité éolienne offshore peut être livrée au coût de 1,6 à 1,8 $ct/kWh avec une éolienne de 3 MW

La section 1 présente le sujet, les objectifs de recherche (section 1.1), la nouveauté et l'impact (section 1.2), la revue générale de la littérature (section 2.3) et la structure de cette thèse (section 1.4).

La section 2 est organisée en seize sections : 2.1 Résumé de (Tsvetkova & Ouarda, 2021), 2.2 Nomenclature utilisée tout au long (Tsvetkova & Ouarda, 2021), 2.3 Liste des abréviations utilisées tout au long (Tsvetkova & Ouarda, 2021), 2.4 Introduction, 2.5 Sensibilité modèles d'analyse de sensibilité, 2.6 Méthodes d'analyse de sensibilité, 2.7 Offshore vs onshore, 2.8 Géographie, 2.9 Logiciel 2.10 Spécificités d'application, 2.11 Synthèse critique, 2.12 Conclusion et perspectives, 2.13 Déclaration d'intérêt concurrent, 2.14 Crédit d'auteur , et 2.15 Remerciements.

Les sections 2.1 à 2.4 sont explicites. La classification d'examen la plus détaillée est basée sur le modèle d'analyse de sensibilité et est donnée à la section 2.5. La portée de cet examen est limitée à l'analyse de sensibilité des mesures d'ajustement (section 4.2.1), de l'énergie

éolienne (2.5.2.2), de production d'énergie (2.5.2.3), de la valeur actualisée nette (2.5.3.1), taux de rendement interne (2.5.3.2), période de récupération (2.5.3.3), coût actualisé de l'énergie (2.5.3.4), dépenses en capital (section 2.5.3.5) et dépenses opérationnelles (section 2.5.3.6).

La section 2.6 passe en revue les méthodes d'analyse de sensibilité rencontrées lors de l'examen de (Tsvetkova et Ouarda, 2021). La section 2.6.1 passe en revue les méthodes d'analyse de sensibilité locale, c'est-à-dire la fameuse analyse de sensibilité une à la fois de la section 2.6.1.1. La section 2.6.2 passe en revue les méthodes d'analyse de sensibilité globale, c'est-à-dire la méthode du nuage de points (section 2.6.2.1), la méthode de Morris (section 2.6.2.2), la méthode de Sobol (section 2.6.2.3), le test d'amplitude de Fourier étendu (section 2.6.2.4), et plus récemment les effets Shapley (Section 2.6.2.5) et PAWN (Section 2.6.2.6).

La section 2.7 organise les études du pool d'examen par applications offshore et onshore. La section 2.8 organise les articles du pool d'examen par pays pour lesquels une étude de cas d'analyse de sensibilité a été rapportée. La section 2.8 fait un zoom sur les lacunes de la recherche dans la littérature d'un point de vue géographique. La section 2.8 est destinée à être une référence rapide sur les régions du monde qui sont sous-étudiées. Au cours du processus d'examen, des études de cas avec des données météorologiques de trente-sept pays (figure 2.3) avec une analyse de sensibilité sous une forme ou une autre a été rencontrées, le tableau 2.5 classe ces résultats en fonction du pays et du modèle d'analyse de sensibilité utilisé, d'où les lacunes sont facilement identifiables. Les rapports mondiaux et nationaux sélectionnés concernant la capacité éolienne installée peuvent être trouvés dans (WindPower, 2021) avec des informations détaillées sur les parcs éoliens existants.

La section 2.9 classe le pool d'articles (articles sélectionnés pour examen) en fonction du logiciel utilisé pour l'analyse de sensibilité et discute de l'influence de chaque outil sur le choix de la méthode d'analyse de sensibilité. (Douglas-Smith et al., 2020) ont identifié le logiciel pour les analyses d'incertitude et de sensibilité et ont fourni un aperçu des tendances générales de la recherche. (Murthy & Rahi, 2017) ont publié une revue des outils logiciels utilisés dans l'évaluation des ressources éoliennes. Les outils logiciels utilisés spécifiquement pour l'analyse de sensibilité dans le domaine de l'évaluation des ressources éoliennes sont répertoriés dans le tableau 4.6. Souvent, les projets liés au vent sont analysés à l'aide d'un logiciel de modélisation professionnel ciblé pour la modélisation de projets d'énergie propre, par exemple, RETScreen (Ressources naturelles Canada : RETScreen, 2020). RETScreen est utilisé pour une évaluation de faisabilité de projets d'énergie propre, par exemple, (Hadi et al., 2020)(Soe et al., 2015)(Salehin et al., 2016), la seule option disponible pour l'analyse de sensibilité du courant net la valeur du projet

dans RETScreen est une à la fois. La nature non linéaire des modèles éoliens et économiques est étonnamment ignorée.

Pour illustrer l'inférence trompeuse ou erronée que l'OATSA peut entraîner pour certains modèles, trois exemples sont examinés à la section 2.10. Le package Sensobol R (Puy et al., 2021) avec une échantillon de taille 1000 a été utilisé pour les trois exemples (2.10.1, 2.10.2, 2.10.3), le script R se trouve à l'annexe I.

Les tendances dévoilées au cours du processus de revue (Tsvetkova & Ouarda, 2021) sont expliquées dans la section 2.11 Synthèse critique. Cinq tendances sont détectées. Premièrement, que tous les modèles couramment utilisés dans le domaine sont non linéaires. Deuxièmement, cette analyse de sensibilité une à la fois prévaut sur le terrain malgré son inapplicabilité aux modèles non linéaires. Troisièmement, plus une étude est technique, plus il est probable qu'une approche globale de l'analyse de sensibilité sera utilisée. Quatrièmement, l'analyse de sensibilité globale devient de plus en plus populaire dans le domaine au fil du temps. Cinquièmement, les implications politiques des résultats d'une analyse de sensibilité ponctuelle non fiables dans l'évaluation de l'énergie éolienne pourraient avoir des conséquences désastreuses et coûteuses. L'examen par (Tsvetkova & Ouarda, 2021) est résumé dans le tableau 4.10. Il indique la prévalence des modèles non linéaires sur le terrain. L'utilisation de mots clés tels qu'une ligne de base, un changement en % ou un diagramme en tornade indique l'utilisation d'une analyse de sensibilité une à la fois.

La section 2.12 présente les conclusions et les perspectives de recherches futures. La section 2.13 contient la déclaration d'intérêts concurrents. Section 2.14 - Contributions des auteurs. Enfin, la section 2.15 énumère les remerciements. La bibliographie de (Tsvetkova & Ouarda, 2021) est donnée dans la section 3.

La section 4 présente le deuxieme article de la série intitulée technique de quasi-Monte Carlo dans l'analyse de sensibilité globale dans l'évaluation des ressources éoliennes avec une étude sur les Émirats Arabes Unis (Tsvetkova & Ouarda, 2019). La section 4.1 contient le résumé de la section 4.2 de l'étude - la nomenclature utilisée tout au long de la section 4.

La section 4 ou (Tsvetkova & Ouarda, 2019) est organisée en quatre sections principales: la introduction (Section 4.3), les méthodes (Section 3.4), les résultats (Section 4.5), les conclusions et les recherches futures (Section 4.5). L'introduction de (Tsvetkova & Ouarda, 2019) a présenté le problème associé à l'analyse de sensibilité dans l'évaluation des ressources éoliennes. La section des méthodes (section 4.4) contient trois sous-sections : les techniques

d'échantillonnage utilisées dans MC/QMC (section 4.4.1), la GSA basée sur la variance (section 4.4.2) et la conception expérimentale (section 4.4.3). La sous-section sur les techniques d'échantillonnage (section 4.4.1) résume les techniques d'échantillonnage utilisées tout au long (Tsvetkova et Ouarda, 2019), à savoir l'échantillonnage pseudo-aléatoire (section 2.4.1.1), l'échantillonnage par hypercube latin (section 4.2.1.2) et l'échantillonnage basé sur les Séquences de Sobol (Section 2.4.1.3). La section 2.4.1.4 compare les trois mentionnés ci-dessus.

La sous-section 4.4.2 de l'analyse de sensibilité globale basée sur la variance passe en revue le calcul de la force brute des indices de sensibilité de premier ordre et d'effet total de Sobol (section 4.4.2.1) et leurs méthodes d'estimation (section 4.4.2.2). La sous-section 4.4.3 de la conception expérimentale contient deux parties : le modèle de test (section 4.4.3.1) et le modèle d'énergie éoliennes dans l'étude de cas de Masdar City (section 4.4.3.2). La section 4.4.3.2 donne des détails sur la configuration de la partie expérimentale de ce travail et les méthodes utilisées dans l'évaluation des ressources éoliennes telles que la distribution de Weibull pour ajuster les données de vitesse du vent et pour calculer la production d'énergie annuelle. Les hypothèses sur les distributions sous-jacentes des variables d'entrée du modèle d'évaluation des ressources éoliennes sont présentées dans cette sous-section. Les variables d'entrée et de sortie de l'expérience Quasi Monte Carlo avec les hypothèses respectives sur les distributions sous-jacentes des variables sont résumées dans le tableau 4.2.

La section 4.5 des résultats fournit les résultats obtenus dans (Tsvetkova & Ouarda, 2019), c'est-à-dire l'analyse de sensibilité globale pour les modèles d'essai (Section 4.5.1) et d'évaluation des ressources éoliennes (Section 4.5.2). Les résultats du modèle de test incluent la comparaison des stratégies d'échantillonnage à la lumière de l'analyse de sensibilité globale dans l'évaluation des ressources éoliennes. Les résultats du modèle d'estimation de l'énergie éolienne contiennent les résultats de l'analyse de sensibilité globale et de l'analyse d'incertitude pour l'évaluation des ressources éoliennes à Masdar City, aux Émirats arabes unis. La section 4.6 des conclusions et des recherches futures présente les conclusions de (Tsvetkova & Ouarda, 2019) avec les suggestions possibles pour l'orientation future des recherches.

Enfin, la section 4.7 contient le conflit d'intérêts pour (Tsvetkova & Ouarda, 2019) et la section 4.8 - les remerciements. La bibliographie de (Tsvetkova & Ouarda, 2019) se trouve dans la section 5.

En travaillant sur (Tsvetkova & Ouarda, 2019), la prévalence des études d'analyse de sensibilité une à la fois dans l'évaluation des ressources éoliennes était ponctuelle, alors que

cette méthode est strictement valable pour les systèmes linéaires. Pour confirmer ce constat intuitif, les travaux sur l'examen complet des pratiques d'analyse de sensibilité dans l'évaluation des recours éoliens ont commencé et ont abouti à (Tsvetkova & Ouarda, 2021). La section 4 présente les travaux entrepris dans (Tsvetkova & Ouarda, 2021).

La section 6 présente des recherches soumises pour publication (Tsvetkova & Ouarda, 2022b) qui introduisent une famille de distribution nouvelle dans le domaine de l'évaluation de l'énergie éolienne. La section 6 est organisée de la manière suivante : 6.1 Résumé de (Tsvetkova & Ouarda, 2022b), 6.2 Notation de (Tsvetkova & Ouarda, 2022b) 6.3 Introduction, 6.4 Méthodes, 6.5 Matériel, 6.6 Résultats et discussion, 6.7 Conclusions et travaux futurs, 6.8 Disponibilité des données, 6.9 Déclaration de conflit d'intérêts, 6.10 Contribution des auteurs à (Tsvetkova & Ouarda, 2022b), et enfin 6.11 Remerciements. La bibliographie de (Tsvetkova & Ouarda, 2022b) se trouve dans la section 7.

La section Méthodes 6.4 comprend l'examen de la famille de distribution Halphen (6.4.1), les classes de distributions à queue lourde dans la théorie des valeurs extrêmes dans la section 6.4.2, la famille de distribution Halphen dans le contexte de la modélisation de la vitesse du vent (6.4.3) et métriques de qualité d'ajustement dans la section 6.4.4. La section 6.5.1 présente une étude de cas sur l'Est du Canada menée dans (Tsvetkova et Ouarda, 2022b). La section 6.6 fournit les résultats généralisés de l'étude de cas de l'Est du Canada, tandis que la section 6.6.1 présente les résultats détaillés pour deux stations spécifiques dans l'étude de cas (une qui a montré la distribution de Weibull à deux paramètres comme étant la mieux ajustée et une autre - comme la distribution Halphen de type A).

La section 8 présente une autre application d'étude d'évaluation des ressources éoliennes aux Émirats arabes unis, mais avec un type de données différent - les données de vitesse du vent par satellite QuickSCAT. La section 8 est organisée en onze sections. La section 8.1 contient le résumé, la section 8.2 – la nomenclature. La section 8.3 énumère les abréviations utilisées dans cette application. La section 8.4 introduit le problème avec une brève revue de la littérature : la section 8.5 couvre les méthodes et les outils utilisés dans ce travail. La section 8.5.1 traite du diffusiomètre SeaWinds/QuikSCAT. La section 8.5.2 décrit les techniques utilisées pour l'évaluation des ressources éoliennes, telles que la distribution couramment utilisée pour décrire le comportement du vent (section 2.2.1), la qualité de l'ajustement (section 2.2.2), l'extrapolation des données de vitesse du vent à la hauteur du moyeu (section 2.2.1). 3) et le volet économique d'un projet éolien (Section 2.2.4). La section 8.6 décrit l'étude de cas adoptée dans le présent travail. La section 8.6.1 décrit la région d'intérêt. Section. 8.6.2 énumère les objectifs de l'étude

de cas. La section 8.6.3 énumère les hypothèses formulées dans l'étude de cas. La section 8.6.4 donne une description détaillée des données de vitesse du vent QuikSCAT. Les résultats sont discutés dans la section 8.7 et les conclusions et les orientations potentielles pour les travaux futurs sont présentées dans la section 8.8. Les sources de soutien et les données sont reconnues dans la section 8.9. Enfin, la déclaration de disponibilité des données et la déclaration de conflit d'intérêts se trouvent respectivement aux sections 8.10 et 8.11. La bibliographie est répertoriée dans la section 9.

La section 10 présente les conclusions générales de cette thèse. La section 11 contient la bibliographie générale de cette thèse. L'annexe I contient le matériel complémentaire à (Tsvetkova & Ouarda, 2021). Les annexes II-V contiennent des annexes à (Tsvetkova & Ouarda, 2023a).

Les cinq pages suivantes seront consacrées aux aspects méthodologiques de cette thèse. Cela couvre brièvement certaines des méthodes d'analyse de sensibilité globale qui sont appliquées dans le domaine de l'évaluation des ressources éoliennes. Saltelli et al. (Saltelli *et al.*, 2008)affirment que l'analyse de sensibilité globale est la notion commune sur laquelle l'analyse de sensibilité de l'ère moderne s'est concentrée au cours des vingt dernières années. Quatre approches principales de l'analyse de sensibilité globale sont distinguées (1) basée sur les dérivés, (2) basée sur la distribution, (3) basée sur le variogramme et (4) basée sur la régression.

Les entrées Xi sont échantillonnées et la réponse du modèle Y(Xi) est enregistrée. Par conséquent, la sortie Y est également échantillonnée. Le tracé de Y(Xi) fournit des informations sur le comportement du modèle. Plus la corrélation entre Y(Xi) et Xi est élevée, plus elle est influente sur Y. Saltelli et al. (Saltelli *et al.*, 2008) affirment que la faible forme du nuage de points sur la plage du facteur d'entrée (comme X1 ou X5 dans la figure 2.7) est un signe certain que l'entrée est moins influente. Saltelli et al. (Saltelli *et al.*, 2008) soulignent que la méthode du nuage de points est un moyen simple et informatif d'effectuer une analyse de sensibilité et que la plupart des mesures d'analyse de sensibilité dérivées par les praticiens visent à préserver la richesse des informations fournies par les nuages de points dans un format condensé . (Saltelli *et al.*, 2008). La fonction plot_scatter du package sensobol R (Puy *et al.*, 2021) est une implémentation de la méthode. Saltelli et al. Recommandent de prendre un échantillon de taille N = 1000. Des diagrammes de dispersion ont été trouvés dans l'analyse de sensibilité dans l'évaluation des ressources éoliennes en (Dykes *et al.*, 2014).

La méthode de Morris (Morris, 1991) pour le dépistage ou l'élimination des facteurs non influents, également connue sous le nom de méthode des effets élémentaires, est généralement

utilisée pour réduire la dimensionnalité des modèles afin que le calcul des méthodes basées sur la variance devienne réalisable. (Morris, 1991) ont introduit une méthode de criblage qui est essentiellement un plan d'échantillonnage OAT divisant l'espace hyper cubé d'entrée k-dimensionnel (pour un modèle $Y = f(X) = f(X_1, X_2, \dots, X_k)$ de k variables) en une grille de niveau p. L'échantillonnage le long de l (généralement l ~ 4-10) trajectoires composées de k + 1 points produit deux mesures de sensibilité moyenne μ (Équation (22)) évaluant l'importance globale de l'entrée et σ (Équation (23)) - les interactions et les effets non linéaires. (Campolongo, Cariboni and Saltelli, 2007) ont proposé une mesure améliorée μ^*(Équation (24)). L'effet élémentaire $d_i(X)$ pour chaque entrée est défini comme Équation (21), où Δ ={0, 1/(p-1), 2/(p-1), … 1}. La méthode est implémentée en tant que fonction de Morris dans le package de sensibilité R [156]. La méthode de Morris a été utilisée pour l'analyse de sensibilité de l'OPEX en une seule étude par (Martin *et al.*, 2016).

La méthode Sobol est une méthode d'analyse de sensibilité globale basée sur la variance bien établie, également appelée « *l'étalon d'or de l'analyse de sensibilité* » (Puy *et al.*, 2020). Il comprend le calcul ou l'estimation des indices de sensibilité (IS) de premier ordre et d'effet total comme mesures pour établir un classement parmi les entrées. (Sobol′, 1990) publié la preuve du théorème sur la décomposition d'une fonction intégrable en sommations de différentes dimensions dans une revue russe et ont défini les SI de Sobol. Les SI sont les mesures de la variance qui entraînent le classement des variables. Dans le cas d'entrées indépendantes, les SI de premier ordre suffisent pour établir un classement des entrées. Si la dépendance de certaines variables d'entrée est présente ou si le modèle est non linéaire, le calcul des indices d'effet total est également nécessaire. Les indices de sensibilité à l'effet total tiennent compte des dépendances et des effets (ou interactions) d'ordre supérieur entre les intrants. Plus tard, les SI Sobol ont fait leur chemin dans la communauté scientifique Anglophone. Les methodes de Sobol′ (2001), Sobol et Kucherenko (2005) et se sont bien établis dans une variété de disciplines (Douglas-Smith et al., 2020; Wagener and Pianosi, 2019; Razavi and Gupta, 2015) en raison de son applicabilité universelle avec l'hypothèse d'indépendance des intrants.

L'essentiel de la méthode Sobol réside dans l'utilisation de la décomposition par analyse de la variance (ANOVA) comme mesure de sensibilité. Si le modèle $Y = f(X) = f(X_1, X_2, \dots, X_k)$ est une fonction de k variables, Équation (25) définit les SI de premier ordre $S_i(Y)$ et Équation (26) – les SI à effet total $T_i(Y)$ pour la fonction [159]. Une multitude d'estimateurs de ces indices (quatre estimateurs de premier ordre et cinq d'ordre total des indices de sensibilité)

peuvent être calculés en appelant la fonction sobol_indices dans le package sensobol R (Puy *et al.*, 2021).

Il existe un certain nombre d'estimateurs des indices d'effet d'ordre total définis dans Équation (26). Dans une récente « *bataille des estimateurs de sensibilité d'ordre total* » (Puy *et al.*, 2020) par Puy et al., l'estimateur (Razavi et Gupta, 2019) a pris le dessus et devrait être préféré en pratique. Une implémentation de cette procédure d'estimation (Razavi and Gupta, 2019) est disponible dans le package sensobol R (Puy *et al.*, 2021). La méthode de Sobol a été utilisée dans l'analyse de sensibilité de l'énergie éolienne (Weekes et Tomlin, 2014; Ulker, Allaire et Willcox, 2017; Aghbalou et al., 2018; Tsvetkova et Ouarda, 2019; Bossavy, Girard et Kariniotakis, 2016); Richter, Wolters et Frank, 2019), NPV (Richter, Wolters et Frank, 2019), IRR (Richter, Wolters et Frank, 2019) et coût actualisé de l'énergie (Mora, Spelling et Weijde, 2021; Richter, Wolters et Frank, 2019), OPEX (Mytilinou et Kolios, 2019) .

Une autre façon de calculer les indices de sensibilité consiste à décomposer la variance en fonction de plusieurs séries de Fourier. Le test de sensibilité à l'amplitude de Fourier (FAST) traduit un SAOV multivarié en une variable de fréquence unique à l'aide de la série de Fourier. Par conséquent, les intégrales requises pour calculer les indices de sensibilité deviennent uni variées, ce qui entraîne des économies de calcul importantes. (Cukier, Levine and Shuler, 1978) ont d'abord suggéré l'utilisation de FAST pour l'analyse de sensibilité globale dans ses recherches sur l'analyse de sensibilité non linéaire, et Saltelli et al. (Saltelli, Tarantola and Chan, 1999)introduit une autre façon de calculer FAST à des fins d'analyse de sensibilité globale, c'est-à-dire le FAST étendu (eFAST). eFAST est implémenté en tant que fonction fast99 dans le package R de sensibilité (Iooss *et al.*, 2021). Les effets des MW sur l'énergie éolienne avec eFAST ont été étudiés dans (McKay et al., 2014; Tong et al., 2015).

(Owen, 2014) introduit le concept de la valeur de Shapley (Shapley, 1951) de la théorie des jeux coopératifs dans l'analyse de sensibilité globale. La valeur de Shapley (Shapley, 1951) est une distribution «*équitable*» des gains totaux aux joueurs du jeu, en supposant qu'ils collaborent tous. (Owen, 2014) ont trouvé la valeur de Shapley des variables individuelles lorsque la «*variance expliquée*» était prise comme leur valeur combinée, et ont montré que les SI de premier ordre et totaux de Sobol comme étant plus faciles à calculer servent de borne pour la nouvelle mesure de sensibilité, qui s'ajoute à la variance totale en cas d'entrées indépendantes. Peu de temps après Song et al. (Song, Nelson and Staum, 2015) ont appelé cette mesure en cas d'entrées dépendantes des effets de Shapley et ont montré comment les indices de sensibilité de premier ordre et à effet total de Sobol, même lorsqu'ils sont utilisés ensemble, peuvent ne pas

mesurer de manière appropriée la sensibilité de la sortie à l'incertitude dans les entrées lorsqu'il existe une dépendance probabiliste ou une interaction structurelle entre les entrées. Ils ont également proposé un algorithme de Monte Carlo efficace pour l'estimation des effets de Shapley (fonction shapleyPermRand dans le package sensitivity dans R (Iooss *et al.*, 2021)). Une autre procédure d'estimation des effets de Shapley a été récemment proposée par Goda (Goda, 2021). L'utilisation des effets Shapley dans l'analyse de sensibilité dans l'évaluation des ressources éoliennes a été trouvée dans un seul article du pool d'examen - l'analyse de sensibilité de WP par Carta et al. (Carta, Díaz and Castañeda, 2020).

Une méthode d'analyse de sensibilité globale nouvelle et efficace appelée PAWN a été introduite par (Pianosi, Sarrazin et Wagener, 2015) . L'essence de PAWN est un calcul efficace des SI basés sur la densité. L'efficacité réside dans la caractérisation des distributions de sortie par leurs fonctions de distribution cumulatives (CDF) au lieu des PDF, car les CDF sont plus faciles à dériver que les PDF (Pianosi, Sarrazin et Wagener, 2015). Pianosi et al. (2015) démontrent les aventajes de PAWN à traversa une serié d'applications à des modèles numériques et environnementaux. PAWN a été conçu pour être une approche complémentaire à l'analyse de sensibilité globale basée sur la variance. Plus tard, une procédure d'estimation générique a été proposée par le même groupe pour faciliter l'application de PAWN pour le praticien (Pianosi, Sarrazin et Wagener, 2015). La méthode est facilement accessible via la boîte à outils SAFE (Pianosi, Sarrazin et Wagener, 2015). Borras Mora et al. (2019) était la seule étude du pool d'examen à appliquer PAWN pour l'analyse de sensibilité du coût actualisé de l'énergie offshore.

La famille est flexible et permet d'ajuster une grande variété de données (El Adlouni and Bobée, 2017). La famille est composée de trois distributions à trois paramètres (échelle et deux paramètres de forme) : Halphen type A (HA), Halphen type B (HB) et Halphen inverse type B (HIB) (El Adlouni et Bobée, 2017). HA est une généralisation de la distribution harmonique à deux paramètres, HB avec distribution gamma comme cas limite et HIB basée sur une fonction factorielle exponentielle avec distribution Gamma inverse comme cas limite (El Adlouni et Bobée, 2017). La famille de distribution Halphen possède un certain nombre de propriétés favorables à la modélisation des données de vent, telles que : limite inférieure à zéro (absence de paramètre de localisation), flexibilité pour couvrir une large gamme de formes, forme explicite des fonctions génératrices de moment (El Adlouni et Bobée, 2017) . Les propriétés de la famille de distribution de Halphen assurent l'optimalité et la cohérence de l'estimateur du maximum de vraisemblance utilisé pour l'estimation des paramètres(El Adlouni et Bobée, 2017) . La famille de distribution de

Halphen appartient à la famille exponentielle des distributions et leurs statistiques suffisantes peuvent être obtenues à partir de leurs formes exponentielles, cela rend l'estimation du maximum de vraisemblance asymptotiquement sans biais et leurs variances correspondantes minimales quelle que soit la taille de l'échantillon d'analyse de sensibilité (S. El Adlouni & Bobée, 2017). Cette caractéristique de la famille de distribution de Halphen est évidemment importante dans les cas où la taille de l'échantillon d'intérêt est limitée. Le tableau 6.3 présente un résumé de la famille de distribution de Halphen.

Une revue concise de la littérature sur la famille de distribution Halphen, son application, sa vulgarisation et ses avancées suivront. La famille de distribution Halphen est une famille de distribution flexible et complète pour s'adapter à des observations indépendantes et distribuées de manière identique qui a été conçue spécifiquement pour les ensembles de données de débit de pointe de rivières par Etienne Halphen pendant la Seconde Guerre mondiale (Morlat, 1956). La création de la famille de distribution Halphen a été motivée par le désir de Halphen de construire ses distributions de manière à répondre à certaines exigences spécifiques d'ajustement des variables hydrologiques (Morlat, 1956). (L. Perreault, Bobée et Rasmussen, 1999a) ont discuté des propriétés statistiques des distributions et plus tard - de l'estimation des paramètres avec estimation du maximum de vraisemblance (estimation du maximum de vraisemblance) et estimation des quantiles. Un important corpus de recherche sur l'importance de la famille de distribution de Halphen dans le domaine de l'analyse de la fréquence des crues a été fourni par (El Adlouni et Bobée, 2017) . (Chebana, El Adlouni et Bobée, 2008) ont discuté de l'estimation des paramètres de la famille de distribution de Halphen avec la méthode des moments et la méthode d'estimation mixte. El Adlouni & Bobee (2007) ont étudié les techniques d'échantillonnage pour la famille de distribution Halphen et ont développé un test discriminatoire (Zhang et Singh, 2021) ont revisité l'application de la famille de distribution Halphen dans l'analyse de la fréquence des crues. Ils ont utilisé 198 ensembles de données de débit de pointe dans leur étude de cas, estimé les paramètres des distributions de Halphen avec la méthode d'estimation du maximum de vraisemblance et utilisé la statistique de Kolmogorov-Smirnov (KS) comme mesure de la qualité de l'ajustement (GOF) et l'erreur quadratique moyenne (RMSE) - comme indicateur de performance. Zhang et Singh (2021) constaté que HA/HB était la distribution préférée pour 190 ensembles de données, et le diagramme du rapport des moments s'est également avéré être un outil fiable pour la sélection de la distribution avec la valeur de l'aplatissement. Plus important encore, l'étude a validé l'utilisation de la famille de distribution de Halphen dans l'analyse de la fréquence des crues. Zhang et Singh (2021) ont comparé les performances de la famille de distribution Halphen avec la distribution log-Pearson de type 3

(LPT3). Chebana, El Adlouni et Bobée (2010) ont mené une étude exploratoire comparant la distribution généralisée des valeurs extrêmes (GEV) à la famille de distribution Halphen. Les comparaisons basées sur la simulation indiquent que la distribution HA est plus flexible que la GEV, ce qui entraîne « un biais et une RMSE raisonnables même lorsque les échantillons sont générés à partir de la distribution GEV» (Chebana, El Adlouni et Bobée, 2010). Delhome et al (2017) introduit la famille de distribution Halphen comme une boîte à outils pour modéliser la variabilité du temps de trajet.

Passant au domaine de l'estimation du potentiel de l'énergie éolienne, des analyses approfondies des distributions statistiques utilisées dans l'industrie éolienne ont été menées dans un certain nombre d'études de Carta et al. (2009), Murthy et Rahi (2017). Jung et Schindler (2019) ont montré que « 115 distributions paramétriques ont été appliquées de 2010 à 2018 » et que la distribution de Weibull à deux paramètres (W2) était « la distribution la plus fréquemment (44 fois) évaluée » (Jung et Schindler, 2019). Ils ont également conclu que W2 était la distribution la plus couramment évaluée et recommandée (Jung & Schindler, 2019). Aries et al. (2018) utilisé le W2, la distribution Gamma à deux paramètres (G2), la distribution de Wald à deux paramètres, la log-normale à deux paramètres (LN2), la valeur extrême de type 1 (EV1) ou Gumbel, GEV, Nakagami, et distribution logistique généralisée pour modéliser la vitesse du vent pour une évaluation approfondie des modèles de distribution de la vitesse du vent pour quatre sites en Algérie. Ouarda et al. (2015) et Ouarda et Charron (2018) ont enrichi la liste avec les trois paramètres log normal (LN3), LPT3 et normal (N). Les distributions utilisées en pratique peuvent ne pas se limiter aux distributions mentionnées ci-dessus, qui ne sont que les distributions les plus fréquemment rencontrées dans la littérature spécialisée. Une évaluation complète des modèles de distribution de la vitesse du vent avec une étude de cas pour le Dakota du Nord par Zhou et al. (2010) incluaient W2, G2, LN2 et la gaussienne inverse. Usta et Kantar (2012) proposent d'utiliser une distribution d'erreur généralisée asymétrique et une distribution t asymétrique. Selon (Jung & Schindler, 2019), les distributions qui ont été appliquées dans au moins quatre études différentes ou dont l'utilisation a été recommandée dans au moins deux études distinctes dans le cadre du WRE sont présentées dans le tableau 6.1. Bien qu'un certain nombre de modèles de mélange aient été appliqués à cette tâche (Shin, Ouarda et Lee, 2016) , les distributions de mélange sortent du cadre de cette étude et sont donc omises. (Jung and Schindler, 2019), concluent qu'il est impossible « d'identifier une distribution unique qui puisse être ajustée universellement » (Jung et Schindler, 2019).

En conclusion, cette thèse était composée de quatre articles (Tsvetkova & Ouarda, 2019)(Tsvetkova & Ouarda, 2021)(Tsvetkova and Ouarda, 2023a)(Tsvetkova and Ouarda, 2022). Les deux premiers portaient sur l'analyse de sensibilité. (Tsvetkova & Ouarda, 2019) est une recherche sur l'échantillonnage utilisé pour l'expérience Quasi-monte Carlo du "golden standard of global sensitivitiy analysis", la méthode Sobol. (Tsvetkova & Ouarda, 2021) est une revue complète des pratiques d'analyse de sensibilité dans le domaine de l'évaluation des ressources éoliennes. (Tsvetkova and Ouarda, 2023a) ont introduit la famille de distribution Halphen, utilisée dans l'analyse de la fréquence des crues, pour modéliser le vent moyen. (Tsvetkova & Ouarda, 2022) est un document d'application de l'évaluation des ressources éoliennes offshore. Le premier et le quatrième article utilisaient des données sur la vitesse du vent provenant des Émirats arabes unis. Le troisième article utilisait des données sur la vitesse du vent provenant de 126 ensembles de données météorologiques historiques dans l'Est du Canada (Tsvetkova, 2022). Le deuxième article était consacré uniquement à l'examen de la sensibilité et à l'analyse extrême de l'incertitude dans l'évaluation des ressources éoliennes.

Le document de recherche (Tsvetkova & Ouarda, 2019) s'est concentré sur les aspects de l'application de la méthode Sobol en tant que méthode d'analyse de sensibilité globale basée sur la variance pour l'évaluation des ressources éoliennes et certains aspects de son application. (Tsvetkova & Ouarda, 2019) ont mené deux études de cas (une sur un modèle de test, une autre - sur un modèle d'énergie éolienne à Masdar City, Émirats arabes unis) et ont conclu que, premièrement, l'échantillonnage basé sur des séquences de Sobol surpassait l'échantillonnage en hypercube latin et le pseudo -échantillonnage aléatoire. Deuxièmement, il a été conclu que le calcul de la force brute des indices de sensibilité du premier ordre et de l'effet total offre une grande précision et est recommandé pour une utilisation dans la plupart des modèles d'évaluation des ressources éoliennes. Lorsque le nombre de variables ne le permet pas, l'estimation de ces indices peut être utilisée. Troisièmement, l'étude de cas des Émirats arabes unis sur l'estimation de la production d'énergie annuelle à Masdar City suggère que « l'influence de la variance des paramètres de Weibull sur la variance de la production d'énergie annuelle pourrait être surestimée, tandis que l'influence de la variance de la densité de l'air pourrait être négligée. Ces résultats sont spécifiques à l'étude de cas et ne doivent pas être généralisés sans effort supplémentaire.

L'étude de cas de Masdar City dans (Tsvetkova & Ouarda, 2019) a illustré comment la méthode Sobol d'analyse de sensibilité globale (qui offre des résultats d'analyse d'incertitude parallèlement) peut être facilement, avec les moyens de l'expérience Quasi Monte, Carlo et sans

frais supplémentaires (R Core Team, R: A Language and Environment for Statistical Computing, 2020) mis en place. La communauté éolienne pourrait bénéficier de l'adaptation de la méthode Sobol, en raison du fait qu'elle fournit des résultats de sensibilité crédibles pour des modèles de production d'énergie annuelle non linéaires dans leur nature. La deuxième raison plaidant en faveur de l'utilisation de Quasi-Monte Carlo est qu'en mettant en place une étude d'analyse de sensibilité globale avec Quasi Monte Carlo, une fonction de densité de probabilité du modèle de sortie (résultats d'analyse d'incertitude) est obtenue avec la même expérience. Enfin, l'expérience quasi Monte Carlo permet d'incorporer diverses données et informations sur un site d'intérêt dans une étude d'incertitude, y compris des analyses d'incertitude et de sensibilité.

Passant aux conclusions de l'examen complet (Tsvetkova & Ouarda, 2021), il a été découvert que les pratiques courantes d'analyse de sensibilité dans le domaine de l'estimation du potentiel éolien correspondent largement à celles de (Mora et al., 2021) dans l'éolien offshore et (Menberg et al., 2016) mais en application aux modèles énergétiques des bâtiments. Tant pour l'énergie éolienne que pour l'énergie des bâtiments, les modèles sont non linéaires (Menberg et al., 2016). La différence est que dans la simulation de construction, l'analyse de sensibilité globale est coûteuse en calcul (Burhenne et al., 2013), alors qu'elle fournit des résultats stables (Menberg et al., 2016). Dans les modèles d'énergie éolienne dans le cadre de l'examen de (Tsvetkova & Ouarda, 2021), la charge de calcul n'est pas un problème (sauf pour le modèle de coût offshore de (Mora et al., 2021)), bien qu'il en soit un pour la recherche météorologique et modèles de prévision modèles informatiques de dynamique des fluides (Tsvetkova & Ouarda, 2019).

Il a également été observé dans l'examen de (Tsvetkova & Ouarda, 2021), que la définition et le but de l'analyse de sensibilité dans l'estimation du potentiel énergétique éolien sont souvent mal interprétés de plusieurs façons. Une définition universelle de l'analyse de sensibilité dans ce domaine fait actuellement défaut. (Tsvetkova & Ouarda, 2021) ont conclu que cette divergence dans la terminologie entraîne une divergence dans la motivation, une incompréhension dans les questions de recherche que l'analyse de sensibilité aborde et les objectifs que l'analyse de sensibilité pourrait aider à atteindre (Section 2.11 pour plus de détails). Le résultat correspond à (Saltelli et al., 2008; Razavi & Gupta, 2015).

(Tsvetkova & Ouarda, 2021) ont constaté que les résultats d'analyse de sensibilité les plus courants parmi les variables d'intérêt utilisées dans l'estimation du potentiel de l'énergie éolienne ont été identifiés comme étant les mesures de qualité de l'ajustement, l'énergie éolienne, l'énergie éolienne ou la production annuelle d'énergie, la production actuelle nette. La valeur, le taux de

rendement interne, le coût actualisé de l'énergie, les dépenses en capital et les dépenses d'exploitation des éoliennes ou des parcs. Tous les éléments mentionnés se sont également révélés non linéaires. La commodité est ce qui est à l'origine de la popularité de l'analyse de sensibilité ponctuelle, mais pas de sa crédibilité. En plus de cela, l'analyse de sensibilité une à la fois s'est déjà révélée inadaptée aux modèles non linéaires par un certain nombre de chercheurs (Harenberg et al., 2018) (Saltelli & Annoni, 2010) (Douglas-Smith et al ., 2020). Néanmoins, l'analyse de sensibilité une à la fois est toujours en plein essor en dominant parmi d'autres méthodes d'analyse de sensibilité dans le domaine de l'estimation du potentiel éolien avec les modèles non linéaires dominants. 53 à 100 % des articles examinés dans chaque catégorie (82 % en moyenne, voir tableau 4.10) ont utilisé la méthode locale (Tsvetkova & Ouarda, 2021). Malgré son manque de fiabilité, des implications politiques ont été faites sur la base des résultats des analyses de sensibilité du coût actualisé de l'énergie dans (Carmichael et al., 2016) (Sliz-Szkliniarz et al., 2019), cela en soi est un motif de grave préoccupation. De plus, des logiciels professionnels conçus pour l'évaluation de projets d'énergie renouvelable, par exemple RETScreen (Ressources naturelles Canada : RETScreen, 2020), encouragent l'utilisation d'analyses non fiables comme moyen d'évaluer les risques associés à l'investissement dans le développement de projets éoliens.

La section 4.8 Géographie de (Tsvetkova & Ouarda, 2021) a révélé que la Grande-Bretagne, les États-Unis et la Chine sont les pays les plus étudiés à cet égard. De plus, le coût actualisé de l'énergie s'est avéré être le modèle le plus populaire dans l'évaluation des projets éoliens. (Tsvetkova & Ouarda, 2021) ont rapporté que "l'éolien offshore revêt une importance particulière pour le Royaume-Uni et l'Espagne". Le secteur de l'énergie éolienne offshore a montré une réduction significative des coûts au cours de la dernière décennie, rendant possible le potentiel plus abondant de l'énergie éolienne offshore pour l'intégrer au réseau. L'évaluation des bénéfices possibles de la prochaine génération de parcs éoliens flottants offshore nécessite des modèles technico-économiques non linéaires complexes qui capturent les nouvelles relations formées en raison des progrès technologiques rapides et des incitations politiques (Mora et al., 2021). Ils rapportent que les relations entre les entrées et les sorties dans les modèles de coûts complexes du secteur éolien offshore sont mal comprises, par conséquent, une analyse de sensibilité globale a été jugée nécessaire pour étudier ces modèles (Mora et al., 2021).

(Pianosi & Wagener, 2018) ont souligné l'importance de l'analyse de sensibilité globale pour l'aide à la décision en matière de politiques. Pourtant, cette voix reste inconnue, bien que l'abondance d'outils logiciels pour GSA ait été montrée dans (Tsvetkova & Ouarda, 2021).

Lorsqu'il a été découvert que la GSA était utilisée dans l'évaluation des ressources éoliennes (Tsvetkova & Ouarda, 2021), la méthode la plus courante était la méthode Sobol, et la moins courante était les effets Shapley (Song et al., 2015) et PAWN (Pianosi & Wagener, 2018).

(Tsvetkova & Ouarda, 2021) se sont concentrés sur les spécificités de l'application et ont discuté de trois exemples illustrant qu'une analyse de sensibilité à la fois peut non seulement être trompeuse pour les modèles non linéaires, mais aussi - pour les modèles linéaires dans certaines circonstances (voir la section 4.10 .1). (Tsvetkova & Ouarda, 2021) avertissent que si l'analyse de sensibilité locale était choisie pour être utilisée, elle "devrait être utilisée avec une extrême prudence, car les résultats de l'AS sont sensibles aux distributions des entrées".

Dans le troisième article de cette thèse (Tsvetkova & Ouarda, 2023a) ont présenté l'application de la famille de distribution Halphen (L. Zhang & Singh, 2021) pour modéliser la vitesse moyenne du vent. (Tsvetkova & Ouarda, 2022a) ont évalué l'efficacité de la famille de distributions de Halphen par rapport à un certain nombre de distributions, telles que la distribution de Weibull à deux paramètres, une autre distribution communément utilisée (tableau 6.6). Les mesures de la qualité de l'ajustement utilisées dans l'étude de cas comprenaient la probabilité logarithmique, le critère d'information d'Akaike, le critère d'information bayésien, la statistique de Kolmogorov-Smirnov, la statistique d'Anderson-Darling et l'erreur quadratique moyenne (tableau 6.5). Les résultats de qualité d'ajustement montrent des résultats très favorables de la performance de la famille de distribution de Halphen.

(Tsvetkova & Ouarda, 2022b) ont trouvé que le modèle le mieux ajusté le plus courant appartenait à la famille de distribution de Halphen (26 % pour Halphen de type A et 38 % pour Halphen de type B). Le deuxième meilleur ajustement a été signalé par (Tsvetkova et Ouarda, 2022b) comme étant la distribution de Weibull à deux paramètres (15%) et la distribution Gamma généralisée (13%). (Tsvetkova et Ouarda, 2022b) ont constaté qu'aucune des données horaires sur la vitesse du vent aux 126 stations de l'Est du Canada ne pouvait être ajustée à la distribution inverse de type B de Halphen. L'ajustement de Halphen-A et Halphen-B s'est avéré supérieur au modèle le plus couramment utilisé pour la tâche d'évaluation des ressources éoliennes (Weibull à deux paramètres), 59 % à 100 % du temps (Tsvetkova et Ouarda, 2022b) selon différentes qualités métriques d'ajustement (tableau 6.5). (Tsvetkova & Ouarda, 2022b) ont recommandé la famille de distribution Halphen pour la modélisation de la vitesse moyenne du vent, qui est étroitement liée à l'estimation du potentiel éolien.

Dans une étude d'application (Tsvetkova & Ouarda, 2022a), les données satellitaires QuikSCAT ont été utilisées aux fins d'évaluation des ressources éoliennes côtières du golfe Persique. L'examen d'un éventuel développement d'applications éoliennes offshore près du rivage dans les Émirats arabes unis est important car les trois plus grandes villes sont situées sur le littoral. Les séries chronologiques de vitesse du vent ont été dérivées de l'ensemble de données QuikSCAT pour une grille de 11 x 20 avec une résolution de 25 km. Ensuite, chacune des séries temporelles a été extrapolée à des hauteurs de moyeu de 100 et 112 m à l'aide de la loi logarithmique, après quoi elles ont été ajustées à la distribution de Weibull à deux paramètres (les paramètres de forme et d'échelle ont été estimés à l'aide de la méthode du maximum de vraisemblance). La moyenne de Weibull, les vitesses de vent énergétique les plus probables et maximales ont été calculées pour chaque cellule de la grille. Les cartes de la vitesse moyenne du vent, de la vitesse du vent la plus attendue et de la vitesse maximale du vent énergétique ont été données dans la Figure 8.3, la Figure 8.4 et la Figure 8.5. La carte du coût annuel de l'énergie éolienne et de l'électricité éolienne côtière (avec l'éolienne Vestas V112) a été fournie respectivement dans la Figure 8.6 et la Figure 8.7. L'électricité éolienne offshore a été estimée entre 1,6 et 1,8 $ct/kW.

(Tsvetkova & Ouarda, 2021) suggèrent que les recherches futures se concentrent sur l'analyse de sensibilité globale dans l'évaluation des ressources éoliennes. (Tsvetkova & Ouarda, 2021) ont constaté qu'aucune étude d'analyse de sensibilité globale sur la qualité de l'ajustement et la période de récupération n'a été repérée. Une autre lacune dans la littérature selon (Tsvetkova & Ouarda, 2021) est le nombre limité d'études traitant de l'analyse de sensibilité des mesures de la qualité de l'ajustement. Calcul des effets Shapley (Song et al., 2015) pour les facteurs contribuant à la valeur actualisée nette et/ou au coût actualisé de l'énergie (comme les sorties les plus populaires (Tsvetkova & Ouarda, 2021)) pour les applications onshore et offshore (en particulier pour l'éolien offshore flottant fermes car c'est l'un des sujets brûlants de l'énergie éolienne (Tsvetkova & Ouarda, 2021)) serait nouveau pour l'industrie (Tsvetkova & Ouarda, 2021). (Martin et al., 2016) ont défini les facteurs les plus influents pour le coût d'exploitation et de maintenance d'un parc éolien offshore flottant et ont suggéré d'affiner leurs distributions et d'effectuer une "analyse de sensibilité globale plus sophistiquée afin de quantifier le degré de sensibilité" (Martin et al., 2016). Ainsi, l'application de Sobol, Shapley ou PAWN à cette conception expérimentale est d'une importance justifiée (Tsvetkova & Ouarda, 2021). (Mytilinou & Kolios, 2019) suggèrent d'augmenter la taille de l'échantillon de la simulation de Monte Carlo pour étudier les interdépendances d'ordre supérieur, cela peut être fait avec effet total Sobol SI.

Enfin, (Guedes Soares, 2021) a suggéré d'étudier la sensibilité du LCOE des OFFWF aux années au cours desquelles chacun des différents coûts se produit (Guedes Soares, 2021).

(Tsvetkova & Ouarda, 2023a) suggèrent de modéliser la vitesse maximale du vent avec la famille de distribution Halphen (Perreault et al., 1999a), car la statistique d'Anderson-Darling favorisant l'ajustement de la queue droite a montré un ajustement amélioré pour Halphen type B (Tsvetkova & Ouarda, 2022a). Dvorak et al. (Dvorak, V., Bobée, B., Boucher, S., Ashkar, 1988) ont souligné que le système de distribution Halphen ne semble pas « aussi riche en une variété de formes et de types que le système Pearson et ils ne remplissent pas certaines exigences particulières comme la facilité de calcul ». Par conséquent, les efforts futurs pourraient également se concentrer sur la poursuite de cette étude de cas dans le but de comparer le système de distribution Halphen avec le système de distribution Pearson (Tsvetkova & Ouarda, 2023a).

TABLE OF CONTENTS

DEDICATION III

ACKNOWLEDGEMENTS IV

ABSTRACT AND KEYWORDS V

RÉSUMÉ ET MOTS-CLÉS VII

SOMMAIRE RECAPITULATIF IX

TABLE OF CONTENTS XXXI

LIST OF FIGURES XXXVII

LIST OF TABLES XLIII

1 GENERAL INTRODUCTION 45

1.1 RESEARCH QUESTIONS 47

1.2 NOVELTY AND IMPACT 49

1.3 A REVIEW OF GENERAL LITERATURE 50

1.3.1 Uncertainty analysis in wind resource assessment *51*

1.3.2 Sensitivity analysis in wind resource assessment *53*

1.3.1 Distributions used in wind resource assessment *55*

1.3.1 Goodness-of-fit metrics used in wind resource assessment *56*

1.3.2 The Halphen distribution family *57*

1.4 STRUCTURE OF DISSERTATION 58

2 A REVIEW OF SENSITIVITY ANALYSIS PRACTICES IN WIND RESOURCE ASSESSMENT 64

2.1 ABSTRACT 65

2.2 NOMENCLATURE 66

2.3 LIST OF ABBREVIATIONS 67

2.4 INTRODUCTION 69

2.5 SENSITIVITY ANALYSIS MODELS 70

2.5.1 Linear vs. nonlinear models *70*

2.5.2 The statistics behind wind resource assessment *71*

2.5.3 The economics of wind resource assessment *77*

2.6 SENSITIVITY ANALYSIS METHODS 91

2.6.1 Local sensitivity analysis *92*

2.6.2 Global sensitivity analysis *93*
2.7 Offshore vs. Onshore 96
2.8 Geography 97
2.9 Software 99
2.10 Specifics of application 101
2.10.1 Example I: Linear model with uniform distributions *101*
2.10.2 Example II: Nonlinear multiplicative model *104*
2.10.3 Example III: Nonlinear levelized cost of energy model *106*
2.11 Critical synthesis 109
2.11.1 Trends *109*
2.11.2 Pitfalls *110*
2.12 Conclusion and outlook 111
2.13 Declaration of competing interest 113
2.14 CRediT authourship contribution 113
2.15 Acknowledgements 113

3 BIBLIOGRAPHY 115

4 QUASI-MONTE CARLO TECHNIQUE IN GLOBAL SENSITIVITY ANALYSIS OF WIND RESOURCE ASSESSMENT WITH A STUDY ON UAE 127

4.1 Abstract 129
4.2 Nomenclature 130
4.3 Introduction 132
4.4 Methods 134
4.4.1 Sampling techniques in MC/QMC experiment *134*
4.4.2 Variance-based global sensitivity analysis (GSA) *140*
4.4.3 Experimental design *143*
4.5 Results 149
4.5.1 Test model results *149*
4.5.2 The UAE case study results *152*
4.6 Conclusions and future research 153
4.7 Conflict of interest 154
4.8 Acknowledgements 154

5 BIBLIOGRAPHY 155

6 USE OF THE HALPHEN DISTRIBUTION FAMILY FOR MEAN WIND SPEED ESTIMATION WITH APPLICATION TO EASTERN CANADA 160

6.1 Abstract 161

6.2 NOMENCLATURE 162
6.3 INTRODUCTION 164
6.4 METHODS 166
6.4.1 Review of Halphen distribution family (HDF) 166
6.4.2 Classes of heavy-tailed distributions in Extreme value theory (EVT) 169
6.4.3 Halphen distribution family in the context of wind speed modelling 170
6.4.4 Goodness-of-fit (GOF) metrics 171
6.5 MATERIALS 173
6.5.1 Eastern Canada case study 173
6.6 RESULTS AND DISCUSSION 178
6.6.1 Results for selected stations 183
6.7 CONCLUSION AND FUTURE WORK 189
6.8 DATA AVAILABILITY 189
6.9 DECLARATION OF COMPETING INTEREST 189
6.10 CREDIT AUTHORSHIP CONTRIBUTION STATEMENT 189
6.11 ACKNOWLEDGEMENTS 190

7 BIBLIOGRAPHY 191

8 OFFSHORE WIND RESOURCE ASSESSMENT WITH QUICKSCAT DATA IN THE UAE 196

8.1 ABSTRACT 197
8.2 NOMENCLATURE 198
8.3 ABBREVIATIONS 199
8.4 INTRODUCTION 200
8.5 MATERIALS AND METHODS 201
8.5.1 SeaWinds/QuickSCAT Scatterometer 201
8.5.2 Wind resource assessment 201
8.6 DESCRIPTION OF THE PERSIAN GULF CASE STUDY 203
8.6.1 Region of interest 203
8.6.2 Objectives 204
8.6.3 Assumptions 204
8.6.4 QuickSCAT wind speed data 205
8.7 RESULTS AND DISCUSSION 206
8.7.1 Wind speed: mean, mode, maximum energy 206
8.7.2 Annucal energy production 208
8.7.3 Electricity cost 210
8.8 CONCLUSIONS AND FUTURE WORK 211

8.9 ACKNOWLEDGEMENTS 211
8.10 DATA AVAILABILITY STATEMENT 211
8.11 DECLARATION OF INTEREST STATEMENT 211
9 BIBLIOGRAPHY 213
10 GENERAL CONCLUSION AND DISCUSSION 217
11 BIBLIOGRAPHY 223
12 APPENDIX I : R SCRIPT FOR EXAMPLE IN SECTION 2.11.1 233
13 APPENDIX II : EASTERN CANADA CASE STUDY STATIONS OVERVIEW 234
14 APPENDIX III: DESCRIPTIVE STATISTICS OF THE WIND SPEED DATA FOR STATIONS OF EASTERN CANADA CASE STUDY 239
15 APPENDIX IV: TEST STATISTICS FOR THE WIND SPEED DATA OF STATIONS IN EASTERN CANADA CASE STUDY 244
16 APPENDIX V: ESTIMATED PARAMETERS FOR HALPHEN DISTRIBUTION FAMILY FOR ALL STATIONS IN EASTERN CANADA CASE STUDY 250

LIST OF FIGURES

FIGURE 2.1 GEOGRAPHICAL REPRESENTATION OF THE REVIEW POOL 97

FIGURE 2.2 ONE-AT-A-TIME SENSITIVITY ANALYSIS RESULTS FOR MODEL L AND UNIFORMLY DISTRIBUTED INPUTS 101

FIGURE 2.3 SCATTER PLOT FOR MODEL L AND UNIFORMLY DISTRIBUTED INPUTS 101

FIGURE 2.4 SOBOL INDICES FOR MODEL L AND UNIFORMLY DISTRIBUTED INPUTS 102

FIGURE 2.5 SHAPLEY EFFECTS FOR MODEL L AND UNIFORMLY DISTRIBUTED INPUTS 102

FIGURE 2.6 ONE-AT-A-TIME SENSITIVITY ANALYSIS RESULTS FOR MODEL L AND X1 ~ N(10,2) , X2 ~ N(1, 0.5), X3 ~ N(100, 50), X4 ~ N(1000, 10), X5 ~ N(0.1, 0.01) 103

FIGURE 2.7 SCATTER PLOT OF MODEL L AND X1 ~ N(10,2) , X2 ~ N(1, 0.5), X3 ~ N(100, 50), X4 ~ N(1000, 10), X5 ~ N(0.1, 0.01) 103

FIGURE 2.8 SOBOL INDICES FOR MODEL L AND X1 ~ N(10,2) , X2 ~ N(1, 0.5), X3 ~ N(100, 50), X4 ~ N(1000, 10), X5 ~ N(0.1, 0.01 103

FIGURE 2.9 SHAPLEY EFFECTS OF MODEL L AND X1 ~ N(10,2) , X2 ~ N(1, 0.5), X3 ~ N(100, 50), X4 ~ N(1000, 10), X5 ~ N(0.1, 0.01) 103

FIGURE 2.10 ONE-AT-A-TIME SENSITIVITY ANALYSIS RESULTS FOR MODEL M AND UNIFORMLY DISTRIBUTED INPUTS 104

FIGURE 2.11 SCATTER PLOT OF MODEL M AND UNIFORMLY DISTRIBUTED INPUTS 104

FIGURE 2.12 SOBOL INDICES FOR MODEL M AND UNIFORMLY DISTRIBUTED INPUTS 104

FIGURE 2.13 SHAPLEY EFFECTS OF M AND UNIFORMLY DISTRIBUTED INPUTS 104

FIGURE 2.14 ONE-AT-A-TIME SENSITIVITY ANALYSIS RESULTS FOR MODEL M AND X1 ~ N(10,2) , X2 ~ N(1, 0.5), X3 ~ N(100, 50), X4 ~ N(1000, 10), X5 ~ N(0.1, 0.01) 105

FIGURE 2.15 SCATTER PLOT OF MODEL M AND X1 ~ N(10,2) , X2 ~ N(1, 0.5), X3 ~ N(100, 50), X4 ~ N(1000, 10), X5 ~ N(0.1, 0.01) 105

FIGURE 2.16 SOBOL INDICES FOR MODEL M AND X1 ~ N(10,2) , X2 ~ N(1, 0.5), X3 ~ N(100, 50), X4 ~ N(1000, 10), X5 ~ N(0.1, 0.01) 105

FIGURE 2.17 SHAPLEY EFFECTS OF MODEL M AND X1 ~ N(10,2) , X2 ~ N(1, 0.5), X3 ~ N(100, 50), X4 ~ N(1000, 10), X5 ~ N(0.1, 0.01) 105

FIGURE 2.18 UNCERTAINTY ANALYSIS RESULTS FOR LEVELIZED COST OF ENERGY MODEL 107

FIGURE 2.19 ONE-AT-A-TIME SENSITIVITY ANALYSIS RESULTS FOR MODEL M AND AND X1 ~ N(10,2) , X2 ~ N(1, 0.5), X3 ~ N(100, 50), X4 ~ N(1000, 10), X5 ~ N(0.1, 0.01) 108

FIGURE 2.20 SCATTER PLOT OF MODEL M AND AND X1 ~ N(10,2) , X2 ~ N(1, 0.5), X3 ~ N(100, 50), X4 ~ N(1000, 10), X5 ~ N(0.1, 0.01) 108

FIGURE 2.21 SOBOL INDICES FOR MODEL M AND AND X1 ~ N(10,2) , X2 ~ N(1, 0.5), X3 ~ N(100, 50), X4 ~ N(1000, 10), X5 ~ N(0.1, 0.01) 109

FIGURE 2.22 SHAPLEY EFFECTS OF MODEL M AND X1 ~ N(10,2) , X2 ~ N(1, 0.5), X3 ~ N(100, 50), X4 ~ N(1000, 10), X5 ~ N(0.1, 0.01) 109

FIGURE 4.1 TWO-DIMENSIONAL PSEUDO-RANDOM SAMPLE 135

FIGURE 4.2 A TWO-DIMENSIONAL LHS SAMPLE (N= 1000) 136

FIGURE 4.3 A TWO-DIMENSIONAL LHS SAMPLE (N = 15, S = 15) 136

FIGURE 4.4 A TWO-DIMENSIONAL SOBOL SAMPLE (N = 1000) 137

FIGURE 4.5 PROJECTIONS OF A THREE-DIMENSIONAL RANDOM (LEFT), LHS (CENTER) AND SOBOL (RIGHT) SAMPLES (N = 1000) 139

FIGURE 4.6 MASDAR CITY LOCATION 147

FIGURE 4.7 ECDF OF AIR DENSITY IN KG/M3, P AT MASDAR CITY 147

FIGURE 4.8 ACCURACY OF S_I FOR THE TEST MODEL USING BRUTE FORCE METHOD WITH A SAMPLE SIZE OF N = 4…64 ($N_R = 1000$) 150

FIGURE 4.9 ACCURACY OF ESTIMATING S_I FOR THE TEST MODEL WITH A SAMPLE SIZE OF N = 4…1024 ($N_R = 1000$) 150

FIGURE 4.10 MEAN ABSOLUTE ERROR OF S_I, $MAE(S_I)$, FOR BRUTE FORCE METHOD (N=4…64, N_R=1000) 151

FIGURE 4.11 MEAN ABSOLUTE ERROR OF S_I, $MAE(S_I)$, FOR ESTIMATION METHOD (N=4…64, N_R=1000) 151

FIGURE 4.12 MEAN ABSOLUTE ERROR OF STI, MAE(STI), FOR BRUTE FORCE METHOD (N=4…64, NR=1000).....151

FIGURE 4.13 MEAN ABSOLUTE ERROR OF STI, MAE(STI), FOR ESTIMATION METHOD (N=4…64, NR=1000).....151

FIGURE 4.14 GSA RESULT OR IMPORTANCE OF INPUTS FOR AEP ACCORDING TO STI.....153

FIGURE 4.15 UA RESULTS OR HISTOGRAM OF AEP AT MASDAR CITY 153

FIGURE 6.1 NESTED CLASSES OF HEAVY-TAILED DISTRIBUTIONS (ADAPTED FROM [15][30]) ..170

FIGURE 6.2 DISTRIBUTIONS COMMONLY USED IN HYDROLOGY, CLASSED ACCORDING TO THEIR TAIL BEHAVIOR (ADAPTED FROM [2][30]).....170

FIGURE 6.3 DISCRIMINATION BETWEEN CLASSES C, D AND E (ADAPTED FROM [2][35]).....170

FIGURE 6.4 126 STATIONS IN EASTERN CANADA THAT PASSED THE MODIFIED MANN-KENDALL TEST [4] 174

FIGURE 6.5 CLOSE UP OF STATIONS AROUND MONTREAL, QUEBEC AND TROIS-RIVIERES IN THE PROVINCE OF QC 175

FIGURE 6.6 CLOSE UP OF STATIONS AROUND MONCTON (NB), HALIFAX (NS) AND CHARLOTTETOWN (PE).....175

FIGURE 6.7 CLOSE UP OF STATIONS AROUND ST. JOHN'S (NL) 176

FIGURE 6.8 DESCRIPTIVE STATISTICS OF THE 126 STATIONS SUMMARIZED IN A BOX PLOT 178

FIGURE 6.9 LL BOX PLOT 179

FIGURE 6.10 AIC BOX PLOT 179

FIGURE 6.11 BIC STATISTIC BOX PLOT 180

FIGURE 6.12 KS BOX PLOT 180

FIGURE 6.13 AD BOX PLOT 180

FIGURE 6.14 RMSE BOX PLOT.....180

FIGURE 6.15 (C_V, C_S) MOMENT RATIO DIAGRAM 183

FIGURE 6.16 ($\Delta 1$, $\Delta 2$) MOMENT RATIO DIAGRAM 183

FIGURE 6.17 HISTOGRAM AND FITTED MODELS FOR STATION ID = 5251 (W2 IS BEST-FIT ACCORDING TO KS) 184

FIGURE 6.18 HISTOGRAM AND FITTED MODELS FOR STATION ID = 6501 (HA IS BEST-FIT ACCORDING TO KS) 184
FIGURE 6.19 TAIL ZOOM-IN OF HISTOGRAM AND FITTED MODELS FOR 5251....184
FIGURE 6.20 TAIL ZOOM-IN OF HISTOGRAM AND FITTED MODELS FOR STATION 6501 184
FIGURE 6.21 SKEWNESS-KURTOSIS PLOT [64] FOR STATION 5251....185
FIGURE 6.22 SKEWNESS-KURTOSIS [64] FOR STATION 6501....185
FIGURE 6.23: LOG-LOG PLOT [36] FOR STATION ID = 5251 (W2 IS BEST-FIT ACCORDING TO KS) 185
FIGURE 6.24: LOG-LOG PLOT [36] FOR STATION ID = 6501 (HA IS BEST-FIT ACCORDING TO KS) 185
FIGURE 6.25 EXPONENTIAL QQ PLOT, MEAN EXCESS PLOT, PARETO QQ PLOT, HILL ESTIMATE OF THE EXTREME VALUE INDICES (EVI) PLOT (HILL, 1975) FOR STATION ID = 5251 (W2 IS BEST-FIT ACCORDING TO KS) 188
FIGURE 6.26 EXPONENTIAL QQ PLOT, MEAN EXCESS PLOT, PARETO QQ PLOT, HILL ESTIMATE OF THE EVI PLOT (HILL, 1975) FOR STATION ID = 6501 (HA IS BEST-FIT ACCORDING TO KS) 188
FIGURE 8.1 REGION OF INTEREST....204
FIGURE 8.2 ONE-DAY QUICKSCAT WIND SPEED IN M/S....206
FIGURE 8.3 WEIBULL MEAN WIND SPEED AT 100 M MAP OF THE PERSIAN GULF 207
FIGURE 8.4 MOST PROBABLE WIND SPEED AT 100 M MAP OF THE PERSIAN GULF 208
FIGURE 8.5 MAXIMUM ENERGY WIND SPEED AT 100 M MAP OF THE PERSIAN GULF 208
FIGURE 8.6 AEP SURFACE OF THE REGION OF INTEREST 209
FIGURE 8.7 AEP WITH V112 MAP OF THE PERSIAN GULF....210
FIGURE 8.8 WIND ELECTRICITY PRODUCTION COST MAP OF THE PERSIAN GULF 210

LIST OF TABLES

TABLE 1.1 RESEARCH SUMMARY OF TOPICS CONSTITUTING THIS DISSERTATION 47

TABLE 2.1 GOODNESS-OF-FIT METRICS USED IN WRA [30][32].....71

TABLE 2.2 SENSITIVITY ANALYSIS INPUT VARIABLES IN [74][124][125] 85

TABLE 2.3 ONE-AT-A-TIME SENSITIVITY ANALYSIS REVIEW POOL ARTICLES ORGANIZED BY SENSITIVITY ANALYSIS OUTPUT VARIABLE 92

TABLE 2.4 REVIEW POOL ARTICLES ORGANIZED BY OBJECTIVE AND APPLICATION.....96

TABLE 2.5 REVIEW POOL ARTICLES ORGANIZED BY COUNTRY AND MODEL 98

TABLE 2.6 REVIEW POOL ARTICLES ORGANIZED BY SOFTWARE AND SENSITIVITY ANALYSIS METHOD 99

TABLE 2.7 OVERVIEW OF SOFTWARE TOOLS FOR GLOBAL SENSITIVITY ANALYSIS [5][8].....100

TABLE 2.8 COMPARISON OF SENSITIVITY ANALYSIS TOOLS AND METHODS IMPLEMENTED.....100

TABLE 2.9 INPUTS TO LEVELIZED COST OF ENERGY MODEL 107

TABLE 2.10 SUMMARY OF THE REVIEW OF SENSITIVITY ANALYSIS IN WIND RESOURCE ASSESSMENT 109

TABLE 4.1 MLE ESTIMATES OF WEIBULL DISTRIBUTION PARAMETERS FOR MASDAR CITY WIND SPEED.....148

TABLE 4.2 VARIABLES USED IN THE WRA MODEL IN THE UAE CASE STUDY 149

TABLE 6.1 DISTRIBUTIONS USED FOR MODELLING MEAN WIND SPEED ACCORDING TO [17] 165

TABLE 6.2 SUFFICIENT STATISTICS FOR THE HDF (ADAPTED FROM [2]) 168

TABLE 6.3 MOMENTS AND MOMENT RATIOS FOR THE HDF (ADAPTED FROM [9]).....168

TABLE 6.4 CASE STUDY STATION IDS LISTED BY PROVINCE 174

TABLE 6.5 GOODNESS-OF-FIT METRICS USED IN THE EASTERN CANADA CASE STUDY 176

TABLE 6.6 DISTRIBUTIONS USED IN THE EASTERN CANADA CASE STUDY 177

TABLE 6.7 BEST-FIT DISTRIBUTION ACCORDING TO ALL GOF METRICS FOR ALL STATIONS OF THE EASTERN CANADA CASE STUDY.....179

TABLE 6.8 BEST-FIT MODEL ACCORDING TO BIC LISTED BY PROVINCE.....181

TABLE 6.9 BEST-FIT MODEL ACCORDING TO KS LISTED BY PROVINCE.....182

TABLE 6.10 SLOPE OF MEAN EXCESS PLOT, SHAPIRO-WILK (SW) LOG-NORMALITY TEST, MODIFIED MANN-KENDALL (MMK) TEST, JACKSON TEST STATISTICS AND P-VALUES FOR SELECTED STATIONS (5251, 6501) 186

TABLE 6.11 SAMPLE STATISTICS FOR SELECTED STATIONS (5251, 6501).....186

TABLE 6.12 SOME SAMPLE STATISTICS ESTIMATIONS BASED ON ESTIMATED MODEL PARAMETERS 187

TABLE 6.13 ESTIMATED PARAMETERS AND MOMENTS FOR HA, HB, W2, GG, AND N DISTRIBUTIONS FOR SELECTED STATIONS (5251, 6501) 187

TABLE 8.1 V112 SPECIFICATION [36].....205

TABLE 13.1 EASTERN CANADA CASE STUDY STATIONS OVERVIEW 234

TABLE 14.1 DESCRIPTIVE STATISTICS OF THE WIND SPEED DATA FOR THE EXAMINED STATIONS239

TABLE 15.1 SLOPE OF MEAN EXCESS PLOT, SHAPIRO-WILK (SW) LOG-NORMALITY TEST, MODIFIED MANN-KENDALL (MMK) TEST, JACKSON TEST STATISTICS AND P-VALUES FOR ALL STATIONS 244

TABLE 16.1 ESTIMATED PARAMETERS FOR HDF FOR ALL STATIONS.....250

1 GENERAL INTRODUCTION

The crises of recent years are urgently calling to address the pressing consequences of climate change. A rapid shift towards clean sustainable energy is now not a matter of new ageism or pure love for the planet, it has become a matter of safety for the human race. Not only do climate crises point in this direction, but also the refugee crises caused by the aggression of fossil fuel-based economies like Russia. Gabor Mate could not have summarized the essence of the problem more bluntly and more to the point than he has in his work on addictions - "*The long-term ill effects of our society's addiction, if not to oil then to the amenities and luxuries that oil makes possible, are obvious. They range from environmental destruction, climate change and toxic effects of pollution on human health to the many wars that the need for oil, or the attachment to oil wealth, has triggered*" (Mate, 2008). Renewables play a pivotal role in such an economic shift. Wind energy is the fastest growing renewable source, but the Paris agreement ('Paris Agreement', 2015) to reduce greenhouse gas emissions requires a more rapid growth. The wind is currently the second best renewable energy source in Canada after hydropower; it contributes to 3.5% of Canada's electricity generation (*About Renewable Energy*, n.d.).

Uncertainty is inherent to the scientific method (Razavi *et al.*, 2020). Sensitivity analysis is the study of how the uncertainty in the output of a mathematical model, system or output variable can be allocated to different sources of uncertainty in its input variables (Andrea Saltelli et al., 2008). Uncertainty analysis is a neighbouring practice. In other words, "*uncertainty analysis and sensitivity analysis are complementary approaches to measuring the robustness of model predictions*" (Saltelli, 2022). Uncertainty analysis focuses on uncertainty quantification, while sensitivity analysis attributes parts of it to the inputs. The questions uncertainty analysis and sensitivity analysis address are different. Uncertainty analysis answers the question of how uncertain the estimated output is, while sensitivity analysis addresses the question of pour la where the uncertainty originates. Sensitivity analysis intends to establish a ranking of inputs. One-at-a-time sensitivity analysis commonly quantifies the impact on the model based on a p% increase and decrease in each input and presented in a so-called tornado plot (Figure 2.6, for instance).

Sensitivity analysis is an important yet undervalued tool in scientific discovery, despite it playing a fundamental part in the reasoning of scientific discovery and human decision-making (Saltelli *et al.*, 2021). "*Sensitivity analysis as a 'formal' and 'standard' component of scientific*

development and policy support is relatively young" claim (Saltelli *et al.*, 2021) in a recent editorial to a special issue of Environmental Modelling and Software. (Saltelli *et al.*, 2021) pinpoint that scientific advances and policies related to them have "*deep but informal roots in sensitivity analysis*" (Saltelli *et al.*, 2021). Moreover, new areas of knowledge that gave birth to modern-day professions, such as data science and machine learning, both benefit from sensitivity analysis (Saltelli *et al.*, 2021).

(Razavi *et al.*, 2020) and (Saltelli, Giampietro and Ravetz, 2016) called for sensitivity analysis to be promoted as an independent discipline due to its unused potential. (Saltelli *et al.*, 2021) claimed that modern sensitivity analysis is currently evolving into a "*formal and independent discipline*" (Saltelli *et al.*, 2021). Although global sensitivity analysis is already a part of several international guidelines for impact assessment (Leinfellner *et al.*, 1990)(Funtowicz and Ravetz, 1990) and disciplinary journals, its uptake is still "*in its infancy*" (Andrea Saltelli et al., 2019). The term sensitivity analysis is vastly stereotyped as the co-called, one-at-a-time sensitivity analysis (Saltelli *et al.*, 2019), even across the scientific community. Sensitivity analysis in wind resource assessment is no exception.

The COVID-19 pandemic gave rise to important aspects of how modelling, science and policy work in today's complex world overwhelmingly flooded with information (Saltelli *et al.*, 2020)(Saltelli *et al.*, 2022)(Saltelli, 2022)(Saltelli and Sarewitz, 2022). When models came to the close inspection of the eye of the public, sensitivity analysis practitioners were actively calling to mind the assumptions, the hubris, the frame, the consequences and the unknown, as (Saltelli, 2022) summarized the aspects allowing for responsible mathematical modelling. The essence of mathematical models is that they are "*simplified representations of real systems or processes*" (Saltelli, 2022). Minding the frame (Saltelli, 2022) refers to the different angles, views of the world, or "*underlying assumptions that guide how individuals, groups, and societies perceive a particular issue*" (Saltelli, 2022). Minding the consequences (Andrea Saltelli, 2022) means that if executed appropriately, mathematical modelling helps society make smarter decisions and vice versa, if executed inappropriately, models can lead to wrong or simply unjustified choices. Finally, minding the unknown (Andrea Saltelli, 2022) meant that "*failure to acknowledge and communicate uncertainties can artificially limit policy options and open the door to unintended consequences*" (Andrea Saltelli, 2022). A recent Nature article (Saltelli *et al.*, 2020) called not for an end to quantification, nor for producing apolitical models, but instead, they call for full and brutally honest disclosure. If these five points are respected it would help to preserve mathematical modelling as a valuable tool (Saltelli *et al.*, 2020). (Saltelli *et al.*, 2020) conclude «*Ignore the five, and model predictions become Trojan horses for unstated interests and values. Model responsibly* ». That

would be all as to the importance of dealing with uncertainty in a prediction or an estimation in the words of a talented simplifier of mathematical modelling in general and sensitivity analysis in particular, Andrea Saltelli.

1.1 Research questions

The research questions that the practices of uncertainty analysis and sensitivity analysis attempt to answer are different. Uncertainty analysis answers the question "*How uncertain is the output?*", while sensitivity analysis answers questions such as "*Where does the uncertainty in the system or mathematical model come from?*", "*Which input is the most and/or least influential in terms of the uncertainty of the output*?", "*What is the ranking of inputs?*", "*How can this level of uncertainty be achieved in the system?*", etc. (Saltelli *et al.*, 2008). (Saltelli *et al.*, 2019) report that uncertainty and sensitivity analyses are at times misinterpreted or the terms used interchangeably, which suggests there is room for improvement in how we as the users of the scientific method reason about uncertainty.

The objectives of this dissertation are the following:

1. to review and assess the quality of sensitivity analysis practices in the field of wind resource assessment;
2. to discourage the use of one-at-a-time sensitivity analysis;
3. to encourage the use of uncertainty and global sensitivity analysis;
4. to introduce methods from other fields;
5. to showcase uncertainty and global sensitivity analysis adding value to the decision support process.

This dissertation is structured into five topics summarized in Table 1.1. Each topic resulted or is about to result in an article in a peer-reviewed journal. The first topic has already resulted in a published article (Tsvetkova and Ouarda, 2019), and the second two topics resulted in (Tsvetkova and Ouarda, 2021). Fourth topic resulted in (Tsvetkova and Ouarda, 2022). Fifth topic resulted in (Tsvetkova and Ouarda, 2022).

Table 1.1 Research summary of topics constituting this dissertation

Section addressing the topic	**Topics**	**Research questions**	**Results**
Section 2	**A review of sensitivity analysis practice**	Are nonlinear models common for wind resource assessment?	Yes one-at-a-time sensitivity

	in wind resource assessment	What sensitivity analysis method is most popular in wind resource assessment? Is one-at-a-time sensitivity analysis prevalent in wind resource assessment? What output variables are commonly used in sensitivity analysis in wind resource assessment?	One-at-a-time sensitivity analysis Yes Goodness-of-fit metrics, wind power, wind energy, net present value, internal rate of return, payback period, levelized cost of energy Refer to (Tsvetkova and Ouarda, 2021) for details.
Section 4	**Quasi-Monte Carlo technique in wind resource assessment with a study on UAE**	Is quasi-Monte Carlo superior to Monte Carlo in the context of wind resource assessment? Does Sampling based on Sobol sequences outperform Latin hypercube sampling and pseudo-random sampling for wind resource assessment context?	Yes Yes See (Tsvetkova and Ouarda, 2019)(Tsvetkova and Ouarda, 2020) for details
Section 2	**Global vs. one-at-a-time sensitivity approach to sensitivity analysis of wind economics variables, such as annual energy production, net present value, payback period, internal rate of return and/or levelized cost of energy**	Does the one-at-a-time sensitivity approach to sensitivity analysis introduce significant error to sensitivity analysis results of annual energy production, net present value, payback period, rate of return, levelized cost of energy compared to global sensitivity analysis?	Yes, an example of OATSA vs GSA of a LCOE model is published (Tsvetkova and Ouarda, 2021)
Section 6	**Halphen distribution family for modelling wind speed in Eastern Canada**	Does the Halphen distribution family reduce estimation uncertainty when modelling mean wind speed compared to the commonly used two-parameter Weibull distribution? Is the Halphen distribution family recommended for use for estimating mean wind speed for wind resource assessment?	Yes Yes Refer to (Tsvetkova and Ouarda, 2023b) for details
Section 8	**Offshore wind resource assessment with QuickSCAT data in the UAE**	Is satellite QuickSCAT data useful for wind resource assessment?	Yes, but the uncertainty of the estimations is under question. See (Tsvetkova and Ouarda, 2022) for details.

1.2 Novelty and impact

The main novelty of this dissertation can be summarized in the following:

1. To the best of author's knowledge, no review of sensitivity analysis in wind resource assessment is currently available in the literature, the review article (Section 2) offers such;

2. Quasi-Monte Carlo technique and the Sobol method of global sensitivity analysis are new to the field of wind resource assessment, research article I (Section 4) bridges mathematical modelling and wind resource assessment;

3. Research article II (or Section 6) introduces the Halphen distribution family from flood frequency analysis to wind resource assessment in general and to mean wind speed estimation in particular.

More details on the novelty and impact of this dissertation follow. Each topic mentioned in Table 1.1 contributes to the state-of-the-art in wind resource assessment. The quasi-Monte Carlo technique has been applied in wind-related studies (Xu and Yan, 2017)(Velarde, Kramhøft and Sørensen, 2019)(Nikishova *et al.*, 2017), but not to wind resource assessment specifically. The Sobol method as a variance-based global sensitivity analysis has received little attention in wind resource assessment (Ulker, Allaire and Willcox, 2017). The main novelty of (Tsvetkova and Ouarda, 2019) is twofold: the use of quasi-Monte Carlo in wind resource assessment and the Sobol method for global sensitivity analysis in wind resource assessment, as both, have not received much attention. The first article (Tsvetkova and Ouarda, 2019) aims to fill in this gap by bridging mathematical modelling and wind resource assessment, as well as popularize global sensitivity analysis and exemplify a global sensitivity analysis study for wind resource assessment. Two case studies were carried out. One using a test model to show that quasi Monte Carlo is superior to Monte Carlo and compare brute force Sobol method with its estimation. Another using UAE data to demonstrate how a global sensitivity analysis (and uncertainty analysis) using quasi Monte Carlo and Sobol method could be set up in the context of wind resource assessment.

The term sensitivity analysis is vastly stereotyped as a one-at-a-time sensitivity analysis (*UNFCCC guidelines on the assessment of investment analysis*, no date), even across the scientific community. The field of wind resource assessment that is "*subject to a great deal of uncertainty*" (Lackner, Rogers and Manwell, 2007) is likely no exception. Several researchers proved one-at-a-time sensitivity's inefficiency for nonlinear models (Saltelli and Annoni, 2010)(Saltelli *et al.*, 2019)(Ferretti, Saltelli and Tarantola, 2016), but are nonLMs common for wind resource assessment? (Tsvetkova and Ouarda, 2021) is structured around this stereotype.

(Tsvetkova and Ouarda, 2019) stated "*one-at-a-time sensitivity approach is commonly used in wind resource assessment*", but more evidence is required to support the argument. The motivation behind (Tsvetkova and Ouarda, 2021) is twofold. First, to provide evidence of sensitivity analysis pitfalls identified in (Saltelli *et al.*, 2019) to be present in wind resource assessment, and, second, to improve the way we reason about uncertainty and rethink how sensitivity analysis should be conducted in wind resource assessment. To the best of the authors' knowledge, no review of sensitivity analysis in wind resource assessment, has been previously published, while reviews of uncertainty analysis have, e.g. (Lackner, Rogers and Manwell, 2007)(Ayodele, 2015). A comprehensive review such as (Tsvetkova and Ouarda, 2021) contributes novelty to the state-of-the-art with its existence. Contribution to the state-of-the-art in (Tsvetkova and Ouarda, 2021) is showcasing how the one-at-a-time sensitivity approach introduces compared to global sensitivity analysis of variables commonly used in wind resource assessment, such as annual energy production, net present value, payback period, internal rate of return, and levelized cost of energy leads to erroneous or misleading results.

The main contributions of the review article (Tsvetkova and Ouarda, 2021) to the state-of-the-art are:

1. providing such a review,
2. providing classifications of sensitivity analysis studies based on method, location and software,
3. identifying the commonly used outputs (sensitivity analysis models) in wind resource assessment,
4. locating gaps in published research,
5. explaining the specific application in wind resource assessment with its advantages and shortcomings (Section 2.10)
6. comparing one-at-a-time sensitivity analysis and global sensitivity analysis for a cost model commonly used in wind resource assessment (2.10.3).

(Tsvetkova and Ouarda, 2023b) are the first to introduce the Halphen distribution family used in hydrology (El Adlouni and Bobée, 2017) into modelling wind speed in Eastern Canada (Tsvetkova, 2022) for the first time offering a superior fit to the most commonly used two-parameter Weibull at 100% of the stations according to the Akaike information criterion.

1.3 A review of general literature

A series of articles on the shortcomings of the common practice of sensitivity analysis raising concern about the credibility of some one-at-a-time sensitivity analysis results have been

published over the past decade. (Saltelli and Annoni, 2010) started the trend in their "*How to avoid a perfunctory sensitivity analysis?*" in 2010, where they offer "*novel geometric proof of the inefficiency of one-at-a-time*" to discourage the use of the one-at-a-time approach to sensitivity analysis and promote a global approach instead. (Ferretti, Saltelli and Tarantola, 2016) report one-at-a-time dominance despite limited applicability among sensitivity analysis studies published and back it up with the evidence of a bibliometric analysis of the trends in sensitivity analysis in the past decade. In their "*Trends in sensitivity analysis practice in the last decade*"(Ferretti, Saltelli and Tarantola, 2016) the authors reported the growing trend of both sensitivity analysis studies published and the share of the global approach to it in the studies published. Finally, (Saltelli *et al.*, 2019) publish their "*Why so many published sensitivity analyses are false: A systematic review of sensitivity analysis practices*". Not only did the authors undertake an extensive systematic multidisciplinary review of sensitivity analysis studies but also they explored the reasons why the one-at-a-time approach is still prevailing, although no dissent has been voiced in the literature as a reaction to the two previous articles. (Saltelli *et al.*, 2019) also identified the common pitfalls of sensitivity analysis to be, first, the discrepancy in the terminology and hence goals, and, second, local instead of a global approach to it.

1.3.1 Uncertainty analysis in wind resource assessment

(Lee and Jason Fields, 2021) provided an immensely useful summary of how the wind energy industry has been quantifying and reducing prediction errors, energy losses, as well as production uncertainties. (Lee and Jason Fields, 2021) presented a literature review of energy production assessment errors across the global wind energy industry. (Lee and Jason Fields, 2021) identified a long-term trend of reduction of overprediction bias, but the uncertainty associated with the prediction error is prominent. Also (Lee and Jason Fields, 2021) summarized the recent advancements in the wind resource assessment process that justify the bias reduction, including improvements in modelling and measurement techniques.

(Kwon, 2010) presented a framework for uncertainty analysis of wind resource assessment with a case study at Kwangyang Bay. He ran a Monte Carlo experiment for estimating annual energy production with several random inputs, such as air density, Weibull parameters, mean wind speed, surface roughness exponent and power performance curve. Air density was modelled by a uniform distribution, mean wind speed – with a Weibull distribution and the rest of the inputs were modelled with the Gaussian distribution. The result was that annual energy

production was fitted best with a normal distribution of a mean of 1 and a standard deviation of 0.11.

(Tsvetkova and Ouarda, 2019)(Tsvetkova and Ouarda, 2020) compared different sampling strategies in a quasi-Monte Carlo experiment for annual energy production at Masdar City. There were five inputs to the annual energy production model. They were: the Weibull parameters modelled with a normal distribution, air density modelled with an empirical cumulative distribution function, and availability and electrical losses both modelled with a uniform distribution (Table 2.2). The results of the global sensitivity analysis suggested the influence of the variance in Weibull parameters on annual energy production might be overestimated, while found to be responsible for 2% of annual energy production uncertainty, and the influence of the variance in air density might be overlooked, while found to account for 94%. The results of uncertainty analysis can be found in Figure 4.15.

According to (Richter, 2020) uncertainty quantification can be divided into two categories of methods: intrusive and non-intrusive: "*Intrusive methods introduce changes to the original problem as the governing equations become statistical, non-intrusive methods on the other hand evaluate the original problem with varying inputs and compute the statistics from these computed results*" (Richter, 2020). (Richter, 2020) claims that for complex problems, non-intrusive methods are often preferred because they require no modification to the original code. Monte Carlo and quasi-Monte Carlo methods fall into the category of non-intrusive methods. From a practical standpoint, (Richter, 2020) ran a Monte Carlo and a quasi-Monte Carlo simulation, as well as applied the stochastic collocation method (Babuska, Nobile and Tempone, 2010) to annual energy production and levelized cost of energy for three existing offshore wind farms. (Richter, 2020) recommended using the quasi-Monte Carlo approach to uncertainty quantification in wind resource assessment.

Recently, (Quan *et al.*, 2020) provided a comprehensive survey of computational intelligence techniques for wind power uncertainty analysis in smart grids. (Quan *et al.*, 2020) introduced prediction intervals as a tool to quantify the uncertainty in wind power forecasts. Various prediction interval evaluation indices, "*including the latest trends in comprehensive evaluation techniques*" (Quan *et al.*, 2020) were compared. Also, computational intelligence-based prediction interval construction methods were summarized and classified as parametric or non-parametric methods. Three methods - stochastic models, fuzzy logic models, and robust optimization – were compared, as well as different power system applications using these techniques were reviewed by (Quan *et al.*, 2020).

1.3.2 Sensitivity analysis in wind resource assessment

No review of sensitivity analysis in wind resource assessment is currently available in the literature, (Tsvetkova and Ouarda, 2021) provided such a comprehensive review of the sensitivity analysis practices in wind resource assessment (Section 4). (Tsvetkova and Ouarda, 2021) offered classifications by sensitivity analysis output variable (or model), method, application, country, and software. The review pool consists of a hundred and two articles with models dealing with statistical and economic aspects of wind resource assessment (goodness-of-fit metrics, wind power, wind energy, the net present value, the payback period, the internal rate of return, the payback period, the levelized cost of energy, capital and operational expenses). Sensitivity analysis studies, where the wind is predicted with weather research and forecasting models, sensitivity analysis of hybrid energy systems with a wind component, and sensitivity analysis of wind turbine fatigue loads, are beyond the scope of the review (Tsvetkova and Ouarda, 2021). (Tsvetkova and Ouarda, 2021) reveals the lack of collective agreement on the definition of sensitivity analysis in the literature, the dominance of nonlinear models (100%), and the prevalence of the one-at-a-time sensitivity analysis method (82%). These findings are consistent with those of (Tsvetkova and Ouarda, 2019)(Saltelli *et al.*, 2019). The review (Tsvetkova and Ouarda, 2021) highlights the existing gaps in the field, and provides evidence of the common pitfalls, possibly leading to costly misinterpretations of the data at the site and hence to erroneous feasibility assessments. The review (Tsvetkova and Ouarda, 2021) urges us to rethink how to conduct sensitivity analysis in wind resource assessment. It also provides a comparison of one-at-a-time sensitivity analysis and global sensitivity analysis for a linear and nonlinear models (Section 2.10).

The trends unveiled in the process of the review (Tsvetkova and Ouarda, 2021) were the following:

1. all models commonly used in wind resource assessment were nonlinear,
2. one-at-a-time sensitivity analysis prevails in wind resource assessment despite its inapplicability to such models,
3. the more technical wind resource assessment study is the more likely for global sensitivity analysis to be employed,
4. global sensitivity analysis is becoming more popular in wind resource assessment over time, and, last but not least,
5. policy implications made on unreliable one-at-a-time sensitivity analysis study results in wind resource assessment might lead to dire consequences.

The summary of the review (Tsvetkova and Ouarda, 2021) can be found in Table 2.10 and it indicates the prevalence of nonlinear models and one-at-a-time sensitivity analysis in wind resource assessment. The use of keywords such as a baseline, a change in %, or a tornado diagram signals the application of one-at-a-time sensitivity analysis.

The review (Tsvetkova and Ouarda, 2021) found evidence of the following pitfalls of sensitivity analysis to be present in the field wind potential estimation:

1. Lack of universal definition of sensitivity analysis in wind resource assessment;
2. Interchangeability of sensitivity analysis and uncertainty analysis;
3. Disregard to the lack of applicability of the one-at-a-time sensitivity method to nonlinear models;

(Tsvetkova and Ouarda, 2021) were not the first to point out the need for a clear standard definition of sensitivity analysis in Earth sciences, it has been voiced before by (Razavi and Gupta, 2015) The motivation behind sensitivity analysis can be diverse. (Saltelli *et al.*, 2008) provided examples of sensitivity analysis objectives, that is to find errors in the model, prioritize research activities, and "*identify critical regions in the space of inputs*" (Saltelli *et al.*, 2008). According to (Tsvetkova and Ouarda, 2021), in some studies selected for review, there was no clear motivation or no research questions for sensitivity analysis study. (Tsvetkova and Ouarda, 2021) often failed to find a ranking of inputs after sensitivity analysis was performed, which (Tsvetkova and Ouarda, 2021) attributed to the lack of a clear research question. (Tsvetkova and Ouarda, 2021) found that some sensitivity analysis studies were used to identify which variables have an effect on the model with the means of one-at-a-time sensitivity analysis. Here two problems exist with this reasoning. First, the statement widely used within this dissertation that one-at-a-time sensitivity analysis is not valid for nonlinear models, and, second, the whole issue of a causal effect is brought to light.

Examples of interchangeability of the terms uncertainty analysis and sensitivity analysis were detected in several studies, (Tsvetkova and Ouarda, 2021) reported. (Tran and Smith, 2018) presented the probability density function of the levelized cost of energy as the result of global sensitivity analysis, when, in fact, they are uncertainty analysis results. (Ayodele, 2015) in an encyclopedia review article on methods for uncertainty analysis of wind turbine output used uncertainty analysis and sensitivity analysis interchangeably. (Heck, Smith and Hittinger, 2016) when reasonably arguing in favour of a Monte Carlo approach for integrating uncertainty into the levelized cost of energy, he stated that *"if uncertainty is included at all, it is usually through a simple sensitivity analysis that uses high/low values for each variable to estimate upper and lower*

bounds on the levelized cost of energy" [121]. With this statement, he shows the common understanding of uncertainties or the interchangeability of uncertainty analysis and sensitivity analysis. (Tsvetkova and Ouarda, 2021) report that only a handful of studies accounted for the nonlinearity of the models common for wind resource assessment, for instance (Tsvetkova and Ouarda, 2019)(Richter, Wolters and Frank, 2019)(Mora, Spelling and van der Weijde, 2019)(Mora *et al.*, 2019). The vast majority of the studies selected for review disregarded model nonlinearity and used one-at-a-time sensitivity analysis (Tsvetkova and Ouarda, 2021).

For the sake of avoiding redundancy, since a review article is part of this dissertation for a detailed review of sensitivity analysis practices in wind resource assessment the reader is kindly asked to refer to Section 2.

1.3.1 Distributions used in wind resource assessment

(Jung and Schindler, 2019)(Carta, Ramírez and Velázquez, 2009)(Ouarda and Charron, 2018)(Zhou *et al.*, 2010)(Wang, Liu and Qian, 2021)(Shi *et al.*, 2021) have published reviews of statistical distributions used in wind resource assessment. (Jung and Schindler, 2019) showed that "*115 parametric distributions were applied 2010–2018*" (Jung and Schindler, 2019) and that the two-parameter Weibull distribution was "*the most frequently (44 times) evaluated distribution*" (Jung and Schindler, 2019). Also (Jung and Schindler, 2019) concluded that the two-parameter Weibull distribution was "*the most commonly evaluated and recommended distribution*" (Jung and Schindler, 2019).

(Aries, Boudia and Ounis, 2018) used the two-parameter Weibull, the two-parameter Gamma distribution, two-parameter Wald distribution, two-parameter lognormal, Gumbel, generalized extreme value distribution, Nakagami, and generalized logistic distribution to model wind speed for deep assessment of wind speed distribution models for four sites in Algeria. (Ouarda and Charron, 2018) enhanced the list with the three-parameter lognormal, log Pearson type 3 and normal. A comprehensive evaluation of wind speed distribution models with a case study for North Dakota by Zhou et al. (Zhou *et al.*, 2010) included the two-parameter Weibull, the two-parameter Gamma, log-normal, and inverse Gaussian. (Usta and Kantar, 2012) propose using skewed generalized error distribution and skewed t distribution. According to (Jung and Schindler, 2019), distributions that were applied at least in four different studies or recommended for use in at least two distinct studies for wind potential estimation are given in Table 6.1. Some mixture models have been applied to this task (Shin, Ouarda and Lee, 2016). Jung et al. (Jung and Schindler, 2019), conclude that is impossible to "*identify a single distribution that can be fitted*

universally" (Jung and Schindler, 2019). The distributions used in practice are not limited to the list mentioned above. Here, the intent was to give a quick overview of the most frequently encountered distributions in specialized literature.

1.3.1 Goodness-of-fit metrics used in wind resource assessment

(Jung and Schindler, 2017) conducted a comparison of goodness-of-fit metrics used in wind resource assessment and found that the Kolmogorov-Smirnov statistic is the most common metric used in such studies. Other goodness-of-fit metrics in popularity order were determined as the following: R_{pp}^2, χ^2, $RMSE_{PP}$, WPE, $RMSE_{PDF}$, Akaike information criterion, Log-likelihood, Bayesina information criterion, R_{PDF}^2, R_{QQ}^2, $RMSE_{QQ}$, *AD*, $RMSE_{power}$, MAE_{QQ}, R_{power}^2.

Several goodness-of-fit metrics include the calculation of the log-likelihood function. The log-likelihood function is given in Eq. (67) (Ouarda, Charron and Chebana, 2016). The higher the value of log-likelihood, the better the fit of the model in question is. One of the widely used goodness-of-fit criteria that include calculation of the log-likelihood is the Akaike information criterion developed by Hirotsugu Akaike (Akaike, 1970). Akaike information criterion can be used as the means for distribution selection: In the case of the Akaike information criterion, the lower the value - the better the model fit. The Akaike information criterion is parsimonious as it takes the number of estimated parameters into account following the concept of Occam's razor (Phil Gibbs, 1997) or also known as the law of parsimony. Another metric that also penalizes the number of parameters of a model is the Bayesian information criterion defined as given in Eq. (69) (Ouarda, Charron and Chebana, 2016). Here again, the lower the value, the better the distribution fit is.

(Ouarda, Charron and Chebana, 2016) mentioned using (β_1, β_2) moment ratio diagram for model selection (See Eq. (70) for definition of order *r, r>1*), where $\beta_1$is the squared coefficient of skewness (Eq. (71)) and β_2 equals the coefficient of kurtosis (Eq. (72)). Moments can be estimated from the data sample in the following manner, as given in Eq. (73). The coefficient of skewness can, hence, be estimated with Eq. (74) and coefficient of kurtosis – Eq. (75).

(Ouarda, Charron and Chebana, 2016) and (Vargas *et al.*, 2019) reviewed goodness-of-fit measures used in wind potential estimation, the summary can be found in Table 2.1.

1.3.2 The Halphen distribution family

A concise literature review of the Halphen distribution family is to follow along with its application, popularization and advances. The Halphen distribution family is a flexible and complete distribution family that was designed specifically for river peak flow datasets by Etienne Halphen during World War II (Dvorak, V., Bobée, B., Boucher, S., Ashkar, 1988). The creation of this distribution family was driven by "*Halphen's desire to construct his distributions to meet some specific requirements of fitting hydrological variables*" (Dvorak, V., Bobée, B., Boucher, S., Ashkar, 1988). The probability density function of the three-member distribution family as well as their moments can be found in Table 6.3.

Perrault et al. (L. Perreault, Bobée and Rasmussen, 1999a) discussed the statistical properties of the distributions in (L. Perreault, Bobée and Rasmussen, 1999a) and later - the parameter estimation with maximum likelihood estimation and quantile estimation (L Perreault, Bobée and Rasmussen, 1999). A significant body of research on the importance of the Halphen distribution family in the field of flood frequency analysis was contributed (El Adlouni and Bobée, 2017). (Chebana, El Adlouni and Bobée, 2008) discussed the estimation of Halphen distribution family parameters with the method of moments and with a mixed estimation method (Chebana, Adlouni and Bobée, 2010). (El Adlouni and Bobée, 2007) studied the sampling techniques for the Halpphen distribution family and developed a discriminatory test (El Adlouni, Salaheddine ; Bobée, 2014). (Zhang and Singh, 2021) revisited the application of the Halphen distribution system in flood frequency analysis. (Zhang and Singh, 2021) used 198 peak flow datasets in the case study, estimated Halphen distribution parameters with the maximum likelihood method and used Kolmogorov-Smirnov statistic as a goodness-of-fit metric and root mean square error – as a performance metric. (Zhang and Singh, 2021) found that HA/HB was the preferred distribution for 190 datasets, also the moment ratio diagram was found to be a reliable tool for distribution selection along with the value of kurtosis. Most importantly, the study of (Zhang and Singh, 2021) validated the use of the Halphen distribution family in flood frequency analysis. (Zhang and Singh, 2021) compared the performance of HDF with log-Pearson type 3 distribution. (El Adlouni, Chebana and Bobée, 2010) conducted an exploratory study comparing generalized extreme value distribution vs. the Halphen distribution family. The simulation-based comparisons point that Halphen type A distribution is more flexible than the generalized extreme value and that it leads to "*reasonable bias and root mean squared error even when samples are generated from generalized extreme value distribution*" (El Adlouni, Chebana and Bobée, 2010). Deholme et al.

(Delhome, Billot and El Faouzi, 2017) introduced the HDF as a toolbox for modelling travel time variability.

For the Halphen distribution family, two-moment ratio diagrams are common - the (C_v, C_s) and the (δ_1, δ_2) moment ratio diagrams (El Adlouni and Bobée, 2017). C_v is the coefficient of variation, defined by Eq. (76) and estimated from sample by Eq. (74). C_s is the coefficient of skewness and was discussed above. According to El Adlouni & Bobee (El Adlouni and Bobée, 2017), δ_1, δ_2 are defined by Eq. (79) and Eq. (80) respectively.

1.4 Structure of dissertation

This paper-based dissertation consists of four articles under the umbrella of uncertainty and sensitivity analyses in the field of wind resource assessment.

Section 1 presents the topic, research objectives (Section 1.1), novelty and impact (Section 1.2), general literature review (Section 2.3) and structure of this thesis (Section 1.4).

Section 2 presents the first article in the series titled Quasi-Monte Carlo technique in global sensitivity analysis in wind resource assessment with a study on United Arab Emirates (Tsvetkova and Ouarda, 2019). Section 2.1 contains the abstract of the study Section 2.2 – the nomenclature used throughout Section 2.

While working on (Tsvetkova and Ouarda, 2019) the prevalence of one-at-a-time sensitivity analysis studies in wind resource assessment was spotted, while this method is strictly valid for linear systems. To confirm this intuitive finding, the work on the comprehensive review of sensitivity analysis practices in wind recourse assessment began and resulted in (Tsvetkova and Ouarda, 2021). Section 4 presents the work undertaken in (Tsvetkova and Ouarda, 2021).

Section 2 is organized in sixteen sections: 2.1 Abstract to (Tsvetkova and Ouarda, 2021), 2.2 Nomenclature used throughout (Tsvetkova and Ouarda, 2021), 2.3 List of abbreviations used throughout (Tsvetkova and Ouarda, 2021), 2.4 Introduction, 2.5 Sensitivity analysis models, 2.6 Sensitivity analysis methods, 2.7 Offshore vs. onshore, 2.8 Geography, 2.9 Software, 2.10 Evolution, 2.11 Specifics of application, 2.12 Critical synthesis, 2.13 Conclusion and outlook, 2.14 Declaration of competing interest, 2.15 CReDiT authorship contribution, and 2.16 Acknowledgements.

Sections 2.1 - 2.4 are self-explanatory. The most detailed review classification is based on the sensitivity analysis model and is given in Section 2.5. The scope of this review is limited to the sensitivity analysis of goodness-of-fit metrics (Section 2.5.1), wind power (2.5.2.1), wind

energy (2.5.2.2), net present value (2.5.3.1), internal rate of return (2.5.3.2), payback period (2.5.3.3), levelized cost of energy (2.5.3.4), capital expense (Section 2.5.3.5), and operational expense (Section 2.5.3.6).

Section 2.6 reviews the sensitivity analysis methods encountered while undertaking the review in (Tsvetkova and Ouarda, 2021). Section 2.6.1 reviews local sensitivity analysis methods, i.e. the famous one-at-a-time sensitivity analysis in Section 2.6.1.1. Section 4.2.2 reviews global sensitivity analysis methods, i.e. the scatterplot method (Section 2.6.2.1), the Morris method (Section 2.6.2.2), the Sobol method (Section 2.6.2.3), extended Fourier amplitude test (Section 2.6.2.4), and more recently developed Shapley effects (Section 2.6.2.5), and PAWN (Section 2.6.2.6).

Section 2.7 organizes the studies in the review pool by offshore vs. onshore applications. Section 2.8 organizes the review pool articles by the country on which a case study of sensitivity analysis has been reported. Section 2.8 zooms into the research gaps in the literature from a geographical standpoint. Section 4.8 is intended to be a quick reference on regions of the world that are understudied. In the process of the review case studies with meteorological data from thirty-seven countries (Figure 2.3) with a sensitivity analysis in one form or another was encountered, Table 2.5 classifies these findings based on the country and sensitivity analysis model used, hence the gaps are easily identifiable. Global and selected country reports concerning installed wind capacity can be found in (WindPower, 2021) with detailed information on existing wind farms.

Section 2.9 classifies the article pool based on the software used for sensitivity analysis and discusses the influence each tool has on the choice of the sensitivity analysis method. (Douglas-Smith *et al.*, 2020) identified the software for both uncertainty and sensitivity analyses and provided an overview of the general research trends. (Murthy and Rahi, 2017) published a review of software tools used in wind resource assessment. The software tools used specifically for sensitivity analysis in the field of wind resource assessment are listed in Table 4.6. Often wind-related projects are analyzed with the use of professional modelling software targeted for modelling clean energy projects, for example, RETScreen (*Natural Resources Canada: RETScreen*, 2020). RETScreen is used for a feasibility assessment of clean energy projects, for instance, (Hadi, Oudah and Al-baldawi, 2020)(Soe, Zheng and Aung, 2015)(Salehin *et al.*, 2016), the only available option for sensitivity analysis of the net present value of the project in RETScreen is one-at-a-time. The nonlinear nature of both wind and economic models is surprisingly disregarded.

To illustrate the misleading or erroneous inference that one-at-a-time sensitivity analysis can entail for some models, three examples are considered in Section 2.10. *Sensobol* R package (Puy *et al.*, 2021) with a sample size of 1000 was used for the three examples (2.10.1, 2.10.2, 2.10.3), the R script can be found in Appendix I.

The trends unveiled in the process of the review (Tsvetkova and Ouarda, 2021) are explained in Section 2.11 Critical synthesis. There are five trends detected. First, all models commonly used in the field are nonlinear. Second, that one-at-a-time sensitivity analysis prevails in the field despite its inapplicability to nonlinear models. Third, the more technical a study is the more likely it is for a global approach to sensitivity analysis to be employed. Fourth, global sensitivity analysis is becoming more popular in the field over time. Fifth, policy implications made on unreliable one-at-a-time sensitivity analysis study results in wind energy assessment might lead to dire and costly consequences. The review by (Tsvetkova and Ouarda, 2021) is summarized in Table 2.10. It indicates the prevalence of nonlinear models in the field. The use of keywords such as a baseline, a change in %, or a tornado diagram indicates the use of one-at-a-time sensitivity analysis.

Section 2.12 presents the conclusions and outlook for further research. Section 2.13 contains a Declaration of competing interest. Section 2.14 - author contributions. Finally, Section 2.15 lists the acknowledgements. Bibliography to (Tsvetkova and Ouarda, 2021) is given in Section 3.

One of the questions kept in mind of this dissertation is to study how much distribution choice affects wind energy estimates. In this realm, Section 6 presents research submitted for publication (Tsvetkova and Ouarda, 2023b) which introduces a distribution family new to the field of wind energy assessment. Section 6 is organized in the following manner: 6.1 Abstract to (Tsvetkova and Ouarda, 2023b), 6.2 Notation for (Tsvetkova and Ouarda, 2023b) 6.3 Introduction, 6.4 Methods, 6.5 Materials, 6.6 Results and discussion, 6.7 Conclusions and future work, 6.8 Data availability, 6.9 Declaration of competing interest, 6.10 Authorship contribution to (Tsvetkova and Ouarda, 2023b), and finally 6.11 Acknowledgements. Bibliography to (Tsvetkova and Ouarda, 2023b) can be found in Section 7.

Section 4 or (Tsvetkova and Ouarda, 2019) is organized into four main sections: introduction (Section 4.3), methods (Section 4.4), results (Section 4.5), conclusions and future research (Section 4.5). The introduction to (Tsvetkova and Ouarda, 2019) presented the problem associated with sensitivity analysis in wind resource assessment. The methods section (Section 4.4) contains three subsections: sampling techniques used in Monte Carlo/quasi-Monte Carlo

(Section 4.4.1), variance-based global sensitivity analysis (Section 4.4.2) and experimental design (Section 4.4.3). The sampling techniques subsection (Section 4.4.1) summarizes the sampling techniques used throughout (Tsvetkova and Ouarda, 2019), namely pseudo-random sampling (Section 4.4.1.1), Latin hypercube sampling (Section 2.2.1.2), and Sampling based on Sobol sequences (Section 4.4.1.3). Section 4.4.1.4 compares the three mentioned above.

Variance-based global sensitivity analysis subsection 4.4.2 reviews brute force calculation of Sobol first-order and total effect sensitivity indices (Section 4.4.2.1) and their estimation methods (Section 4.4.2.2). Experimental design subsection 4.4.3 contains two parts: the test model (Section 4.4.3.1) and the wind energy model at Masdar City case study (Section 4.4.3.2). Section 4.4.3.2 gives details on the setup of the experimental part of this work and methods used in wind resource assessment such as the Weibull distribution to fit wind speed data and to calculate annual energy production. The assumptions about underlying distributions of input variables to the wind resource assessment model are given in this subsection. The input and output variables in the quasi-Monte Carlo experiment with the respective assumptions about the underlying distributions of the variables are summarized in Table 4.2.

The results section 4.5 provides the results obtained in (Tsvetkova and Ouarda, 2019), i.e. global sensitivity analysis for the test (Section 4.5.1) and wind resource assessment (Section 4.5.2) models. Test model results include the comparison of sampling strategies in light of global sensitivity analysis in wind resource assessment. Wind energy estimation model results contain results of global sensitivity analysis and uncertainty analysis for wind resource assessment at Masdar City, United Arab Emirates. The conclusions and future research (Section 4.6) presents conclusions made in (Tsvetkova and Ouarda, 2019) with some possible suggestions for future research direction. Finally, Section 4.7 contains the conflict of interest for (Tsvetkova and Ouarda, 2019) and Section 4.8 – the acknowledgements. The bibliography for (Tsvetkova and Ouarda, 2019) can be found in Section 5.

The Methods section 6.4 includes the review of the Halphen distribution family (6.4.1), classes of heavy-tailed distributions in extreme value theory in Section 6.4.2, Halphen distribution family in the context of wind speed modelling (6.4.3) and goodness-of-fit metrics in Section 6.4.4. Section 6.5.1 presents Eastern Canada cases study conducted in (Tsvetkova and Ouarda, 2023b). Section 6.6 provides generalized results of the Eastern Canada case study, while Section 6.6.1 presents detailed results for two specific stations in the case study (one that showed the two-parameter Weibull distribution as best-fit and another - as Halphen type A distribution).

Section 8 presents another application wind resource assessment study in the United Arab Emirates, but with a different kind of data – satellite QuickSCAT wind speed data. Section 8 is organized into eleven sections. Section 8.1 contains the abstract, and section 8.2 is the nomenclature. Section 8.3 lists the abbreviations used in this application. Section 8.4 introduces the problem with a brief literature review: Section 8.5 covers the methods and tools used in this work. Section 8.5.1 covers SeaWinds/QuikSCAT scatterometer. Section 8.5.2 describes techniques used for wind resource assessment, such as the distribution commonly used to describe wind behaviour (Section 2.2.1), goodness-of-fit (Section 2.2.2), extrapolating wind speed data to hub height (Section 2.2.3) and the economic side of a wind project (Section 2.2.4). Section 8.6 describes the case study adopted in the present work. Section 8.6.1 describes the region of interest. Section. 8.6.2 lists the case study objectives. Section 8.6.3 lists the assumptions made in the case study. Section 8.6.4 gives a detailed description of QuikSCAT wind speed data. The results are discussed in Section 8.7 and the conclusions and potential directions for future work are presented in Section 8.8. Sources of support and data are acknowledged in Section 8.9. Finally, the data availability statement and the declaration of interest statement can be found in Section 8.10 and Section 8.11 respectively. The bibliography of Section 8 is listed in Section 9.

Section 10 presents the general conclusions of this dissertation. Section 11 holds the general bibliography of this dissertation. Appendix I contains the supplementary material (Tsvetkova and Ouarda, 2021). Appendices II- V contain appendices to (Tsvetkova and Ouarda, 2023b).

2 A REVIEW OF SENSITIVITY ANALYSIS PRACTICES IN WIND RESOURCE ASSESSMENT

Titre de l'article :

UNE REVUE DES PRATIQUES D'ANALYSE DE SENSIBILITE DANS L'EVALUATION DES RESSOURCES EOLIENNES

Authors :

Olga Tsvetkova, INRS-ETE

Taha B.M.J. Ouarda, INRS-ETE

Titre of book or journal :

Energy Conversion and Management

Date of publication : 2021/06/15

DOI : https://doi.org/10.1016/j.enconman.2021.114112

Contribution of authors :

Olga Tsvetkova: Conceptualization, Methods, Writing - Original draft preparation.

Taha B.M.J. Ouarda: Funding acquisition, Supervision, Writing - Reviewing and Editing.

2.1 Abstract

A review of sensitivity analysis in wind resource assessment is presented, offering classifications by sensitivity analysis output variable (or model), method, application, country, and software. No review of sensitivity analysis in wind resource assessment is currently available in the literature. The review pool consists of 102 articles with models dealing with statistical and economic aspects of wind resource assessment (goodness-of-fit metrics, wind power, wind energy, the net present value, the payback period, the internal rate of return, the payback period, the levelized cost of energy, capital and operational expenses). Sensitivity analysis studies, where the wind is predicted with weather research and forecasting models, sensitivity analysis of hybrid energy systems with a wind component, and sensitivity analysis of wind turbine fatigue loads, are beyond the scope of this review. This review reveals the lack of collective agreement on the definition of sensitivity analysis in the literature, the dominance of nonlinear models (100%), and the prevalence of one-at-a-time sensitivity analysis method (82%). The review highlights the existing gaps in the field, provides evidence of the common pitfalls, possibly leading to costly misinterpretations of the data at the site and hence to erroneous feasibility assessments. The review urges to rethink how to conduct sensitivity analysis in wind resource assessment. It also includes comparison of one-at-a-time sensitivity analysis and global sensitivity analysis for a linear and nonlinear models.

2.2 Nomenclature

μ_i	The mean of elementary effect of Morris [1]
μ_i^*	The improved sensitivity measure of [2] based on the Morris method [1]
P_{WT}	Wind turbine rating
P_{WF}	Installed windfarm capacity
S_i	Sobol first-order sensitivity indices [3][4]
T_i	Sobol total effect sensitivity indices [3][4]
V_{T_i}	a variance based on the total effect for a factor X_i
V_i	a variance based on the first-order effect for a factor X_i
$X_{\sim i}$	$N \times (k-1)$ matrix of all factors but X_i
X_i	Generic sensitivity analysis input variables
WD	Water depth
D	Distance to shore
d_i	Elementary effect of Morris [1]
σ_i	The standard deviation of elementary effects of Morris [1]
A	$N \times k$ sample matrix of inputsIVs used
AEP	Annual energy production
B	Benefit in cost-benefit analysis
C	Cost in cost-benefit analysis
CAPEX	Capital expense
E	Energy
h_0	Roughness length
H	Wind turbine height
LCOE	Levelized cost of energy
OPEX	Operational expense
A	Cross sectional area of a wind turbine rotor
P	Power
N	Sample size
R	Discount rate
T	Time
W	Wind speed
Y	Function, response, model, output
Λ	Scale parameter of the two-parameter Weibull distribution
P	Air density
c	Shape parameter of the two-parameter Weibull distribution
k	Number of inputs

2.3 List of abbreviations

AEP	Annual energy production
ANN	Artificial neural network
ANOVA	Analysis of variance
ARIMA	Auto-regressive integrated moving average
CAPEX	Capital expenditure
CBA	Cost-benefit analysis
CDF	Cumulative distribution function
CF	Capacity factor
CS	Case study
DOE	Design of experiment
DM	Distribution model
DR	Discount rate
DWP	Dispersed wind power
D&C	Costs of development and consenting of a wind project
eFAST	Extended Fourier sensitivity analysis test
FAST	Fourier amplitude sensitivity test
FC	Foundation costs
FIT	Feed-in tariff
FOFFWF	Floating offshore wind farm
FS	Feasibility study
FUSED-Wind	Framework for unified systems engineering and design of wind plants [5]
GIS	Geographical information system
GOF	Goodness-of-fit
GOFM	Goodness-of-fit metric
GSA	Global sensitivity analysis
GSAR	Global sensitivity analysis result
HES	Hybrid energy system
HH	Hub height
IR	Interest rate
IRR	Internal rate of return
IV	Input variable
JUV	Jack up vessel
KS	Kolmogorov-Smirnov statistic
LCOE	Levelized cost of energy
LM	Linear model
LSA	Local sensitivity analysis
MAE	Mean absolute error
MC	Monte Carlo
MLP	Multi-layer perceptron
MSE	Mean standard error
MTTF	Mean time to failure
NG	Natural gas
nonLM	Nonlinear model
NPV	Net present value
NREL	National Renewable Energy Laboratory
O&M	Operation and maintenance
OAT	One-at-a-time
OATSA	One-at-a-time sensitivity analysis

OATSAR	One-at-a-time sensitivity analysis result
OFFWF	Offshore wind farm
ONWF	Onshore wind farm
OPEX	Operational expenditure
OV	Output variable
PAWN	Distribution based method of global sensitivity analysis [6]
PC	Power curve
PDF	Probability density function
PO	Power output
PP	Payback period
PPA	Power purchase agreement
P&A	Production and aquisition
QMC	Quasi-Monte Carlo
RA	Risk analysis
RC	Repowering cost
R&D	Research and development
RL	Roughness length
RMSE	Root mean square error
SA	SA
SAFE	Sensitivity analysis for everyone [7]
SAIV	Sensitivity analysis input variable
SAOV	Sensitivity analysis output variable
SAR	Sensitivity analysis result
SD	Standard deviation
SI	Sensitivity index
SP	Superposition principle
SR	Surface roughness
SWD	System of wind speed distributions
TD	Tornado diagram
TEA	Techno-economic assessment
TS	Time series
UA	Uncertainty analysis
UNFCCC	United Nations Framework Convention on Climate Change
UQ	Uncertainty quantification
W2	The two-parameter Weibull distribution
WE	Wind energy
WF	Wind farm
WFPO	Wind farm power output
WM	Wake model
WP	Wind power
WRA	Wind resource assessment
WRF	Weather research and forecasting
WRFM	Weather research and forecasting model
WS	Wind speed
WSC	Wind shear coefficient
WSTS	Wind speed time series
WT	Wind turbine
WTFL	Wind turbine fatigue load

2.4 Introduction

Uncertainty is inherent to the scientific method [4]. Sensitivity analysis (SA) is the study of how the uncertainty in the output of a mathematical model, system or output variable (OV) can be allocated to different sources of uncertainty in its input variables (IV) [4]. Uncertainty analysis (UA) is a neighbouring practice. UA focuses on the uncertainty quantification (UQ), while SA attributes parts of it to the inputs. The questions UA and SA address are different. UA answers the question of how uncertain the output is, while SA - where the uncertainty originates . SA means to establish a ranking of inputs. One-at-a-time (OAT) SA (OATSA) commonly quantifies the impact on the model of based on a p% increase and decrease in each input.

Saltelli et al. [8] called for SA to be promoted as an independent discipline due to its unused potential. Although, global SA (GSA) is already a part of a number of international guidelines for impact assessment [9][10] and disciplinary journals , its uptake is still "*in its infancy*" [11].The term SA is vastly stereotyped as OATSA [12], even across the scientific community. This review is conceptualized around this stereotype. SA in WRA is no exception. Tsvetkova et al. [13] stated that OATSA is typical for WRA (evidence required) and voiced concern about the validity of OATSA for nonlinear models (nonLMs) in WRA. However, are nonLMs typical for WRA? The review intends to provide evidence of SA pitfalls present in WRA [13], OATSA and nonLMs prevalence in WRA. Reviews of UA in WRA exist in the literature, e.g. [14], but a review of SA in WRA does not. A recent review of Azavedo et al. [15] identified the main impact factors on economical feasibility of wind projects and suggested performing SA of NPV, IRR, PP based on the identified inputs. There is a growing interest in SA in relation to WRA.

The main contributions of this paper are: (1) providing such a review, (2) providing classifications of SA studies based on method, location and software, (3) identifying the commonly used outputs (SA models) in WRA, (4) locating gaps in published research (Section 10), (5) explaining the specific application in WRA with its advantages and shortcomings (Section 8) (6) comparing OATSA and GSA for a cost model commonly used in WRA. The goals of this review are to (1) shed light on the inconsistencies present in the use of SA in the field, (2) encourage the use of UA/SA in WRA studies, and (3) promote the use of appropriate SA methods for the models used in WRA, so that policy implications were made on credible results.

The review is organized in ten sections: 2.4 Introduction, 2.5 Sensitivity analysis models, 2.6 Sensitivity analysis methods, 2.7 Offshore vs. onshore, 2.8 Geography, 2.9 Software, 2.10 Specifics of application, 2.11 Critical synthesis, and 2.12 Conclusion and outlook. The most detailed review classification is based on the SA model and is given in Section 2.5. The scope of

this review is limited to SA of goodness-of-fit metrics (GOFMs), wind power (WP), wind energy (WE), net present value (NPV), internal rate of return (IRR), payback period (PP), and levelized cost of energy (LCOE). There are four significant clusters of ongoing research in neighbouring topics outside the review's scope: (1) SA of wind turbine fatigue loads (WTFLs), (2) SA of weather research and forecasting models (WRFM's), (3) SA of hybrid energy systems (HES's) with a wind component, and (4) SA used in wind farm (WF) layout optimization [16]. SA of WTFL tends to use universal GSA, and of WRFMs – OATSA [13]. SA of HES's mostly employs OATSA [17]. WRFM's predict the WS (often with WP or WE), OATSA of WRFM's can be justified by the computational burden and many SAIV typical for such models [13].

2.5 Sensitivity analysis models

Section 2.5.1 discusses model linearity and explains why it is crucial when choosing a SA method. Section 2.5 walks the reader through the typical process in WRA, discusses which WRA variables act as SAOVs. Section 2.5.3 reviews the economic variables found to be a SAOV.

2.5.1 Linear vs. nonlinear models

In mathematics, a linear system is a system satisfying the superposition principle (SP) [18] - that for all linear systems, the response caused by multiple stimuli, is the sum of individual responses [19]. The essence of the SP is in additivity (Eq. (1)) and homogeneity (Eq. (2)). A linear function Y is one satisfying the SP. In SA, LMs exhibit behaviour described in Eq. (3) [4].

$$Additivity: F(X_1 + X_2) = F(X_1) + F(X_2) \tag{1}$$

$$\textit{Homogeneity: } F(aX) = aF(X) \tag{2}$$

$$Y = b_0 + \sum_{r=1}^{k} b_r X_i = b_0 + b_1 X_1 + b_2 X_2 + \cdots + b_k X_k \tag{3}$$

For a model to be linear, all the relationships between inputs X_i and *Y* should be linear (Eq. (4)). Vice versa, to classify a model as nonlinear, it is sufficient to show that at least one relationship between X_i and *Y* is nonlinear.

$$Linear\ relationship: Y \sim X_i \tag{4}$$

$$Nonlinear\ relationship: Y \sim 1/X_i, Y \sim {X_i}^n, Y \sim \ln X_i, Y \sim e^{X_i} \ldots \tag{5}$$

The local or OAT approach is limited to LMs [20][21][22], while GSA is a universal tool applicable to any model.

2.5.2 The statistics behind wind resource assessment

WRA starts with statistically modelling the WS. WS time series (WSTS) is fitted with a distribution model (DM), most commonly with the two-parameter Weibull (W2) distribution (Eq. (6)) [23]-[27], although other DMs are possible [27]-[31].

$$f(w) = \frac{c}{\lambda}\left(\frac{w}{\lambda}\right)^{c-1} e^{-\left(\frac{w}{\lambda}\right)^{c}}, \tag{6}$$

2.5.2.1 Goodness-of-fit metrics

Then the goodness-of-fit (GOF) is evaluated by calculating GOFMs characterizing the fit between the collected WSTS and a DM. Ouarda et al. [30] and Vargas et al. [32] reviewed GOFMs used in WRA (summarized in Table 2.1). All the studies mentioned in this section used OATSA, despite the eye-catching nonlinearity of GOFMs.

Table 2.1 Goodness-of-fit metrics used in WRA [30][32]

GOFM	Formula	Comment
Log-likelihood (LL)	$\ln L = \ln \sum_{i=0}^{N} f(w_i)$	w_i is the WSTS
Akaike information criterion (AIC)	$AIC = -2\ln L + 2k$	*k* is the number of parameters of a distribution
Bayesian information criterion (BIC)	$BIC = -2\ln L + k\ln N$	*N* is the WS sample size
Coefficient of determination	$R^2 = 1 - \frac{\sum_{i=0}^{n}(w_i - v_i)^2}{\sum_{i=0}^{n}(w_i - v_{ave})^2}$	
Coefficient of determination giving the degree of fit between the theoretical cumulative distribution function and the empirical cumulative probabilities of WS data	$R^2{}_{PP} = 1 - \frac{\sum_{i=0}^{n}(F_i - \widehat{F_i})^2}{\sum_{i=0}^{n}(F_i - \bar{F})^2}$	
Coefficient of determination giving the degree of fit between the theoretical WS quantiles and the WS data	$R^2{}_{QQ} = 1 - \frac{\sum_{i=0}^{n}(w_i - \widehat{w_i})^2}{\sum_{i=0}^{n}(w_i - \bar{w})^2}$	
The adjusted coefficient of determination	$R^2{}_a = 1 - (1 - R^2)\frac{N-1}{N-d}$	*N* is the WS sample size, and *d* is the number of parameters in a statistical model
Root mean square error (RMSE)	$RMSE = \sqrt{\frac{\sum_{i=0}^{n}(w_i - \widehat{w_i})^2}{n}}$	

Chi-square test statistic	$\chi^2 = \frac{\sum_{i=0}^{n}(O_i - E_i)^2}{\sum_{i=0}^{n} E_i}$	
Kolmogorov-Smirnov statistic (KS)	$\mathrm{D} = \max_{1 \le i \le n} F_i - \widehat{F_i}$	
Anderson-Darling statistic (AD)	$A = -n - \sum_{i=1}^{n} \frac{2i-1}{n} (\ln(\widehat{F_i}) + \ln(1 + \widehat{F_{n-i+1}}))$	
Mean absolute error (MAE)	$MAE = \sum_{i=1}^{n} \lvert w_i - \widehat{w_i} \rvert$	
Mean absolute percentage error (MAPE)	$MAPE = \frac{1}{n} \sum_{i=0}^{n} \frac{w_i - \widehat{w_i}}{w_i}$	
Standard deviation	$\sigma = \sqrt{\frac{1}{n-1} \sum_{i=0}^{n} (w_i - \overline{w_i})^2}$	

Only two studies on SA of GOFMs of some distributions to fit WSTS were found [33][34]. Alavi et al. [33] pursued SA of four DMs (lognormal, gamma, Rayleigh, W2) with actual and truncated WSTS with an Iranian case study (CS). They pointed to the lack of SA studies of GOFMs to the accuracy of measured data. OATSA of GOFMs (such as MSE, normalized MSE, normalized RMSE, MAE, RMSE, mean absolute relative error, coefficient of determination, and coefficient of efficiency) to the change in the accuracy of WS at five locations was conducted. GOF of the original and truncated to integer values WSTS were compared, showing that the lognormal distribution is best-fit to the original WSTS, while W2 - to the truncated WSTS [33].

Jung et al. [34] investigated the effect of WSTS quality on ten GOFMs for a system of WS distributions (SWD) comprised of the Burr-Generalized Extreme Value, Kappa, and Wakeby distributions. The GOFMs were KS, ${R^2}_{PP}$, ${R^2}_{QQ}$, $RMSE_{PP}$, $RMSE_{QQ}$, MAE_{PP}, MAE_{QQ}, relative error of the mean of the cubes of WS, annual energy production (AEP) error, and percentage of AEP error. WSTS from 187 German locations were used. Jung et al. [34] emphasized the lack of results in the literature for fitting a distribution to poor quality WSTS. The percentage of missing data, the data resolution, and the temporal resolution were altered, and the AEP was calculated. The goal was to evaluate the robustness of SWD against measurement errors, missing values, and low temporal resolution. SWD was found robust against all the SAIVs, despite the application of OATSA [34].

2.5.2.2 Wind power

Once WS data are fitted to a DM, WP can be assessed. Both GSA [35]-[42] (47%) and OATSA [43]-[50](53%) were conducted for WP. Weekes et al. [35] performed GSA of WP density

of a small-scale onshore WT in the UK with the Sobol method using GUI-HDMR [51]. The SAIVs were regional displacement height, roughness length (RL), blending height, and W2 shape factor. GSA results (GSARs) differed across ten locations. On average W2 shape was top-ranked, explaining 37% in WP variance. McKay et al. [36] and Tong et al. [37] used extended Fourier amplitude sensitivity testing (eFAST) to study the effects of wake models (WMs) on WP. SAIVs in [36] were yaw angle, rotor speed, blade pitch angle, WS, ambient temperature, main bearing temperature, WS standard deviation (SD), and yaw angle SD, in [37] - WS, ambient turbulence, land area per MW installed, land aspect ratio, and nameplate capacity. The GSARs accounting for wake effects in [36] ranked WS and WS SD as the top contributing to WP variance. Tong et al. [37] found that (1) when the WS is less than the WT rated WS, its effect is dominant regardless of the WM used, (2) the relative importance of each IV is less sensitive to the choice of WM for WFs with optimized layouts. Finally, Ulker et al. [38] conducted a GSA of both onshore WT and WF power output (PO) for WT micro-siting. The SAIVs was the W2 parameters, power turbulence intensity, power wind shear, and operational pitch control. SARs in [38] ranked the W2 scale at the top - responsible for 63-77% of WT and 69-83% of WF PO variance. WT PO in [38] was calculated as (32). Wake effects influence on AEP variance was found negligible in [52] and significant in [53]. Also, the use of very accurate WMs was found overstated in [52].

A recent study by Carta et al. [39] proposed a GSA method tailored to wind farm power output (WFPO) estimation models. Moreover, in [39] Sobol indices were compared to Shapley effects [54] and regular vine copula was used to simulate the dependency among the inputs. The model used in the CS of [39] for WFPO proposed by Diaz et al. [55] was fed with sixteen meteorological and six operational inputs. The data used in the CS of [39] is historical operational data of the Gorona del Viento wind-hydro power plant (El Hierro-Canary Islands-Spain). Carta et al. [39] found that the WS, active power set-point and turbulence intensity variables accounted for 98.58% of the variance in the WFPO model, while the wind direction, nacelle orientation and air density – for only 1.42%. They also found that Shapley effects overcame the difficulty of the presence of correlation of inputs to the WFPO model as compared to the Sobol indices that operate based on the assumption that the inputs are statistically independent.

$$P_{ave} = \int_0^{\infty} \mathrm{P(w)}\, \pi_w(w)\, dw = \int_0^{\infty} \mathrm{P(w)}\, \frac{c}{\lambda}\left(\frac{w}{\lambda}\right)^{c-1} e^{-\left(\frac{w}{\lambda}\right)^{c}} dw, \tag{7}$$

Where the WT power curve (PC) is $P(w)$, $\pi_w(w)$ is the WS probability distribution function (PDF), c and λ are the W2 parameters.

Aghbalou et al. [42] conducted a probabilistic assessment approach for WT-site matching with a GSA of performance function and probability of operating based for a CS ot two sites in Morocco. The performance function was defined as the difference between electrical power and critical power. The WS and rated WS show most influence on the performance of a WT.

Much risk in WRA is associated with the volatile nature of the wind. Naturally, the WS or its DM parameters often serve as SAIVs. The relationship between the WS and WP is known to be cubical (Eq. (8)) [25], so whenever the WS or its DM parameters are present among SAOVs, OAT is not acceptable. Numerous attempts at quantifying the uncertainty in WP associated with the WS were made [35]-[45][44], some - with OATSA [43]-[45]. He et al. [45] sharply observed that all relationships between SAIVs (WS threshold, slope threshold, elevation threshold, and bathymetry threshold) and the SAOV were nonlinear, but used OATSA nonetheless.

$$P = \frac{1}{2} C_p \rho A w^3, \tag{8}$$

Where C_p is the coefficient of performance (that depends on the yaw angle, rotor speed, and blade pitch angle), ρ is the air density (inversely proportional to the mean bearing temperature), *A* is the cross-sectional area of the rotor and *w* is the WS.

Eisa et al. [44] studied sensitivity of mechanical power with the model of a type-3 DFAG/DFIG wind turbine generator with close attention to behaviour at higher wind speeds with the pitch control activated. The goal was to understand how fast the pith angle needs to respond to the WS change[44]. Although the study focus was on SA, Eisa et al. [44] studied "*sensitivity of the state variables to the parameters by analyzing the effect of changing one parameter while fixing the others*" [44]. Along with the WS, WT pitch control parameters and grid characteristics served as inputs to SA.

Two studies on OATSA of WP [45][46] used GIS tools. He et al. [45] assessed where, when and how much wind is available in China by using ten years of hourly WSTS for two hundred Chinese sites. Nguyen [46] assessed WE potential in Vietnam and reasoned about the development status and future implications. Nguyen [46] claimed that wind potential primarily depends on the assumed discount rate (DR) and specific investment cost. The SA objective in [46] was to provide policymakers with more accurate potential assessment, but research questions were unclear, and no ranking was established.

Kubik et al. [47] compared the log law (Eq. 9) and the power law (Eq. 10) to translate ground WS to hub height (HH) WS with OATSA of WP output to surface roughness (SR) and wind

shear coefficient (WSC) for West Freugh, Scotland. As the names and Equations (9)-(10) suggest, the research question calls for GSA due to nonlinearity, but instead, OATSA was used.

$$w(h) = \frac{w_*}{k}\ln(\frac{h}{h_0}), \tag{9}$$

$$w_2 = w_1\left(\frac{h_2}{h_1}\right)^{\alpha},\ \alpha = \ln(w_2) - \ln(w_1))/(ln(h_2) - \ln(h_1)), \tag{10}$$

Where h_0 is RL and α is the WSC.

Nedjari et al. [48] studied the wind potential of seventy-four coastal Algerian locations, identified the optimal windy sites, and evaluated wind power's sensitivity (OATSA) to the data time interval. WP density was calculated with different ten-year intervals.

Two recent studies used SA of WT power for PC modelling. A recent study by Saint-Drenan et al. [49], included a parametric model for wind turbine power curves that incorporated environmental conditions. It included a "*univariate*" SA of qualitative nature (OATSA) of the power curve with respect to rotor diameter, nominal power, cut-in and cut-out speed, minimum and maximum rotation speed. Rotor diameter and nominal power are reported to have most impact on the power curve, yet "*their level of uncertainty is negligible as they both are design parameters and most manufacturers mention them directly in the name of the turbine*" [49]. Gonzalez et al. [56] explored using high-frequency SCADA data for WT performance monitoring and found it highly beneficial for this purpose. Sensitivity of power curve models to site specific conditions, seasonality, input relevance and sampling rate was studied with an interesting angle to SA.

Two groups of researchers considered uncertainties in aeroelastic blade models. Kumar et al. [40] studied GSA of model uncertainty in aeroelastic blade element momentum models for WT output with the Sobol method by the means of UQLab [57] tool. The GSA results showed "*the importance of the lift coefficient, especially for the axial force prediction*" [40].The study of Murcia et al. [41] on uncertainty propagation through an aeroelastic blade model using polynomial surrogates included GSA of WTPO, inter alia.

Finally, Haces-Fernandes et al. [50] recently showed improvement of WFPO with selected turbine deactivation, and OATSA of WFPO with regard to turbine rotor diameter was part of the study. The new deactivation concept offered larger PO improvement for WFs with larger turbines installed [50].

2.5.2.3 Wind energy

Energy is power in a given time, so the nonlinearity concern holds. Yet OATSA of wind energy (WE) [58]-[66] (71%) is more common than GSA [13][52][53][67] (29%). Zhou et al. [58] and Hoogwijk et al. [59] conducted OATSA of global onshore WE potential and generation costs. The SAIVs in [58] were WS, SR, HH, turbine density, land suitability, turbine cost, finance rate, and transmission cost, and WS was found most influential. Zhou et al. [58] used nonlinear (Eq (11)) to calculate global onshore wind potential. A "one-factor" SA [59] was referred to as "*not complex as most relationships are linear*" [59].

$$E_a = f \sum_{i=1}^{8760} \eta_1 \eta_2 \left(\frac{\mathrm{A}\delta}{1.5}\right) P_i \tag{11}$$

Where *f* denotes land suitability factor, *A* is the area of each grid cell, η_1 is the availability factor, η_2 is the array efficiency, δ is turbine density, P_i is the hourly WP output that depends on the HH and the RL.

SA of WE is frequent in techno-economic assessments (TEAs). A TEA and UQ of a Finnish onshore WF (ONWF) [60] included OATSA of deterministic and stochastic models of AEP and NPV. A TEA of a real WF repowering experience in Malpica, Spain [61] based on [60] included OATSA (+/-5% of the baseline scenario) of AEP, present value costs, cost of energy, NPV, IRR, PP, and minimum spot price. Inputs to SA of AEP in [61] were W2 parameters, air density and WT power curve, Weibull scale was found most influential on AEP. Khalid et al. Another TEA [62] included OATSA of a hypothetical WF in Pakistan with RETScreen [68]. The SAIVs were initial project cost, electricity export rate, electricity price, escalation rate, debt interest rate (IR), capacity factor (CF), emission reduction income. The SAOVs were net energy produced, generation cost and NPV. The SARs were presented as a plot of NPV depending on the CF. No ranking of inputs was established, and instead, conclusions about the strong dependency were made [62]. A TEA of onshore wind on the Canary Islands [63] implemented OATSA of AEP and LCOE. The singe SAIV was HH. Although SA is meant to establish an input ranking, the analysis was nevertheless referred to as SA [63]. The results showed that for the mountainous islands, no pattern could be established, but in the case of flat islands, the highest HH of 100 m correlated with lower generation cost [63]. Also, Tautz-Weinert et al. [64] performed "*what-if*" SA (OATSA) of an ONWF maintenance decision with performance and revenue analyses. The SAOV was normalized

energy production, and SAIVs were optimization delay, additional downtime, shifting of the intervention icing, wind direction, country, taxed revenue, and subsidy. Bistline et al. [65] studied the economic drivers of wind and solar penetration in the US with OATSA of future WE share. The SAIVs were investment costs, natural gas (NG) price, the potential for new inter-regional transmission, availability of low-cost energy storage, and CO2 policy. It was found that "*no single factor unilaterally determines wind and solar deployment*" [65], this statement alone calls for GSA with SAIVs varying simultaneously in contrast to OATSA. The Sobol method was used to account for the WE model nonlinearity [13][52][53][67]. Tsvetkova et al. [13] and Richter et al. [52] applied quasi-Monte Carlo (QMC) technique in GSA in WRA and discussed the related sampling [13][52] and computation problems at length [52]. A non-specific turbine CS on UAE was conducted in [13], and an assessment of four offshore WFs (OFFWFs) - in [52]. SAOV was AEP [13][52], and NPV, IRR, LCOE [52]. The SAIVs in [13] were air density, turbine availability, electric losses, and the W2 parameters, in [52] - WS, wake effect, PC, SR, plant performance, capital cost, O&M cost, DR, and energy price. Air density was found to be most influential in [13], accounting for 94% of AEP variance, WS and PC - in [52] accounting for 80% and 3-9%.

Dykes et al. [53] applied a systems engineering approach to WT key design parameters by using the Sobol, correlation and scatterplot methods to evaluate a US ONWF performance. GSA studies of AEP were conducted with NREL WISDEM [69]. Rotor diameter and WT rated power were found most influential on AEP [53]. Bossavy et al. [67] conducted a GSA of the technical potential GIS assessment of onshore wind and solar technologies. They discovered that parameters related to availability are more influential rather than those related to technology. Sensitivity indices for energy production in Brittany and Provence-Alpes-Cote d'Azur were calculated. The inputs were CF increase ratio from the use of new wind technology, the proportion of fresh wind installed capacity, a parameter indicating whether or not protected natural areas are constraints to WP capacity implantation, and a parameter indicating whether or not protected natural areas are constraints to the wind and solar power capacity implantation. Among other inputs, there was maximum altitude for plant installation, maximum altitude gradient for plant installation, minimum CF suitable for plant installation, and installed capacity by the surface unit at power plant scale. The relative influence of the parameters involved in defining surface availability was estimated at 65-75%.

2.5.3 The economics of wind resource assessment

The economics of WRA is expressed with cost-benefit analysis (CBA) characterizing a project by NPV, IRR, PP, LCOE, all using AEP in their definition, hence here too the nonlinearity

concern persists. Moreover, Harenberg et al. [20] showed that only GSA accounts for nonlinearities and variable interactions and that both are present in economic models.

2.5.3.1 Net present value

Despite the various nonlinearities among frequent IVs to SA of NPV (WS, DR, lifetime), GSA is rarely used – a single study [52] of the twenty five reviewed (5%). All studies calculated NPV as:

$$NPV = \sum_{i=0}^{N} \frac{B - C}{(1+r)^i} = \sum_{i=0}^{N} \frac{AEP_i\ FIT - CAPEX_i - OPEX_i}{(1+r)^i}, \quad (12)$$

Where *B* is the benefit (depends on AEP), *C* is the cost, *i* is the time (usually a year), *N* is the project lifetime, and *r* is the DR.

One common input in SA of NPV is the DR [52][70]-[77], the only GSA among these was [52]. (37) shows the nonlinear relationship between the DR and NPV. Nordman [70] performed WRA in Kenya with OATSA of NPV with the initial cost, debt IR, DR, WS, and electricity price as SAIVs. With SARs presented in a table, the conclusion consisted of a determined threshold WS value necessary for a positive NPV [70]. Kongham et al. [71] formulated the investment strategy as a mixed-integer programming problem with the constraints specified as intervals and the NPV as the objective. After finding an optimum solution, OATSA was performed to test the effects of DR, electricity rate, O&M cost, and lifetime on NPV. Higher DR and O&M costs were found to yield higher generation cost [71]. Lozano-Minguez et al. [72] performed multi-criteria assessment of different OFFWT support structures (monopole, tripod and jacket) with OATSA of NPV. The varied parameter was the DR. The SAR was that a DR increase yields NPV decrease [72]. Alonzo et al. [77] quantified the uncertainty of the NPV of virtual onshore and offshore windfarms in France, Germany and Denmark and evaluated the cost of support mechanisms needed to guarantee their profitability under present and future climate. Their study included OATSA of NPV based on DR as "*DR is a parameter that strongly impacts the NPV and as a consequence the profitability of an asset*" [77].

OATSA of NPV conducted in TEAs [60][61][78][79] studied onshore [60][61][78] and offshore [79] wind applications. Afanasyeva et al. [60] pursued technical, economic and uncertainty modelling of a Finnish ONWF with OATSA of a deterministic and stochastic model of AEP and NPV. The SARs were presented in a so-called tornado diagram (TD), commonly used for presenting OATSA results (OATSARs). A TD (Figure 4.6) shows the importance of inputs for

SAOV according to the percent change in SAOV compared to the defined baseline scenario. Afanasyeva et al. [60] report that high impact on NPV has electricity price and O&M cost, while average WS, PC and IR have a common effect. The effect of air density and wake effect was reported insignificant. [61] included OATSA of NPV with SAIVs of AEP, spot energy price, electricity generation tax, general company expenses, WT O&M costs, electrical infrastructure O&M cost, inflation rate, ONWF depreciation, profit tax rate, risk-free rate, debt risk premium, country risk premium, levered beta, and market premium. NPV was found most sensitive to the SP [minimum spot price], the inflation rate, the AEP and the depreciation rate [61]. Hadi et al. [78] performed a preliminary FS for Al-Shehabi, Iraq, which included OATSA of NPV, IRR, and PP with the use of RETScreen [68]. The most influential factors on NPV, IRR and PP were found to be initial investment, electricity export rate, and DR [78]. Ali et al. [79] conducted a TEA of WE potential at three locations in South Korea using long-term WSTS with different HH's.

OATSA of the NPV of onshore applications in Serbia [75] was performed with Oracle Crystall Ball [80], in Myanmar [73] with RETScreen [68], and in Indonesia [81] with @RISK [82]. No ranking of IVs was established with RETScreen [68]. Instead, the change in NPV triggered by the difference in the inputs was reported [73]. Loncar et al. [75] varied CF, risk-adjusted DR, regular price escalation, corporate income tax, specific investment costs, the inflation rate in Euro-zone, specific O&M costs, operational expenditure (OPEX), capital expenditure (CAPEX), and DR and found CF most influential on NPV. Ismail et al. [81] conducted an economic feasibility study (FS) of an ONWF in the coastal South Purworejo. The SAIVs were equity portion, capital investment cost, and O&M cost. The capital investment cost and O&M cost were found influential on NPV [75].

OATSA of the NPV of onshore wind applications in Thailand was found in [76][83][84] and Brazil in [85]-[87]. SAIVs in [76] were WS, DR, tax, salvage value, in [83] - AEP, cost of the turbine, sale of electricity, crude oil price, and inflation rate, in [84] - AEP, project costs, and average tariff,. WS caused the most variance of NPV in [76], AEP - in [83] (similar finding in [88]), and no ranking was established in [84]. WRA and comparative economic assessment using AMOS data of a 30 MW WF in Korea included OATSA of NPV and IRR [84]. The inputs were AEP, renewable energy certificate price, CAPEX, OPEX, and system marginal price. NPV was found most sensitive to AEP and least vulnerable to OPEX [84]. Onshore WP economic feasibility under uncertainty in Brazil was studied in [85]. The SAOV was NPV of an ONWF. The methods of SA used were OATSA, and a novel by using an artificial neural network (ANN). The SAIVs were WS, investment, and energy tariff, while the other parameters were fixed at their baseline

values. The SARs were presented as a TD and in a bar plot. TD summarized the OATSARs and bar chart consisted of relative importance (RI) measures for ANN SARs. WS (56%), energy tariff (27%) and the investment amount (16%) were found most relevant factors based on the ANN SARs [85]. WP FS under uncertainty in Brazilian electricity market was conducted in [86]. NPV of WP plant was calculated given a set of assumptions. MC was used for UA and OAT for – SA. IVs to UA/SA were average WS, energy price, investment, O&M, losses in transition lines, insurance, and CO2 ton average price in the European market, emission factor, and leasing, administrative expenses, transmission wheeling charges, annual economic benefit, and ONS/CCEE tax. The SARs were presented as linear plots of NPV (percentage of change to baseline). WS, energy prices, and investment costs were found most significant. Using ANN in SA of NPV of microgeneration of wind energy for small businesses in Brazil is continued by Lacerda et al. [87]. Three states were chosen for feasibility analysis - Rio Grande do Norte, Rio Grande do Sul, and Minas Gerais – with MC UA and ANN based SA. A multi-level perceptron (MLP) was trained with Statistica[89] as proposed by Chakrabarty et al. [90] for economic viability of biogas and green self-employment opportunities. A MLP produces synoptic weights are used for calculation of relative importance that is in turn used as a sensitivity measure on NPV of the project. Most impact on NPV had WS, investment, third party capital, tariff energy, and depreciation [87].

A few recently published studies follow the evident trend of using OAT as SA method of NPV of onshore wind applications [91][92]. The first one studied onshore wind farm siting prioritization based on investment profitability for Greece by Sakka et al. [91]. It included OATSA of NPV and IRR with respect to variance in detailed CAPEX and OPEX costs for a cases study of Lemnos. O&M costs were found most influential on both metrics. Also, Ammizud et al. [92] conducted SA and UA of economic feasibility of establishing a ONWF in Kerman, Iran. OATSA of NPV with respect to inflation and currency rates was considered.

OATSA NPV of OFFWFs was found in [64][74][93]-[97]. OATSA of NPV was part of [64]. NPV in [64] was found equally sensitive to icing and wind direction. A lifecycle techno-economic model of OFFWF for different entry and exit instances for a UK CS was created in [93]. The SAIVs were CAPEX parameters, OPEX parameters, revenue parameters, and financial expenditure parameters. OATSA revealed that financial and revenue parameters had a greater influence on the NPV of the investment in comparison to CAPEX and OPEX parameters [93]. The ranking of financial, OPEX and CAPEX parameters was established [93]. SA of NPV of a Spanish floating OFFWF (FOFFWF) was conducted in [74] using Oracle Crystall Ball [80]. The SAIVs included: wave parameters, W2 parameters, depth, distances, number of turbines, electric tariff, number of

diameters between WTs, the diameter of WT, the diameter of the tower of WT, the height of the tower of the WT, WT cost, cost of direct labour in the shipyard, direct index labour in the shipyard, annual amortization in a mean shipyard, number of offshore wind floating platforms constructed by a shipyard in a year, percentage of financing, DR and cost of steel. W2 scale and the electric tariff was found most influential [74]. Shigina recently considered a design and a TEA of an OFFWF to be located in Murmansk region of Russia. Shigina [96] recently considered a design and TEA of an OFFWF to be located in Murmansk Region of Russia, as "*adjacent Barents and White Seas are considered promising for wind energy utilization*" [96]. Her analysis included OATSA of NPV and IRR based on varying CAPEX and O&M costs. Ioannou et al. [97] published a preliminary techno-economic comparison of grid-connected and non grid-connected OFFWFs that included a OATSA of NPV presented in a spider diagram.

Although MC UA results can be easily translated into GSA results [13], OATSA of the NPV of an ONWF [76][86] and OFFWFs [94][95] was preferred to GSA. Pookpunt et al. [76] presented their comprehensive TEA for optimally placed WFs ambitiously calling it "*an ideal decision-making tool considering technical efficiency and profitability*" [76] that included both MC UA and OATSA of NPV. Haughton et al. [94] conducted an economic assessment of an OFFWF in Nantucket Sound, US, through MC UA and OATSA of NPV. The SAIVs were equipment and construction costs, WS, energy prices, the value of CO2 reduction, the value of SOx decline, the share of NG in electricity generation, O&M cost, the value of NOx reduction, the value of energy independence, and price of green credits. Equipment and construction costs and WS were reported to have the most impact on NPV. The SARs were presented in a sensitivity chart, widely known as TD. Ioannou et al. [95] looked into the stochastic financial appraisal of OFFWFs. They presented a probabilistic appraisal framework of OFFWF, used an ANN to model O&M costs and an ARIMA model to predict future electricity prices, and applied the MC approach to assessing system uncertainties. Although MC was used for UA, it was not used for SA. Instead, OATSA of NPV was implemented by increasing and decreasing twenty parameters by 20% from their baseline (expected values). The SARs were presented as a TD. The cost of the turbine component, the mean time to failure (MTTF), the foundation costs (FC's), the working hours and the weather adjustment factor were found to be most influential on the NPV [95]. The authors have a significant publication record on the topic of costs of an OFFWF, often use the MC approach [93][95][98][99], and consistently use SA in their analyses, but unfortunately always OATSA that do not provide reliable figures. An overview of different cost models for an OFFWF was found in [100].

2.5.3.2 Internal rate of return

IRR is calculated by solving Eq. (12) for *r*, entailing nonlinear relationships between all SAIVs and IRR, hence GSA should be used. Nevertheless, a single study [52] of the fourteen studies (8%) with IRR as SAOV used GSA instead of OATSA (92%). This statement serves as evidence of the prevalence of OATSA over GSA of IRR in WRA.

$$NPV = \sum_{i=0}^{N} \frac{B - C}{(1 + r)^i} = 0 \qquad => \qquad r = IRR \tag{13}$$

Richter et al. [52] conducted GSA of IRR alongside QMC UQ of three existing OFFWFs. The SAIVs included WS, wake effect, PC, SR, plant performance, capital cost, O&M cost, DR, and energy price. Wind contributes more than 80% of the uncertainty in IRR [52]. The other vital sensitivities include the PC, the O&M and capital costs. The wake effect has a negligible impact on IRR [52].

OATSA of IRR is commonly used [61][73][78][81][88] [91][96][101]-[106] (See Section 2.5.3.2 for detailed accounts of [73][78][81][88][91][96][101]). Several FS's applied OATSA of IRR. Rafique et al. [102] conducted the thermo-economic feasibility of a Saudi ONWF for different climatic conditions (five locations) with RETScreen [68]. SA and risk analysis (RA) were included. The SARs were presented as a plot of IRR depending on the debt ratio. SA showed that zero-interest governmental loans were found to play an important role in the development of wind energy in Saudi Arabia [102]. Then results of RA were presented in the form of a plot resembling a TD. RA showed that the initial cost and O&M costs have the most impact on feasibility [102].

OATSA of IRR was also found in repowering studies [61][103] and GIS studies [104]. Villena-Ruiz et al.[61] found IRR to be most sensitive to the spot price. Colmenar-Santos et al. [103] looked into an actual possibility for WE in Spain in a new scenario without a feed-in tariff (FIT), i.e. repowering. IVs to SA of IRR were spot price, WT generator price, financial leverage, and profit taxes. The SARs were presented as plots of IRR vs. each input.

In GIS-related studies, SA seems to have a slightly different meaning from the mainstream. Grassi et al. [104] published GIS research with large-scale TEA of onshore WE potential for a CS in Iowa. The CS included a SA of the impact of the power purchase agreement on the land profitability [104]. All factors significantly affecting the cash flow of a wind project were accounted for (initial investment and O&M phase). Economic assumptions were made, but the core of the study referred to as SA were the five values of PPA, for which corresponding graphs

of exploitable land area depending on IRR of wind project were plotted. From the mathematical modelling standpoint, such analysis, although useful and necessary in WRA, is not SA as SA aims to identify the IVs that make the most influence on the OV.

Again, a combination of MC UA and OATSA, this time of IRR, was found in [105], where financial additionality and viability of clean design mechanism projects under uncertainty was studied. Carmichael et al. [105] varied cash flows from their most likely values with and without carbon emission reduction. UNFCCC guidelines on the assessment of investing analysis were used, suggesting that SA covers "*a range of +10% and 10%*" [12]. Clearly, SA is unfortunately understood here solely as OATSA.

Zhang et al. [107] recently published a technical and institutional economics analysis of whether dispersed WP could take off in China. The study included SA of IRR and LCOE of dispersed WP under current institutional arrangement. Although the SA was used to "*ensure credibility of the results*" [107], OAT approach was used. SA inputs were initial investment, annual operational hours and financial arrangement, i.e. loan capital ratio and loan interest. Zhang et al. [107] report that SARs suggest that although all inputs have an effect on DWP, no matter the inputs there is considerate profitability in DWP. Based on this OATSA, policy implications were proposed [107].

Finally, Estanqueiro et al. [106] assessed maximum wind power penetration in weak grids using dynamic wind farm models. The inputs were the WS, lifetime, fuel, WT and O&M costs. The OATSAR was presented in a spider diagram with no established ranking.

A feasibility study by Sakka et al. [91] included an OATSA of IRR, for a detailed review refer to the previous Section.

2.5.3.3 Payback period

The payback period (PP) is the time necessary for capital investment to pay off. Roughly, a WT PP would amount to (39), where FIT is the wind electricity sell price. Eq. 14 is not a LM. Hence OATSA is not applicable, but the six studies reviewed in this section used OAT. Hence, the absolute predominance of OATSA of PP is detected. OATSA of PP is also commonly used for hybrid systems with a wind component [108]–[112] that are outside the scope of this review. If the discounting of money in time is to be considered, it only adds to the nonlinearity of Eq. (14).

$$PP = \frac{CAPEX}{\mathrm{AEP} * \mathrm{FIT} - \mathrm{OPEX}}, \tag{14}$$

An early influential OAT study by Kaldellis et al. [113] on WT PP sensitivity equated the terms SA and OATSA: *"[…] it is important to define the central point of the proposed SA*". For example, Kongnam et al. [71] and a recent study of Tautz-Weinert et al. [64] are citing [113] and continue to apply OAT to SA of economic nonLMs. Kaldellis has an extensive publication record on SA of wind hybrid applications [110][111][112]. The SAIVs considered in [113] were capital cost, return on investment index, local inflation rate index, electricity price escalation rate, installation CF, M&O cost, turn-on key cost of the power plant, and rated power. Kaldellis et al. [113] found PP to be most sensitive to the capital cost, CF, and electricity escalation rate. A recent RETScreen [68] FS of a Saudi WF [102] (Section 2.3.2) included SA of PP with SAIVs such as electricity exported to the grid, electricity export rate, initial costs, O&M costs, debt ratio, and debt term. Waewsak et al. [84] (Section 2.3.1) conducted OATSA of PP with inputs such as project costs, AEP, and average tariff, but no ranking has been established as a result. Villena-Ruiz et al. [61] also conducted OATSA of PP in their repowering of a Spanish WF study (Section 2.5.3.1) with SAIVs such as spot price, WT generator price, financial leverage, and profit taxes. Villena-Ruiz et al. [61] found PP was most sensitive to SP, AEP, depreciation rate and O&M costs. Hadi et al. [78] performed OATSA of PP with RETScreen [68] for a single location in Iraq, initial cost was determined as most influential. Sgobba [114] recently defended her PhD thesis on on-site energy generation for a decarbonized Irish manufacturing industry, it included OATSA of wind application PP to DR, carbon tax, electricity and gas prices. Sensitivity of each input was considered individually and SA results were presented and plots of PP depending on DR, etc.

A common way to present OATSARs is in a TD. TD for PP of WFs can be found in SARs in [61][102].

2.5.3.4 Levelised cost of energy

LCOE is a popular SAOV in WRA, as this section is most populated. The interest in LCOE can be attributed to LCOE as a means to reason about grid parity [115] and the breakeven price of wind electricity [116]. Five [52][117]-[120] of the thirty nine studies (13%) reviewed used GSA, and 87% - OATSA, serving as evidence of the prevalence of OATSA of LCOE in WRA. Moving towards the use of the global MC approach to UA and SA of LCOE has been identified in [121]-[123]. Heck et al. [121] argued to use MC approach to integrate uncertainty into LCOE, instead of point estimates when assessing LCOE, especially that the technique is relatively simple. Lerch et al. [122] identified MC UA as a direction for future work. Aldersey-Williams et al. [123] brought forward a theoretical justification and critical assessment of LCOE and urged to use of the MC approach to model LCOE.

LCOE is a frequent SAOV in offshore WRA [52][74][95][116][117][120][122][124]-[132]. Borras Mora et al. [123] claim that "*a financial metric typically used in the energy sector to evaluate the financial performance of a project is the LCOE*" [133]. Recently Borras Mora et al. [120] applied GSA to offshore cost modelling. The study [120] included a GSA of LCOE based on the model, offshore cost modelling tool, developed and explained in detail in [123]. Also in [123] it was found that reducing the uncertainty in estimated mean WS does not necesserily improve the LCOE, and floating LIDAR technology is the optimal measurement campaign tool for offshore. Borras Mora et al. [120] point out that LCOE is a theoretical metric and as a result has a number of weaknesses, but it is commonly used in offshore wind. In [120] the variance (the Sobol) and density based (PAWN) GSA methods were compared with the results of SA of offshore LCOE. The total order ranking provided by the two methods coincided, the differences was in in secord order effects [120]. The key factors to drive the LCOE were found to be the WS (significantly higher than all others), target equity rate of return, WT costs, drilling costs, and debt service coverage ratio [120].

SA of LCOE of the forefront wind technology – FOFFWFs - was recently conducted [74][95][122][124][125][126], all used OATSA. [74][124] [125] used the same baseline of 100 5-MW WTs. Shafiee et al. [125] state this fact enabled them to compare their results to previous studies and validate the model. The same applies to the comparison of OATSARs of [74][124][125] that all use Eq. 15 to calculate LCOE. In Eq. (15) ($CAPEX_i$ denotes investment in year i, $OPEX_i$ – maintenance in year i, AEP_i – energy generated in year i, and r denotes the DR. Here, the same observation as for the model of NPV can be made - the model is nonlinear. More ways to calculate LCOE can be found in [123] and [134]. SAIVs in [74][124][125] are given in Table 2.2.

$$LCOE = \frac{\sum_{i=1}^{N}(CAPEX_i + OPEX_i)/(1+r)^{\mathrm{i}}}{\sum_{i=1}^{N} AEP_i/(1+r)^{\mathrm{i}}} \tag{15}$$

LCOE was found most sensitive to DR, distance from shore, farm size and depth in [124], W2 scale - in [74], and installed capacity of a WF, the distance from the beach, and the fault detection capability of a condition monitoring system – in [125].

Table 2.2 Sensitivity analysis input variables in [74][124][125]

	Castro-Santos et al. [74]	**Myhr et al. [124]**	**Shafiee et al. [125]**
SAIVs	wave height, wave period, W2 parameters, depth, farm-to-shore distance, distance from farm to the platform construction place, distance from farm to the component storage place, number of turbines, electric tariff, number of diameters between WTs, the diameter of WT, the diameter of the tower of WT, the height of the tower of	farm size, distance to shore, water depth, project life span, eport cable, steel	the capacity of OFFWF, site location, IR and the quality of fault detection

	the WT, WT cost, cost of direct labour in the shipyard, index direct labour in the shipyard, annual amortization in a mean shipyard, number of offshore wind floating platforms constructed by a shipyard in a year, percentage of financing, DR and cost of steel	price, vessel rate, turbine, load factor, DR, contingency, and cost reduction	

Lerch et al. [122] proposed a methodology for calculating LCOE for a specific FOFFWF and performed an extensive yet local SA with hundreds of SAIVs. Turbine, substructure and mooring system manufacturing cost, power cable cost was found to be the most influential variable besides the common DR and energy losses. Ioannou et al. [132] developed a parametric model for LCOE (Eq. 16), CAPEX (Eq. 19), and OPEX (Eq. 20) based on WT rating, distance from shore, water depth, and WF capacity, the study included a OATSA of these outputs presented as plots of each output depending on each input. Ioannou et al. [95] performed a stochastic financial appraisal of OFFWF based on the deterministic lifecycle techno-economic model. They reported based on OATSA that the cost of the turbine, MTTF (hence, O&M cost), and FC to be most influential on the NPV and LCOE.They provide a thorough overview of costs related to OFFWF and assumptions for modelling them. Spyroudi [126] reported on the cost modelling analysis of floating wind technologies and assessed the potential of TLPWIND [135]. TLPWIND [135] is a 5MW Tension Leg Platforms floating technology for OFFWTs explicitly tailored for UK waters (Aberdeen coast). Spyroudi [126] conducted an OATSA of LCOE for TLPWIND [135]. SAIVs were exchange rate, turbine, fabrication, other OPEX, mooring and auxiliaries, O&M, export cable, installation, development, array cables, offshore substation, steel price, onshore substation, construction facilities, decommissioning, and landfall. LCOE was found in [126] to be most sensitive to the exchange rate and CAPEX.

$$LCOE = 110.37P_{WT}^{-2.226} + 0.167WD + 0.004D^2 + 2.889\,10^9\,P_{WF}^{-3.339} + 95.045, \quad (16)$$

Where P_{WT} is WT rating, *WD* is water depth, *D* is distance from shore and P_{WF} is WF capacity.

SA of LCOE in conventional OFFWFs was found in [52][99][116][127][129][131]. A GSA (Sobol method) of LCOE of an OFFWF was found as part of the UQ in OFFWF [52] (Section 2.5.2.3). Levitt et al. [116] studied offshore WP pricing and conducted OATSA of breakeven price or LCOE when the NPV of costs is equal to the NPV of benefits:

$$\sum_{i=0}^{N} \frac{C_i}{(1+r)^i} = \sum_{i=0}^{N} \frac{AEP_i P_i + B_i}{(1+r)^i}, \quad (17)$$

where C_i is the total cash expenditure including debt service payments, is the annual energy production, includes tax benefits and capacity payments, and is the resulting LCOE (payback price equivalent to the possible energy price that year). The SAIVs were CAPEX, OPEX, CF, and DR. The OATSARs were presented as a linear plot of breakeven price vs. percentage of change. LCOE was found most sensitive to CAPEX, the DR, and CF in [116]. Yeter et al. [127] conducted a risk-based lifecycle assessment of offshore WT support structures accounting for economic constraints that contained an OATSA of LCOE. The SAIVs were DR, annual production, WTG price, FIT, steel price, OPEX, tax, and overhead. A TD demonstrated that the highest contribution to LCOE variation originated in the DR. Finally, Cavazzi et al. [129] used an offshore WE geographic information system (OWE-GIS) for the assessment of the UK's offshore WE potential. The study included OATSA of LCOE (calculated as (43)) based on changing values in IR, WF lifetime, availability, CAPEX, average WS, bad weather factor (double installation times were used to represent adverse weather conditions). SARs were presented as TDs [129]. The ranking of factors was established with IR and lifetime having the most significant influence on LCOE [129]. Jadali et al. [99] recently published their TEA of decommissioning (full and partial) vs. repowering of a hypothetical OFFWF in UK waters with a OATSA of LCOE. Inputs to SA were AEP, DR, installation and commissioning costs, O&M costs, production and acquisition costs, partial and full decommissioning costs, and repowering costs. The study included MC UA but OATSA of LCOE, SA found AEP to be most influential on LCOE. Xu et al. [131] recently reported on the status of offshore wind energy in China that included a OATSA of LCOE with respect to expected annual hours of utilization and unit cost and policy recommendations.

$$LCOE = \frac{1}{AEP} CAPEX * \frac{r}{1-(1+r)^{-n}} + OPEX, \tag{18}$$

Ebenbach et al. [136] compared the economics of conventional bottom-fixed and floating substructures used in OFFWFs with OATSA of LCOE for both. Inputs to SA of LCOE with bottom-fixed structures involved were the following: gross load factor, water depth, distance to shore, turbine size, and wind farm capacity. O&M, concrete price and weighted average of cost capital, were added to the list of inputs to SA of LCOE for FOFFWF design. The gross load factor was found most influential on both designs, while the influence of water depth is, understandably, more prominent on the conventional design.

Findings in this review concerning SA of LCOE in OFFWFs are in accordance with those outlined in "*Developments in Renewable Energy Offshore*" [137]. According to [137], economic factors like DR and lifetime have extensively been studies through SA [93][122][125][138], but "*sensitivity of the results to the years in which each of the costs occur has not been considered*"

[137]. What is left to mention that although [93][122][125][138] made a significant input to the state-of-the-art of OFFWFs, all of them used OATSA.

Two studies with SA of both onshore and offshore borne LCOE are available in the literature [117][128]. Tran et al. [117] conducted a broad comparison study on LCOE of different energy sources (including onshore and offshore wind) that used the Sobol method [117]. Tran et al. [117] incorporated performance-based GSA and UA into LCOE calculations for emerging renewable energy technologies. SA for everyone (SAFE) toolbox [7] was used to conduct MC based GSA of LCOE for wave, tidal, pressure retarded osmosis, geothermal, biomass, hydropower, onshore wind, offshore wind, solar thermal, solar photovoltaic, nuclear, NG, and coal. The SAIVs were overnight capital cost, O&M cost, variable O&M cost, CF, lifetime, and lifecycle emissions. The GSARs were presented in a table with the mean, median and variance columns. Hence importance ranking was not established, despite having used GSA. The UA results labelled as GSA results signalled that UA and SA were used interchangeably. Schmidt et al. [128] assessed the costs of photovoltaic and WP (onshore and offshore) in six developing countries (Brazil, Egypt, Kenya, Nicaragua, India, Thailand). They conducted OATSA of LCOE and the incremental cost of wind electricity based on the changes in the target share of renewable energy technology (RET) in the electricity mix. Schmidt et al. [128] called the analysis SA, but only two values of a single input were calculated, and no further discussion of claimed SARs ensued. Such operation of the concept of SA in reputable journals such as Nature Climate Change points to the lack of standards concerning SA in the field of WRA. [1]

LCOE is often used in assessing onshore wind applications. Khalid et al. [62] conducted OATSA of generation cost for a 40 MW hypothetical Pakistani WF with RETScreen [23]. The SARs in [62] showed that the electricity production cost strongly depended on the initial project cost, electricity export price and electricity price escalation rate [62]. Tu et al. [115] studied the effects of DR, learning rate, curtailment rate, O&M cost, and CF for Chinese onshore wind electricity to reach grid parity in 2020. To this end, the OATSA of LCOE was conducted. Tu et al. [115] reported that high DR and O&M costs delay the moment of grid parity [115], with no ranking established. Ohunakin et al. [139] economically assessed WE conversion systems using LCOE and present value cost methods in Nigeria. OATSA of LCOE based on +/-10-80% changes in CF, civil cost, WT cost, project life, O&M cost, and IR was part of the analysis. The SARs were

[1] This problem is not unique to WRA.

presented as a spider diagram. The SA revealed that the CF and the WT lifetime have a positive impact on LCOE, while the rest of SAIVs – a negative [139]. Gass et al. [140] assessed the economic WP potential in Austria. The changes in DR, lifetime, investment and O&M costs were considered [140]. The OATSA of LCOE [140] showed the existing FIT necessary to reach the set policy targets [140]. Also, DR had a significant impact on the resulting installed capacity [140]. Dong et al. [118] showed that QMC is superior to MC in WRA setting and found air density to be as important as Weibull scale parameter for a 1.5 MW WT operating in Zhangzhou onshore wind farm, both findings are similar to those of Tsvetkova et al. [13]. Recently, Dong et al. [119] published GSA results of a 1.5MW WT in commissioning Qingjing onshore wind farm in Eastern China, where Weibull scale parameter was found most influential. Both SA studies [118][119] used air density, Weibull shape and scale parameters as inputs, LCOE as output, and Sobol SI as SA method. Sgobba [141] published on sensitivity of on-site renewable electricity production and self consumption for manufacturing industry in Ireland to techno-economic conditions, the article included a OATSA of wind LCOE to normalized CAPEX and DR.SA of LCOE based on changes in HH was part of [140] (Section 2.2.3). Since the input was only one, it automatically classifies this instance of SA as OAT. Adaramola et al. [142] assessed WP generation along the coast of Ghana with OATSA of LCOE for the location of Oshiyie. SAIVs were project lifetime, DR, CF, cost WT, and civil cost contribution. Adaramola et al. [142] classified SAIVs into two groups: CF and the useful lifetime of the WT had a positive effect on LCOE, while the rest – harmful. Herran et al. [143] performed a global assessment of coastal WP resources, considering the distance to urban areas. OATSA of LCOE was part of the study. Aggregated distance to an urban area, transmission losses, transmission cost, visibility, land use factors (land suitability factor, the density of capacity), technical factors (array efficiency, availability), and economic factors (capital cost, DR, lifetime) were considered for the SA. The SARs were presented in a TD. SAR suggests that the distance to urban areas is insignificant for the global availability of onshore wind resources [143]. Sunderland et al. [144] compared urban WTs and solar PV systems in Ireland with OATSA of LCOE produced by HOMER [145]. The IVs to SA referred to as “design of experiment analysis” [144], were the following: capital, resource and IR, but no ranking of inputs was established. The SARs revealed dependency rather than ranking, i.e. the WT productivity was concluded to be dependent on wind speed [144]. Ali et al. [79] (Section 2.3.1) conducted OATSA of LCOE for three locations in South Korea.

Tizgui et al. [100] estimated wind LCOE in Morocco. The SAIV were IR, O&M costs, AEP, lifetime, which all were found to have a significant influence on LCOE, except for O&M costs according to plots of LCOE depending on each input. Allouhi et al. [101] conducted an energetic,

exergetic, economic and environmental (4E) assessment of onshore WP generation in Morocco with OATSA of LCOE. The SAIVs were air temperature, DR, and CF. Allouhi et al. [101] found LCOE to be most sensitive to the CF, and DR. Galvez et al. [102] researched how the change in DR, O&M costs and investment costs affect LCOE (SA) for a CS in Mexico. The SA [102] revealed the need to implement financial mechanisms like a FIT to decrease the electricity production cost in low-potential areas. Barutha et al. [130] evaluated the commercial feasibility of a new tall wind tower design concept using a stochastic LCOE model.

Carriveau et al. [146], Rubert et al. [147][148], and Jadali et al. [99] recently contributed to the important and necessary debate on extending options for ONWFs, all reasoned based on unreliable OATSA of LCOE. Carriveau et al. [146] looked at the situation in Canada as "*the wind fleet in North America is aging, with farms approaching and surpassing the halfway points of their power purchase agreements*" [146], while Rubert et al. [147][148] and Jadali et al. [99] – in the UK.

2.5.3.5 Capital expense (CAPEX)

Mytilinou et al. [149] recently conducted a techno-economic optimisation of OFFWFs based on life cycle cost analysis in the UK, where GSA of CAPEX and OPEX with respect to layout, number of WTs, WT size and site name was part of the study. GSA included calculation of total, first and second order Sobol indices. Second order Sobol indices correspond to pairwise sensitivity, or more precisely determine the amount of output variance that is explained by the respective pairwise interaction. It also included OATSA of CAPEX and OPEX for the optimal layout solution determined. SA was carried out with SALib [150]. The SA completed depicted "*the highly complex nature of the decision variables and their interdependencies, where the combinations of site-layout and site-turbine size captured above 20% of the variability in CAPEX and OPEX*" [149].

Martinez-Luengo [151] developed guidelines and showed a CBA of the structural health monitoring implementation in offshore wind with a CS on the UK. The study included a OATSA of CAPEX and OPEX. OPEX reduction due to structural health monitoring implementation was observed.

Two studies by a prominent group of researchers in offshore wind, Ioannou et al. [132], [152], applied OATSA to CAPEX. In [132] they developed a parametric model for CAPEX (44) based on WT rating, distance from shore, water depth, and WF capacity, a OATSA of CAPEX was presented as plots depending on each input. In [152] they presented a preliminary parametric

techno-economic study of offshore wind floater concepts. Eq. (19) shows the underlying nonlinear relationships. Borras Mora [120] too argued in favor of GSA for cost models in offshore wind due to the complex nature of the relationships between the inputs and outputs of such models.

$$CAPEX = -1.48510^{11}P_{WT}^{0.001} + 2.35310^{6}WD + 2.5310^{6}D + 2.45110^{6}P_{WF} + 1.48710^{6} \quad (19)$$

Where P_{WT} is WT rating, *WD* is water depth, *D* is distance from shore and P_{WF} is WF capacity

2.5.3.6 Operational expense (OPEX)

Martin et al. [153] thoroughly considered the project three stages of OFFWFs in terms of O&M costs, as they account for 14–40% of project life expenditure. Qualitative screening SA (the Morris method [1]) was applied, and the results showed that "*access and repair costs along with failure rates for both minor and major repairs*" are the factors contributing the most to total O&M costs [153]. The use of the Morris method is rightfully justified as the OFFWF O&M model used in [153] had over a hundred inputs, and the model execution time was measured in minutes. SA framework, recently announced to no longer be available for downloading, SimLab [154] was used for the described SA experiment. Sensobol R package [11] can be now used instead.

Aforementioned Ioannou et al. [132] developed a parametric model for OPEX (Eq. (20)), a OATSA of CAPEX was accompanying. Eq. 20 shows the underlying nonlinear relationships.

$$OPEX = -6.34910^{8}P_{WT}^{0.187} + 2.59510^{-19}e^{0.83D} + 8{,}41410^{5}P_{WF} + 9.50610^{8} \quad (20)$$

Where P_{WT} is WT rating, *WD* is water depth, *D* is distance from shore and P_{WF} is WF capacity.

Some articled reviewed in previous section included SA of OPEX in them. For a detailed review of Mytilinou et al. [149] and Martinez-Luengo [151], refer to the previous Section, and of Dykes [53] – to Section 4.5.2.2.

2.6 Sensitivity analysis methods

This section briefly explains the SA methods that were encountered during the review to be used in WRA. Section 2.6 classifies the review pool articles based on the class of SA method used: 2.6.1 Local sensitivity analysis including subsection.

Local SA (LSA) uses derivative-based measures of sensitivity that characterize an individual effect of each input at a specific point in space (base point), hence the name local. Such

measures are only valid locally, in close vicinity to the base point. The exception is the linear model when the first partial derivative is constant.

One-at-a-time sensitivity analysis oi not a method of SA per se, rather it is an example of convenience sampling from the design of experiment (DOE) point of view. Nevertheless, the review reveals that OATSA is especially popular in WRA.

The choice of the proper SA method depends on the following considerations:

- The computational cost (number of model runs) of calculating the model for a given point in space (a combination of inputs)
- The number of inputs
- Linearity/nonlinearity of the model
- The consideration of interactions among the inputs in the model (typical for nonLMs)

2.6.1 Local sensitivity analysis

Local SA (LSA) uses derivative-based measures of sensitivity $\partial Y/\partial X_i$ that characterize an individual effect of each input at a specific point in space (base point), hence the name *local*. Such measures are only valid locally, in close vicinity to the base point. The exception is the linear model when the first partial derivative is constant.

2.6.1.1 One-at-a-time sensitivity analysis

Misinterpretation of SA as the practice of changing one parameter at a time, and tracking the effect such change has on the OV is frequent. In such studies, a baseline case is chosen. Then an increase or decrease of a certain amount usually measured in percent is applied to one parameter, and the result it has on the variable of interest is analyzed. Hence the name - one-at-a-time (OAT) or one-factor-at-a-time. OATSA was called "*one-factor*" in [59] and "*what-if*" analysis in [64]. OATSARs are often presented in TDs (Figure 5). OAT is one of the most common and most straightforward approaches to SA. Despite its simplicity, it does not explore input space adequately - the higher the number of inputs, the weaker the exploration of space [13]. OATSA is invalid for nonlinear models [21]. Moreover, OAT does not account for interactions among the inputs [4]. OATSA approximates LSA. Therefore, the validity of OATSARs holds only for linear models. OATSA is commonly used for SA in WRA [13]. OAT was applied for SA of GOFMs, WP, WE, NPV, IRR, PP, LCOE. CAPEX and OPEX in WRA (Table 2.3).

Table 2.3 One-at-a-time sensitivity analysis review pool articles organized by sensitivity analysis output variable

SAOV	Reference
GOFMs	[26][27]
WP	[28][35]-[39]
WE	[43][49]-[56]

NPV	[43][51][60]-[109]
IRR	[43][52][63][71][78][90]-[95]
PP	[52][74][91][102]
LCOE	[43][64][85][105][109][11]-[116]

2.6.2 Global sensitivity analysis

The present section briefly covers some of the GSA methods that are applied in the field of WRA. Saltelli et al. [155][8] claim that GSA is the common notion that modern-era SA has focused on in the last twenty years. A recent overview of state-of-the-art of SA distinguished four major GSA approaches: (1) derivative-based, (2) distribution-based, (3) variogram-based, and (4) regression-based [8].

2.6.2.1 Scatterplot method

If inputs X_i are sampled and the model's response $Y(X_i)$ is recorded. Hence output Y is sampled too. Plotting $Y(X_i)$ provides information about the model's behaviour. The higher the correlation between $Y(X_i)$ the most influential it is on Y. Saltelli et al. [4] claim that little shape of the cloud of points over the range of the input factor (like X1 or X5 in Figure 4.7) is a definite sign that the input is less influential. Saltelli et al. [4] point out that the scatterplot method is a straightforward and informative way to conduct SA and that "*most SA measures derived by practitioners aim to preserve the rich information provided by the scatterplots in a condensed format*" [4]. Function plot_scatter of sensobol R package [11] is one implementation of the method. Saltelli et al. recommend taking a sample of size N = 1000. Scatterplots were found in SA in WRA in [53].

2.6.2.2 The Morris method

The Morris method [1] for screening, or eliminating non-influential factors, also known as the elementary effects method, is usually used for reducing models dimensionality so that computation of variance-based methods would become feasible. In 1991 Morris [1] introduced a screening method that is in essence a OAT sampling design dividing the k-dimensional input hypercube space (for a model $Y = f(X) = f(X_1, X_2, \dots, X_k)$ of k variables) into p level grid. Sampling along l (typically l ~ 4-10) trajectories consisting of k+1 points produces two sensitivity measures mean μ (Eq. (22)) assessing the overall importance of the input and σ (Eq. (23)) – the interactions and nonlinear effects. Campolongo et al. [2] offered an improved measure μ^* (Eq. (24)). The elementary effect $d_i(X)$ for each input is defined in Eq. (21), where Δ={0, 1/(p-1), 2/(p-1), … 1}. The method is implemented as *morris* function in sensitivity R package [156]. The Morris method was used for SA of OPEX in a single study by Martin et al. [153].

$$d_i(X) = \frac{f(X_1, \dots, X_i + \Delta, \dots, X_k) - f(X)}{\Delta} \tag{21}$$

$$\mu_i = \frac{1}{l}\sum_{j=1}^{l} d_i\left(X^{(j)}\right) \tag{22}$$

$$\sigma_i = \sqrt{\frac{1}{l-1}\sum_{j=1}^{l}(d_i(X^{(j)}) - \mu_i)^2} \tag{23}$$

$$\mu_i^* = \frac{1}{l}\sum_{j=1}^{l} |d_i\left(X^{(j)}\right)| \tag{24}$$

2.6.2.3 The Sobol method

The Sobol method is a well established variance-based method of GSA, also referred to as "*the golden standard of SA*" [157]. It includes the calculation or estimation of first-order and total-effect sensitivity indices (SIs) as measures for establishing a ranking among the inputs. In 1990 Sobol [3] published the proof of the theorem about the decomposition of an integrable function into summands of different dimensions in a Russian journal and defined the Sobol SIs. The SIs are the measures of variance that brings about the ranking of variables. In the case of independent inputs, the first-order SIs are sufficient for establishing a ranking of inputs. If the dependency of some IVs is present, or the model is nonlinear, the calculation of total-effect indices is necessary as well. Total-effect SI's account for dependencies and higher-order effects (or interactions) among the inputs. Later the Sobol SIs made their way into the English speaking scientific community [158][159] and well established itself in a variety of disciplines [22][160][161] due to its universal applicability with the assumption of input independence.

The crux of the Sobol method lies in using analysis of variance (ANOVA) decomposition as a sensitivity measure. If the model $Y = f(X) = f(X_1, X_2, \dots, X_k)$ is a function of k variables, Eq. (25) defines the first-order SI's $S_i(Y)$ and Eq. (26) – the total-effect SI's $T_i(Y)$ for the function [159]. A multitude of estimators of these indices (four estimators of first order and five - of total order SI's) can be calculated by calling sobol_indices function in sensobol R package [11].

$$S_i(Y) = \frac{V_i}{V(Y)} = \frac{V_{X_i}(E_{X\sim i}(Y|X_i))}{V(Y)} \tag{25}$$

$$T_i(Y) = \frac{V_{T_i}}{V(Y)} = \frac{E_{X\sim i}(V_{X_i}(Y|X_i))}{V(Y)} = 1 - \frac{V_{X_{\sim i}}\left(E_{Xi}(Y|X_{\sim i})\right)}{V(Y)}, \quad (26)$$

Where *V(Y)* is the model variance, $V_{X_i}(E_{X\sim i}(Y|X_i))$ is the variance based on the first-order effect for the input variable X_i. $X_{\sim i}$ excludes the effect of the variable X_i.

There is a number of estimators of the total order effect indices defined in (30). In a recent "*battle of total-order sensitivity estimators*" [157] by Puy et al., the estimator by Razavi & Gupta [162] took over the rest and should be preferred in practice. An implementation of this estimation procedure by Razavi & Gupta [162] is available in sensobol R package [11]. Sobol's method was used in SA of WP [35][38][42], WE [13][52][53][67], NPV [52], IRR [52] and LCOE [52][117][120], OPEX [149].

2.6.2.4 Extended Fourier amplitude sensitivity test

Another way to calculate SI's is through variance decomposition based on multiple Fourier series. The Fourier amplitude sensitivity test (FAST) translates a multivariate SAOV into a single frequency variable with the use of the Fourier series. Therefore, the integrals required to calculate the SI's become univariate, resulting in significant computational savings. Cukier et al. [163] first suggested the use of FAST for GSA in his research on nonlinear SA, and Saltelli et al. [164] introduced an alternative way to compute FAST for GSA purposes, i.e. the extended FAST (eFAST). eFAST is implemented as *fast99* function in sensitivity R package [165][156]. The effects of WMs on WP with eFAST were studied in [36][37].

2.6.2.5 Shapley effects

Owen [166] introduced the concept of the Shapley value [167] from cooperative game theory into GSA. Shapley value [167] is a "*fair*" distribution of the total gains to the players of the game, assuming they all collaborate. Owen [166] found the Shapley value of individual variables when "*variance explained*" was taken as their combined value, and showed that Sobol first-order and total SIs as being easier to compute serve as the bound for the new sensitivity measure, which adds up to total variance in case of independent inputs. Soon after Song et al. [54] called this measure in case of dependent inputs Shapley effects and showed how Sobol first-order and total effect SIs, "*even when used together, may fail to appropriately measure how sensitive the output is to uncertainty in the inputs when there is probabilistic dependence or structural interaction among the inputs*" [54]. They also proposed an efficient MC algorithm for estimation of Shapley effects (function shapleyPermRand in sensitivity R package [156]). Another estimation

procedure for Shapley effects was recently proposed by Goda [168]. The use of Shapley effects in SA in WRA was found in a single review pool article – SA of WP by Carta et al. [39].

2.6.2.6 PAWN

A novel and efficient GSA method called PAWN was introduced by Pianosi et al. [6] in 2015. The essence of PAWN is an efficient computation of density-based SI's. The efficiency lies in characterization of output distributions by their Cumulative Distribution Functions (CDF) instead of PDFs, as CDFs are easier to derive than PDFs [6]. Pianosi et al. [6] demonstrate the advantages of PAWN through a series of applications to numerical and environmental models. PAWN was designed to be a complementary approach to variance-based GSA [6]. Later in 2018 a generic estimation procedure was proposed by the same group to make the application of PAWN easier for the practitioner [169]. The method can be easily accessed through SAFE toolbox [7]. Borras Mora [120] was the only study in the review pool to apply PAWN for SA of offshore LCOE.

2.7 Offshore vs. Onshore

This section classifies the reviewed article pool into offshore and onshore wind applications (Table 2.4). Not a single GSA of GOFM or PP was found in the literature. No SA of PP of offshore applications was detected.

According to the review, offshore wind development is of special significance to the UK and Spain. The costs of offshore wind has been dropping in the last years, making the more abundant offshore wind potential feasible for integrating into the grid. According to Borras Mora [120], "*simple cost models are no longer suitable*" [120] for assessing profitability of the next generation OFFWFs, "tailored techno-economic cost models are being developed" [120], those that capture the new relationships formed due to rapid technological advancement and policy incentives. GSA is necessary to study these models are complex and the relationships between inputs and outputs are poorly understood [120].

As a side note, novel methods of GSA are used in structural analysis and safety studies in offshore applications. Teixeira et al. [170] used transformed Kullback-Leibler divergence for GSA of short-term stress damage rate of an offshore WT. Velarde et al. [171] performed variance-based GSA of offshore wind foundation loads using MC. Such studies are outside the scope of this review but are worth mentioning due to the application of GSA to offshore wind. Zhou et al. [172] conducted GSA on the semisubmersible substructure of a WT of a FOFFWF.

Table 2.4 Review pool articles organized by objective and application

	GOFM	WP	WE	NPV	IRR	PP	LCOE	CAPEX	OPEX
Offshore	-	[37] [42] [43]	[52]	[52][72] [74][77] [94][95] [97]	[52]	-	[52][74] [95][99] [116]-[129] [131][132]	[132] [151] [153]	[132] [149] [151] [153]
Onshore	[33] [44]	[35][36] [38][39] [45]-[48]		[60][61] [70][71][73] [75]-[78] [80][81][83] -[86][87] [91][92] [96][122]	[61] [73][78] [81][88][88] [96][101]- [106] [107]	[61] [78] [84] [102] [113] [114]	[62][79] [107] [115][117]- [119] [128][129] [139]-[173]		[53]

2.8 Geography

Section 2.8 intends to uncover research gaps in the literature. Since there is plenty of wind data available online, when designing a WRA CS for scientific purposes, this section serves as a quick reference on understudied regions of the world. In the process of the review case studies with meteorological data from thirty-seven countries (Figure 2.1) with SA in one form or another were encountered, Table 2.5 classifies these findings based on the country and SA model. Global and selected country reports concerning installed wind capacity can be found in [174] with detailed information on existing WFs.

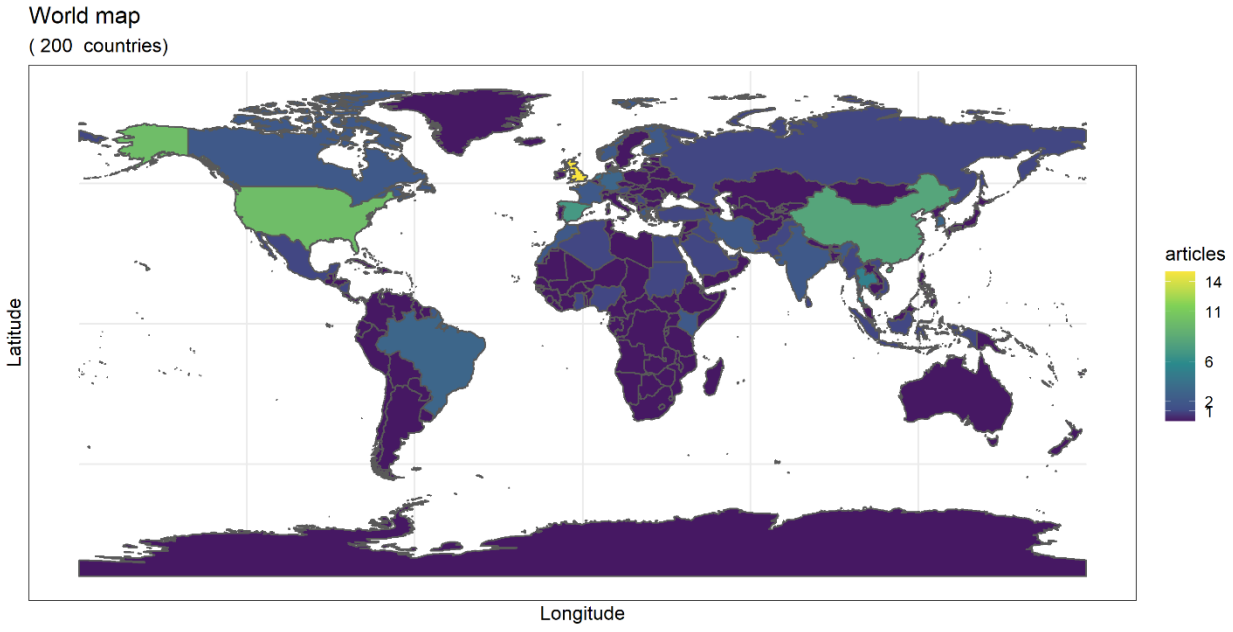

Figure 2.1 Geographical representation of the review pool

The main review findings from the geography standpoint are that (1) LCOE is the most popular SAOV, and (2) the UK and the US are the most studied countries in terms of the number of SA studies in the literature.

Table 2.5 Review pool articles organized by country and model

	GOFM	WP	WE	NPV	IRR	PP	LCOE	CAPEX	OPEX
Algeria		[48]							
Austria							[140]		
Brazil				[85]-[87]			[128]		
Canada		[36]					[146]		
China		[45]			[107]		[81][107] [118] [119] [131] [175][176]		
Egypt							[128]		
France			[67]				[122]		
Finland			[60]	[60][67]					
Germany	[34]			[52][77]	[52]				
Ghana							[142]		
Greece				[91]	[91]	[113]			
India							[128][177]		
Indonesia				[81]	[81]				
Iran	[33]			[92]					
Iraq				[78]	[78]	[78]			
Kenya				[70]			[128]		
Mexico							[173]		
Morocco							[178][179]		
Myanmar				[73]	[73]				
Netherlands			[52] [64]	[64][77][95]	[52]		[52][95]		
Nigeria							[139]		
Nicaragua							[128]		
Norway		[38]					[124]		
Pakistan			[62]				[62]		
Russia				[96]	[96]				
Saudi Arabia					[102]	[102]			
Serbia				[75]					
South Korea				[79][88][180]	[88]		[79]		
Spain		[39]	[61] [63] [64]	[61][64][74]	[61][74] [103] [106]	[61]	[74][63]		
Sri Lanka							[181]		
Sudan				[182]					
Turkey				[101]	[101]				
Thailand				[71][76][83][84]	[84]	[84]	[128]		
UAE			[13]						
UK		[35]	[64]	[64] [72]		[114]	[99] [120][122]	[132] [149]	[132] [149]

				[93][97] [183]			[123][129] [132] [141][144] [147][148]	[151]	[151] [153]
US		[53]	[53]	[53][65][94] [184]	[104]		[116][1117] [122][130]		[53]
Vietnam		[46]							

2.9 Software

Section 2.9 classifies the article pool based on the software used for SA and discusses the influence each tool has on the choice of the SA method. Douglas-Smith et al. [22] identified the software for UA and SA and provided an overview of the general research trends. Murphy et al. [185] published a review of software tools used in WRA[2]. The software used for SA in WRA is listed in Table 4.6. Often wind-related projects are analyzed with the use of professional modelling software targeted for modelling clean energy projects, for example, RETScreen [68][110]. RETScreen[3] is used for a feasibility assessment of clean energy projects [62][68][73][78][102], the only available option for SA of NPV in RETScreen is OAT. The nonlinear nature of models in WRA and economics is disregarded.

Pianosi et al. [7] created a Matlab toolbox called "*Sensitivity analysis for everyone*" (SAFE) aiming to popularize GSA[4]. Tsvetkova et al. [13] used R for GSA. Sensitivity package in R [156] provides easy-to-use access to screening and GSA methods. Noacco et al. [186] provided a handy set of workflow scripts (R/Matlab) and discussed the critical choices that potential GSA users would face [186].

Oracle Crystall Ball [80] User Guide [187] gives information both on TDs implying OATSA [188] and correlation coefficients implying GSA [189]. Commercial software [80][82][135] commonly use OATSA regardless of the model at hand. Open source toolboxes specializing in SA [7][165] are using GSA methods. For instance, a framework for unified systems engineering and design of wind plants (FUSED-Wind), an open-source framework intended or multi-disciplinary optimization and analysis of wind energy systems, that defines key interfaces, methods and inputs and outputs "*to achieve a system level analysis capability of wind turbine plants with multiple levels of fidelity*" [5], implements the Sobol method.

Table 2.6 Review pool articles organized by software and sensitivity analysis method

Software tool/SA method	**OAT**	**Morris**	**Sobol**	**Scatterplot**
Excelbased @RISK [82]	[81]			

[2] The list included RETScreen, RETScreen Plus, FOCUS, FAST, QBlade, Vortexje, WAsP, OpenWind, WindPRO, Windsim, and Metodyn [185].
[3] Developed by Natural Resources of Canada.
[4] Developed by Natural Resources of Canada.

Excelbased Oracle Crystal Ball [80]	[74][75][122]			
Matlab based GUI-HDMR [51]			[35]	
Matlab/R/python based SAFE [7]			[117]	
Matlab-based UQLab [7]			[40]	
Python based WISDEM [57]			[53]	[53]
Python based SALib [150]	[149]		[149]	
Python based FUSED-Wind [5]			[53]	
R [162]			[13]	
Standalone RETScreen [68]	[62][73][78][102]			
Standalone SimLab [154]		[155]		

Although the application of GSA is yet in its infancy, the availability of software tools and packages for GSA is surprisingly vast [11] for any taste and budget. Therefore, unavailability of tools is not the reason for slow uptaking of GSA. The authors used the sensobol R package [190] for the examples in Section 2.10 and found it very easy to use (R script can be found in Appendix I).

Table 2.7 Overview of software tools for global sensitivity analysis [5][8]

Software tool/Language of implementation	**R**	**Matlab/Octave**	**Python**	**C**	**C#**	**C++**	**julia**
SALib [150]			x				
SAFE [7]	x	x	x				
UQLab [191]		x					
sensobol [11]	x						
sensitivity [190]	x						
fast [192]	x						
multisensi [193]	x						
SobolGSA [194]		x	x		x		
Dakota [195]						x	
OpenTURNs [196]			x			x	
PSUADE [197]				x			
VARS-Tool [198]		x		x			
MADS.jl [199]							x
FUSED-wind [5]			x				

For scientists more familiar with SA looking to compare, for instance, different estimators of Sobol indices for a given model, can do so with the new *sensobol* package, that offers four estimators (classic Sobol [200] and Jansen [201] estimators, plus more recent [202]). According to the benchmark of Puy et al. *sensobol* [11] is twice as fast as *sensitivity* R package [190].

Table 2.8 Comparison of sensitivity analysis tools and methods implemented

Software tool/SA method	**Shapley effects [54]**	**Morris method [1]**	**Borgonovo indices [191]**	**Sobol indices [159]**	**Kucherencko indices [57]**	**FAST**	**PAWN [6]**
SA Lib [150]		x		x		x	
SAFE [7]		x		x			x
UQLab [191]		x	x	x	x		
sensobol [11]				x			
sensitivity [165]	x	x		x		x	
fast [192]						x	
Multisensi [193]				x		x	

2.10 Specifics of application

To illustrate the misleading or erroneous inference that OATSA can entail for some models, consider three examples in this section. *Sensobol* R package [11] with a sample size of a 1000 was used for the three examples, the R script is provided in Appendix I.

2.10.1 Example I: Linear model with uniform distributions

Consider a simple example: a linear model described by Eq. (27) with all inputs uniformly distributed in [0,1].

$$L = X_1 + X_2 + X_3 + X_4 + X_5, \tag{27}$$

For such a simple model obviously OATSA and complex GSA methods would produce identical results (Figure 2.2 - Figure 2.5). It's worth mentioning that Sobol indices provide more information about the model at hand. For a linear model, no interactions of factors are present, similar values of first order and total effect indices in Figure 4.6 confirm this.

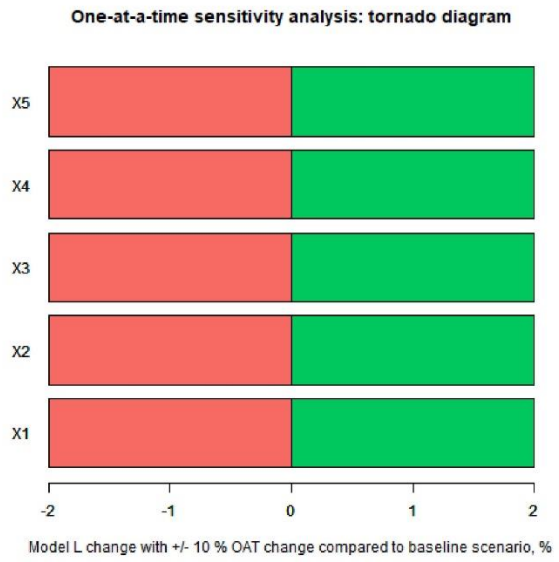

Figure 2.2 One-at-a-time sensitivity analysis results for model L and uniformly distributed inputs

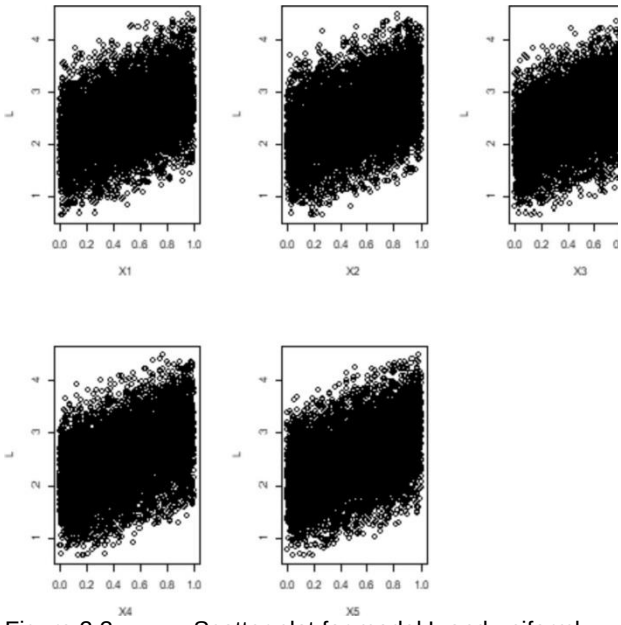

Figure 2.3 Scatter plot for model L and uniformly distributed inputs

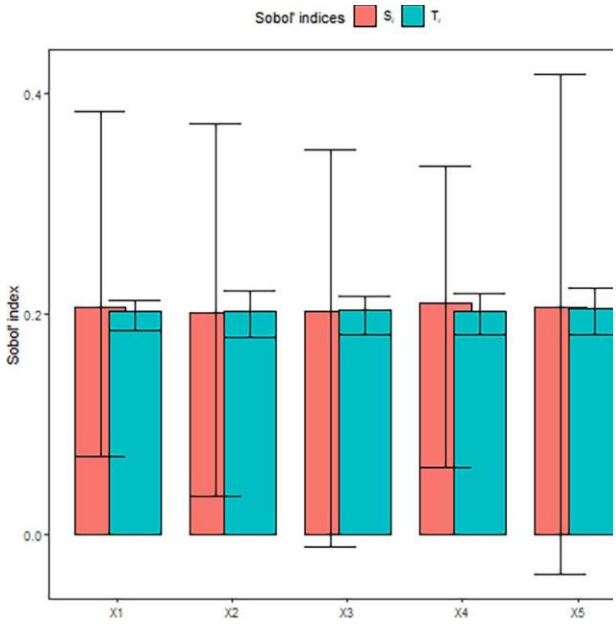

Figure 2.4 Sobol indices for model L and uniformly distributed inputs

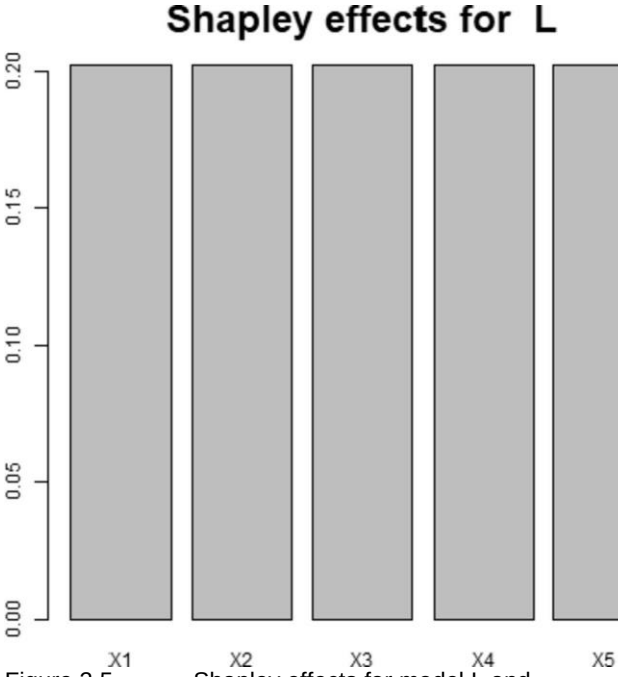

Figure 2.5 Shapley effects for model L and uniformly distributed inputs

If the variables would now be distributed normally in the following manner X1 ~ N(10,2) , X2 ~ N(1, 0.5), X3 ~ N(100, 50), X4 ~ N(1000, 10), X5 ~ N(0.1, 0.01), SA results would be quite different and this subtle change in distributions would only be detected by the savvy GSA methods (Figures 2.7 - 2.9). According to OATSA X4 is most influential on L, while the GSA methods - scatterplot, Sobol and Shapley – all agree that it is X3. This example illustrates that OATSA can even be misleading for a LM, because SA results depend on the model, the distributions of the inputs, and interactions among the factors.

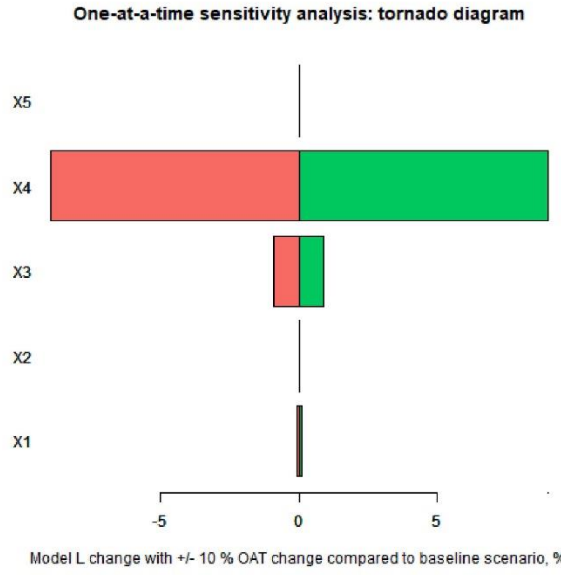

Figure 2.6 One-at-a-time sensitivity analysis results for model L and X1 ~ N(10,2) , X2 ~ N(1, 0.5), X3 ~ N(100, 50), X4 ~ N(1000, 10), X5 ~ N(0.1, 0.01)

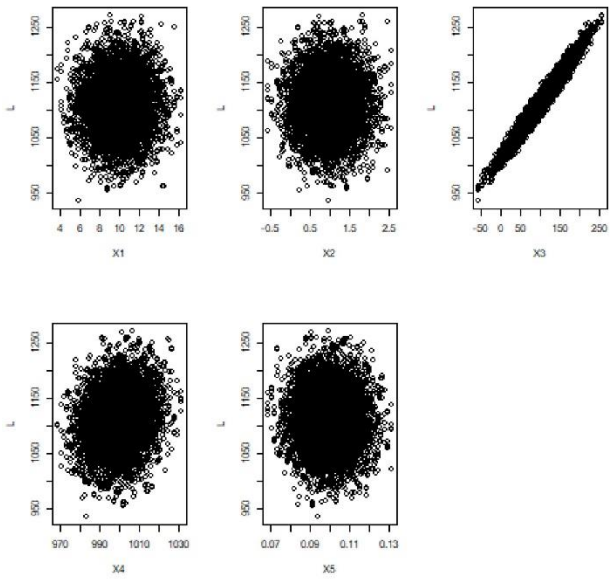

Figure 2.7 Scatter plot of model L and X1 ~ N(10,2) , X2 ~ N(1, 0.5), X3 ~ N(100, 50), X4 ~ N(1000, 10), X5 ~ N(0.1, 0.01)

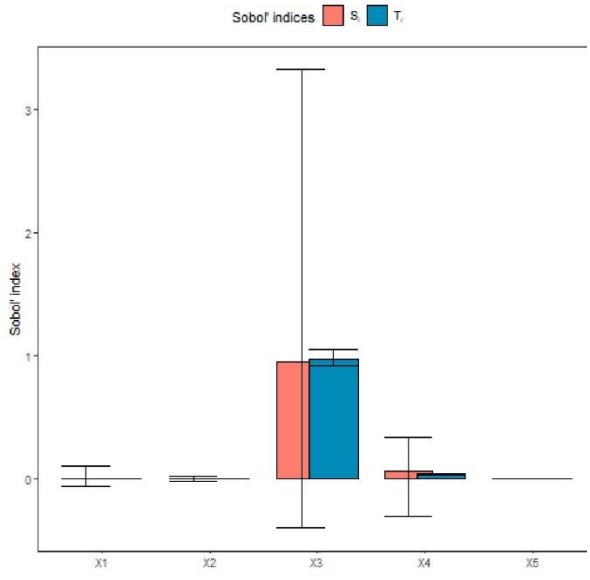

Figure 2.8 Sobol indices for model L and X1 ~ N(10,2) , X2 ~ N(1, 0.5), X3 ~ N(100, 50), X4 ~ N(1000, 10), X5 ~ N(0.1, 0.01

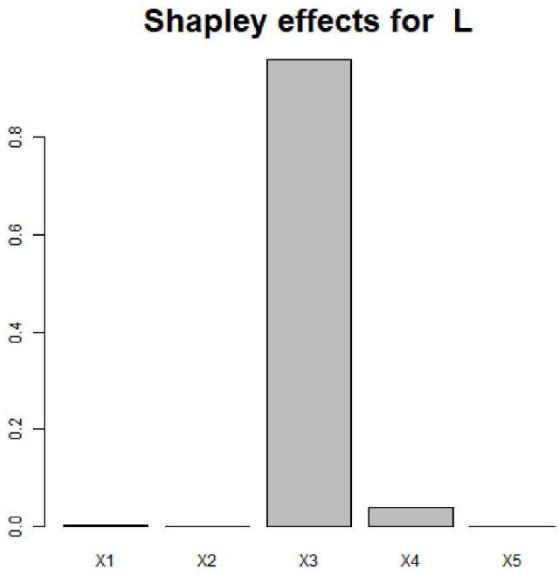

Figure 2.9 Shapley effects of model L and X1 ~ N(10,2) , X2 ~ N(1, 0.5), X3 ~ N(100, 50), X4 ~ N(1000, 10), X5 ~ N(0.1, 0.01)

2.10.2 Example II: Nonlinear multiplicative model

Now consider a multiplicative model *M = X1*X2*X3*X4*X5* with all inputs uniformly distributed in [{0,1]. Although, OATSA (Fig. 2.10) and GSA results coincide in this particular instance (Figures 2.10 - 2.13), it can be seen in Fig. 4.12 that for model M, all factors interact with one another (values of total effect SI's are much greater than first order SI's). This is an example of the Sobol method providing fuller information about the model compared to the OATSA, even when the ranking provided by both are the same.

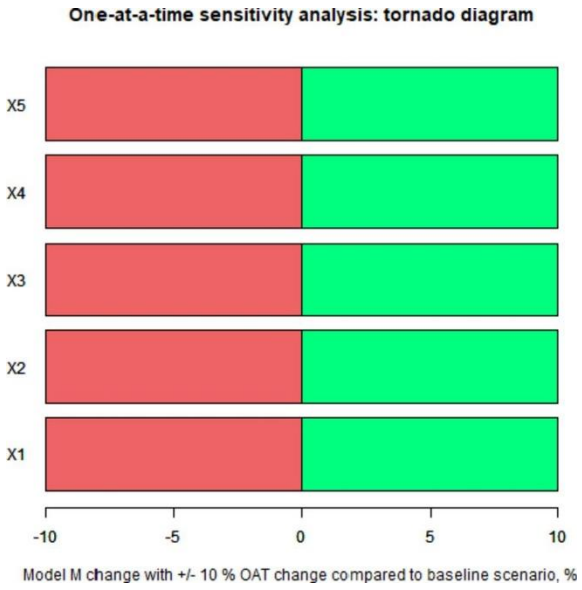

Figure 2.10 One-at-a-time sensitivity analysis results for model M and uniformly distributed inputs

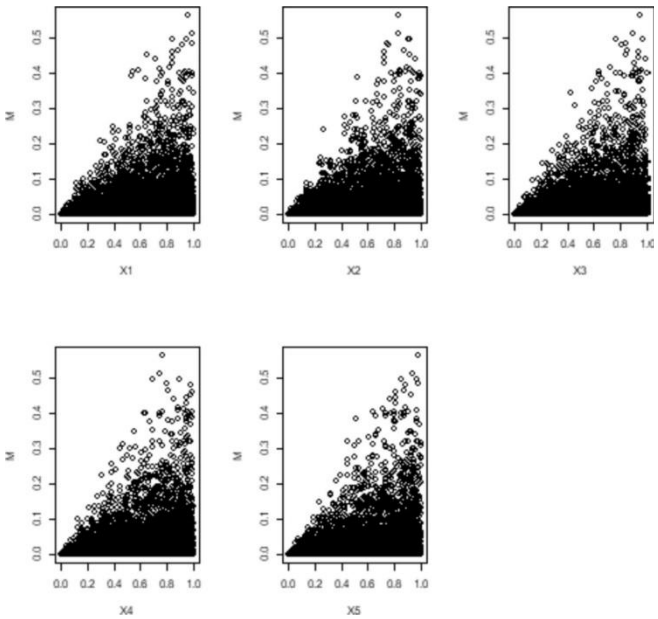

Figure 2.11 Scatter plot of model M and uniformly distributed inputs

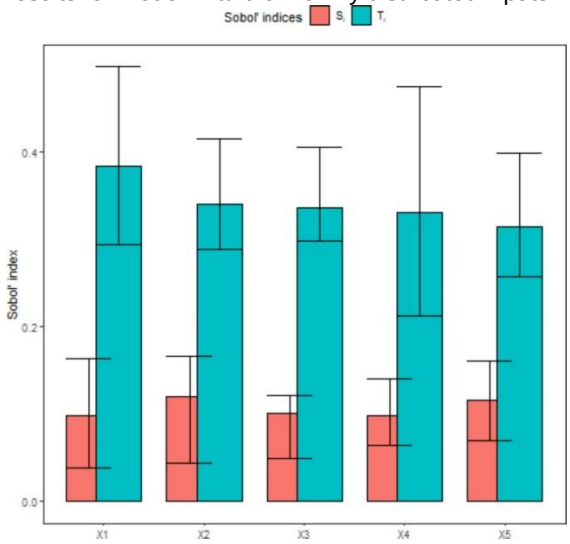

Figure 2.12 Sobol indices for model M and uniformly distributed inputs

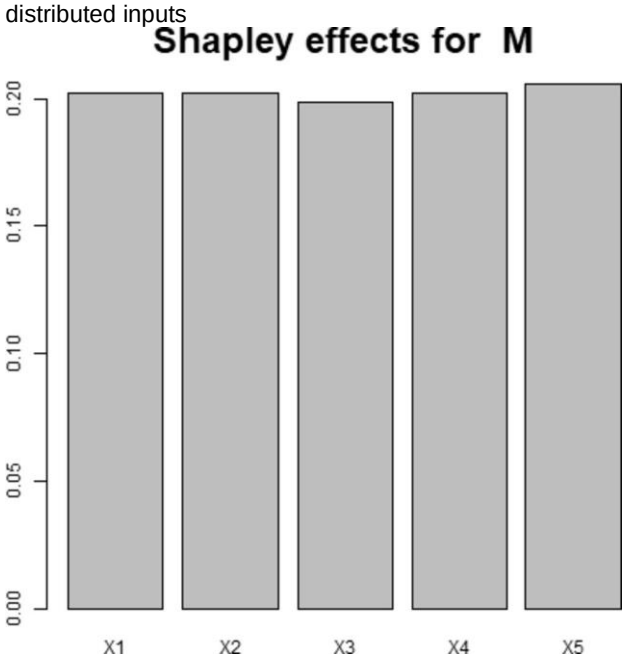

Figure 2.13 Shapley effects of M and uniformly distributed inputs

Now again the variables are distributed normally in the following manner *X1 ~ N(10,2), X2 ~ N(1, 0.5), X3 ~ N(100, 50), X4 ~ N(1000, 10), X5 ~ N(0.1, 0.01)*. This change again remains unnoticed to the OATSA (Fig. 2.14), but is picked up by the GSA methods, that again agree in their findings on the most influential factors being X2 and X3 (Fig. 2.15 - 2.17).

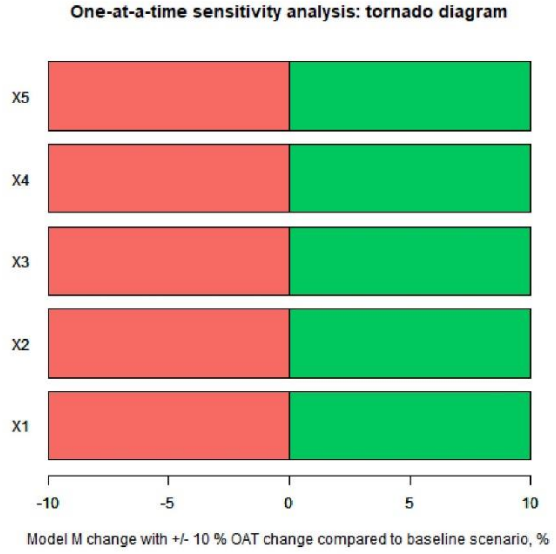

Figure 2.14 One-at-a-time sensitivity analysis results for model M and X1 ~ N(10,2) , X2 ~ N(1, 0.5), X3 ~ N(100, 50), X4 ~ N(1000, 10), X5 ~ N(0.1, 0.01)

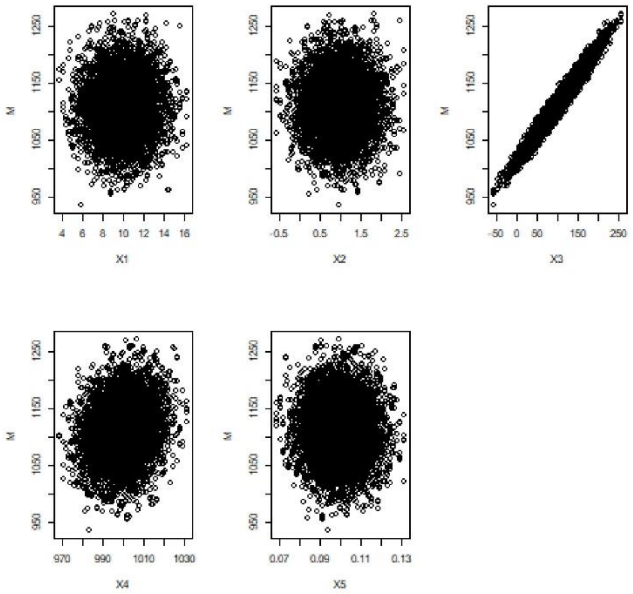

Figure 2.15 Scatter plot of model M and X1 ~ N(10,2) , X2 ~ N(1, 0.5), X3 ~ N(100, 50), X4 ~ N(1000, 10), X5 ~ N(0.1, 0.01)

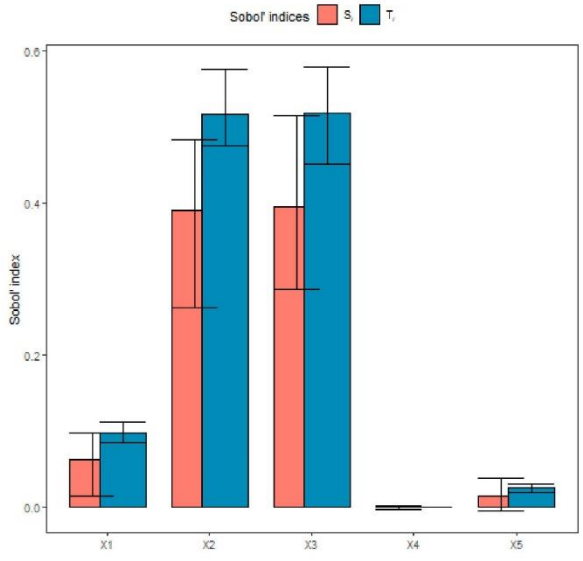

Figure 2.16 Sobol indices for model M and X1 ~ N(10,2) , X2 ~ N(1, 0.5), X3 ~ N(100, 50), X4 ~ N(1000, 10), X5 ~ N(0.1, 0.01)

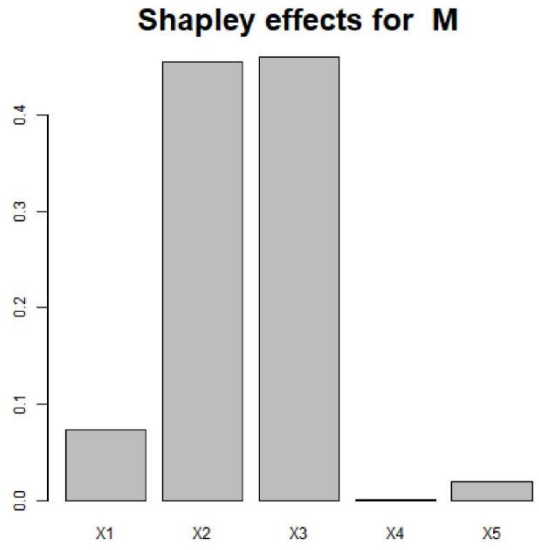

Figure 2.17 Shapley effects of model M and X1 ~ N(10,2) , X2 ~ N(1, 0.5), X3 ~ N(100, 50), X4 ~ N(1000, 10), X5 ~ N(0.1, 0.01)

2.10.3 Example III: Nonlinear levelized cost of energy model

Now consider a realistic LCOE model adapted from the recent study of Jadali et al. [99] that compared full and partial decommissioning vs. repowering end-of-life scenarios for a OFFWF with a TEA, which included a MC UA but a OATSA of LCOE. Inputs to SA were AEP, DR, cost of development and consenting (D&C), installation and commissioning costs (I&C), O&M costs, production and acquisition (P&A) costs, partial and full decommissioning costs, and repowering costs (RC). The study included UA with MC simulation but OATSA of LCOE. LCOE was calculated with Eq. (40).

The case study focused on a realistic but hypothetical OWF deployed in UK waters. It consisted of a deterministic analysis and stochastic analysis. For the deterministic analysis, the AEP was assumed to be constant and equal to 1734792 MWh/year. The operating time of a OWF is considered 20 years. The stochastic part consisted on MC UA and OATSA of LCOE for partial and full decommissioning and repowering scenarios. For the MC experiment, random sampling was used with the size of N = 100000 iterations. The distributions of variables for the UA in [99] are given in Table 2.9.

There are no major concerns on the UA part, only that quasi random sampling could be used for in order to reach the same level of accuracy with a significantly less sample size, but the chosen sample size of 100000 is big enough to overcome the inhomogeneity ever present in any random sample. The major shortcoming of SA in [99] is that OAT was used. OAT is a good an example of convenience sampling. It is popular and easy to integrate in any analysis. In [99] the baseline is the deterministic result, but the amount of percent is omitted altogether. The reader is invited to explore what happens to the sample when OATSA is used.

There were seven variables in SA in [99]. By increasing and decreasing the baseline by p% one variable at a time, 14 new points in input space are sampled. So in [99] a sample of 100000 points was used for UA, but a sample of 15 (14 + baseline) points was used for SA. Even without going into the nuances of the calculation procedure, it is obvious that the sample sizes for UA and SA are drastically different, several magnitudes apart to be precise. So how can OATSA results be reliable to make a decision whether to decommission or repower a OFFWF? Tsvetkova & Ouarda [13] argued that the same sample can be used for both UA and global SA. Why not integrate variation in AEP into the sample used for MC experiment and then use the results for SA? That way sample size for UA and SA would be identical

An alternative experiment design is for the repowering case is proposed. The sample size is reduced to 1000, as quasi random sampling is used. The p% for OATSA is assumed to be 10,

although the value of p is of little importance, as the underlying sampling for OATSA is not sufficient. The deficiency of the OAT approach is alleviated somewhat by the Morris method [1] that uses a sufficient enough sampling and then from the sampled points assesses the OAT effects on the model. The baseline value of the DR is assumed to be 8%, the distribution for AEP is assumed to be normal (1734792, 173479), and the distribution for the DR - to be normal N(0.08, 0.02).

Table 2.9 Inputs to levelized cost of energy model

Variable name	**Meaning**	**Distribution**	**Distribution parameters**
D&C	Cost of development and consenting	Normal	N(205750, 20575) [99]
P&A	Production & acquisition costs	Normal	N(1040229, 10422) [99]
I&C	Installation & commissioning costs	Normal	N(305742, 30574) [99]
O&M	Operation & maintanence costs	Normal	N(56597, 5659) [99]
RC	Repowering costs	Normal	N(707035, 70703) [99]
AEP	Annual energy production	Normal	N(1734792, 173479)
DR	Discount rate	Normal	N(0.08, 0.02)

The UA results in Fig. 2.18 show a skewness of the LCOE distribution not found in [99]. The UA results are not the focus of this example, but are considered worth mentioning in the context of reasoning and approaching uncertainty.

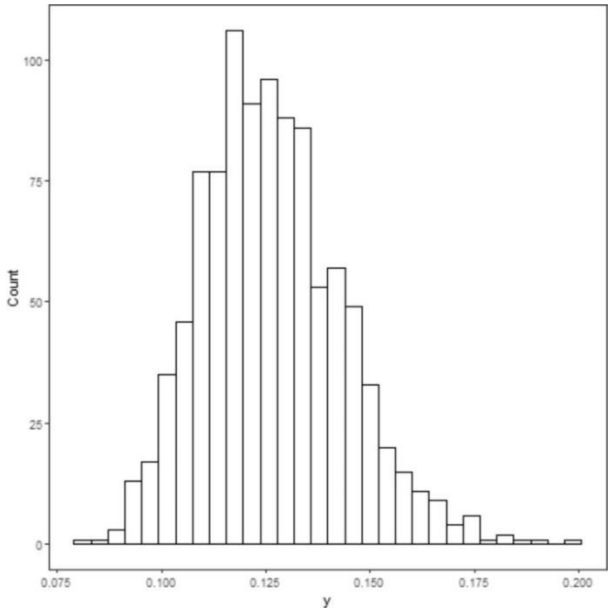

Figure 2.18 Uncertainty analysis results for levelized cost of energy model

The results of SA, i.e. the ranking of the inputs according to the degree it influences the variance of LCOE, would be different. The OATSA results in Fig. 2.19 suggest that P&A costs are most influential after the AEP. The scatterplot of LCOE in Fig. 2.20 does not provide clarity on the second most influential factor in this case. The Sobol method (Fig. 2.21) and Shapley effects (Fig. 2.22) identify DR to take the second place and P&A – the third. For this case, surprisingly the difference between OATSA and GSA methods for a nonlinear LCOE model were not as eye-catching as in the previous examples, but one must keep in mind that the LCOE model of Jadali [99] although realistic but is still hypothetical and all distributions are taken with the same value of standard deviation.

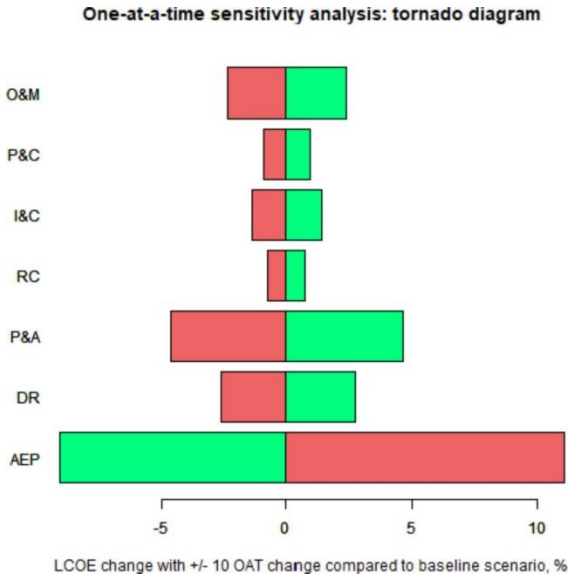

Figure 2.19 One-at-a-time sensitivity analysis results for model M and and X1 ~ N(10,2) , X2 ~ N(1, 0.5), X3 ~ N(100, 50), X4 ~ N(1000, 10), X5 ~ N(0.1, 0.01)

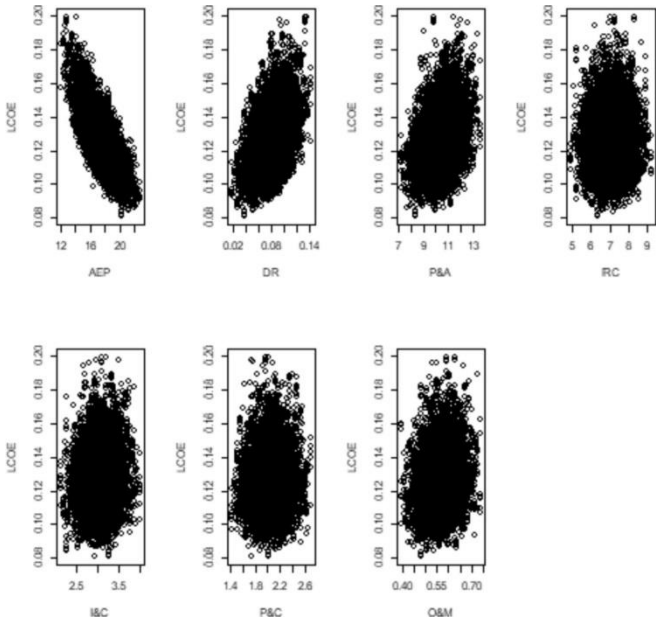

Figure 2.20 Scatter plot of model M and and X1 ~ N(10,2) , X2 ~ N(1, 0.5), X3 ~ N(100, 50), X4 ~ N(1000, 10), X5 ~ N(0.1, 0.01)

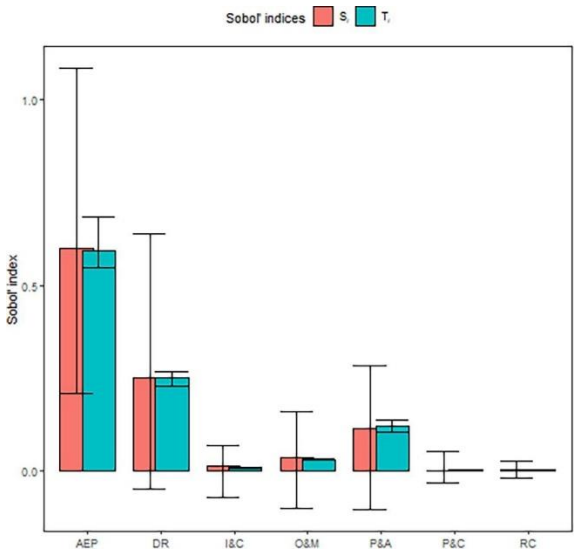

Figure 2.21 Sobol indices for model M and and X1 ~ N(10,2) , X2 ~ N(1, 0.5), X3 ~ N(100, 50), X4 ~ N(1000, 10), X5 ~ N(0.1, 0.01)

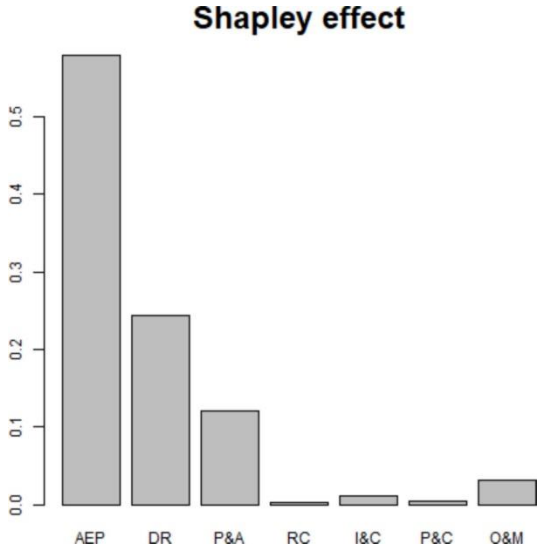

Figure 2.22 Shapley effects of model M and X1 ~ N(10,2) , X2 ~ N(1, 0.5), X3 ~ N(100, 50), X4 ~ N(1000, 10), X5 ~ N(0.1, 0.01)

The previous simplified examples demonstrated that, although for some cases OATSA results do coincide with GSA results, OATSA if used at all are to be used with extreme caution, as the results are sensitive to the distributions of the inputs.

2.11 Critical synthesis

Section 2.11 synthesizes critical remarks on the review article pool, observations and generalizations encountered in the process of the review.

2.11.1 Trends

The trends unveiled in the process of this review are (1) all model commonly used in WRA are nonlinear (2) OATSA prevails in WRA despite its inapplicability to such models, (3) the more technical WRA study is the more likely for GSA to be employed, (4) GSA is becoming more popular in WRA over time, and, last but not least, (5) policy implications made on unreliable OATSA study results in WRA might lead to dire consequences.

The review summary (Table 2.10) indicates the prevalence of nonLMs and OATSA in WRA. The use of keywords such as a baseline, a change in %, or a tornado diagram indicates OATSA.

Table 2.10 Summary of the review of sensitivity analysis in wind resource assessment

SA model	Non-linearity of model	Relationship to key inputs	#of articles in review	References of the reviewed articles	OATSA	GSA

GOFM	Yes	$R^2 = 1 - \frac{\sum_{i=0}^{n}(w_i - v_i)^2}{\sum_{i=0}^{n}(w_i - v_{ave})^2}$	2	[33][34]	100%	0%
WP	Yes	$P = \frac{1}{2} C_p \rho A w^3$	174	[35][36][37][38][39] [40][41][42][43][44] [45][46][47][48][49][50][56]	53%	47 %
WE	Yes	$AEP = 8760 \frac{1}{2} C_p \rho A w^3$	14	[13][52][53][56][66] [58][59][60][61][62][63] [64][65][67]	71%	29 %
NPV	Yes	$\sum_{i=0}^{N} \frac{AEP_i\ FIT - CAPEX_i - OPI}{(1+r)^i}$	27	[52][60][61][64] [70][71][72][73][74][75][78] [77] [79][81][83][84][85][86][87] [88] [91][92][93][94][95][96][97]	96%	4%
IRR	Yes	$IRR \sim \sqrt[n]{r}$	14	[52][61] [73][78][81][88][91][96] [101][102][103][104][105][106]	93%	7%
PP	Yes	$PP = \frac{CAPEX}{\text{AEP} * \text{FIT} - \text{OPEX}}$	6	[61][78][84][102][113][114]	100%	0%
LCOE	Yes	$LCOE = \frac{\sum_{i=1}^{N}(CAPEX_i + OPEX_i)/(1+}{\sum_{i=1}^{N} \text{AEP}/(1+r)^{\text{i}}}$	39	[52][74][95][99][107] [115][116][117][118][119] [120][122][123][124][125] [126][127][128][129][130][131] [134][132][136][139][140][141] [142][143][144][146][147][148] [173][178][179]	87%	13 %
CAPEX	Yes	$CAPEX = -1.48510^{11} P_{WT}^{0.001} + 2.35310^6 WD + 2.5310^6 D + 2.45110^6 P_{WF} + 1.48710^6$	4	[132][149][151][152]	75	25
OPEX	Yes	$OPEX = -6.34910^8 P_{WT}^{0.187} + 2.59510^{-19} e^{0.83D} + 8{,}41410^5 P_{WF} + 9.50610^8$	5	[53][132][149][151][153]	60	40
Average	**100%**		**102**		**82%**	**18 %**

2.11.2 Pitfalls

The review found evidence of the following pitfalls of SA to be present in WRA:

(1) Lack of universal definition of SA in WRA;

(2) Interchangeability of SA and UA;

(3) Disregard to the lack of applicability of OAT method to nonLMs;

The need for a clear standard definition of SA in Earth sciences was voiced by Razavi et al. [161]. The motivation behind SA can be diverse. Saltelli et al. [4] provide examples of SA objectives, i.e. to find errors in the model, prioritize research activities, and "*identify critical regions in the space of inputs*" [4]. In some studies, no clear motivation (research questions for SA) was found [46][102]. Often no ranking of SAIVs was established after a SA was performed [84][102], which is attributed to the lack of a clear research question. Sometimes SA is used to identify which variables have a positive and a negative effect on the model, for example [139][142]. SA is also used to make inferences about the dependency of SAIVs and SAOV [62][144]. Examples of interchangeability of the terms UA and SA were detected in [14][117][121]. Tran et al. [117] presented the PDFs of LCOE as GSARs, when, in fact, they are UA results. Ayodele et al. [14] in an encyclopedia review article of methods for UA of WT output uses UA and SA interchangeably. Heck et al. [121] reasonably argues in favor of a MC approach for integrating uncertainty into LCOE, he states that *"if uncertainty is included at all, it is usually through a simple sensitivity analysis that uses high/low values for each variable to estimate upper and lower bounds on the LCOE*" [121]. With this statement, he shows the common understanding of uncertainties or the interchangeability of UA and SA. Only a handful of studies accounted for the nonlinearity of the models common for WRA [13][36][37][39] [42][52][53][118][120]. The rest disregarded model nonlinearity and used OATSA.

2.12 Conclusion and outlook

The review findings of common SA practices in the field of WRA greatly correspond with those of Morras Bora et al. [120] in offshore wind and Menberg et al. [203] but in the field of building energy models. Building energy models, like the models used in WRA, are nonlinear [204], and GSA is computationally expensive while it provides stable results [205]. In WRA, computational burden for the WRA models mentioned in this review is not an issue (except for the offshore cost model [120]), although it is one for WRF and CFD models [13].

The definition and purpose of SA in WRA is often misconstrued in a number of ways. A universal definition of SA in the field is absent. This discrepancy in terminology causes discrepancy in motivation, misunderstanding in the research questions SA addresses and goals SA could help achieve (Section 4.11 for details). This finding corresponds with the those of [4][161]. In Section 2, the most common SA outputs among variables of interest used in WRA have been identified as GOFM, WP, WE, NPV, IRR, PP, LCOE, CAPEX, and OPEX. All were shown to be nonlinear. OATSA is popular mainly due to its convenience but not credibility. Moreover, OATSA has been previously shown to be unsuitable for nonlinear models [20]-[22].

Nonetheless, it is flourishing by dominating among other SA methods in the field of WRA with prevailing nonlinear models. 53-100% of articles reviewed in each category (82% on average, Table 10) used OATSA. Despite its unreliability, policy implications were made based on results of OATSA of LCOE [105][138], which is a call for serious concern. To make matters worse, professional software designed for renewable energy assessment, such as RETScreen [68], is promoting the use of unreliable OATSA as a tool for reasoning about uncertainty and risks associated with investing in wind energy.

Section 2.8 Geography found based on the number of SA studies in the literature that LCOE is the most popular model in WRA, and that the UK, the US and China are the most studied countries. Offshore wind is of special significance to the UK and Spain. The costs of offshore wind has been dropping in the last years, making the more abundant offshore wind potential feasible for integrating into the grid. Profitability assessment of the next generation of OFFWFs require complex nonlinear techno-economic models that capture the new relationships formed due to rapid technological advancement and policy incentives [120]. Borras Mora et al. [120] call GSA necessary to study these complex models, as relationships between inputs and outputs are poorly understood [120]. The significance of GSA for decision support in policy in general was emphasized in [7]. Yet the voice in favor of GSA remains unheard, despite the abundancy of software tools for GSA. When GSA was found to be used in WRA [13][36][37][39] [42][52][53][118][120], the most common GSA method was the variance-based Sobol method, the least common – Shapley effects [54] and PAWN [6]. Section 7 focused on the specifics of application and discussed three examples illustrating that OATSA can even be misleading for a LM, let alone nonLMs, as SA results depend on the model, the distributions of the inputs, and interactions among the factors. It also showed that although OATSA results do coincide with GSA results in some particular cases, OATSA if used at all should be used with extreme caution, as SA results are sensitive to the distributions of the inputs.

Future research should focus on GSA in WRA. Notably, not one GSA study of GOFMs and PP in WRA was detected. The limited amount of studies dealing with SA of GOFMs indicates a necessity for GSA of GOFMs. Calculating Shapley effects [54] for factors contributing to NPV and/or LCOE (as the most popular economic SAOVs used in FS's) for ONWF and OFFWF (especially for FOFFWFs as it is one the hot topics in WE) would be ground-breaking. Martin [153] defined most influential factors for O&M cost of a OFFWF and suggested refining their distributions and running a "more sophisticated GSA in order to quantify the amount of sensitivity" [153], so applying Sobol, Shapley or PAWN to this experimental design is of justified importance.

Mytilinou et al. [149] suggest increasing the sample size of MC simulation to study the higher order interdependencies, this can be done with total effect Sobol SI's. Also, [137] suggested studying "*sensitivity of LCOE of OFFWFs to the years in which each of the different costs occur*" [137].

2.13 Declaration of competing interest

There is no conflict of interest regarding this publication.

2.14 CRediT authourship contribution

Olga Tsvetkova: Conceptualization, Methods, Writing - Original draft preparation.

Taha B.M.J. Ouarda: Funding acquisition, Supervision, Writing - Reviewing and Editing.

2.15 Acknowledgements

The authors are thankful to the Editor Neven Duic and the anonymous reviewers for their insightful input, that helped improve the quality of the manuscript significantly. This review was supported by the Canada Research Chair Program and the Natural Sciences and Engineering Research Council of Canada (NSERC).

3 BIBLIOGRAPHY

[1] M.D. Morris, Factorial sampling plans for preliminary computational experiments, Technometrics, 33 (2) (1991), pp. 161-174

[2] F. Campolongo, J. Cariboni, A. Saltelli, An effective screening design for sensitivity analysis of large models, Environ Model Softw, 22 (10) (2007), pp. 1509-1518

[3] Sobol I.′, “ОБ ОЦЕНКЕ ЧУВСТВИТЕЛЬНОСТИ НЕЛИНЕЙНЫХ МАТЕМАТИЧЕСКИХ МОДЕЛЕЙ (On sensitivity estimation for nonlinear mathematical models),” Математическое моделирование (Matem. Model., vol. 2, no. 1, pp. 12–18, 1990.

[4] A. Saltelli, et al., Global Sensitivity Analysis: The Primer, John Wiley & Sons Ltd (2008)

[5] “Overview — FUSED-Wind documentation.” [Online]. Available: https://www.fusedwind.org/. [Accessed: 05-Feb-2021].

[6] F. Pianosi, T. Wagener, A simple and efficient method for global sensitivity analysis based on cumulative distribution functions, Environ Model Softw, 67 (2015), pp. 1-11

[7] F. Pianosi, F. Sarrazin, T. Wagener, A Matlab toolbox for Global Sensitivity Analysis, Environ Model Softw, 70 (2015), pp. 80-85

[8] Razavi S. et al., “The Future of Sensitivity Analysis: An Essential Discipline for Systems Modeling and Policy Support,” Environ. Model. Softw., p. 104954, Dec. 2020.

[9] Mara TA, Azzini I, Listorti G, Rosati R. “Uncertainty and sensitivity analysis for policy decision making - Publications Office of the EU,” Joint Research Centre (European Commission), 2020. [Online]. Available: https://op.europa.eu/en/publication-detail/-/publication/ff3cf22c-35e1-11eb-b27b-01aa75ed71a1/language-en. [Accessed: 01-Feb-2021].

[10] Gilbertson, “An approach for using probabilistic risk assessment in risk-informed decisions on plant-specific changes to the licensing basis,” 2018.

[11] Puy A. Saltelli A. Levin SA, Jan CO. “sensobol : an R package to compute variance-based sensitivity indices,” arXiv Prepr. arXiv2101.10103, 2021.

[12] “UNFCCC guidelines on the assessment of investment analysis.” .

[13] Tsvetkova O. Ouarda TBMJ. “Quasi-Monte Carlo technique in global sensitivity analysis of wind resource assessment with a study on UAE,” J. Renew. Sustain. Energy, vol. 11, no. 5, 2019.

[14] Ayodele TR. “Wind Turbines : Uncertainty Analysis Approaches,” Encyclopedia of Energy Engineering and Technology, Second Edition, no. June 2015. Taylor and Francis: New York, pp. 2251–2262, 2015.

[15] Azevêdo RDO. “Identification and analysis of impact factors on the economic feasibility of wind energy investments,” no. September, pp. 1–27, 2020.

[16] M. Rezaei, et al., Sensitivity analysis of criteria to optimize wind farm localizing: A case study

Wind Eng, 44 (3) (2020), pp. 294-312

[17] T. Blackler, M.T. Iqbal, Pre-feasibility study of wind power generation in Holyrood, Newfoundland

Renew Energy, 31 (4) (2006), pp. 489-502

[18] G. Boeing, Visual analysis of nonlinear dynamical systems: chaos, fractals, self-similarity and the limits of prediction, Systems, 4 (4) (2016), p. 37

[19] V. Illingworth (Ed.), The Penguin Dictionary of Physics, Penguin Books, London (1991)

[20] D. Harenberg, S. Marelli, B. Sudret, V. Winschel, Uncertainty quantification and global sensitivity analysis for economic models, Quant Econom, 10 (1) (2018), pp. 1-41

[21] A. Saltelli, P. Annoni, How to avoid a perfunctory sensitivity analysis, Environ Model Softw, 25 (12) (2010), pp. 1508-1517

[22] Douglas-Smith D. Iwanaga T, Croke BFW, Jakeman AJ. “Certain trends in uncertainty and sensitivity analysis: An overview of software tools and techniques,” Environmental Modelling and Software, vol. 124. Elsevier Ltd, p. 104588, 01-Feb-2020.

[23] U.C. Ben, A.E. Akpan, C.C. Mbonu, C.H. Ufuafuonye

Integrated technical analysis of wind speed data for wind energy potential assessment in parts of Southern and Central Nigeria, Clean Eng Technol (2021), p. 100049

[24] M.A. Saeed, Z. Ahmed, S. Hussain, W. Zhang, Wind resource assessment and economic analysis for wind energy development in Pakistan, Sustain Energy Technol Assessments, 44 (2021), Article 101068

[25] J.F. Manwell, J.G. McGowan, A.L. Rogers, Wind energy explained : theory, design and application, Wiley (2009)

[26] K. Azad, M. Rasul, P. Halder, J. Sutariya, Assessment of wind energy prospect by Weibull distribution for prospective wind sites in Australia, Energy Procedia, 160 (2019), pp. 348-355

[27] Z.H. Hulio, W. Jiang, S. Rehman, Techno-Economic assessment of wind power potential of Hawke’s Bay using Weibull parameter: A review, Energy Strateg Rev, 26 (Nov. 2019), Article 100375

[28] G.K. Gugliani, Comparison of different multi-parameters probability density models for wind resources assessment, J Renew Sustain Energy, 12 (6) (2020), Article 063303

[29] K. Mohammadi, O. Alavi, J.G. McGowan, Use of Birnbaum-Saunders distribution for estimating wind speed and wind power probability distributions: A review, Energy Convers Manag, 143 (2017), pp. 109-122

[30] T.B.M.J. Ouarda, C. Charron, F. Chebana, Review of criteria for the selection of probability distributions for wind speed data and introduction of the moment and L-moment ratio diagram methods, with a case study, Energy Convers Manag, 124 (2016), pp. 247-265

[31] J. Jia, Z. Yan, X. Peng, X. An, A new distribution for modeling the wind speed data in Inner Mongolia of China, Renew Energy, 162 (2020), pp. 1979-1991

[32] S.A. Vargas, G.R.T. Esteves, P.M. Maçaira, B.Q. Bastos, F.L. Cyrino Oliveira, R.C. Souza, Wind power generation: A review and a research agenda, J Clean Prod, 218 (2019), pp. 850-870

[33] O. Alavi, A. Sedaghat, A. Mostafaeipour, Sensitivity analysis of different wind speed distribution models with actual and truncated wind data: A case study for Kerman, Iran, Energy Convers Manag, 120 (2016), pp. 51-61

[34] C. Jung, D. Schindler, Sensitivity analysis of the system of wind speed distributions, Energy Convers Manag, 177 (2018), pp. 376-384

[35] S.M. Weekes, A.S. Tomlin, Low-cost wind resource assessment for small-scale turbine installations using site pre-screening and short-term wind measurements, IET Renew Power Gener, 8 (4) (2014), pp. 349-358

[36] P.M. McKay, R. Carriveau, D.-S.-K. Ting, J.L. Johrendt, Global sensitivity analysis of wind turbine power output, Wind Energy, 17 (7) (2014), pp. 983-995

[37] W. Tong, S. Chowdhury, A. Mehmani, A. Messac, J. Zhang, Sensitivity of wind farm output to wind conditions, land configuration, and installed capacity, under different wake models, J Mech Des Trans ASME, 137 (6) (2015), pp. 1-11

[38] F. Ulker, D. Allaire, K. Willcox, Sensitivity-guided decision-making for wind farm micro-siting, Int J Numer Meth Fluids, 83 (1) (2017), pp. 52-72

[39] J.A. Carta, S. Díaz, A. Castañeda, A global sensitivity analysis method applied to wind farm power output estimation models, Appl Energy, 280 (2020), Article 115968

[40] P. Kumar, B. Sanderse, K. Boorsma, M. Caboni, Global sensitivity analysis of model uncertainty in aeroelastic wind turbine models, J Phys Conf Ser, 1618 (2020), p. 42034

[41] J.P. Murcia, et al., Uncertainty propagation through an aeroelastic wind turbine model using polynomial surrogates, Renew Energy, 119 (2018), pp. 910-922

[42] N. Aghbalou, A. Charki, S.R. Elazzouzi, K. Reklaouiб A probabilistic assessment approach for wind turbine-site matchingб Int J Electr Power Energy Syst, 103 (2018), pp. 497-510

[43] A.R. Grilli, M.L. Spaulding, Offshore wind resource assessment in Rhode Island waters, Wind Eng, 37 (6) (2013), pp. 579-594

[44] Eisa SA, Wedeward K, Stone W. “Sensitivity analysis of a type-3 DFAG wind turbine’s dynamics with pitch control,” in 2016 IEEE Green Energy and Systems Conference, IGSEC 2016, 2016.

[45] G. He, D.M. Kammen, Where, when and how much wind is available? A provincial-scale wind resource assessment for China, Energy Policy, 74 (2014), pp. 116-122

[46] K.Q. Nguyen, Wind energy in Vietnam: Resource assessment, development status and future implications, Energy Policy, 35 (2) (2007), pp. 1405-1413

[47] Kubik ML, Coker PJ, Hunt C. “Using Meteorological Wind Data to Estimate Turbine Generation Output: A Sensitivity Analysis,” Proc. World Renew. Energy Congr. – Sweden, 8–13 May, 2011, Linköping, Sweden, vol. 57, pp. 4074–4081, 2011.

[48] H. Daaou Nedjari, S.K. Haddouche, A. Balehouane, O. Guerri, Optimal windy sites in Algeria: Potential and perspectives, Energy, 147 (2018), pp. 1240-1255

[49] Y.M. Saint-Drenan, et al., A parametric model for wind turbine power curves incorporating environmental conditions, Renew Energy, 157 (2020), pp. 754-768

[50] F. Haces-Fernandez, H. Li, D. Ramirez, Improving wind farm power output through deactivating selected wind turbines, Energy Convers Manag, 187 (2019), pp. 407-422

[51] T. Ziehn, A.S. Tomlin, GUI-HDMR - A software tool for global sensitivity analysis of complex models

Environ Model Softw, 24 (7) (2009), pp. 775-785

[52] P. Richter, P.R.J. Wolters, R.Ç.A.V.M. Frank, Uncertainty Quantification of Offshore Wind Farms

Wind Energy (2019)

[53] Dykes K Ning A, King R, Graf P, Scot G, Veers P. “Sensitivity analysis of wind plant performance to key turbine design parameters: A systems engineering approach,” 32nd ASME Wind Energy Symp., no. February, 2014.

[54] Song E. Nelson BL, Staum J. “Shapley Effects for Global Sensitivity Analysis: Theory and Computation,” 2015.

[55] S. Díaz, J.A. Carta, A. Castañeda, Influence of the variation of meteorological and operational parameters on estimation of the power output of a wind farm with active power control, Renew Energy, 159 (2020), pp. 812-826

[56] E. Gonzalez, B. Stephen, D. Infield, J.J. Melero, Using high-frequency SCADA data for wind turbine performance monitoring: A sensitivity study, Renew Energy, 131 (2019), pp. 841-853

[57] S. Marelli and B. Sudret, “UQLab: A Framework for Uncertainty Quantification in Matlab,” Vulnerability, Uncertainty, Risk Quantif. Mitigation, Manag. - Proc. 2nd Int. Conf. Vulnerability Risk Anal. Manag. ICVRAM 2014 6th Int. Symp. Uncertain. Model. a, no. October, pp. 2554–2563, 2014.

[58] Y. Zhou, P. Luckow, S.J. Smith, L. Clarke, Evaluation of Global Onshore Wind Energy Potential and Generation Costs, Environ Sci Technol, 46 (14) (2012), pp. 7857-786

[59] M. Hoogwijk, B. de Vries, W. Turkenburg, Assessment of the global and regional geographical, technical and economic potential of onshore wind energy, Energy Econ, 26 (5) (2004), pp. 889-919

[60] S. Afanasyeva, J. Saari, M. Kalkofen, J. Partanen, O. Pyrhönen, Technical, economic and uncertainty modelling of a wind farm project, Energy Convers Manag, 107 (2016), pp. 22-33

[61] R. Villena-Ruiz, F.J. Ramirez, A. Honrubia-Escribano, E. Gómez-Lázaro, A techno-economic analysis of a real wind farm repowering experience: The Malpica case, Energy Convers. Manag., 172 (2018), pp. 182-199

[62] A. Khalid, S. Lodi, and M. Mahmood, “Power Potential Assessment and Sensitivity Analysis of a Wind Farm Power,” no. March, 2012.

[63] J. Schallenberg-Rodríguez, J. Notario-del Pino, Evaluation of on-shore wind techno-economical potential in regions and islands, Appl Energy, 124 (2014), pp. 117-129

[64] J. Tautz-Weinert, N.Y. Yürüşen, J.J. Melero, S.J. Watson, Sensitivity study of a wind farm maintenance decision - A performance and revenue analysis, Renew. Energy, 132 (2019), pp. 93-105

[65] J. Bistline, D. Young, Economic drivers of wind and solar penetration in the U.S, Environ Res Lett (2019)

[66] M. Lackner, A.L. Rogers, J.F. Manwell, M.A. Lackner, P.D. Student, “Uncertainty Analysis in MCP-Based Wind Resource, Assessment and Energy Production” (2008)

[67] A. Bossavy, R. Girard, G. Kariniotakis, Sensitivity analysis in the technical potential assessment of onshore wind and ground solar photovoltaic power resources at regional scale, Appl Energy, 182 (2016), pp. 145-153

[68] “Natural Resources Canada: RETScreen,” 2020. [Online]. Available: https://www.nrcan.gc.ca/maps-tools-publications/tools/data-analysis-software-modelling/retscreen/7465. [Accessed: 13-Aug-2020].

[69] “Systems Engineering Models and Tools.” [Online]. Available: https://www.nrel.gov/wind/systems-engineering-models-tools.html. [Accessed: 13-Aug-2020].

[70] E.E. Nordman, Energy transitions in Kenya’s tea sector: A wind energy assessment

Renew. Energy, 68 (2014), pp. 505-514

[71] C. Kongnam and S. Nuchprayoon, “Development of investment strategies for wind power generation,” 2007 IEEE Canada Electr. Power Conf. EPC 2007, no. November 2007, pp. 308–313, 2007.

[72] E. Lozano-Minguez, A.J. Kolios, F.P. Brennan, Multi-criteria assessment of offshore wind turbine support structures, Renew. Energy, 36 (11) (2011), pp. 2831-2837

[73] T.T. Soe, M. Zheng, Z.N. Aung, Assessment of economic feasibility on promising wind energy sites in Myanmar, Int. J. Renew. Energy Res., 5 (3) (2015), pp. 699-707

[74] L. Castro-Santos, V. Diaz-Casas, Sensitivity analysis of floating offshore wind farms, Energy Convers. Manag., 101 (2015), pp. 271-277

[75] D. Loncar, I. Milovanovic, B. Rakic, and T. Radjenovic, “Compound real options valuation of renewable energy projects: The case of a wind farm in Serbia,” Renewable and Sustainable Energy Reviews, vol. 75. Elsevier Ltd, pp. 354–367, 2017.

[76] S. Pookpunt, W. Ongsakul, N. Madhu, A comprehensive techno-economic analysis for optimally placed wind farms, Electr Eng, 102 (4) (2020), pp. 2161-2179

[77] B. Alonzo, S. Concettini, A. Creti, P. Tankov, Wind farm revenues in Western Europe in present and future climate, Soc. Sci. Res. Netw. (2021), pp. 1-55

[78] F.A. Hadi, S.S. Oudah, R.A. Al-baldawi, An Economic Study of a Wind Energy Project Using Different Sources of Wind Data, Iraqi J. Sci., 61 (2) (2020), pp. 322-332

[79] S. Ali, S. M. Lee, and C. M. Jang, “Techno-economic assessment of wind energy potential at three locations in South Korea using long-Term measured wind data,” Energies, vol. 10, no. 9, 2017.

[80] “Oracle Crystal Ball: Technical Information,” 2019. [Online]. Available: https://www.oracle.com/middleware/technologies/crystalball.html. [Accessed: 17-Dec-2019].

[81] S. Kamal Ismail, Sarjiya Purnomo, B. Hartono, Economic Feasibility of Wind Farm: A Case Study for Coastal Area in South Purworejo, Indonesia,Energy Procedia, 65 (2015), pp. 146-154

[82] “@RISK for risk analysis.” [Online]. Available: https://www.palisade.com/risk/. [Accessed: 13-Aug-2020].

[83] P. Quan, T. Leephakpreeda, Assessment of wind energy potential for selecting wind turbines: An application to Thailand, Sustain. Energy Technol. Assessments, 11 (2015), pp. 17-26

[84] J. Waewsak, C. Kongruang, Y. Gagnon, Assessment of wind power plants with limited wind resources in developing countries: Application to Ko Yai in southern Thailand, Sustain. Energy Technol. Assessments, 19 (2017), pp. 79-93

[85] P. Rotela Junior et al., “Wind power economic feasibility under uncertainty and the application of ANN in sensitivity analysis,” Energies, vol. 12, no. 12, 2019.

[86] G. Aquila, P. Rotela Junior, E. de Oliveira Pamplona, A.R. de Queiroz, Wind power feasibility analysis under uncertainty in the Brazilian electricity market, Energy Econ, 65 (2017), pp. 127-136

[87] L.S. Lacerda, et al., Microgeneration of Wind Energy for Micro and Small Businesses: Application of ANN in Sensitivity Analysis for Stochastic Economic Feasibility, IEEE Access, 8 (2020), pp. 73931-73946

[88] H. Kim, B. Kim, Wind resource assessment and comparative economic analysis using AMOS data on a 30MW wind farm at Yulchon district in Korea, Renew. Energy, 85 (Jan. 2016), pp. 96-103

[89] TIBCO, “TIBCO StatisticaTM Trial Download for Windows | TIBCO Software,” 2021. [Online]. Available: https://www.tibco.com/resources/product-download/tibco-statistica-trial-download-windows. [Accessed: 04-Feb-2021].

[90] S. Chakrabarty, F.I.M.M. Boksh, A. Chakraborty, Economic viability of biogas and green self-employment opportunities, Renew Sustain Energy Rev, 28 (Dec. 2013), pp. 757-766

[91] E.G. Sakka, D.V. Bilionis, D. Vamvatsikos, C.J. Gantes, Onshore wind farm siting prioritization based on investment profitability for Greece, Renew. Energy, 146 (Feb. 2020), pp. 2827-2839

[92] M.M. Amirrud, M. Shahin, Sensitivity and Uncertainty Analysis of Economic Feasibility of Establishing Wind Power Plant in Kerman, Iran, Renew. Energy Res. Appl., 1 (2) (Jul. 2020), pp. 247-260

[93] A. Ioannou, A. Angus, F. Brennan, A lifecycle techno-economic model of offshore wind energy for different entry and exit instances, Appl Energy, 221 (2018), pp. 406-424

[94] J. Haughton, D.G. Tuerck, An Economic Analysis of a Wind Farm in Nantucket Sound, Economic Analysis (2004)

[95] A. Ioannou, A. Angus, F. Brennan, Stochastic financial appraisal of offshore wind farms, Renew. Energy, 145 (Jan. 2020), pp. 1176-1191

[96] A. Shigina, “Offshore wind power plant in Murmansk region: techno-economic evaluation.”.

[97] A. Ioannou and F. Brennan, “A preliminary techno-economic comparison between a grid-connected and non-grid connected offshore floating wind farm,” in 2019 Offshore Energy and Storage Summit, OSES 2019, 2019.

[98] A. Ioannou, A. Angus, and F. Brennan, “Stochastic Prediction of Offshore Wind Farm LCOE through an Integrated Cost Model,” Energy Procedia, vol. 107, no. September 2016, pp. 383–389, 2017.

[99] A.M. Jadali, A. Ioannou, K. Salonitis, A. Kolios, Decommissioning vs. repowering of offshore wind farms—a techno-economic assessment, Int J Adv Manuf Technol (2021), pp. 2519-2532

[100] A. Garcia-Teruel and H. Jeffrey, “The economics of floating offshore wind – A comparison of different methods,” no. November, 2020.

[101] B. Ozerdem, S. Ozer, M. Tosun, Feasibility study of wind farms: A case study for Izmir, Turkey

J Wind Eng Ind Aerodyn, 94 (10) (2006), pp. 725-743

[102] M. Rafique, S. Rehman, M. Alam, L. Alhems, Feasibility of a 100 MW Installed Capacity Wind Farm for Different Climatic Conditions, Energies, 11 (8) (Aug. 2018), p. 2147

[103] A. Colmenar-Santos, S. Campíñez-Romero, C. Pérez-Molina, and F. Mur-Pérez, "Repowering: An actual possibility for wind energy in Spain in a new scenario without feed-in-tariffs," Renewable and Sustainable Energy Reviews, vol. 41. Elsevier Ltd, pp. 319–337, 2015.

[104] S. Grassi, N. Chokani, R.S. Abhari, Large scale technical and economical assessment of wind energy potential with a GIS tool: Case study Iowa, Energy Policy, 45 (Jun. 2012), pp. 73-85

[105] D.G. Carmichael, K.A. Lea, M.C.A. Balatbat, The financial additionality and viability of CDM projects allowing for uncertainty, Environ Dev Sustain, 18 (1) (Feb. 2016), pp. 129-141

[106] A.I. Estanqueiro, J.M.F. De Jesus, J.O. Tande, H. Bindner, Maximum Wind Power Penetration Assessment in Weak Grids Using Dynamic Wind Park Models, Eur. Wind Energy Conf. Exhib. (1997), pp. 1-4

[107] Y. Zhang, J. Yuan, C. Zhao, L. Lyu, Can dispersed wind power take off in China: A technical & institutional economics analysis, J. Clean. Prod., 256 (May 2020), Article 120475

[108] R. N. S. R. Mukhtaruddin, H. A. Rahman, and M. Y. Hassan, "Economic analysis of grid-connected hybrid photovoltaic-wind system in Malaysia," in 4th International Conference on Clean Electrical Power: Renewable Energy Resources Impact, ICCEP 2013, 2013, pp. 577–583.

[109] D. Al Katsaprakakis, et al., Introduction of a wind powered pumped storage system in the isolated insular power system of Karpathos-Kasos, Appl Energy, 97 (2012), pp. 38-48

[110] M. Kapsali, J.S. Anagnostopoulos, J.K. Kaldellis, Wind powered pumped-hydro storage systems for remote islands: A complete sensitivity analysis based on economic perspectives, Appl Energy, 99 (2012), pp. 430-444

[111] J.K. Kaldellis, K.A. Kavadias, Cost-benefit analysis of remote hybrid wind-diesel power stations: Case study Aegean Sea islands, Energy Policy, 35 (3) (2007), pp. 1525-1538

[112] J.K. Kaldellis, An integrated model for performance simulation of hybrid wind-diesel systems

Renew. Energy, 32 (9) (2007), pp. 1544-1564

[113] J.K. Kaldellis, T.J. Gavras, The economic viability of commercial wind plants in Greece. A complete sensitivity analysis, Energy Policy, 28 (8) (2000), pp. 509-517

[114] A. Sgobba, "On-site energy generation for a decarbonized Irish manufacturing industry," Trinity College Dublin, 2020.

[115] Q. Tu, R. Betz, J. Mo, Y. Fan, Y. Liu, Achieving grid parity of wind power in China – Present levelized cost of electricity and future evolution, Appl Energy, 250 (2019), pp. 1053-1064

[116] A.C. Levitt, W. Kempton, A.P. Smith, W. Musial, J. Firestone, Pricing offshore wind power

Energy Policy, 39 (10) (Oct. 2011), pp. 6408-6421

[117] T.T.D. Tran, A.D. Smith, Incorporating performance-based global sensitivity and uncertainty analysis into LCOE calculations for emerging renewable energy technologies

Appl Energy, 216 (Apr. 2018), pp. 157-171

[118] M. Dong, Y. Li, D. Song, B. Liu, L. Fang, and Q. Lv, "Uncertainty analysis of wind power based on levelized cost of energy," in 2020 15th IEEE Conference on Industrial Electronics and Applications (ICIEA), 2020, pp. 443–448.

[119] M. Dong, et al., Uncertainty and global sensitivity analysis of levelized cost of energy in wind power generation, Energy Convers. Manag., 229 (Feb. 2021), Article 113781

[120] E. B. Mora, J. Spelling, and A. H. Weijde, “Global sensitivity analysis for offshore wind cost modelling,” Wind Energy, p. we.2612, Jan. 2021.

[121] N. Heck, C. Smith, E. Hittinger, A Monte Carlo approach to integrating uncertainty into the levelized cost of electricity, Electr. J., 29 (3) (Apr. 2016), pp. 21-30

[122] M. Lerch, M. De-Prada-Gil, C. Molins, G. Benveniste, Sensitivity analysis on the levelized cost of energy for floating offshore wind farms, Sustain. Energy Technol. Assessments, 30 (Dec. 2018), pp. 77-90

[123] J. Aldersey-Williams, T. Rubert, Levelised cost of energy – A theoretical justification and critical assessment, Energy Policy, 124 (2019), pp. 169-179

[124] A. Myhr, C. Bjerkseter, A. Ågotnes, T.A. Nygaard, Levelised cost of energy for offshore floating wind turbines in a lifecycle perspective, Renew. Energy, 66 (Jun. 2014), pp. 714-728

[125] M. Shafiee, F. Brennan, I.A. Espinosa, A parametric whole life cost model for offshore wind farms

Int J Life Cycle Assess, 21 (7) (Jul. 2016), pp. 961-975

[126] A. Spyroudi, “Angeliki Spyroudi October 2016,” 2016.

[127] B. Yeter, Y. Garbatov, C. Guedes Soares, Risk-based life-cycle assessment of offshore wind turbine support structures accounting for economic constraints

Struct Saf, 81 (2019), p. Nov

[128] T.S. Schmidt, R. Born, M. Schneider, Assessing the costs of photovoltaic and wind power in six developing countries, Nat. Clim. Chang., 2 (7) (Jul. 2012), pp. 548-553

[129] S. Cavazzi, A.G. Dutton

An Offshore Wind Energy Geographic Information System (OWE-GIS) for assessment of the UK’s offshore wind energy potential, Renew. Energy, 87 (Mar. 2016), pp. 212-228

[130] P. Barutha, A. Nahvi, B. Cai, H.D. Jeong, S. Sritharan, Evaluating commercial feasibility of a new tall wind tower design concept using a stochastic levelized cost of energy model, J. Clean. Prod., 240 (2019)

[131] Y. Xu, K. Yang, and J. Yuan, “Levelized cost of offshore wind power in China,” Environ. Sci. Pollut. Res., pp. 1–14, Jan. 2021.

[132] A. Ioannou, A. Angus, F. Brennan, “Parametric CAPEX, OPEX, and LCOE expressions for offshore wind farms based on global deployment parameters”, Energy Sources, Part B Econ, Planning, Policy, 13 (5) (May 2018), pp. 281-290

[133] E.B. Mora, J. Spelling, A.H. van der Weijde, E.M. Pavageau, The effects of mean wind speed uncertainty on project finance debt sizing for offshore wind farms, Appl Energy, 252 (Oct. 2019), Article 113419

[134] A. Bergmann et al., “A review of levelised cost of energy as applied to the offshore wind industry. An independent report for SeaEnergy PLC & the Energy Technology Partnership (ETP),” 2015. [Online]. Available:https://www.researchgate.net/publication/320410287_A_REVIEW_OF_LEVELISED_COST_OF_ENERGY_AS_APPLIED_TO_THE_OFFSHORE_WIND_INDUSTRY. [Accessed: 20-Feb-2020].

[135] “TLPWIND,” 2018. [Online]. Available: https://ore.catapult.org.uk/stories/tlp-wind/. [Accessed: 21-Jan-2020].

[136] R. Ebenhoch, D. Matha, S. Marathe, P.C. Muñoz, C. Molins, Comparative levelized cost of energy analysis, Energy Procedia, 80 (2015), pp. 108-122

[137] C. Guedes Soares, Ed., Developments in Renewable Energies Offshore, Marine Tec. CRC Press, Taylor & Francis Group, 2021.

[138] B. Sliz-Szkliniarz, J. Eberbach, B. Hoffmann, M. Fortin, Assessing the cost of onshore wind development scenarios: Modelling of spatial and temporal distribution of wind power for the case of Poland

Renew Sustain Energy Rev, 109 (Jul. 2019), pp. 514-531

[139] O. S. Ohunakin, O. M. Oyewola, and M. S. Adaramola, “Economic analysis of wind energy conversion systems using levelized cost of electricity and present value cost methods in Nigeria,” Int. J. Energy Environ. Eng., vol. 4, no. 1, 2013.

[140] V. Gass, J. Schmidt, F. Strauss, E. Schmid, Assessing the economic wind power potential in Austria

Energy Policy, 53 (Feb. 2013), pp. 323-330

[141] A. Sgobba, C. Meskell, On-site renewable electricity production and self consumption for manufacturing industry in Ireland: Sensitivity to techno-economic conditions, J. Clean. Prod., 207 (Jan. 2019), pp. 894-907

[142] M.S. Adaramola, M. Agelin-Chaab, S.S. Paul, Assessment of wind power generation along the coast of Ghana, Energy Convers. Manag., 77 (2014), pp. 61-69

[143] D. Silva Herran, H. Dai, S. Fujimori, T. Masui, Global assessment of onshore wind power resources considering the distance to urban areas, Energy Policy, 91 (2016), pp. 75-86

[144] K. Sunderland, M. Narayana, G. Putrus, and M. Conlon, “Levelised cost of energy analysis: A comparison of urban (micro) wind turbines and solar PV systems,” in Proceedings - 2016 51st International Universities Power Engineering Conference, UPEC 2016, 2016, vol. 2017-Janua, pp. 1–6.

[145] “Homer Pro software,” HOMER Pro, 2020. [Online]. Available: https://www.homerenergy.com/products/pro/index.html. [Accessed: 13-Aug-2020].

[146] R. Carriveau, L. Miller, Economic Sensitivities and Options Surrounding Wind Farm Life Extension

J Phys Conf Ser, 1452 (1) (2020), p. 12047

[147] T. Rubert, P. Niewczas, D. McMillan, Life Extension for Wind Turbine Structures and Foundations

Int. Conf. Offshore Renew. Energy - (2016), pp. 1-12

[148] T. Rubert, D. McMillan, P. Niewczas, A decision support tool to assist with lifetime extension of wind turbines, Renew. Energy, 120 (May 2018), pp. 423-433

[149] V. Mytilinou, A.J. Kolios, Techno-economic optimisation of offshore wind farms based on life cycle cost analysis on the UK, Renew. Energy, 132 (Mar. 2019), pp. 439-454

[150] J. Herman and W. Usher, “SALib : Sensitivity Analysis Library in Python (Numpy). Contains Sobol , SALib : An open-source Python library for Sensitivity Analysis,” vol. 41, no. April, pp. 2015–2017, 2018.

[151] M. Martinez-Luengo, M. Shafiee, Guidelines and cost-benefit analysis of the Structural Health Monitoring implementation in offshore wind turbine support structures, Energies, 12 (6) (2019), pp. 1-26

[152] A. Ioannou, Y. Liang, M.L. Jalón, F.P. Brennan, A preliminary parametric techno-economic study of offshore wind floater concepts, Ocean Eng, 197 (Feb. 2020), Article 106937

[153] R. Martin, I. Lazakis, S. Barbouchi, L. Johanning, Sensitivity analysis of offshore wind farm operation and maintenance cost and availability, Renew. Energy, 85 (2016), pp. 1226-1236

[154] S. Tarantola, W. Becker, “SIMLAB Software for Uncertainty and Sensitivity Analysis”, in Handbook of Uncertainty Quantification, Springer International Publishing (2015), pp. 1-21

[155] A. Saltelli, S. Tarantola, F. Campolongo, Sensitivity analysis as an ingredient of modeling

Stat. Sci., 15 (4) (Nov. 2000), pp. 377-395

[156] “sensitivity-package: Sensitivity Analysis in sensitivity: Global Sensitivity Analysis of Model Outputs.” [Online]. Available: https://rdrr.io/cran/sensitivity/man/sensitivity-package.html. [Accessed: 01-Feb-2021].

[157] A. Puy, W. Becker, S. Lo Piano, and A. Saltelli, “The battle of total-order sensitivity estimators,” arXiv, vol. 9, 2020.

[158] I. Sobol′, Global sensitivity indices for nonlinear mathematical models and their Monte Carlo estimates, Math Comput Simul, 55 (1–3) (Feb. 2001), pp. 271-280

[159] I.M. Sobol, Global sensitivity indices for nonlinear mathematical models. Review, Math Comput Simul, 55 (1–3) (2001), pp. 271-280

[160] T. Wagener and F. Pianosi, “What has Global Sensitivity Analysis ever done for us? A systematic review to support scientific advancement and to inform policy-making in earth system modelling,” Earth-Science Reviews, vol. 194. Elsevier B.V., pp. 1–18, 01-Jul-2019.

[161] S. Razavi, H.V. Gupta, What do we mean by sensitivity analysis? the need for comprehensive characterization of ‘global’ sensitivity in Earth and Environmental systems models, Water Resour Res, 51 (5) (May 2015), pp. 3070-3092

[162] S. Razavi, H.V. Gupta, A new framework for comprehensive, robust, and efficient global sensitivity analysis: 1. Theory, Water Resour Res, 52 (1) (Jan. 2016), pp. 423-439

[163] R. I. Cukier, H. B. Levine, and K. E. Shuler, “Nonlinear sensitivity analysis of multiparameter model systems,” Journal of Computational Physics, vol. 26, no. 1. Academic Press, pp. 1–42, 01-Jan-1978.

[164] A. Saltelli, S. Tarantola, K.P.S. Chan, A quantitative model-independent method for global sensitivity analysis of model output, Technometrics, 41 (1) (1999), pp. 39-56

[165] “R Core Team, R: A Language and Environment for Statistical Computing.” R Foundation for Statistical Computing, Vienna, Austria, 2020.

[166] A.B. Owen, Sobol’ indices and Shapley value, SIAM/ASA J. Uncertain. Quantif., 2 (1) (2014), pp. 245-251

[167] L.S. Shapley, Notes on the n-Pearson game – II: the value of the n-Pearson game

Santa Monica, California (1951)

[168] T. Goda, “A simple algorithm for global sensitivity analysis with Shapley effects.”.

[169] F. Pianosi, T. Wagener, Distribution-based sensitivity analysis from a generic input-output sample

Environ. Model. Softw., 108 (Oct. 2018), pp. 197-207

[170] R. Teixeira, A. O’Connor, M. Nogal, Probabilistic sensitivity analysis of offshore wind turbines using a transformed Kullback-Leibler divergence, Struct Saf, 81 (Nov. 2019), Article 101860

[171] J. Velarde, C. Kramhøft, and J. D. Sørensen, “Global sensitivity analysis of offshore wind turbine foundation fatigue loads,” Renew. Energy, vol. 140, pp. 177–189, Sep. 2019.

[172] S. Zhou, K. Müller, C. Li, Y. Xiao, P.W. Cheng, Global sensitivity study on the semisubmersible substructure of a floating wind turbine: Manufacturing cost, structural properties and hydrodynamics

Ocean Eng, 221 (Feb. 2021), Article 108585

[173] G. Hernández Galvez, et al., Wind resource assessment and sensitivity analysis of the levelised cost of energy. A case study in Tabasco, Mexico, Renew. Energy Focus, Jun., 29 (2019), pp. 94-106

[174] WindPower, “Countries - Online access - The Wind Power - Wind energy Market Intelligence,” 2021. [Online]. Available: https://www.thewindpower.net/country_list_en.php. [Accessed: 04-Feb-2021].

[175] Z. Lv, Z. Wang, and W. Xu, “A techno-economic study of 100% renewable energy for a residential household in China,” Energies, vol. 12, no. 11, 2019.

[176] W. Ma, J. Fan, S. Fang, and G. Liu, “Techno-economic potential evaluation of small-scale grid-connected renewable power systems in China,” Energy Conversion and Management, vol. 196. Elsevier Ltd, pp. 430–442, 15-Sep-2019.

[177] G. Nagababu, S.S. Kachhwaha, V. Savsani, Estimation of technical and economic potential of offshore wind along the coast of India, Energy, 138 (2017), pp. 79-91

[178] I. Tizgui, F. El Guezar, H. Bouzahir, A.N. Vargas, Estimation and analysis of wind electricity production cost in Morocco, Int. J. Energy Econ. Policy, 8 (3) (2018), pp. 58-66

[179] A. Allouhi, Energetic, exergetic, economic and environmental (4 E) assessment process of wind power generation, J. Clean. Prod., 235 (Oct. 2019), pp. 123-137

[180] K. T. Kim, D. J. Lee, and S. J. Park, “Evaluation of R&D investments in wind power in Korea using real option,” Renewable and Sustainable Energy Reviews, vol. 40. Elsevier Ltd, pp. 335–347, 2014.

[181] A. T. D. Perera, R. A. Attalage, and K. K. C. K. Perera, “Optimal design of a grid connected hybrid electrical energy system using evolutionary computation,” 2013 IEEE 8th Int. Conf. Ind. Inf. Syst. ICIIS 2013 - Conf. Proc., pp. 12–17, 2013.

[182] M.R. Elkadeem, S. Wang, S.W. Sharshir, E.G. Atia, Feasibility analysis and techno-economic design of grid-isolated hybrid renewable energy system for electrification of agriculture and irrigation area: A case study in Dongola, Sudan, Energy Convers. Manag., 196 (2019), pp. 1453-1478

[183] C. Diyoke, M. Aneke, M. Wang, C. Wu, Techno-economic analysis of wind power integrated with both compressed air energy storage (CAES) and biomass gasification energy storage (BGES) for power generation, RSC Adv, 8 (39) (2018), pp. 22004-22022

[184] E.A. Martinez-Cesena, J. Mutale, Wind power projects planning considering real options for the wind resource assessment, IEEE Trans. Sustain. Energy, 3 (1) (2012), pp. 158-166

[185] K. S. R. Murthy and O. P. Rahi, “A comprehensive review of wind resource assessment,” Renewable and Sustainable Energy Reviews, vol. 72. Elsevier Ltd, pp. 1320–1342, 2017.

[186] V. Noacco, F. Sarrazin, F. Pianosi, T. Wagener

Matlab/R workflows to assess critical choices in Global Sensitivity Analysis using the SAFE toolbox

MethodsX, 6 (2019), pp. 2258-2280

[187] C. Ball, “Crystal Ball 7.2.2 ®.” [Online]. Available: http://www.uca.edu.sv/facultad/clases/maestrias/mafi/m230106/CB7 User Manual.pdf. [Accessed: 17-Dec-2019].

[188] Oracle, “Oracle Crystall Ball 11.1.2 User Guide: Benefits and limitations of sensitivity charts,” 2012. [Online]. Available: https://docs.oracle.com/cd/E17236_01/epm.1112/cb_user/frameset.htm?ch07s04s01.html.

[189] “The Crystall Ball charts: Sensitivity,” 2017. [Online]. Available: https://www.oracle.com/technetwork/middleware/crystalball/overview/sensitivity-chart-128074.pdf. [Accessed: 17-Dec-2019].

[190] A. B. looss et al., “Package ‘ sensitivity ,’” 2021. [Online]. Available: https://cran.r-project.org/web/packages/sensitivity/sensitivity.pdf. [Accessed: 02-Aug-2021].

[191] E. Borgonovo, A new uncertainty importance measure, Reliab Eng Syst Saf, 92 (6) (2007), pp. 771-784

[192] “fast: Implementation of the Fourier Amplitude Sensitivity Test (FAST) version 0.64 from CRAN.” [Online]. Available: https://rdrr.io/cran/fast/. [Accessed: 01-Feb-2021].

[193] “multisensi-package: Multivariate sensitivity Analysis in multisensi: Multivariate Sensitivity Analysis.” [Online]. Available: https://rdrr.io/cran/multisensi/man/multisensi-package.html. [Accessed: 01-Feb-2021].

[194] S. Kucherenko and O. Zaccheus, “SobolGSA Software | Research groups | Imperial College London,” Imperial College London, 2021. [Online]. Available: https://www.imperial.ac.uk/process-systems-engineering/research/free-software/sobolgsa-software/. [Accessed: 01-Feb-2021].

[195] B. M. Adams et al., “Dakota A Multilevel Parallel Object-Oriented Framework for Design Optimization Parameter Estimation Uncertainty Quantification and Sensitivity Analysis: Version 6.12 User?s Manual.,” Albuquerque, NM, and Livermore, CA (United States), May 2020.

[196] M. Baudin, A. Dutfoy, B. Looss, A.L. Popelin

“OpenTURNS: An industrial software for uncertainty quantification in simulation”, in Handbook of Uncertainty Quantification, Springer International Publishing (2017), pp. 2001-2038

[197] C. Tong, “PSUADE Reference Manual,” pp. 1–26, 2015.

[198] S. Razavi, R. Sheikholeslami, H.V. Gupta, A. Haghnegahdar

VARS-TOOL: A toolbox for comprehensive, efficient, and robust sensitivity and uncertainty analysis, Environ. Model. Softw., 112 (2019), pp. 95-107

[199] V.V. Vesselinov, B.S. Alexandrov, D. O’Malley, Nonnegative tensor factorization for contaminant source identification, J Contam Hydrol, 220 (2019), pp. 66-97

[200] I.M. Sobol, Global sensitivity indices for nonlinear mathematical models and their Monte Carlo estimates, Math Comput Simul, 55 (1–3) (Feb. 2001), pp. 271-280

[201] M.J.W. Jansen, Analysis of variance designs for model output, Comput Phys Commun, 117 (1) (1999), pp. 35-43

[202] A. Puy, S. Lo Piano, and A. Saltelli, “Is VARS more intuitive and efficient than Sobol’ indices?,” Sep. 2021.

[203] K. Menberg, Y. Heo, R. Choudhary, Sensitivity analysis methods for building energy models: Comparing computational costs and extractable information, Energy Build, 133 (2016), pp. 433-445

[204] S. Burhenne, O. Tsvetkova, D. Jacob, G.P. Henze, A. Wagner, Uncertainty quantification for combined building performance and cost-benefit analyses, Build Environ, 62 (2013), pp. 143-154

[205] O. Tsvetkova, Uncertainty and sensitivity analysis for decision support in building design, Albert Ludwig University of Freiburg (2011)

4 QUASI-MONTE CARLO TECHNIQUE IN GLOBAL SENSITIVITY ANALYSIS OF WIND RESOURCE ASSESSMENT WITH A STUDY ON UAE

Titre de l'article :

TECHNIQUE QUASI-MONTE CARLO DANS L'ANALYSE DE SENSIBILITÉ GLOBALE DE L'ÉVALUATION DES RESSOURCES ÉOLIENNES AVEC UNE ÉTUDE SUR LES EAU

Authors :

Olga Tsvetkova, INRS-ETE

Taha B.M.J. Ouarda, INRS-ETE

Titre of book or journal :

Journal of Renewable and Sustainable Energy

Date of publication : 2019/10/7

DOI : https://doi.org/10.1063/1.5120035

Contribution of authors :

Olga Tsvetkova: Conceptualization, Methods, Writing - Original draft preparation.

Taha B.M.J. Ouarda: Funding acquisition, Supervision, Writing - Reviewing and Editing.

4.1 Abstract

The present paper bridges mathematical modeling and wind resource assessment. Sensitivity analysis links portions of output variance to the variance in each input variable. Global sensitivity analysis explores inputs globally. One-at-a-time sensitivity analysis is dominating in wind resource assessment, while global sensitivity analysis is often overlooked. Compared to traditional methods global sensitivity analysis offers potential improvement by the means of quasi-Monte Carlo technique with its elaborate sampling designs enabling faster convergence. The main novelty of this work is twofold: the use of quasi-Monte Carlo in wind resource assessment and Sobol method as a variance-based global sensitivity analysis method in wind resource assessment. This paper is among a few using global sensitivity analysis in wind resource assessment. Two case studies were conducted. One shows that quasi-Monte Carlo with sampling based on Sobol sampling outperforms Latin hypercube sampling and pseudo-random sampling. It also shows that in terms of accuracy of results brute-force calculation of Sobol sensitivity indices should be used whenever the model allows it, otherwise sensitivity indices can be estimated. Another case study demonstrates a valid global sensitivity analysis study for wind resource assessment at Masdar City, United Arab Emirates. The results suggest the influence of the variance in Weibull parameters on annual energy production might be overestimated, while found to be responsible for 2% of annual energy production uncertainty, and the influence of the variance in air density might be overlooked, while found to account for 94%. Wind resource assessment studies would benefit greatly from using quasi-Monte Carlo and the Sobol method. The Sobol method is a universal global sensitivity analysis method providing valid results for nonlinear models typical for wind resource assessment and quasi-Monte Carlo provides global scalability, model independence, and flexibility in uncertainty quantification.

4.2 Nomenclature

$\widehat{S_{T_i}}$	Estimates of Sobol total effect sensitivity indices with the use of Jansen estimator [1][2]
$\widehat{S_i}$	Estimates of Sobol first-order sensitivity indices with the use of Saltelli estimator [2]
$A_B^{(i)}$	$N \times k$ matrix where all columns except for *i*-th come from *A* and *i*-th column comes from *B*
N_r	Number of replicas of a Monte Carlo/quasi-Monte Carlo experiment
R_{spec}	Specific gas constant of dry air, $R_{spec} = 287.058 \frac{J}{kg\,K}$
S_{T_i}	Sobol total effect sensitivity indices [3]
S_i	Sobol First-order sensitivity indices [3]
V_{T_i}	a variance based on total effect for a factor X_i
V_i	a variance based on first-order effect for a factor X_i
$X_{\sim i}$	$N \times (k-1)$ matrix of all factors but X_i
X_i	Generic input variable, vector of $N \times 1$
$a_{j,k}$	Binary coefficients in Sobol sequence generation
g_i	Terms of analytical G-function used as the test model
$m_{j,k}$	Sobol sequence generation
s_j	Order of a polynomial used in Sobol sequence generation
$v_{j,k}$	Direction numbers in Sobol sequence generation
$x_{i,j}$	j^{th} component of the i^{th} point in a Sobol sequence
AEP	Annual energy production
CFD	Computational fluid dynamics
ECDF	Empirical cumulative distribution function
FiT	Feed-in tariff
FOWF	Floating offshore windfarm
GOF	Goodness-of-fit
GSA	Global sensitivity analysis
IRR	Internal rate of return
LCOE	Levelised cost of energy
LHS	Latin hypercube sampling
MAE	Mean absolute error as defined in [2]
MC	Monte Carlo
MCP	Measure-correlate-predict
MLE	Maximum likelihood estimation
NPV	Net present value
OAT	One-at-a-time
OWF	Offshore wind farm
O&M	Operation and maintenance
PDF	Probability density function
PRNG	Pseudo-random number generator
PRS	Pseudo-random sampling
QMC	Quasi-Monte Carlo
SA	Sensitivity analysis
SBSS	Sampling based on Sobol sequences
SI	Sensitivity indices
SS	Stratified sampling

UA	Uncertainty analysis
UAE	United Arab Emirates
W2	The two-parameter Weibull distribution
WRA	Wind resource assessment
WRF	Weather research and forecasting
λ	Scale parameter of the two-parameter Weibull distribution
ρ	Air density
A	$N \times k$ sample matrix of input variables used
AEP	Annual energy production at Masdar City
B	$N \times k$ sample matrix of input variables used
EL	Electric losses
$MAE(\widehat{S_{T_i}})$	Mean absolute error of total effect sensitivity indices [2]
$MAE(\widehat{S_i})$	Mean absolute error of first-order sensitivity indices [2]
N	Sample size used in MC/QMC experiments (number of model runs)
T	$2N \times 2k$ sample matrix of input variables used to implement radial design described by Saltelli in [2]
V	Total variance of a model
X	$N \times k$ matrix of all input variables
Y	Vector model output of $N \times 1$
a	Availability of a wind turbine for energy production
c	Shape parameter of the two-parameter Weibull distribution
k	Number of input variables
p	Atmospheric pressure
s	Number of strata in case of Latin hypercube sampling
t	Absolute air temperature
w	Wind speed time series

4.3 Introduction

Sensitivity analysis (SA) is a study of apportioning the uncertainty in the output variable of interest to the uncertainty in each input variable [3]. Although SA is an important practice related to uncertainty analysis (UA) [3] and is meant to complement UA [4], SA may be performed perfunctorily [4][5]. The problems with SA practices at large are unveiled across engineering fields by recent systematic reviews of Feretti et al. [5] and Saltelli et al. [6]. This paper looks at how SA is performed in WRA and offers possible improvement to current practice. Global SA (GSA) explores each input variable over its entire range of interest and provides valid results for any model [3]. The main drawback of GSA as Wagener & Pianosi have pointed out "*is the possibly significant impact of the chosen input distributions, which should be carefully scrutinized*" [7]. Although "a sign of improvements in the take up of GSA" is marked, GSA is "*still applied by a minority of researchers*" [5]. Instead, easy to implement one-at-a-time (OAT) methods [8] that vary one parameter while keeping all others fixed are widely used [4][5][6], although one should be cautious of such methods as they are "predicated on assumptions of model linearity" [6]. Saltelli et al. voiced reasonable concern about OAT SA results by publishing geometric proof of its inefficiency as "*a convincing … argument against OAT*" [4]. Nonetheless, researchers "*seem reluctant to abandon this [OAT] practice*" [4]. Although an attempt to popularize GSA and increase SA quality in the environmental modelling community has already been made by Pianosi et al. by introducing a Matlab toolbox for GSA [9], it has come to the authors' attention that OAT is commonly used in WRA [10][11][12][13][14][15], hence the authors intend to continue this effort.

It is expensive to explore variable input space as the number of dimensions grows, yet it is not a reason to practice OAT for nonlinear models. In fact, GSA (variance-based or other) offers ways to globally explore high-dimension models with the use of quasi-Monte Carlo (QMC) technique [16]. To conduct a variance-based GSA study it is necessary to run a Monte Carlo (MC) or a QMC experiment. MC is a "*universal uncertainty quantification tool with applications across all engineering fields with only computational cost being a limiting factor*" [17]. QMC helps mitigate this barrier by using elaborate sampling designs as the results of a QMC experiment converge faster than those of a MC experiment [17][18][19]. The difference between a MC and a QMC experiment lies in how random numbers are generated. A MC experiment uses common pseudo-random sampling (PRS), while QMC uses other sampling strategies, for example, Latin hypercube sampling (LHS) or sampling based on low discrepancy Sobol sequences (SBSS).

WRA mostly deals with estimates (often point [20][21][22]) of wind power or annual energy production (AEP) cubically proportional to the wind speed. MC in WRA is usually used for

windfarm layout optimization [23][24] or profitability UA [10] [25][26][27][28][29] often with no SA accompanying. In wind turbine specific studies, MC was also used for stochastic blade flutter analysis [30], turbine reliability [31] and fatigue loads [32][33] assessments. To the best of authors' knowledge, SA in WRA commonly uses OAT methods [10][11][12][13][14][15], that disregard model nonlinearity [4][5][6]. Only a few WRA studies have used GSA [34][35][36]. Di et al. used multivariate adaptive regression for optimizing numerous parameters of a weather research and forecasting (WRF) model for more accurate wind power prediction [34]. McKay et al. used Fourier amplitude sensitivity test for wind power output [35]. Ulker et al. studied sensitivity-guided decision-making for wind farm micro-siting and Sobol method was part of the study [36]. It is worth mentioning a broader study on levelised cost of energy (LCOE) of different energy sources (including onshore and offshore wind) that used Sobol method [37].

The main reason for using QMC in WRA is that it enables the application of GSA methods, such as Sobol method, that account for model nonlinearity. There are also several benefits to using QMC in general, such as global scalability, model independence, and flexibility. The first benefit is that QMC is what makes GSA practically feasible in case of numerous input variables. Second, QMC provides a way to conduct a GSA regardless of the computational demand the model of interest imposes. In application to WRA, one can model wind with a distribution (Weibull [38][39] or other [40][41]) or using more time-consuming computational fluid dynamics (CFD) [42][43][44] or WRF [45][46] models. The third benefit is flexibility. One might have limited data about the variables of the output model or assumptions about the underlying distributions of input variables. One might use parametric or non-parametric models to describe input variables. Whichever the case, one can incorporate all the knowledge about a particular site available into a GSA study with the use of QMC. As more data or knowledge become available, the GSA study can be elaborated and results that are more accurate can be obtained. There is also a side benefit to using QMC for GSA – the same QMC experiments yields both UA and GSA results. UA shows how uncertain the estimate of the output variable is and GSA apportions output uncertainty to uncertainty in the input variables.

QMC technique has been applied in wind related studies [18][33][47], but not to WRA specifically. Sobol method as a variance-based GSA, the focus of this study, has received little attention in WRA [36]. Estimation of Sobol indices has not yet been used in WRA. Therefore, the main novelty of this work is twofold: the use of QMC in WRA and Sobol method for GSA in WRA, as both have not received much attention. The present paper aims to fill in this gap by bridging mathematical modelling and WRA, as well as popularize GSA and exemplify a GSA study for

WRA. Two case studies were carried out. One using a test model to show QMC is superior to MC and compare brute force Sobol method with its estimation. Another using UAE data to demonstrate how a GSA (and UA) using QMC and Sobol method could be set up in the context of WRA.

This paper is organized into four main sections: introduction, methods, results, conclusions and future research. The introduction presented the problem associated with SA in WRA. The methods section contains three subsections: sampling techniques used in MC/QMC, variance-based GSA and experimental design. Sampling techniques subsection summarizes sampling techniques used throughout this paper, namely PRS, LHS, SBSS. Variance-based GSA subsection reviews brute force calculation of Sobol first-order and total effect sensitivity (SI) and their estimation. Experimental design subsection contains two parts: the test model and the WRA model in Masdar City case study. It gives details on the setup of the experimental part of this work and methods used in WRA such as the Weibull distribution to fit wind speed data and to calculate AEP. The assumptions about underlying distributions of input variables to the WRA model are given in this subsection. The results section provides the results of GSA for the test and WRA models. Test model results include the comparison of sampling strategies in the light of GSA in WRA. WRA model results contain results of GSA and UA for WRA at Masdar City, UAE. The conclusions and future research section presents conclusions made along with the suggestions for possible directions for future research.

4.4 Methods

In this section the methods used are explained, the experimental design of the two case studies is presented, and the details about the data and the assumptions used in the UAE case study are provided.

4.4.1 Sampling techniques in MC/QMC experiment

Sampling is the foundation of any MC/QMC experiment. It is important to understand how different sampling strategies affect the results of MC/QMC simulations. As mentioned in the introduction, a QMC experiment differs from a MC experiment in the way random numbers are generated. A MC uses PRS, while QMC uses sampling strategies other than PRS aimed to reduce computational cost of MC by enabling faster convergence of results. The computational cost of MC is an important barrier to its applicability, but in most cases it can be overcome with a good sampling strategy [17].

4.4.1.1 Pseudo-random sampling (PRS)

Pseudo-random sampling (PRS) generates a sequence of random numbers with a pseudo-random number generator (PRNG). PRNG is an algorithm for generating a sequence of numbers determined by the initial key, called a seed, for generating a sequence [46]. The main weakness of random sampling in relation to the problem of GSA is poor dimensional distribution. A random sample typically has gaps and clusters [3] which can play a significant role in the results of GSA, meaning it does not provide a uniform exploration of the variable space. Figure 4.1 exhibits a two-dimensional pseudo-random sample and one can see the gaps and clusters of sampled points with a naked eye.

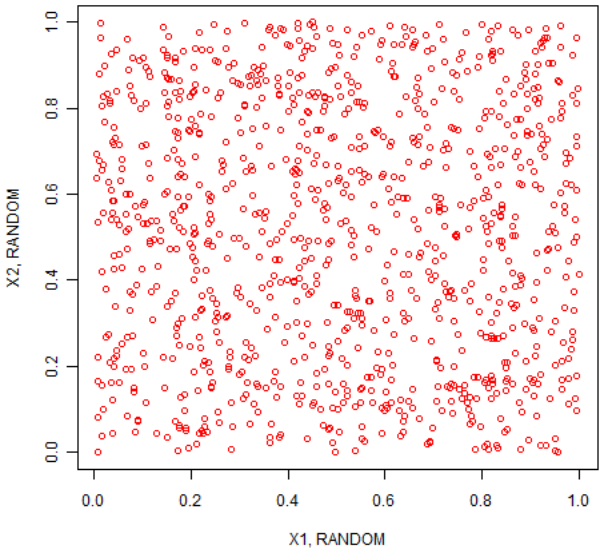

Figure 4.1 Two-dimensional pseudo-random sample

4.4.1.2 Latin hypercube sampling (LHS)

In a GSA problem setting, a homogeneous sample is a critical point as it allows a homogeneous input space exploration and stratified sampling aims at avoiding gaps and clusters typical in PRS. Figure 4.2 exhibits a large two-dimensional LHS sample (N = 1000). More homogeneity in Figure 4.2 can be observed compared to the pseudo-random sample in Figure 2.1.

As a way to overcome the flaws of PRS, stratified sampling (SS) was invented. SS is sampling with a PRNG but at different intervals or strata providing a somewhat more “homogeneously” distributed sample. LHS is a particular kind of SS. The main goal of LHS is to

make sure each variable is individually stratified over s levels (s>2), and that each level contains an equal number of points [48]. Figure 4.3 emphasizes this property. Each of the fifteen horizontal and vertical strata in Figure 4.3 contains strictly one point. The rectangles in Figure 4.3 outline this very property.

The conditions of LHS require that s divides into the sample size N [3]. As a result of such sampling design, LHS has some attractive advantages [3]:

The estimate of the mean converges faster to the true value compared to the one corresponding to a random sample. This means that smaller sample size is necessary for QMC experiment to converge compared to MC. When the model is computationally expensive, it adds up to a significant time difference between MC and QMC experiments;

When the output function is monotonic in each of the inputs X_i, a sample would have less uncertainty with LHS compared to PRS at any sample size N [3].

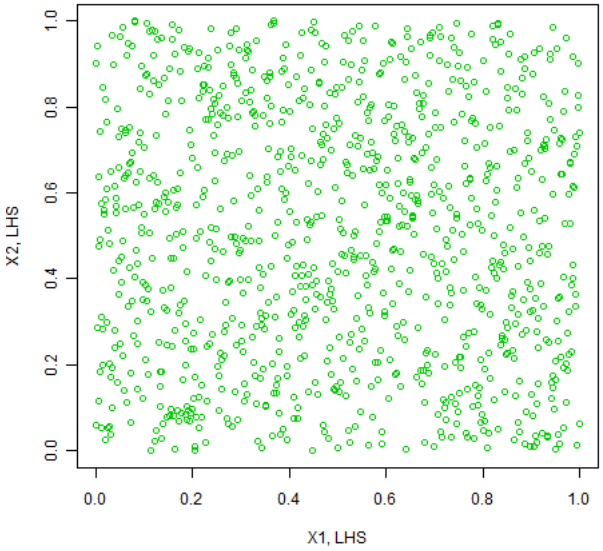

Figure 4.2 A two-dimensional LHS sample (N= 1000)

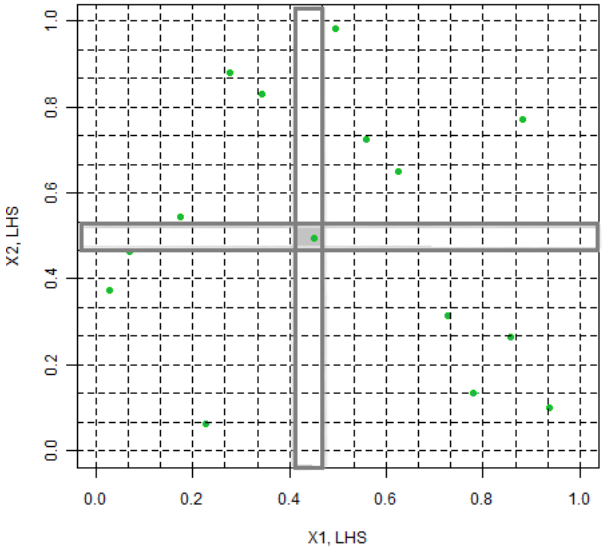

Figure 4.3 A two-dimensional LHS sample (N = 15, s = 15)

LHS could be perceived as a compromise between PRS and stratified sampling, and the LHS procedure produces more stable results compared to those of PRS [48]. The superiority of LHS over PRS has been corroborated often enough, and LHS is generally recommended for use instead of PRS, as it is "*an undemanding upgrade, but it substantially boosts convergence and applicability*" [17].

4.4.1.3 Sampling based on Sobol sequences (SBSS)

Another sampling used in QMC is sampling based on low-discrepancy sequences, such as Sobol sequences that use two as a base and uniformly partition given interval by a recursive algorithm. The recursive component in the algorithm is the principal difference between SBSS and other sampling strategies. Sobol sequences are examples of low-discrepancy sequences (sequences, with a low distance between sampled points) , that were first introduced by Sobol in 1967 [49]. The lower the discrepancy of a sample, the better it is for the purpose of conducting GSA [3]. Low-discrepancy sequences have a very important property: as the sequence length N increases, the discrepancy decreases.

Figure 4.4 exhibits a two-dimensional Sobol sample. One can notice the low distance between sampled points and more order and homogeneity in Figure 4.4 compared to LHS (Figure 4.2), and to the pseudo-random sample in Figure 4.1.

Bratley & Fox provide an implementation algorithm of generating Sobol sequences in [50]. A procedure of defining the j^{th} component of points in a Sobol sequence is summarized below.

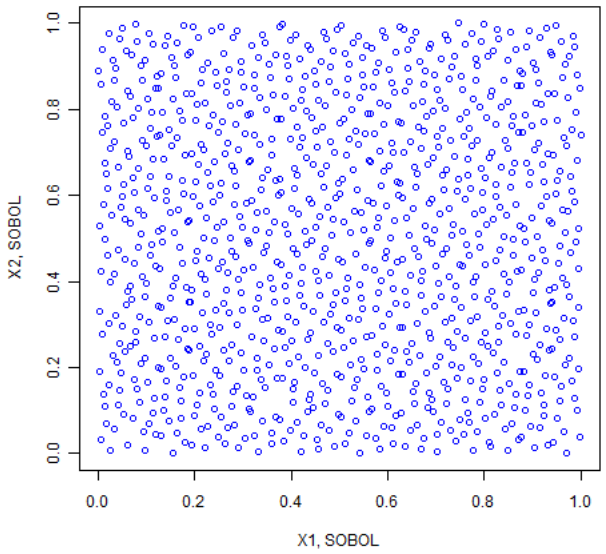

Figure 4.4 A two-dimensional Sobol sample (N = 1000)

A primitive polynomial of the degree s_j of the form given in Eq. (28) should be chosen:

$$x^{s_j} + a_{1,j}x^{s_j-1} + \cdots + a_{s_j-1,j}x + 1, \tag{28}$$

Where coefficients $a_{1,j}, \ldots, a_{s_j-1,j}$ are binary.

The coefficients $a_{1,j}, \ldots, a_{s_j-1,j}$ are used to define a sequence $\{m_{1,j}, m_{2,j}, \ldots\}$ consisting of positive integers with the following recursive function:

$$m_{k,j} = 2a_{1,j}m_{k-1,j}XOR2^2a_{2,j}m_{k-2,j}XOR \ldots \tag{29}$$

$$\ldots XOR\ 2^{s_j-1}a_{s_j-1}m_{k-s_j+1,j}\ XOR\ 2^{s_j}m_{k-s_j,j}XOR\ m_{k-s_j,j},$$

For $k \geq s_j + 1$. *XOR* is a bit-by-bit exclusive *OR* operator. Initial values of $m_{k,j}, k = 1 \ldots s_j$ should satisfy the condition of being odd and less than 2^k.

The so-called direction numbers $v_{k,j}, , k = 1 \ldots s_j$ are defined as:

$$v_{k,j} = {}^{m_{k,j}}/_{2^k} \tag{30}$$

Finally, the *j*th component of the *i*th point in a Sobol sequence is:

$$x_{i,j} = b_1v_{1,j}XORb_2v_{2,j}XOR \ldots, \tag{31}$$

This algorithm is implemented in *randtoolbox* package in R [51].

4.4.1.4 PRS, LHS, SBSS comparison

Section 4.4.1.4 touches on the quality of space exploration in a MC/QMC experiment and how the properties of samples are responsible for it. To this end, two-dimensional samples produced by PRS (Figure 4.1), LHS (Figure 4.2), and SBSS (Figure 4.4) are compared. A pseudo-random sample (Figure 4.1) has many holes and clusters and is the opposite of homogeneity, a property important for thorough input space exploration necessary for GSA. LHS produces a more homogeneous sample (Figure 4.2) compared to PRS, yet it still has some holes and clusters, although almost not visible with a naked eye. But the homogeneity of a Sobol sample (Figure 4.4) is evident compared to both pseudo-random (Figure 4.1) and LHS samples (Figure 4.2).

Moving on to multidimensional space exploration in a MC/QMC experiment using PRS, LHS, and SBSS, Figure 4.5 exhibits projections of the three-dimensional uniformly distributed pseudo-random, LHS and Sobol samples on to *X1X2*, *X2X3* and *X1X3* planes. In Figure 2.5 one can see the same shift from non-homogeneity in a pseudo-random sample to homogeneity in a Sobol sample observed when comparing Figures 4.1, 4.2 and 4.4, but now in every two-

dimensional projection (Figure 4.5). Now imagine we move to an *N*-dimensional hypercube of a MC/QMC experiment with *N* input variables. Obviously, the non-homogeneity of PRS becomes more of a problem as the sample size grows.

The discrepancy decrease is the reason SBSS produces an increased quality of the multivariate sample in terms of homogeneity and therefore better input space exploration. Figure 4.5 aims to exhibit precisely this property in case of a three-dimensional problem. Figure 4.5 emphasizes the fact that requirements to the quality of a multivariate sample increase as the number of inputs increases, and the famous curse of dimensionality manifests itself[5]. Tarantola et al. investigated this problem in [52] where they compared convergence properties of SBSS and LHS and recommended using SBSS for most practical cases.

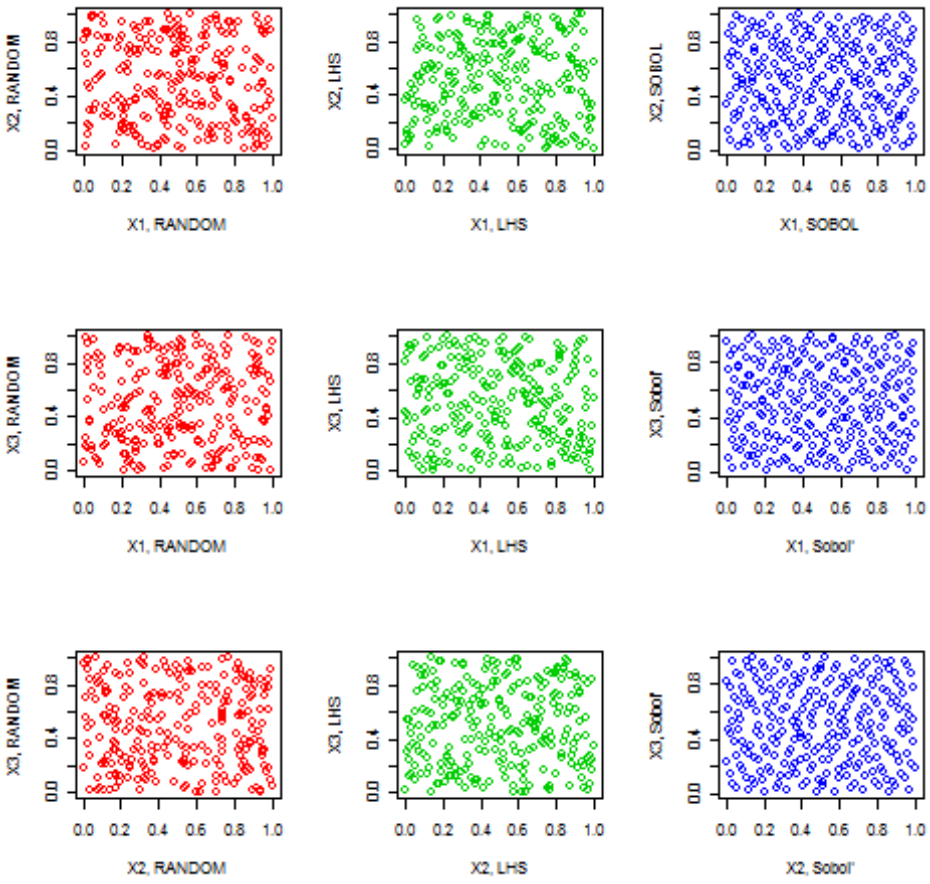

Figure 4.5 Projections of a three-dimensional random (left), LHS (center) and Sobol (right) samples (N = 1000)

[5] As the dimensionality grows, the volume of the hypercube explodes making a sample sparse. This sparsity stands in the way of any method that requires statistical significance. The amount of data necessary to back up a statistically sound result grows with the dimensionality.

4.4.2 Variance-based global sensitivity analysis (GSA)

Variance-based methods constitute a class of GSA based on decomposing the variance of model output. The most interesting features of variance-based GSA methods account for nonlinearity, provide a tool for investigating the influence of the full range of variation of the inputs, and provide the capacity to work with groups of factors [3].

The main drawback of GSA as mentioned in the introduction is the impact of assumptions about underlying distributions of the input variables [7]. Another drawback of variance-based methods is the same as of any MC simulation as they use MC/QMC, i.e. their computational cost in case of complex models and numerous inputs. Although this is not a concern for the presented UAE case study, it could be if distribution parameters were evaluated for every model run. Although numeric wind models are outside the scope of this paper, if a CFD or a WRF was used to model the wind SBSS would be useful and would serve as a significant timesaver for the QMC experiment.

Among GSA methods there are also moment-independent methods [53] and density or distribution based methods [54][75]. For a review of GSA in earth system modeling refer to Pianosi et al. [7], for a review of global and local SA methods – to Borgonovo & Plischke [55]. Also Plischke et al. published a detailed review of global sensitivity measures [56]. Guidelines for application of GSA can be found in [4]. For a comparison of variance-based methods to moment- methods refer to Zadeh et al. [53].

4.4.2.1 Sobol method: brute force

Among GSA methods “the most well-established and widely-applied one is probably the variance-based method of Sobol” [53]. This method is sometimes referred to as Sobol SI method, Sobol SA or simply Sobol method. The Sobol method is based on calculating global sensitivity indices (SI) - first-order and total effect – and was first mentioned by Sobol & Kucherenko in 1990 [57]. SI are calculated for each input factor and serve as a measure of importance of this factor in relation to the influence on model output. The term “importance” is used to express the relative contribution of variable to the uncertainty in the output. Sobol published a review of global SI in [58].

If a model is given in the form $Y = f(X) = f(X_1, X_2, \dots, X_k)$, the variance based on first-order effect for a factor X_i can be written as $V_i = V_{X_i}(E_{X_{\sim i}}(Y|X_i))$ where $X_{\sim i}$ denotes the matrix of all factors but X_i [2]. The meaning of the inner expectation operator is that the mean of Y is taken

over all possible values of $X_{\sim i}$ while keeping the X_i factor fixed. The outer variance is taken over all possible values of X_i. The associated sensitivity measure, first-order sensitivity index, is equal to:

$$S_i(Y) = \frac{V_i}{V(Y)} = \frac{V_{X_i}(E_{X\sim i}(Y|X_i))}{V(Y)} \tag{32}$$

Where *V(Y)* is defined as the variance of model output.

The first-order SI defined in (5) are the main measure used for ranking input factors according to their influence on the model output.

The total effect sensitivity index S_{T_i} of a factor i measures the total effect of this factor on model output, that includes first and higher order effects (or interactions) of factor X_i. One way to visualize the meaning of a total effect sensitivity index is by considering that $V_{X_{\sim i}}(E_{Xi}(Y|X_{\sim i}))$ is the first-order effect of $X_{\sim i}$, so that $V(Y)$ minus $V_{X_{\sim i}}(E_{Xi}(Y|X_{\sim i}))$ must give the contribution of all terms in the variance decomposition which include X_i. This measure gives extra information about the input factors, i.e. how active a factor is in interacting with other factors (dependence of input factors).

Ideally, input factors should be independent from one another, which is hardly the case in real world applications. In case of independent input factors, the first-order SI are sufficient. When some factors are not independent, the calculation of total effect indices is necessary along with calculation of first-order SI. The definition of a total effect sensitivity index [2] is:

$$S_{T_i}(Y) = \frac{V_{T_i}}{V(Y)} = \frac{E_{X\sim i}(V_{X_i}(Y|X_i))}{V(Y)} = 1 - \frac{V_{X_{\sim i}}(E_{Xi}(Y|X_{\sim i}))}{V(Y)} \tag{33}$$

Both first-order and total effect SI can be calculated with a brute force method, i.e. according to their definitions in (5) and (6). Brute force is only applicable in the case of a simple model and a small number of inputs, such as the case study on UAE presented in this paper. As the number of input variables increases or the model becomes too complex, SI brute force calculation is no longer computationally affordable. In such cases estimation of SI can be used. For example, if CFD or WRF models were to be used to model wind, estimation of SI can be used instead.

4.4.2.2 Sobol method: Saltelli and Jansen estimators

SI estimation provides ways to estimate SI instead of computing them using brute force which could be computationally not feasible when the curse of dimensionality is an issue for a given experimental design. There is ongoing research on the ways of estimating global Sobol SI

[59][60][61]. A number of estimation methods are ready for use in Sensitivity package in R [51]. The estimation method of global SI the authors used for the test model case study is referred to simultaneous computation of estimates of first-order SI and total effect indices with the use of Sobol sampling, radial design and Jansen estimator described in [1].

Model variance $V(Y)$ can be calculated as follows [3]:

$$V(Y) = \frac{1}{N}\sum_{j=1}^{N}\left(f(A)_j^2\right) - \left(\frac{1}{N}\sum_{j=1}^{N}\left(f(A)_j\right)\right)^2 \tag{34}$$

Saltelli et al. compared different schemes for estimating SI in [2] and found that the first order SI S_i should be computed according to Eq. (35), and total effect SI S_{T_i} – according to Eq. (36).

Eq. (35) is also called Saltelli estimator (Saltelli *et al.*, 2010) and Eq. (36) is referred to as Jansen estimator (Jansen, 1999).

$$S_i(Y) = \frac{V_{X_i}(E_{X\sim i}(Y|X_i))}{V(Y)} = \frac{\frac{1}{N}\sum_{j=1}^{N} f(B)_j\left(f(A_B^{(i)})_j - f(A)_j\right)}{\frac{1}{N}\sum_{j=1}^{N}\left(f(A)_j^2\right) - \left(\frac{1}{N}\sum_{j=1}^{N}\left(f(A)_j\right)\right)^2}, \tag{35}$$

$$S_{T_i}(Y) = \frac{E_{X\sim i}(V_{X_i}(Y|X_i))}{V(Y)} = \frac{\frac{1}{2N}\sum_{j=1}^{N}\left(f(A_B^{(i)})_j - f(A)_j\right)^2}{\frac{1}{N}\sum_{j=1}^{N}\left(f(A)_j^2\right) - \left(\frac{1}{N}\sum_{j=1}^{N}\left(f(A)_j\right)\right)^2} \tag{36}$$

The matrix T of size $(2k, 2N)$ is generated with the use of SBSS. Then, the matrix A would be assigned the value of the upper left matrix of size (k, N) and B – the lower right matrix of the same size as A. This is what Saltelli et al. call the radial design [2].

$$T = \begin{pmatrix} A & \vdots \\ \ldots & B \end{pmatrix} \tag{37}$$

$$A = \begin{pmatrix} a_{11} & \ldots & a_{1k} \\ a_{21} & \ldots & a_{1k} \\ \vdots & \ddots & \vdots \\ a_{N1} & \ldots & a_{Nk} \end{pmatrix} \qquad B = \begin{pmatrix} b_{11} & \ldots & b_{1k} \\ b_{21} & \ldots & b_{1k} \\ \vdots & \ddots & \vdots \\ b_{N1} & \ldots & b_{Nk} \end{pmatrix} \tag{38}$$

The matrices A, B are used to form the $A_B^{(i)}$ matrices. The matrices $A_B^{(i)}$ are generated according to Eq. (39), all of the columns come from matrix A, except for the i^{th} column which comes from matrix B [2];

$$A_B^{(i)} = \begin{pmatrix} a_{11} & \cdots & b_{1i} & \cdots & a_{1k} \\ \vdots & \ddots & \vdots & \ddots & \vdots \\ a_{N1} & \cdots & b_{Ni} & \cdots & a_{Nk} \end{pmatrix} \quad (39)$$

The implementation this estimation procedure is summarized below:

1. Sample the matrices *A, B* with SBSS according to Eq. (37);
2. Generate $A_B^{(i)}$ matrices according to Eq. (39);
3. Calculate model outputs *Y(A)*, *Y(B)* and *Y($A_B^{(i)}$);*
4. Compute first-order and total effect SI according to Eq. (35) and (36) respectively.

Sensitivity package in R offers an implementation of this procedure called *soboljansen* [51].

4.4.3 Experimental design

The numerical experiment consisted of two parts:

1. Testing sampling strategies on a test model for which analytical values of SI are available and choosing the best performance variance-based GSA method and sampling strategy according to test model results;
2. Performing GSA with the sampling strategy identified as best performing for the WRA model, i.e. annual energy production *AEP.*

The numerical experiment with the test model is aimed at defining the best GSA method and sampling strategy for the WRA model. To obtain robust results, a high number of replicas N_r of calculating a set of first-order SI S_i is used (number of replicas of experiment $N_r = 1000$). The ranking accuracy is calculated as:

$$Accuracy = \frac{N_{identical}}{N_r} \times 100\%, \quad (40)$$

Where $N_{identical}$ is the number of replicas when the ranking obtained in a numerical experiment matches the analytical ranking and N_r is the overall number of replicas of MC/QMC experiment.

Saltelli et al. used the following definitions of mean absolute error (MAE) for numerical experiments of convergence of first-order and total effect SI for a set of test functions in [2]:

$$MAE(\widehat{S_i}) = \frac{1}{Nr} \sum_{j=1}^{Nr} \sum_{i=1}^{k} \left| \widehat{S_i}(j) - S_i \right| \quad (41)$$

$$MAE(\widehat{S_{T_i}}) = \frac{1}{Nr}\sum_{j=1}^{Nr}\sum_{i=1}^{k}\left|\widehat{S_{T_i}}(j) - S_{T_i}\right| \tag{42}$$

Where $\widehat{S_i}(j)$, $\widehat{S_{T_i}}(j)$ are estimates of first-order and total effect SI and S_i, S_{T_i} are the analytical values.

In order to compare results of the test model with the results of Saltelli et al. reported in (Saltelli *et al.*, 2010) $MAE(\widehat{S_i})$ and $MAE(\widehat{S_{T_i}})$ are calculated. All numeric experiments were set up and run using R [51].

4.4.3.1 Test model

A specific G-function described by Saltelli et al. in [2] was chosen to be the test model as the one being closest (multiplicative) to the WRA model of AEP given in Eq. (52):

$$G = G(X_1, X_2, \dots, X_k, a_1, a_2, \dots, a_k) = \prod_{i=1}^{k} g_i, \tag{43}$$

$$g_i = \frac{|4X_i - 2| + a_i}{1 + a_i}, \tag{44}$$

Where $a_i = i, k = 4$ and all input variables are uniformly distributed in the interval [0,1].

The variance based on first-order effect V_i, the variance based on total effect V_{T_i} and the total variance V can be calculated according to Eq. (45), (46) and (47) respectively [12]:

$$V_i = V_{X_i}\left(E_{X\sim i}(Y|X_i)\right) = \frac{1}{3(1+a_i)^2} = \frac{1}{3(1+i)^2} \tag{45}$$

$$V_{T_i} = V_i\prod_{i\neq j}(1+V_j) = \frac{1}{3(1+i)^2}\prod_{i\neq j}(1+\frac{1}{3(1+j)^2}) \tag{46}$$

$$V = \prod_{i=1}^{k}(1+V_i) - 1 = \prod_{i=1}^{4}(1+V_i) - 1 = \prod_{i=1}^{4}\left(1+\frac{1}{3(1+i)^2}\right) - 1 \tag{47}$$

The analytical form of the first-order SI for the chosen multiplicative test model is:

$$S_i = \frac{V_i}{V} = \frac{1}{3(1+i)^2\left[\prod_{i=1}^{4}\left(1+\frac{1}{3(1+i)^2}\right)-1\right]} \tag{48}$$

The analytical form of total effect SI for the chosen test model can be calculated as:

$$S_{T_i} = \frac{V_{T_i}}{V} = \frac{\prod_{i \neq j}(1 + \frac{1}{3(1+j)^2})}{3(1+i)^2\left[\prod_{i=1}^{4}\left(1 + \frac{1}{3(1+i)^2}\right) - 1\right]} \quad (49)$$

All QMC experiments for the test function were conducted with the sample size of N = 1024.

4.4.3.2 Wind resource assessment model (WRA) model in the UAE case study

Wind energy is proportional to the cube of wind speed, intuitively making wind energy most sensitive to the variance in the wind or wind model parameters (Eq. (52)). Uncertainty is inherent but not limited to the wind. There are also turbine related uncertainties, such as uncertainties associated with turbine lifetime, necessary turbine maintenance, and losses. Distance to the grid, interest rate, inflation rate, investment cost, operation and maintenance (O&M) costs also add a great deal of economic uncertainty to wind economics that rely on WRA. What is of interest here is whether it is possible to quantify the uncertainty originating from various sources of uncertainty. To what extent are wind model parameters responsible for the variance in wind energy? These are the research questions this case study is aiming to answer, and luckily variance-based GSA [2] is tailored to address such research questions.

When designing this case study, the authors looked into how other researchers designed their MC experiments in WRA. For instance, Kwon used variables such as Weibull shape and scale parameters, air density, mean wind speed, surface roughness exponent, and measure-correlate-predict (MCP) residual as inputs to MC simulation for AEP UA [62]. Montes et al. included economic uncertainties to assess wind farm profitability using a MC approach and obtained a probability distribution function (PDF) for the net present value (NPV) of costs and internal rate of return (IRR) [25]. Amirinia et al. conducted a MC based offshore WRA study of the Persian Gulf [26]. They presented UA results as PDF of AEP and used two-scenario economic analysis. Caralis et al. used MC method for assessing profitability of twelve offshore wind projects. They integrated MC simulation into a classical financial model thus accounting for various sources of uncertainty related to expected changes in feed-in tariff (FiT) legislation in Greece [27]. The results demonstrate how difficult it is to propose a common FiT for all offshore wind farms, despite Greece's small size.

What output variables were of interest in SA studies performed in WRA? Several studies on SA of LCOE in WRA have been published in the last years [10][11][12][13][29][37]. Ioannou et al. performed a stochastic financial appraisal of offshore wind farms (OWF) based on deterministic lifecycle techno-economic model and reported based on a local SA, that the cost of turbine, the mean time to failure (hence, O&M cost), and foundation cost to be most influential on NPV and LCOE [10]. They provide a thorough overview of costs related to OWF and assumptions for modelling them. Castro-Santos & Diaz-Casas used Oracle Crystal Ball to set up a MC simulation to get SA results of floating OWF (FOWF) [11]. Their results indicate that the most important variables are the wind scale parameter and the electric tariff for the LCOE, discounted pay-back period, IRR, NPV, and cost of power. Lerch et al. proposed a methodology for calculating LCOE for a specific FOWF and performed an extensive yet local SA with 325 input variables [12]. They found that turbine, substructure and mooring system manufacturing cost as well as power cable cost are the most influential variables besides the common discount rate and energy losses. Galvez et al. recently reported results of a local SA in WRA for Tabasco, Mexico [13]. The authors looked at how the change in discount rate, O&M costs as well as investment costs affect LCOE, and with the use of SA revealed the need to implement financial mechanisms like FiT to decrease the cost of electricity generation in places with relatively low wind potential.

Although, most SA in WRA studies used LCOE [10][11][12][13][29][37] or goodness-of-fit (GOF) measures [14][15] as the output variable, the authors decided to define AEP as model output, because other variables of interest like LCOE, IRR, NPV all rely on AEP. Conducting GSA with a GOF measure as the output variable is planned to be reported in a following paper. Masdar City (24.420° N, 54.613° E) is located in the coastal area inside the city of Abu Dhabi, UAE (Figure 2.6). The authors chose it for the case study because Naizghi et al. have pointed out a high wind power generation potential in the coastal and mountainous regions of the UAE [63] and there were temperature and atmospheric pressure measurements available for the location as a non-wind-turbine-specific study was intended.

The meteorological station at Masdar City consists of a meteorological tower with 5 calibrated Hersteller Thies Cilma cup anemometers [64], two wind vanes, one Campbell CR1000 data logger, and three sensors of temperature, barometric pressure and humidity [65]. Ten-minute interval data of wind speed, temperature, atmospheric pressure, and humidity was collected at the height of 50 m from July 2007 - August 2008 and from January 2010 to January 2011.

These data were used for the QMC experiment for GSA. Extrapolation to hub height of a hypothetical wind turbine was not necessary as the measurements were taken at the height of 50 m. The length of available data is limited to two years only. A MCP method can be used to extend

it, but this step is omitted, as AEP was chosen as the variable of interest. Inter-annual variability could be taken into account in later refined GSA study of Masdar City if found fit and necessary.

Figure 4.6 Masdar City location

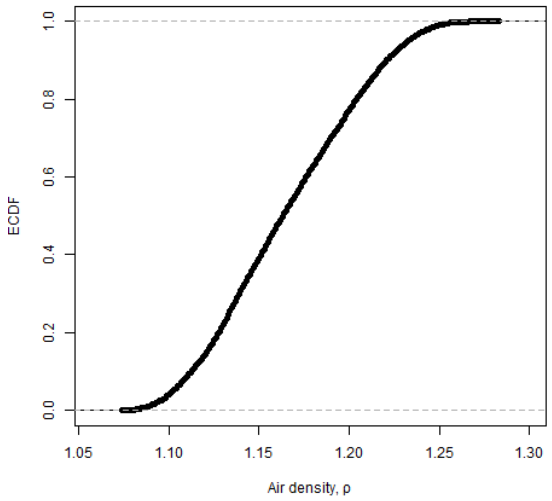

Figure 4.7 ECDF of air density in kg/m3, ρ at Masdar City

The importance of accounting for the variance in air density in WRA was pointed out by Jung & Schindler in [66]. Air density was calculated according to Eq. (50) with the collected data of temperature and atmospheric pressure at Masdar City. The ECDF of air density (Figure 4.7) based on the calculated values was used for distributional modeling of air density. For alternative ways to account for the variability in air density in WRA refer to [66].

$$\rho = \frac{p}{R_{spec}T}, \tag{50}$$

Where $R_{spec} = 287.058\ \frac{J}{kg\ K}$ is the specific gas constant of dry air, *t* is air temperature in K, *p* is the atmospheric pressure.

The two-parameter Weibull (W2) distribution is widely accepted in the wind energy field [38][39]. It is also most frequently used and often assumed best-fit distribution for wind data. A lot of researchers used W2 in recent WRA studies [21][67][68][69][70][71]. The PDF of the W2 distribution is:

$$f(w) = \frac{c}{\lambda}\left(\frac{w}{\lambda}\right)^{c-1} e^{-\left(\frac{w}{\lambda}\right)^{c}}, \tag{51}$$

Where *w* is the sample of wind speed data, *c* is the shape parameter and *λ* is the scale parameter.

Ouarda et al. showed the W2 exhibits best GOF for modeling wind speed in the UAE among two-parameter distributions and performs better than most three-parameter distributions, such as the generalized extreme value and the three-parameter lognormal distributions [72]. Hence, the W2 was chosen to model the wind at Masdar City, UAE.

When W2 is used to model wind and electric losses *EL* (in percent) are taken into account, the AEP can be calculated according to Eq. (52) [38]. Generally, electrical losses include cable losses, transformation losses, and losses in the substation.

$$AEP = \frac{(100 - EL)}{100}\frac{a}{2}\rho\lambda^3\Gamma\left(\frac{c+3}{c}\right)8760, \tag{52}$$

Where *a* is the availability of a wind turbine to generate electricity in percent of the time during the year available for electricity production (not down for maintenance) [38], ρ is the air density, Γ is the gamma function, *c* is the shape parameter and λ is the scale parameter of the W2.

According to Manwell et al., the availability due to no maintenance of a wind turbine lies within 97 – 99% interval [38]. Madariaga et al. report that the electrical losses in wind energy conversion systems are in the range of 3.25 – 4.75% [73], therefore the expected value of electrical losses was estimated to be 4%. When nothing else apart from a range of a variable is known, we make the most general assumption that turbine availability is uniformly distributed in [97, 99] and electrical losses are uniformly distributed in [3.25, 4.75].

Weibull shape and scale parameters were estimated using maximum likelihood (ML) estimation. The results of MLE for wind speed data at Masdar City are given in Table 4.1. For the QMC experiment we assume Weibull shape and scale parameter are both normally distributed with the mean corresponding to the respective ML estimate and standard deviation - to standard error of the respective MLE estimate. Similar assumptions about Weibull parameters were made by Amirinia et al. in a MC UA study of the Persian Gulf [26]. The value of Kolmogorov-Smirnov statistic for the W2 fit to Mascar City wind speed data at 50 m is equal to 0.015.

Table 4.1 MLE estimates of Weibull distribution parameters for Masdar City wind speed

	MLE estimate	**Standard error of MLE estimate**
Shape parameter of the Weibull distribution, *c*	2.1073	0.0049
Scale parameter of the Weibull distribution, λ	4.9368	0.0075

The input and output variables in QMC experiment with the respective assumptions about the underlying distributions of the variables are summarized in Table 4,2. The authors defined the output variable of interest for WRA in this study as the commonly used AEP in MWh (Equation 25). All QMC experiments for the AEP were conducted using brute force calculation of Sobol SI with the sample size of N = 1024.

Table 4.2 Variables used in the WRA model in the UAE case study

Type	Variable	Definition
Input	Weibull scale, λ	Gaussian(4.9368, 0.0049) according to (Amirinia, Mafi and Mazaheri, 2017)
Input	Weibull shape, c	Gaussian(2.1072, 0.0075) according to (Amirinia, Mafi and Mazaheri, 2017)
Input	Availability a, % per year	Uniform [97, 99] according to (Manwell, McGowan and Rogers, 2009)
Input	Electrical losses EL, %	Uniform[3.25, 4.75] according to (Madariaga *et al.*, 2017)
Input	Air density ρ, kg/m3	The ECDF of air density (Figure 4.7)
Output/model	Annual energy production, *AEP*	$\frac{(100-EL)}{100}\frac{a}{2}\rho\lambda^3\Gamma\left(\frac{c+3}{c}\right)8760$

4.5 Results

This section presents the results of the two case studies conducted.

4.5.1 Test model results

The results of calculating the accuracy of ranking according to the first-order SI using the brute force method for the test model are given in Figure 4.8. Random, LHS and Sobol samples converge to the analytical ranking with 100% ranking accuracy as the sample size becomes greater than 64. So, if the model at hand allows a sample size of 64, then all sampling strategies are equivalent. If a sample size smaller than 64 has to be used, the maximum accuracy can be achieved with SBSS or LHS. One can see that LHS and SBSS always outperform PRS. For small sample sizes of 2 and 4 LHS sampling outperforms SBSS. As the sample size increases without reaching the value of 64, LHS performs slightly better than SBSS.

The accuracy of ranking results with an estimation of the first-order SI for the test model is shown in Figure 4.9. The accuracy of estimated indices is significantly lower compared to the brute force method (4.5% as opposed to 100% for N = 1024). Therefore, the brute force should

be used for the WRA model since the model is not complicated and computational time allows it. One can see that there is a drop in the accuracy with growing sample size of all sampling strategies. This was not observed in the case of the brute force method. For LHS the drop occurs the earliest at sample size N = 8, PRS exhibits the drop at N = 16 and SBSS shows the drop at N = 64.

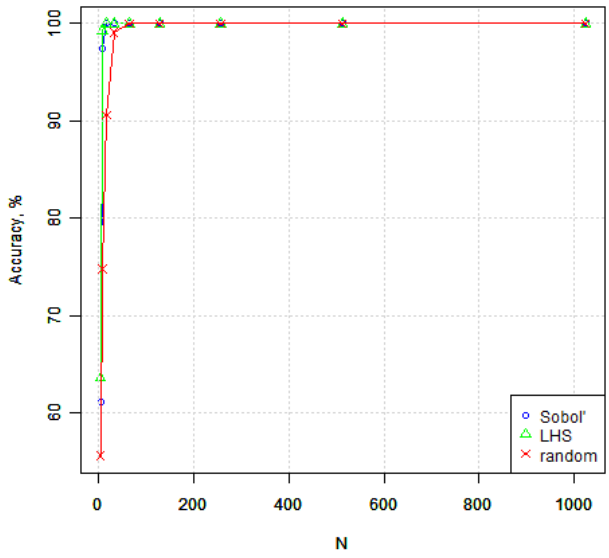

Figure 4.8 Accuracy of S_i for the test model using brute force method with a sample size of N = 4…64 ($N_r = 1000$)

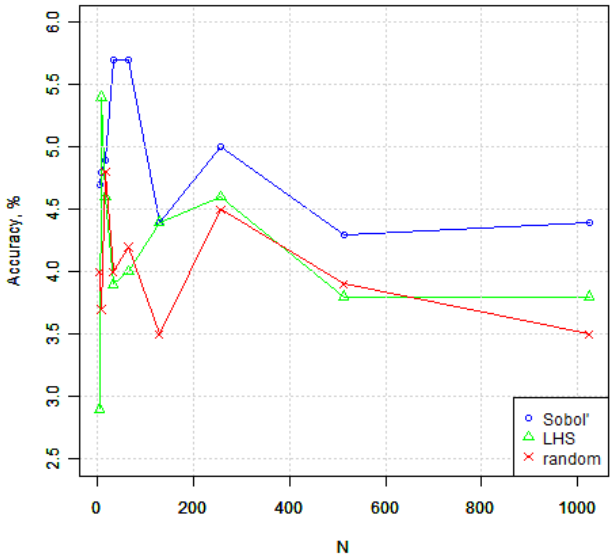

Figure 4.9 Accuracy of estimating S_i for the test model with a sample size of N = 4…1024 ($N_r = 1000$)

Mean absolute errors (MAE) were calculated for both sets of indices (first-order and total effect) for the two methods being compared: brute force and best-practice estimation. Figure 4.10 and Figure 4.11 show $MAE(\widehat{S_i})$ as a function of sample size (N = 4…64) for brute force and estimation methods respectively. Figures 4.12 and 4.13 exhibit $MAE(\widehat{S_{T_i}})$ as a function of sample size (N = 4…64) for brute force and estimation methods respectively. From these graphs one can see that:

- MAE for SBSS is always smaller compared to other sampling strategies for the sample sizes of N = 8, …, 1024;
- LHS outperforms SBSS only with a sample size of N = 8 which is not commonly used for QMC simulation;
- $MAE(\widehat{S_i})$ for the estimation method converges to a higher value than in the case of the brute force method;

- $MAE(\widehat{S_{T_i}})$ for the estimation method converges to a higher value than in the case of the brute force method;
- When considering estimation method, $MAE(\widehat{S_i})$ is one order smaller than $MAE(\widehat{S_{T_i}})$;
- When considering the brute force method, $MAE(\widehat{S_i})$ is of the same magnitude as $MAE(\widehat{S_{T_i}})$.

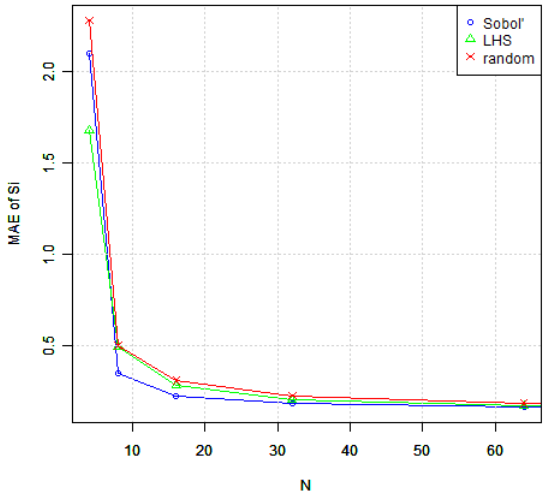

Figure 4.10 Mean absolute error of S_i, $MAE(\widehat{S_i})$, for brute force method (N=4…64, Nr=1000)

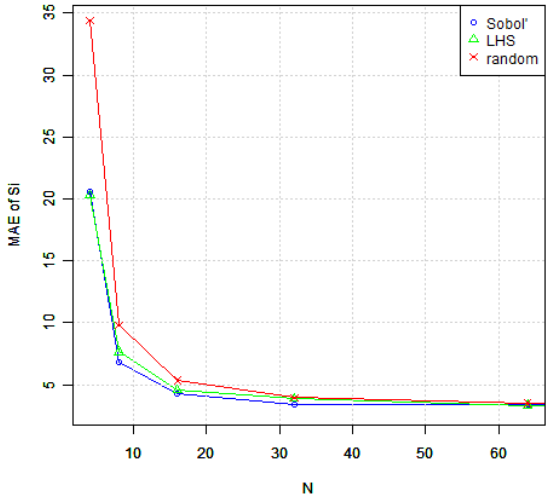

Figure 4.11 Mean absolute error of S_i, $MAE(\widehat{S_i})$, for estimation method (N=4…64, Nr=1000)

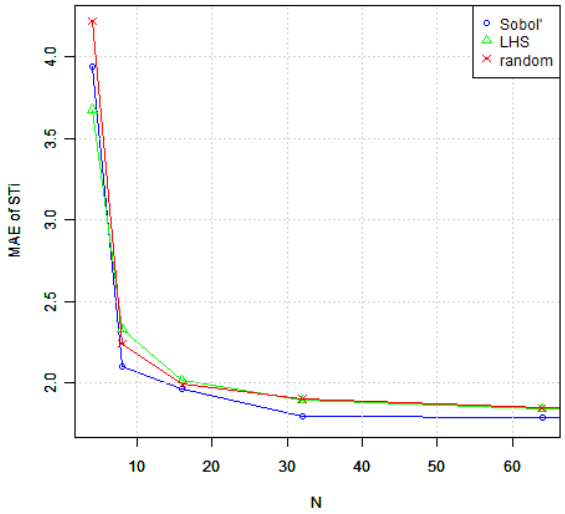

Figure 4.12 Mean absolute error of S_{T_i}, $MAE(\widehat{S_{T_i}})$, for brute force method (N=4…64, Nr=1000)

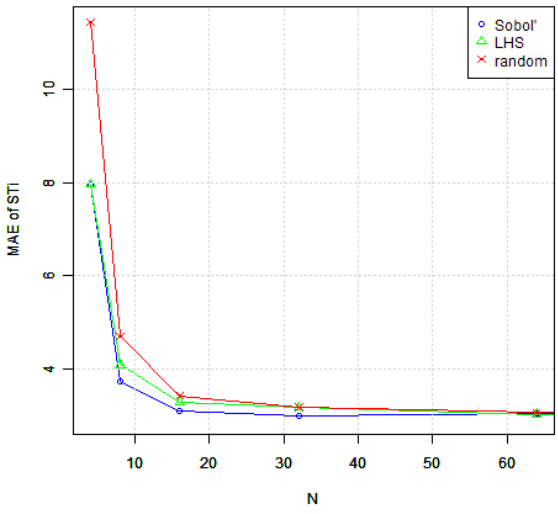

Figure 4.13 Mean absolute error of S_{T_i}, $MAE(\widehat{S_{T_i}})$, for estimation method (N=4…64, Nr=1000)

Test model results are summarized below:

1) Sampling strategies have been tested on the G-function ($a_i = i, k = 4$). LHS and SBSS outperform PRS in all cases tested. In some limited cases LHS slightly outperforms SBSS but the difference is not significant. In the majority of cases tested SBSS exhibits better

performance and is therefore recommended for practical use. This finding is similar to the recommendation of Tarantola et al. in [52].

2) MAE for SBSS is always smaller compared to other sampling strategies for sample size *N* = 8…1024. LHS outperforms SBSS only with a sample size of *N* = 8 which is too small for QMC simulation;
3) $MAE(\widehat{S_i})$ for estimation method is always higher than $MAE(\widehat{S_i})$ for brute force method. $MAE(\widehat{S_{T_i}})$ for estimation method is also always higher than $MAE(\widehat{S_{T_i}})$ for brute force method;
4) When considering estimation method, $MAE(\widehat{S_i})$ is one order smaller than $MAE(\widehat{S_{T_i}})$. When considering the brute force method, $MAE(\widehat{S_i})$ is of the same magnitude as $MAE(\widehat{S_{T_i}})$;
5) GSA brute force and estimation methods have been compared using the G-function ($a_i = i, k = 4$). Brute force method shows 100% accuracy for ranking order at sample size of *N* = 64 with any sampling strategy. Brute force is recommended for WRA, when wind is modeled with a distribution, else estimation should be used.

4.5.2 The UAE case study results

The GSA results of the AEP at Masdar City are given as a bar chart of total effect SI S_{T_i} in Figure 4.14. 94 % of variance in the AEP is explained by the variance in air density, 2.7 % by the variance in turbine availability, and Weibull scale parameter and electrical losses contribute the same amount of variance to the AEP, which is equal to 1.6%. The least influential factor to the AEP is Weibull shape parameter responsible for 0.4% of the AEP variance. Despite the AEP calculated in cubical proportion to Weibull scale parameter, the Weibull scale parameter surprisingly contributes only 1.6 % of the variance in the AEP. Thus, research questions posed have been answered. Note that the variance from all inputs considered adds up to 100%, as the AEP is calculated based on a simple multiplicative model, and proves that the QMC experiment converged. The ranking obtained is surprising, as well as the magnitude of difference in variance contribution. The contribution to the overall variance in AEP by the variance in air density is underestimated and should be further investigated.

The UA results of the AEP at Masdar City are presented in Figure 4.15. The PDF of the AEP was obtained with the same QMC experiment (*N* = 1024) set up to obtain the GSA results. Presenting a PDF is always superior to presenting point estimates. From Figure 4.15 one can see

that the AEP at Masdar City lies in the range of 67 to 81 MWh. The mean value of the AEP is 72 MWh.

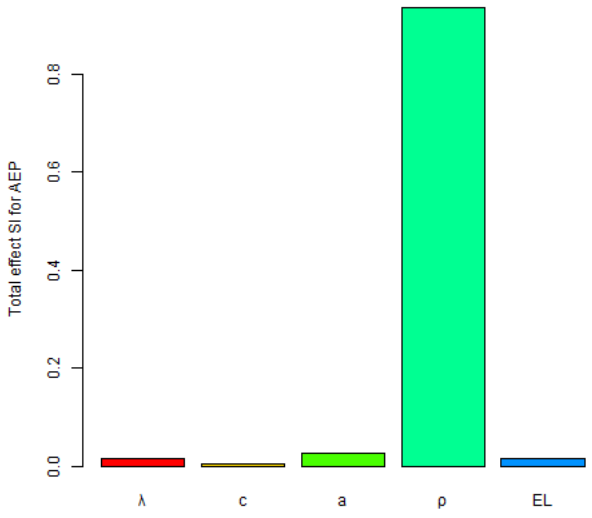

Figure 4.14 GSA result or importance of inputs for AEP according to S_{T_i}

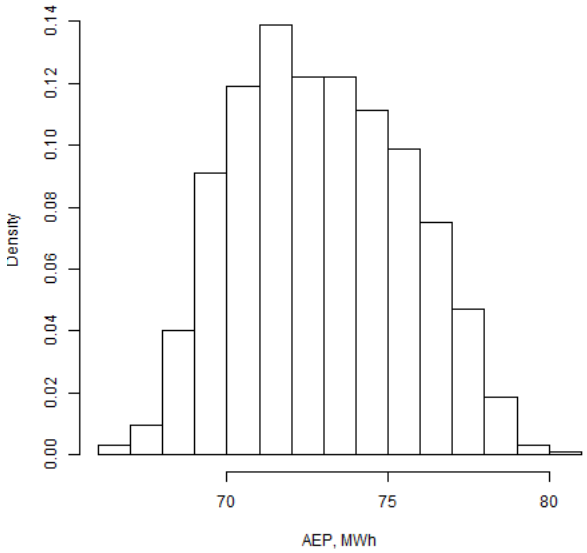

Figure 4.15 UA results or histogram of AEP at Masdar City

4.6 Conclusions and future research

The present paper is focused on Sobol method as a variance-based GSA method for WRA and the aspects of its application. The conclusions from both conducted case studies are:

1. SBSS outperforms LHS and PRS, and is recommended for use in QMC in WRA;
2. Brute force SI calculation offers high accuracy of results, and is recommended for use whenever the model and number of input variables allows it (similar to the UAE case study), otherwise their estimation can be used;
3. The UAE case study results suggest that the influence of variance in Weibull parameters on the AEP might be overestimated, while the influence of the variance in air density on the AEP might be overlooked. These results are specific to the case study and should not be generalized without further effort.

Masdar City case study illustrated that variance-based GSA can be easily, with the means of QMC, and at no extra cost (by using R [51]) set up in a WRA study. The wind community would benefit greatly from adapting the use of QMC and Sobol method, due to the following reasons:

1. First, QMC enables calculating global Sobol SI that provide a valid measure of importance for WRA models nonlinear in their nature;

2. Second, by setting up a GSA study with QMC, a PDF of the output model or the UA results are obtained with the same QMC experiment;
3. Third, it allows for miscellaneous data and information about a site of interest to be incorporated in a GSA study in WRA.

Future research should focus on the influence of air density in a more general context, for instance through running GSA similar to the one performed for the UAE case study but for a number of sites with longer datasets available. Future efforts should consider wind turbine specific studies with fitting air density to candidate distributions as recently suggested by Jung & Schindler [66], modeling air density with the best-fit and calculating AEP with air density corrected power curves [66]. Including economic uncertainties to the problem setup and conducting GSA for LCOE as defined in [37] could be carried out with the use of mixture distribution models instead of Weibull for AEP estimation as suggested by Ouarda et al. in [72] and Shin et al. in [74]. The idea of combining wind-related and economic uncertainties originated in [75] and [76]. Another interesting direction of research is performing a GSA study of how the quality of wind speed data (missing value percentage, measurement accuracy, and temporal step) affects GOF and/or wind speed distribution parameter estimation accuracy, enhancing the work of Jung & Schindler [14].

4.7 Conflict of interest

The authors declare that there is no conflict of interest regarding the publication of this paper.

4.8 Acknowledgements

This research was supported by the Natural Sciences and Engineering Research Council of Canada (NSERC) and the Canada Research Chair Program. The authors are very grateful to the Editor-in-Chief Carlos F.M. Coimbra and the Editorial Board of Journal of Renewable and Sustainable Energy for their time, valuable input, patience and understanding. The authors are also very grateful to the two anonymous reviewers for thoughtful and detailed reviews that helped improve the UAE case study and the overall quality of the manuscript significantly.

5 BIBLIOGRAPHY

[1] M. J. W. Jansen, “Analysis of variance designs for model output,” Comput. Phys. Commun., vol. 117, no. 1, pp. 35–43, 1999.

[2] A. Saltelli, P. Annoni, I. Azzini, F. Campolongo, M. Ratto, and S. Tarantola, “Variance based sensitivity analysis of model output. Design and estimator for the total sensitivity index,” Comput. Phys. Commun., vol. 181, no. 2, pp. 259–270, 2010.

[3] A. Saltelli et al., Global Sensitivity Analysis: The Primer. John Wiley & Sons, Ltd, 2008.

[4] A. Saltelli and P. Annoni, “How to avoid a perfunctory sensitivity analysis,” Environ. Model. Softw., vol. 25, no. 12, pp. 1508–1517, 2010.

[5] F. Ferretti, A. Saltelli, and S. Tarantola, “Trends in sensitivity analysis practice in the last decade,” Sci. Total Environ., vol. 568, pp. 666–670, 2016.

[6] A. Saltelli et al., “Why so many published sensitivity analyses are false: A systematic review of sensitivity analysis practices,” Environ. Model. Softw., vol. 114, pp. 29–39, 2019.

[7] T. Wagener and F. Pianosi, “What has Global Sensitivity Analysis ever done for us? A systematic review to support scientific advancement and to inform policy-making in earth system modelling,” Earth-Science Reviews, vol. 194. Elsevier B.V., pp. 1–18, Jul. 01, 2019, doi: 10.1016/j.earscirev.2019.04.006.

[8] “Global sensitivity analysis,” EU Science hub. https://ec.europa.eu/jrc/en/samo/methods (accessed May 30, 2019).

[9] F. Pianosi, F. Sarrazin, and T. Wagener, “A Matlab toolbox for Global Sensitivity Analysis,” Environ. Model. Softw., vol. 70, pp. 80–85, 2015.

[10] A. Ioannou, A. Angus, and F. Brennan, “Stochastic financial appraisal of offshore wind farms,” Renew. Energy, vol. 145, pp. 1176–1191, Jan. 2020.

[11] M. Lerch, M. De-Prada-Gil, C. Molins, and G. Benveniste, “Sensitivity analysis on the levelized cost of energy for floating offshore wind farms,” Sustain. Energy Technol. Assessments, vol. 30, pp. 77–90, Dec. 2018.

[12] L. Castro-Santos and V. Diaz-Casas, “Sensitivity analysis of floating offshore wind farms,” Energy Convers. Manag., vol. 101, pp. 271–277, 2015.

[13] G. Hernández Galvez et al., “Wind resource assessment and sensitivity analysis of the levelised cost of energy. A case study in Tabasco, Mexico,” Renew. Energy Focus, vol. 29, pp. 94–106, Jun. 2019.

[14] C. Jung and D. Schindler, “Sensitivity analysis of the system of wind speed distributions,” Energy Convers. Manag., vol. 177, pp. 376–384, Dec. 2018.

[15] O. Alavi, A. Sedaghat, and A. Mostafaeipour, “Sensitivity analysis of different wind speed distribution models with actual and truncated wind data: A case study for Kerman, Iran,” Energy Convers. Manag., vol. 120, pp. 51–61, Jul. 2016.

[16] I. . Sobol′, “Global sensitivity indices for nonlinear mathematical models and their Monte Carlo estimates,” Math. Comput. Simul., vol. 55, no. 1–3, pp. 271–280, Feb. 2001.

[17] H. Janssen, “Monte-Carlo based uncertainty analysis: Sampling efficiency and sampling convergence,” Reliab. Eng. Syst. Saf., vol. 109, pp. 123–132, Jan. 2013, doi: 10.1016/J.RESS.2012.08.003.

[18] X. Xu and Z. Yan, “Probabilistic load flow calculation with quasi-Monte Carlo and multiple linear regression,” Int. J. Electr. Power Energy Syst., vol. 88, pp. 1–12, Jun. 2017, doi: 10.1016/J.IJEPES.2016.11.013.

[19] S. Burhenne, D. Jacob, and G. P. Henze, “Sampling based on Sobol sequences for Monte Carlo techniques applied to building simulations,” in Proceedings of Building Simulation 2011, 2011, pp. 1816–1823.

[20] M. Shoaib, I. Siddiqui, S. Rehman, S. Khan, and L. M. Alhems, “Assessment of wind energy potential using wind energy conversion system,” J. Clean. Prod., vol. 216, pp. 346–360, Apr. 2019, doi: 10.1016/J.JCLEPRO.2019.01.128.

[21] T. Aukitino, M. G. M. Khan, and M. R. Ahmed, “Wind energy resource assessment for Kiribati with a comparison of different methods of determining Weibull parameters,” Energy Convers. Manag., vol. 151, pp. 641–660, Nov. 2017.

[22] M. Y. Kazet, R. Mouangue, A. Kuitche, and J. M. Ndjaka, “Wind Energy Resource Assessment in Ngaoundere Locality,” Energy Procedia, vol. 93, pp. 74–81, Aug. 2016, doi: 10.1016/J.EGYPRO.2016.07.152.

[23] G. Marmidis, S. Lazarou, and E. Pyrgioti, “Optimal placement of wind turbines in a wind park using Monte Carlo simulation,” Renew. Energy, vol. 33, no. 7, pp. 1455–1460, Jul. 2008, doi: 10.1016/J.RENENE.2007.09.004.

[24] L. Wang, J. Yuan, M. E. Cholette, Y. Fu, Y. Zhou, and A. C. Tan, “Comparative study of discretization method and Monte Carlo method for wind farm layout optimization under Weibull distribution,” J. Wind Eng. Ind. Aerodyn., vol. 180, pp. 148–155, Sep. 2018, doi: 10.1016/J.JWEIA.2018.07.021.

[25] G. M. Montes, E. P. Martin, J. A. Bayo, and J. O. Garcia, “The applicability of computer simulation using Monte Carlo techniques in windfarm profitability analysis,” Renew. Sustain. Energy Rev., vol. 15, no. 9, pp. 4746–4755, 2011, doi: 10.1016/j.rser.2011.07.078.

[26] G. Amirinia, S. Mafi, and S. Mazaheri, “Offshore wind resource assessment of Persian Gulf using uncertainty analysis and GIS,” Renew. Energy, vol. 113, pp. 915–929, Dec. 2017.

[27] G. Caralis et al., “Lessons learnt from the evaluation of the feed-in tariff scheme for offshore wind farms in Greece using a Monte Carlo approach,” J. Wind Eng. Ind. Aerodyn., vol. 157, pp. 63–75, Oct. 2016, doi: 10.1016/J.JWEIA.2016.08.008.

[28] C. bin Li, G. shu Lu, and S. Wu, “The investment risk analysis of wind power project in China,” Renew. Energy, vol. 50, no. 2013, pp. 481–487, 2013, doi: 10.1016/j.renene.2012.07.007.

[29] V. Gass, F. Strauss, J. Schmidt, and E. Schmid, “Assessing the effect of wind power uncertainty on profitability,” Renew. Sustain. Energy Rev., vol. 15, no. 6, pp. 2677–2683, 2011.

[30] S. Li and L. Caracoglia, “Surrogate Model Monte Carlo simulation for stochastic flutter analysis of wind turbine blades,” J. Wind Eng. Ind. Aerodyn., vol. 188, pp. 43–60, May 2019, doi: 10.1016/J.JWEIA.2019.02.004.

[31] Y. F. Li, S. Valla, and E. Zio, “Reliability assessment of generic geared wind turbines by GTST-MLD model and Monte Carlo simulation,” Renew. Energy, vol. 83, pp. 222–233, Nov. 2015, doi: 10.1016/J.RENENE.2015.04.035.

[32] R. Teixeira, A. O’Connor, and M. Nogal, “Probabilistic sensitivity analysis of offshore wind turbines using a transformed Kullback-Leibler divergence,” Struct. Saf., vol. 81, p. 101860, Nov. 2019.

[33] J. Velarde, C. Kramhøft, and J. D. Sørensen, “Global sensitivity analysis of offshore wind turbine foundation fatigue loads,” Renew. Energy, vol. 140, pp. 177–189, Sep. 2019, doi: 10.1016/J.RENENE.2019.03.055.

[34] Z. Di et al., “Improving WRF model turbine-height wind-speed forecasting using a surrogate- based automatic optimization method,” Atmos. Res., vol. 226, pp. 1–16, Sep. 2019, doi: 10.1016/J.ATMOSRES.2019.04.011.

[35] P. M. McKay, R. Carriveau, D. S.-K. Ting, and J. L. Johrendt, “Global sensitivity analysis of wind turbine power output,” Wind Energy, vol. 17, no. 7, pp. 983–995, Jul. 2014.

[36] F. Ulker, D. Allaire, and K. Willcox, “Sensitivity-guided decision-making for wind farm micro-siting,” Int. J. Numer. Methods Fluids, vol. 83, no. 1, pp. 52–72, Jan. 2017.

[37] T. T. D. Tran and A. D. Smith, “Incorporating performance-based global sensitivity and uncertainty analysis into LCOE calculations for emerging renewable energy technologies,” Appl. Energy, vol. 216, pp. 157–171, Apr. 2018.

[38] J. F. Manwell, J. G. McGowan, and A. L. Rogers, Wind energy explained : theory, design and application. Wiley, 2009.

[39] P. Wais, “A review of Weibull functions in wind sector,” Renew. Sustain. Energy Rev., vol. 70, pp. 1099–1107, Apr. 2017, doi: 10.1016/J.RSER.2016.12.014.

[40] T. B. M. J. Ouarda, C. Charron, and F. Chebana, “Review of criteria for the selection of probability distributions for wind speed data and introduction of the moment and L-moment ratio diagram methods, with a case study,” Energy Convers. Manag., vol. 124, pp. 247–265, 2016.

[41] D. Villanueva and A. Feijóo, “Wind power distributions: A review of their applications,” Renew. Sustain. Energy Rev., vol. 14, no. 5, pp. 1490–1495, 2010, doi: 10.1016/j.rser.2010.01.005.

[42] X.-Y. Tang, S. Zhao, B. Fan, J. Peinke, and B. Stoevesandt, “Micro-scale wind resource assessment in complex terrain based on CFD coupled measurement from multiple masts,” Appl. Energy, vol. 238, pp. 806–815, Mar. 2019, doi: 10.1016/J.APENERGY.2019.01.129.

[43] C. L. Defforge, B. Carissimo, M. Bocquet, R. Bresson, and P. Armand, “Improving CFD atmospheric simulations at local scale for wind resource assessment using the iterative ensemble Kalman smoother,” J. Wind Eng. Ind. Aerodyn., vol. 189, pp. 243–257, Jun. 2019, doi: 10.1016/J.JWEIA.2019.03.030.

[44] E. Arteaga-López, C. Ángeles-Camacho, and F. Bañuelos-Ruedas, “Advanced methodology for feasibility studies on building-mounted wind turbines installation in urban environment: Applying CFD analysis,” Energy, vol. 167, pp. 181–188, Jan. 2019, doi: 10.1016/J.ENERGY.2018.10.191.

[45] D. J. Willis et al., “Wind energy research: State-of-the-art and future research directions,” Renew. Energy, vol. 125, pp. 133–154, Sep. 2018, doi: 10.1016/J.RENENE.2018.02.049.

[46] E. B. Barker and J. M. Kelsey, “Recommendation for random number generation using deterministic random bit generators,” Gaithersburg, MD, 2012. doi: 10.6028/NIST.SP.800-90a.

[47] A. Nikishova, A. Kalyuzhnaya, A. Boukhanovsky, and A. Hoekstra, “Uncertainty quantification and sensitivity analysis applied to the wind wave model SWAN,” Environ. Model. Softw., vol. 95, pp. 344–357, Sep. 2017, doi: 10.1016/J.ENVSOFT.2017.06.030.

[48] J. C. Helton and F. J. Davis, “Latin hypercube sampling and the propagation of uncertainty in analyses of complex systems,” Reliab. Eng. Syst. Saf., vol. 81, no. 1, pp. 23–69, 2003, doi: 10.1016/S0951-8320(03)00058-9.

[49] I. . Sobol’, “On the distribution of points in a cube and the approximate evaluation of integrals,” USSR Comput. Math. Math. Phys., vol. 7, no. 4, pp. 86–112, Jan. 1967, doi: 10.1016/0041-5553(67)90144-9.

[50] P. Bratley and B. L. Fox, “ALGORITHM 659: implementing Sobol’s quasirandom sequence generator,” ACM Trans. Math. Softw., vol. 14, no. 1, pp. 88–100, 2002, doi: 10.1145/42288.214372.

[51] “R Core Team, R: A Language and Environment for Statistical Computing.” R Foundation for Statistical Computing, Vienna, Austria, 2020, [Online]. Available: https://www.r-project.org/.

[52] S. Tarantola, W. Becker, and D. Zeitz, “A comparison of two sampling methods for global sensitivity analysis,” Comput. Phys. Commun., vol. 183, no. 5, pp. 1061–1072, 2012, doi: 10.1016/j.cpc.2011.12.015.

[53] F. Khorashadi Zadeh et al., “Comparison of variance-based and moment-independent global sensitivity analysis approaches by application to the SWAT model,” Environ. Model. Softw., vol. 91, pp. 210–222, 2017.

[54] F. Pianosi and T. Wagener, “Distribution-based sensitivity analysis from a generic input-output sample,” Environ. Model. Softw., vol. 108, pp. 197–207, Oct. 2018.

[55] E. Borgonovo and E. Plischke, “Sensitivity analysis: A review of recent advances,” Eur. J. Oper. Res., vol. 248, no. 3, pp. 869–887, Feb. 2016, Accessed: Sep. 05, 2019. [Online]. Available: https://www.sciencedirect.com/science/article/pii/S0377221715005469#sec0009.

[56] E. Plischke, E. Borgonovo, and C. L. Smith, “Global sensitivity measures from given data,” Eur. J. Oper. Res., vol. 226, no. 3, pp. 536–550, May 2013, Accessed: Sep. 04, 2019. [Online]. Available: https://www.sciencedirect.com/science/article/pii/S0377221712008995?dgcid=raven_sd_recommender_email.

[57] I. Sobol and S. Kucherenko, “On global sensitivity analysis of quasi-Monte Carlo algorithms, Monte Carlo Methods and Applications,” Monte Carlo Methods Appl., vol. 11, no. 1, pp. 1–9, 2005.

[58] I. M. Sobol, “Global sensitivity indices for nonlinear mathematical models. Review,” Math. Comput. Simul., vol. 55, no. 1–3, pp. 271–280, 2001.

[59] L. Pronzato, “Sensitivity analysis via Karhunen–Loève expansion of a random field model: Estimation of Sobol’ indices and experimental design,” Reliab. Eng. Syst. Saf., vol. 187, pp. 93–109, Jul. 2019, doi: 10.1016/j.ress.2018.01.010.

[60] L. Gilquin, E. Arnaud, C. Prieur, and A. Janon, “Making the best use of permutations to compute sensitivity indices with replicated orthogonal arrays,” Reliab. Eng. Syst. Saf., vol. 187, pp. 28–39, Jul. 2019.

[61] S. Kucherenko, O. V. Klymenko, and N. Shah, “Sobol’ indices for problems defined in non-rectangular domains,” Reliab. Eng. Syst. Saf., vol. 167, pp. 218–231, Nov. 2017.

[62] S. D. Kwon, “Uncertainty analysis of wind energy potential assessment,” Appl. Energy, vol. 87, no. 3, pp. 856–865, 2010, doi: 10.1016/j.apenergy.2009.08.038.

[63] M. S. Naizghi and T. B. M. J. M. J. Ouarda, “Teleconnections and analysis of long-term wind speed variability in the UAE,” Int. J. Climatol., vol. 37, no. 1, pp. 230–248, Jan. 2017.

[64] Measnet, “ANEMOMETER CALIBRATION Version 2 October 2009,” Measurement, no. October, 2009, [Online]. Available: http://www.measnet.com/wp-content/uploads/2011/06/measnet_anemometer_calibration_v2_oct_2009.pdf.

[65] I. Janajreh and I. Talab, “Wind Data Collection and Analyses at Masdar City for Wind Turbine Assessment,” 01-902-664-9706, vol. 1, no. 1, pp. 43–50, 2010, doi: 10.5383/ijtee.01.01.007.

[66] C. Jung and D. Schindler, “The role of air density in wind energy assessment – A case study from Germany,” Energy, vol. 171, pp. 385–392, Mar. 2019, doi: 10.1016/J.ENERGY.2019.01.041.

[67] K. Azad, M. Rasul, P. Halder, and J. Sutariya, “Assessment of wind energy prospect by Weibull distribution for prospective wind sites in Australia,” in Energy Procedia, 2019, vol. 160, pp. 348–355.

[68] S. Ali, S.-M. M. Lee, and C.-M. M. Jang, “Statistical analysis of wind characteristics using Weibull and Rayleigh distributions in Deokjeok-do Island – Incheon, South Korea,” Renew. Energy, vol. 123, pp. 652–663, Aug. 2018, Accessed: Jul. 12, 2019. [Online]. Available: https://www.sciencedirect.com/science/article/pii/S0960148118302313?via%3Dihub.

[69] Z. H. Hulio, W. Jiang, and S. Rehman, “Techno-Economic assessment of wind power potential of Hawke’s Bay using Weibull parameter: A review,” Energy Strateg. Rev., vol. 26, p. 100375, Nov. 2019.

[70] J. C. Aririguzo and E. B. Ekwe, “Weibull distribution analysis of wind energy prospect for Umudike, Nigeria for power generation,” Robot. Comput. Integr. Manuf., vol. 55, pp. 160–163, Feb. 2019, doi: 10.1016/J.RCIM.2018.01.001.

[71] M. H. Soulouknga, S. Y. Doka, N.Revanna, N.Djongyang, and T.C.Kofane, “Analysis of wind speed data and wind energy potential in Faya-Largeau, Chad, using Weibull distribution,” Renew. Energy, vol. 121, pp. 1–8, Jun. 2018, doi: 10.1016/J.RENENE.2018.01.002.

[72] T. B. M. J. Ouarda et al., “Probability distributions of wind speed in the UAE,” Energy Convers. Manag., vol. 93, pp. 414–434, Mar. 2015.

[73] A. Madariaga, C. J. Martinez de Ilarduya, S. Ceballos, I. Martinez de Alegria, and J. L. Martin, “Electrical losses in multi-MW wind energy conversion systems,” Renew. Energy Power Qual. J., pp. 322–327, 2017, doi: 10.24084/repqj10.305.

[74] J.-Y. Shin, T. B. M. J. Ouarda, and T. Lee, “Heterogeneous mixture distributions for modeling wind speed, application to the UAE,” Renew. Energy, vol. 91, pp. 40–52, Jun. 2016.

[75] O. Tsvetkova, “Uncertainty and sensitivity analysis for decision support in building design,” Albert Ludwig University of Freiburg, 2011.

[76] S. Burhenne, O. Tsvetkova, D. Jacob, G. P. Henze, and A. Wagner, “Uncertainty quantification for combined building performance and cost-benefit analyses,” Build. Environ., vol. 62, pp. 143–154, Apr. 2013, doi: 10.1016/j.buildenv.2013.01.013.

6 USE OF THE HALPHEN DISTRIBUTION FAMILY FOR MEAN WIND SPEED ESTIMATION WITH APPLICATION TO EASTERN CANADA

Titre de l'article :

FAMILLE DE DISTRIBUTION HALPHEN POUR LA MODÉLISATION DE LA VITESSE MOYENNE DU VENT : ÉTUDE DE CAS SUR L'EST DU CANADA

Authors :

Olga Tsvetkova, INRS-ETE

Taha B.M.J. Ouarda, INRS-ETE

Titre of book or journal :

Energy Conversion and Management

Date of publication : 2022/11/29

DOI : https://doi.org/10.1016/J.ENCONMAN.2022.116502

Contribution of authors :

Olga Tsvetkova: Methods, Writing - Original draft preparation

Taha B.M.J. Ouarda: Idea & conceptualization, Funding acquisition, Supervision, Writing - Reviewing and Editing.

6.1 Abstract

We introduce the Halphen distribution family (HDF) to model average wind speed for the purpose of wind energy estimation. The family is flexible and is used to fit a large variety of data. The family is composed of three three-parameter distributions (scale and two shape parameters): Halphen type A (HA), Halphen type B (HB) and Halphen inverse type B (HIB). HA is a generalization of the two-parameter Harmonic distribution, HB has the gamma distribution as a limiting case, and HIB is based on the exponential factorial function and has the inverse Gamma distribution as a limiting case. The HDF has a number of properties favorable to model wind data, such as lower bound at zero (absence of location parameter), flexibility to cover a large range of shapes, and explicit form of moment generating functions. Properties of the HDF ensure optimality and consistency of maximum likelihood estimators used for distribution parameter estimation. We examined 126 stations in Eastern Canada. We found that HDF provides fit superior to the most commonly used distribution for this purpose, the two-parameter Weibull distribution, in 98% of the stations according to the Akaike information criterion (AIC) and in 99% of the stations according to the Bayesian information criterion (BIC). The most common best-fit distribution for the stations in the Eastern Canada case study is the HDF (84% according to AIC and BIC). The results of the case study show that wind observations cannot be fit by the HIB, but can be very well modeled by HA (best-fit for 38% of the stations according to AIC and BIC) or HB (best-fit for 46% of the stations according to AIC and BIC). We encourage the use of HDF in wind resource estimation studies that are based on mean wind speed estimation.

.

6.2 Nomenclature

$\widehat{C_s}$	Biased estimator of coefficient of skewness $\widehat{C_s} = \frac{1}{n}\sum_{i=1}^{n}(x_i - \bar{x})^3 \,/\, \left(\frac{1}{n}\sum_{i=1}^{n}(x_i - \bar{x})^2\right)^{3/2}$ [1]
$\widetilde{C_s}$	Classical correction to the biased estimator $\widehat{C_s}$ [1] $\widetilde{C_s} = \widehat{C_s}\frac{\sqrt{n(n-1)}}{n-2}\left(1+\frac{8.5}{n}\right) = \frac{1}{n}\sum_{i=1}^{n}(x_i - \bar{x})^3 \,/\, \left(\frac{1}{n}\sum_{i=1}^{n}(x_i - \bar{x})^2\right)^{3/2} \frac{\sqrt{n(n-1)}}{n-2}\left(1+\frac{8.5}{n}\right)$
$\mu_r(D)$	The r-th central moment of the distribution D
$\mu'_r(D)$	The r-th non-central moment of the distribution D
C_k	Coefficient of kurtosis μ_4/μ_2^2 [2]
C_s	Coefficient of skewness $\mu_3/\mu_2^{3/2}$ [2]
C_v	Coefficient of variation $\sqrt{\mu_2}/\mu'_1$ [3]
$K_v(.)$	Bessel function, $K_v(2\alpha) = \frac{1}{2m^v}\int_0^\infty x^{v-1}e^{-\alpha\left(\frac{x}{m}+\frac{m}{x}\right)}dx$ [2][3]
$ef_v(.)$	Exponential factorial function $ef_v(\alpha) = 2\int_0^\infty x^{2v-1}e^{-\alpha(-x^2+\alpha x)}dx$ [2]
n_{par}	Number of parameters of a model
x_M	Mode of a sample
x_i	*i*-th observation of the wind speed time series
β_1	Skewness squared
β_2	Kurtosis
δ_1	Moment ratio $\delta_1 = \ln(A/G)$ [2]
δ_2	Moment ratio $\delta_2 = \ln(G/H)$ [2]
AD	Anderson-Darling statistic
AIC	Akaike information criterion
BIC	Bayesian information criterion
CDF	Cumulative distribution function. CDF describes the probability that a random variable X with a given probability distribution will be found at a value less than or equal to x $(P(X) \leq x)$.
EV1	Extreme value type 1 distribution or Gumbel distribution
EV2	Extreme value type 2 distribution or Frechet distribution
EV3	Extreme value type 3 distribution or three-parameter Weibull distribution
EVI	Extreme value indices
EVT	Extreme value theory
G2	The two-parameter Gamma distribution
GEV	Generalized extreme value distribution
GOF	Goodness-of-fit
HA	Halphen type A distribution
HB	Halphen type B distribution
HDF	Halphen distribution family
HIB	Halphen inverse type B distribution
HLY	Hourly
IG	Inverse Gamma distribution
k	Shape parameter of the Weibull distribution
KS	Kolmogorov-Smirnov statistic
L	Likelihood function
m	Scale parameter of Halphen distributions [2]

MK	Mann-Kendall test [4][5]
ML	Maximum likelihood
MMK	Modified Mann-Kendall test [5][6]
N	Gaussian (normal) distribution
NB	The province of New Brunswick
NL	The province of New Foundland and Labrador
NS	The province of Nova Scotia
PDF	Probability distribution function. PDF is a mathematical way of describing the range of possible values that a random variable can have and the respective probability of such an event occurring.
PEI	The province of Prince Edward Island
QC	The province of Quebec
QQ	Quantile-quantile
RMSE	Root mean squared error
SW	Shapiro-Wilk test [7]
W2	2-paramter Weibull distribution
WRE	Wind resource estimation
x	Wind speed time series
α	Shape parameter of Halphen and Gamma distributions [2]
λ	Scale parameter of the Weibull distribution
ν	Shape parameter of Halphen distributions [2]
σ	Standard deviation
A	Arithmetic mean of a sample $A = \sum_{i=1}^{N} x_i$
F	Cumulative distribution function
$F(x)$	Cumulative distribution function
G	Geometric mean of a sample $G = (\prod_{i=1}^{N} x_i)^{1/N}$
H	Harmonic mean of a sample $H = \frac{N}{\sum_{i=1}^{N} 1/x_i}$
$M(a,b,z)$	confluent hypergeometric function $M(a,b,z) = \frac{\Gamma(b)}{\Gamma(b-a)\Gamma(a)} \int_0^1 e^{zt}\, t^{a-1}(1-t)^{b-a-1} dt$ [2]
Q	Quadratic moment $Q = \sum_{i=1}^{N} x_i^2$ [2]
$f(x)$	Probability distribution function (density)

6.3 Introduction

The Halphen distribution family (HDF) initially designed to specifically model annual and seasonal flows in flood frequency analysis [2] is introduced to model wind speed for the purpose of wind resource estimation (WRE). With this article we present the use of three-parameter HDF (scale and two shapes) to model mean wind speed necessary for assessing sites for the purpose of wind energy development with a case study of 126 sites in Eastern Canada. Whether HDF is useful for this task is the main research question of this paper. In other words, is Halphen type A (HA), Halphen type B (HB) or Halphen inverse type B (HIB) superior to distributions commonly used for wind resource assessment?

A concise literature review of the HDF, its application, popularization and advances follow. The HDF is a flexible and complete distribution family to fit independent and identically distributed observations that was designed specifically for river peak flow datasets by Etiene Halphen during World War II [8]. The creation of HDF was driven by "*Halphen's desire to construct his distributions so as to meet some specific requirements of fitting hydrological variables*" [8]. Perrault et al. [9] discussed the statistical properties of the distributions in [9] and later - the parameter estimation with maximum likelihood estimation (MLE) and quantile estimation in [10]. A significant body of research on the significance of the HDF in the field of flood frequency analysis was contributed by El Adlouni & Bobee [2]. Chebana, El Adlouni & Bobee discussed the estimation of HDF parameters with the method of moments in [11] and mixed estimation method in [1]. El Adlouni & Bobee [12] studied the sampling techniques for HDF and developed a discriminatory test in [13]. Zhang & Singh [14] revisited the application of HDF in flood frequency analysis. They used 198 peak flow datasets in their case study, estimated Halphen distributions parameters with the MLE method and used Kolmogorov-Smirnov statistic (KS) as a goodness-of-fit (GOF) metric and root mean square error (RMSE) – as a performance metric. Zhang & Singh [14] found that HA/HB was the preferred distribution for 190 datasets, also the moment ratio diagram was found to be a reliable tool for distribution selection along with the value of kurtosis. Most importantly, the study validated the use of HDF in flood frequency analysis. Zhang & Singh [14] compared the performance of HDF with log-Pearson type 3 (LPT3) distribution. El Adlouni et al. [15] conducted an exploratory study comparing generalized extreme value distribution (GEV) vs. HDF. The simulation-based comparisons point that HA distribution is more flexible than the GEV that leads to "*reasonable bias and RMSE even when samples are generated from GEV distribution*" [15]. Deholme et al. [16] introduced the HDF as a toolbox for modelling travel time variability.

Moving on to the field of WRE, extensive reviews of statistical distributions used in the wind industry have been conducted in a number of review studies [17]-[22]. Jung et al. [17] showed that "*115 parametric distributions were applied 2010–2018*" [17] and that the two-parameter Weibull distribution (W2) was "*the most frequently (44 times) evaluated distribution*" [17]. They also concluded that W2 was "*the most commonly evaluated and recommended distribution*" [17]. Aries et al. [23] used the W2, the two-parameter Gamma distribution (G2), two-parameter Wald distribution, two-parameter lognormal (LN2), the extreme value type 1 (EV1) or Gumbel, GEV, Nakagami, and generalized logistic distribution to model wind speed for deep assessment of wind speed distribution models for four sites in Algeria. Ouarda et. al. [19] enhanced the list with the three-parameter lognormal (LN3), LPT3, and normal (N). The distributions used in practice might not be limited to the above mentioned distributions, which are merely the most frequently encountered distributions in specialized literature. A comprehensive evaluation of wind speed distribution models with a case study for North Dakota by Zhou et al. [20] included W2, G2, LN2, and inverse Gaussian. Usta et al. [24] propose using skewed generalized error distribution and skewed t distribution. According to Jung et al. [17], distributions that were applied at least in four different studies or recommended for use in at least two distinct studies for the purpose of WRE are given in Table 6.1. Although a number of mixture models have been applied to this task [25], mixture distributions are outside the scope of this study and therefore omitted. Jung et al. [17], conclude that is impossible to "*identify a single distribution that can be fitted universally*" [17].

Table 6.1 Distributions used for modelling mean wind speed according to [17]

Group of distributions	**List of distributions**
One-parameter distributions	*Exponential, Rayleigh,*
Two-parameter distributions	*Birnbaum-Sanders, Erlang, Gamma, Gumbel, Inverse Gamma, Inverse Gaussian, inverse Weibull, logistic, log-Logistic, lognormal, Nakagami, Normal, Weibull*
Three-parameter distributions	*Beta, Burr, Dagum, Generalized extreme value, generalized Pareto, lognormal, log-Pearson type 3, Weibull, generalized Gamma*
Four-parameter distributions	*Kappa*
Five-parameter distributions	*Wakeby*

The article is organized in the following manner: 6.3 Introduction, 6.4 Methods, 6.5 Materials, 6.6 Results and discussion, and 6.7 Conclusions and future work. The Methods section 6.4 includes the review of the HDF (6.4.1), classes of heavy-tailed distributions in extreme value theory (EVT) in Section 6.4.2, HDF in the context of wind speed modelling (6.4.3) and goodness-of-fit (GOF) metrics in Section 6.4.4.

6.4 Methods

This section describes the methods used, the data chosen and the experiment designed – the Eastern Canada case study. The methods include a review of the Halphen distribution family, mentioning of other distribution models the HDF was compared against, and the goodness-of-fit (GOF) metrics used to assess a model's performance.

6.4.1 Review of Halphen distribution family (HDF)

The family is flexible and is used to fit a large variety of data [2]. The family is composed of three three-parameter distributions (scale and two shape parameters): Halphen type A (HA), Halphen type B (HB) and Halphen inverse type B (HIB) [2]. HA is a generalization of the two-parameter Harmonic distribution, HB with gamma distribution as a limiting case and HIB based on exponential factorial function with inverse Gamma distribution as a limiting case [2]. The HDF has a number of properties that are favorable for wind data modeling, such as: lower bound at zero (absence of location parameter), flexibility to cover a large range of shapes, explicit form of moment generating functions [2]. The properties of the HDF ensure optimality and consistency of maximum likelihood estimator (MLE) used for parameter estimation [2]. HDF "belong to the exponential family of distributions and their sufficient statistics can be obtained from their exponential forms" [26], it makes the MLE "*asymptotically unbiased and their corresponding variances minimal regardless of the sample size*" [26]. This characteristic of the HDF is obviously of importance in cases when the sample size of interest is limited.

HA distribution was introduced in 1941 as a generalization of the two-parameter harmonic distribution with the following probability distribution function (PDF):

$$f_{HA}(x, m, \alpha, v) = \frac{1}{2m^{v}K_{v}(2\alpha)} x^{v-1} e^{-\alpha\left(\frac{x}{m}+\frac{m}{x}\right)}, \tag{53}$$

Where m>0 is the scale parameter, α>0 and v∈R are shape parameters. $K_{v}(.)$ is the modified Bessel function of second kind [2](National Bureau of Standards, 1972) (Eq.(54)), can be computed by calling *bessely* function in Matlab (MathWorks, no date) or *BesselK* function of *GPBayes* package in R.

$$K_{v}(2\alpha) = \frac{1}{2}\int_{0}^{\infty} e^{-\alpha\left[t+\frac{1}{t}\right]} t^{v-1} dt = \frac{1}{2m^{v}}\int_{0}^{\infty} e^{-\alpha[w/m+m/w]} w^{v-1} dw \tag{54}$$

So,

$$f_{HA}(x,m,\alpha,v\,)=\frac{x^{v-1}e^{-\alpha\left(\frac{x}{m}+\frac{m}{x}\right)}}{\int_0^{\infty}e^{-\alpha[x/m+m/x]}\,x^{v-1}dx}, \tag{55}$$

The HB distribution exhibits a different kind of asymptotic behaviour near zero compared to HA distribution [2]. The PDF of the HB distribution is given in Eq.(56):

$$f_{HB}(x,m,\alpha,v\,)=\frac{2}{m^{2v}ef_v(\alpha)}x^{2v-1}e^{-\alpha[-\left(\frac{x}{m}\right)^2+\alpha\frac{x}{m}]} \tag{56}$$

Where *m*>0 is the scale parameter, α∈R and v> 0 are shape parameters and $ef_v(\alpha)$ is the exponential factorial function [2] given in Eq. (57).

$$ef_v(\alpha)=2\int_0^{\infty}x^{2v-1}e^{-\alpha\left(-x^2+\alpha x\right)}\,dx \tag{57}$$

So,

$$f_{HB}(x,m,\alpha,v\,)=\frac{x^{2v-1}e^{-\alpha[-\left(\frac{x}{m}\right)^2+\alpha\frac{x}{m}]}}{m^{2v}\int_0^{\infty}x^{2v-1}e^{-\alpha(-x^2+\alpha x)}\,dx} \tag{58}$$

For easier computation, the relationship between the exponential factorial function $ef_v(\alpha)$ and confluent hypergeometric function $M(a,b,z)$ (Eq. (60)) defined by Abromovitz and Stegan [3] is given in Eq.(59) [2]. The confluent hypergeometric function can be computed with *hypergeom* function in Matlab [27] and *hypergeo* function of package *hypergeo* [30] in R [29].

$$M(a,b,z)=\frac{\Gamma(b)}{\Gamma(b-a)\Gamma(a)}\int_0^1 e^{zt}\,t^{a-1}(1-t)^{b-a-1}dt \tag{59}$$

$$ef_v(\alpha)=\Gamma(v)M\left(v,\frac{1}{2},\frac{\alpha^2}{4}\right)+\alpha\Gamma\left(v+\frac{1}{2}\right)M\left(v+1/2,\frac{3}{2},\frac{\alpha^2}{4}\right) \tag{60}$$

Finally, Morlat (1956) introduced the Halphen inverse type B (HIB) distribution to complete the distribution family. The PDF of the HIB distribution is given in Eq. (61). A summary of the HDF is provided for reference in Table 6.3.

$$f_{HIB}(x,m,\alpha,v)=\frac{2}{m^{-2v}ef_v(\alpha)}x^{-2v-1}e^{-\alpha\left[-\left(\frac{x}{m}\right)^2+\alpha\frac{x}{m}\right]}=\frac{x^{-2v-1}e^{-\alpha\left[-\left(\frac{x}{m}\right)^2+\alpha\frac{x}{m}\right]}}{m^{-2v}\int_0^\infty x^{2v-1}e^{-\alpha(-x^2+\alpha x)}\,dx} \tag{61}$$

All distributions of the HDF possess an important quality, i.e. they all have triplets of so-called sufficient statistics (El Adlouni and Bobée, 2017), the summary of which is given in Table 6.2. The concept of a sufficient statistic, first introduced by Fisher in 1922 and refined by Neyman in 1935, carries as much information as the full dataset (El Adlouni and Bobée, 2017). Sufficient statistics also enable efficient parameter estimators, which was the driving force behind Halphen's research pursuit (El Adlouni and Bobée, 2017).

Table 6.2 Sufficient statistics for the HDF (adapted from [2])

Distribtion	**HA**	**HB**	**HIB**
Sufficient statistics	H^{-1}	$ln(G)$	IQ^{-1}
	$ln(G)$	A	H^{-1}
	A	Q	$ln(G)$

Definitions of arithmetic, geometric, harmonic and quadratic means are given in Eq. (62) - Eq. (65) respectively:

$$A=\sum_{i=1}^{N}x_i \tag{62}$$

$$G=\left(\prod_{i=1}^{N}x_i\right)^{1/N} \tag{63}$$

$$H=\frac{N}{\sum_{i=1}^{N}1/x_i} \tag{64}$$

$$Q=\sum_{i=1}^{N}x_i^2 \tag{65}$$

For more in details information on HDF refer to Perreault et al. [27].

Table 6.3 Moments and moment ratios for the HDF (adapted from [9])

	HA	**HB**	**HIB**
f	$\frac{1}{2m^vK_v(2\alpha)}x^{v-1}e^{-\alpha\left(\frac{x}{m}+\frac{m}{x}\right)}$ $x > 0$, $m > 0$, $\alpha > 0$ and $v \in R$	$\frac{2}{m^{2v}ef_v(\alpha)}x^{2v-1}e^{\left(-\frac{x^2}{m}+\alpha\frac{m}{x}\right)}$ $x > 0$, $m > 0$, $\alpha \in R$, $v > 0$	$\frac{2}{m^{-2v}ef_v(\alpha)}x^{-2v-1}e^{\left(-\frac{m^2}{x}+\alpha\frac{m}{x}\right)}$ $x > 0$, $m > 0$, $\alpha \in R$, $v > 0$
x_M	$m\left[\frac{v-1}{2\alpha}+\sqrt{\left(\frac{v-1}{2\alpha}\right)^2+1}\right]$	Can either have no mode, have a unique mode or possess one mode and one anti-mode (L. Perreault, Bobée and Rasmussen, 1999b)	$m\left[-\frac{\alpha}{4v+2}+\sqrt{\left(\frac{\alpha}{4v+2}\right)^2+\frac{2}{2v+1}}\right]$
μ_r'	$\frac{m^rK_{v+r}}{K_v}$	$\frac{m^ref_{v+r/2}(\alpha)}{ef_v(\alpha)}$	$\frac{m^ref_{v-r/2}(\alpha)}{ef_v(\alpha)}$

μ_1'	$\frac{mK_{v+1}}{K_v}$	$\frac{mef_{v+1/2}(\alpha)}{ef_v(\alpha)}$	$\frac{mef_{v-1/2}(\alpha)}{ef_v(\alpha)}$
μ_2'	$m^2/K_v^2(K_vK_{v+2}-K_{v+1}^2)$	$\frac{m^2(ef_vef_{v+1}-ef_{v+1/2}^2)}{ef_v^2}$	$\frac{m^2(ef_vef_{v-1}-ef_{v-1/2}^2)}{ef_v^2}$
μ_3'	$\frac{m^3}{K_v^3}(K_v^2K_{v+3}-3K_vK_{v+1}K_{v+3}+2K_{v+1}^3)$	$\frac{m^3}{ef_v^3}(ef_v^2ef_{v+1/2}-3ef_vef_{v+1/2}ef_{v+1}+2ef_{v+1/2}^3)$	$\frac{m^3}{ef_v^3}(ef_v^2ef_{v-1/2}-3ef_vef_{v-1/2}ef_{v-1/2}+2ef_{v-1/2}^3)$
μ_4'	$\frac{m^4}{K_v^4}(K_v^3K_{v+4}-4K_{v+1}K_v^2K_{v+3}+6K_vK_{v+1}^2K_{v+2}-3K_{v+1}^4)$	$\frac{m^4}{ef_v^4}(ef_v^3ef_{v+2}-4ef_{v+1/2}ef_v^2ef_{v+3/2}+6ef_vef_{v+1/2}^2ef_{v+1}-3ef_{v+1/2}^4)$	$\frac{m^4}{ef_v^4}(ef_v^3ef_{v-2}-4ef_{v-1/2}ef_v^2ef_{v-3/2}+6ef_vef_{v-1/2}^2ef_{v-1}-3ef_{v-1/2}^4)$
C_v	$\frac{\sqrt{K_vK_{v+2}-K_{v+1}^2}}{K_{v+1}}$	$\frac{\sqrt{ef_vef_{v+1}-ef_{v+1/2}^2}}{ef_{v+1/2}}$	$\frac{\sqrt{ef_{v-1}ef_v-ef_{v-1/2}^2}}{ef_{v-1/2}}$
C_s	$\frac{K_v^2K_{v+3}-3K_vK_{v+1}K_{v+2}+2K_{v+1}^3}{(K_vK_{v+2}-K_{v+1}^2)^{3/2}}$	$\frac{ef_v^2ef_{v+3/2}-3ef_vef_{v+1/2}ef_{v+1}+2ef_{v+1/2}^3}{(ef_vef_{v+1}-ef_{v+1/2}^2)^{3/2}}$	$\frac{ef_v^2ef_{v-3/2}-3ef_{v-1}ef_{v-1/2}ef_v+2ef_{v-1/2}^3}{(ef_vef_{v-1}-ef_{v-1/2}^2)^{3/2}}$

Note: K_v denotes $K_v(\alpha)=\frac{1}{2m^v}\int_0^\infty x^{v-1}e^{-\alpha\left(\frac{x}{m}+\frac{m}{x}\right)}dx$, ef_v *denotes* $ef_v(\alpha)=2\int_0^\infty x^{2v-1}e^{-\alpha\left(-x^2+\alpha x\right)}dx$

Dvorak et al. [8] studied the HDF in an attempt to classify and find links to known distributions and recognized that HDF form "*their own system of frequency functions*" [8]. To sum up, the main properties of the HDF are the presence of sufficient statistics, non-existence of location parameter and the power to represent different kinds of shapes of frequency distributions [2].

6.4.2 Classes of heavy-tailed distributions in Extreme value theory (EVT)

The 4th moment (kurtosis) of a normal distribution equals to 3. If X is a random variable and μ_x and σ_x are the mean and the standard deviation of that variable, then the distribution is called heavy-tailed (alternatively, fat-tailed or long-tailed), given Eq. (66) holds [2][33].

$$C_k = E\left[\left(\frac{X-\mu_x}{\sigma_x}\right)^4\right] > 3, \tag{66}$$

Different classes of heavy-tailed distributions exist that are nested into one another [33][34] (See Figure 6.1). In Figure 6.1, class E represents distributions with non-existence of exponential moments, class D - sub-exponential distributions, class C stands for regularly varying distributions, class B – for Pareto-type tail distributions, and class A - for α-stable (non-normal) distributions [2][34][35]. Note, that HA and HB belong to class D\C (i.e., a class of sub-exponential distributions that are not regularly varying [35]), and HIB – to class C\B (Figure 6.2).

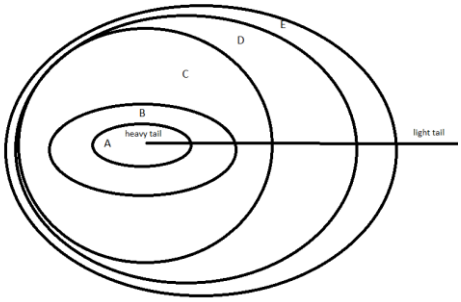

Figure 6.1 Nested classes of heavy-tailed distributions (adapted from [15][30])

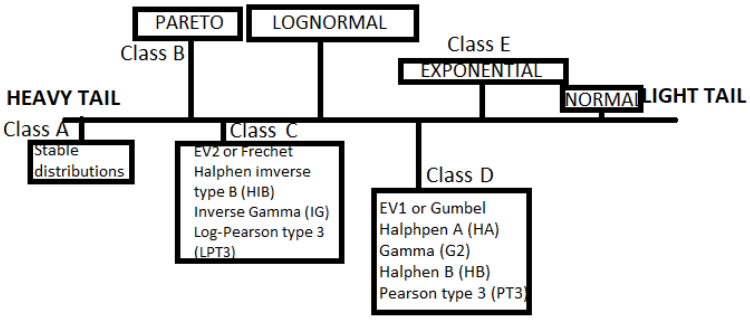

Figure 6.2 Distributions commonly used in hydrology, classed according to their tail behavior (adapted from [2][30])

El Adlouni & Bobee [2] proposed a decision support system to discriminate between the classes of heavy-tailed distributions. Log-log plot [36] helps discriminate between class C and class D, the plot of mean excess function [37] - between classes D and E, while Jackson's statistic [38] and Hill's ratio [39] are used to confirm the conclusions drawn previously using the aforementioned plots. Summary of the decision support system can be found in Figure 6.3 (adapted from [40]).

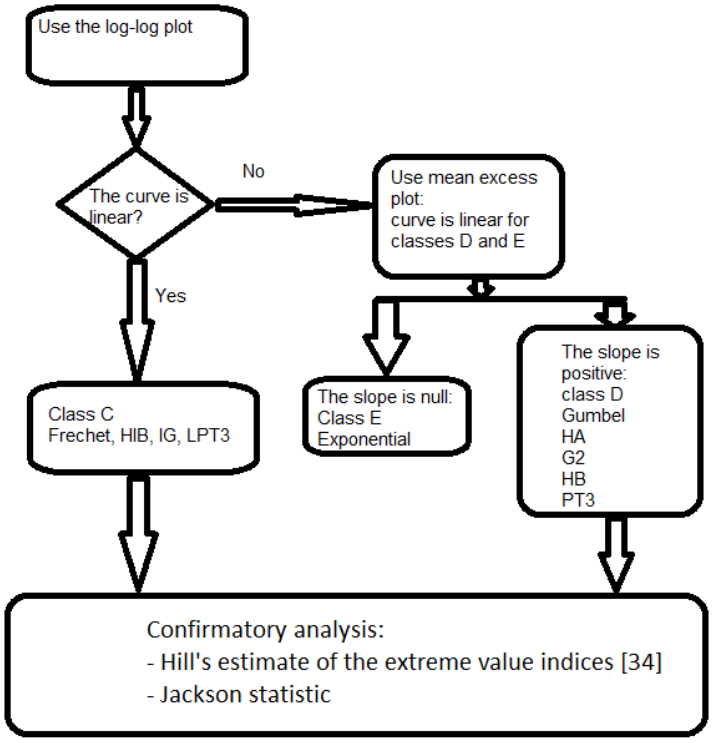

Figure 6.3 Discrimination between classes C, D and E (adapted from [2][35])

6.4.3 Halphen distribution family in the context of wind speed modelling

The analysis of wind speed data often reveals that the following are typical for such data:

(1) Asymmetry and positive skewness are often present

(2) The empirical distribution has a lower bound (0 m/s)

(3) The empirical distribution typically starts at 0, reaches the maximum and then approaches 0 again at a varying rate

All of the three characteristics are also typical for hydrological data [41]. These characteristics are not limited to the field of hydrology and wind energy but are also common in other fields. According to Bobee & Ashkar [41], such limitations imposed by the real world data lead statisticians like Karl Pearson to search for a way of constructing a family of distributions that could model such data.

6.4.4 Goodness-of-fit (GOF) metrics

Jung et al. [17] found that *KS* is the most common GOF used in the WRE studies. Other GOF metrics in popularity order were R_{pp}^2, χ^2, $RMSE_{PP}$, WPE, $RMSE_{PDF}$, *AIC, LL, BIC*, R_{PDF}^2, R_{QQ}^2, $RMSE_{QQ}$, *AD*, $RMSE_{power}$, MAE_{QQ}, R_{power}^2.

A number of goodness-of-fit (GOF) metrics include on the calculation of the likelihood function. The log-likelihood function is given in Eq. (67) [42]. The higher the value, the better the fit.

$$ln(L) = ln\left(\prod_{i=1}^{N} f_{\hat{\vartheta}}(x_i)\right) \tag{67}$$

Where $f_{\hat{\vartheta}}(x_i)$ is the PDF of the model with the estimated parameters $\hat{\vartheta}$.

One of the widely used goodness-of-fit criteria that involves the log-likelihood is the Akaike information criterion (AIC) developed by Hirotsugu Akaike [43]. AIC can be used as the means for model (distribution) selection:

$$AIC = -2\ln(L) + 2n_{par} \tag{68}$$

Where $ln(L)$ is the log-likelihood function calculated according to Eq. (67), n_{par} is the number of estimated parameters in the model. A lower value indicates better model fit.

The AIC is a parsimonious criterion because it takes the number of estimated parameters into account following the concept of Ockham's razor or also known as the law of parsimony.

Another GOF metric that also penalizes the number of parameters of a model (but stronger than AIC for samples with $N \geq 8$ [42]) is the Bayesian information criterion (BIC) defined as given in Eq. (69) [42]. Again, the lower the value, the better the model fit is.

$$BIC = -2 \ln L + k \ln N \tag{69}$$

Ouarda et al. [42] mention using (β_1, β_2) moment ratio diagram for model selection (See Eq. (70) for definition of order *r, r>1*), where $\beta_1$is the squared coefficient of skewness (Eq. (71)) and β_2 equals the coefficient of kurtosis (Eq. (72)).

$$C_r = \frac{\mu_r}{\mu_2^{r/2}} = \frac{E(X-\mu)^r}{\mu_2^{r/2}} \tag{70}$$

$$\beta_1 = {C_s}^2 = {C_3}^2 = \frac{\mu_3}{\mu_2^{3/2}} \tag{71}$$

$$\beta_2 = C_k = C_4 = \frac{\mu_4}{\mu_2^2} \tag{72}$$

Moments can be estimated from the data sample in the following manner, as given in Eq. (73):

$$m_r = \frac{1}{N}\sum_{i=1}^{N}(x_i - \bar{x})^r \tag{73}$$

The coefficient of skewness can, hence, be estimated with Eq. (74) and coefficient of kurtosis – Eq. (75):

$$\widehat{C_s} = \frac{m_3}{m_2^{3/2}} = \frac{1}{n}\sum_{i=1}^{n}(x_i - \bar{x})^3 \Big/ \left(\frac{1}{n}\sum_{i=1}^{n}(x_i - \bar{x})^2\right)^{3/2} \tag{74}$$

$$\widehat{C_k} = \frac{m_4}{m_2^2} = \frac{1}{n}\sum_{i=1}^{n}(x_i - \bar{x})^4 \Big/ \left(\frac{1}{n}\sum_{i=1}^{n}(x_i - \bar{x})^2\right)^{2} \tag{75}$$

For the HDF, two moment ratio diagrams are common - the (C_v, C_s) and the (δ_1, δ_2) moment ratio diagrams [2]. C_v is the coefficient of variation, defined by Eq. (76) and estimated

from sample by Eq. (74). C_s is the coefficient of skewness and was discussed above. Chebana et al. [1] showed that Eq. (78) is a biased estimator of C_s and gives a correction with Eq. (78).

$$C_v = \frac{\sigma}{\mu} \tag{76}$$

$$\widehat{C_v} = \frac{s}{\bar{x}} \tag{77}$$

$$\widetilde{C_s} = \widehat{C_s}\frac{\sqrt{N(N-1)}}{N-2}\left(1+\frac{8.5}{n}\right) = \frac{1}{N}\sum_{i=1}^{N}(x_i-\bar{x})^3 \Big/ \left(\frac{1}{n}\sum_{i=1}^{N}(x_i-\bar{x})^2\right)^{3/2}\frac{\sqrt{N(N-1)}}{N-2}\left(1+\frac{8.5}{N}\right) \tag{78}$$

According to El Adlouni & Bobee [2], δ_1, δ_2 are defined by Eq. (79) and Eq. (80) respectively.

$$\delta_1 = \ln\left(\frac{A}{G}\right) = \ln\left(\frac{\sum_{i=1}^{N} x_i}{(\prod_{i=1}^{N} x_i)^{1/N}}\right) \tag{79}$$

Where *A* and *G* are the arithmetic and geometric means respectively.

$$\delta_2 = \ln\left(\frac{G}{H}\right) = \ln\left(\frac{(\prod_{i=1}^{N} x_i)^{1/N}}{\frac{N}{\sum_{i=1}^{N} 1/x_i}}\right) \tag{80}$$

Where *G* and *H* are the geometric and harmonic means respectively.

6.5 Materials

This section presents the description of the Eastern Canada case study conducted in the practical part of this work. The case study was performed with the use of Matlab [27] and R [29].

6.5.1 Eastern Canada case study

The case study includes observations of the wind speed at 126 stations across the Eastern part of Canada (see Figure 6.4). The study included 13 stations in the province of New Brunswick (NB), 35 – in New Foundland and Labrador (NL), 23 – in Nova Scotia (NS), 5 – in Prince Edward Island (PE), and 50 in the province of Quebec (QC). Refer to Table 6.4 for the stations IDs for each province. Canada and can be obtained for reproducibility in [45], the initial meteorological data source is [46].

Table 6.4 Case study station IDs listed by province

NB	NL	NS	PE	QC
15, 16, 34, 35, 37, 71,78, 91, 102, 112,113,119, 121	20-33, 44, 56-60, 66, 72, 74, 75, 77, 96, 97, 100, 101, 103,107, 111, 116, 117, 126	17-19, 36, 38-40, 49, 53, 63, 67, 84, 85, 88-90, 92-95,98, 110, 114	55, 76, 83, 86, 115	1-14, 41-43, 45-48, 50-52, 54, 61, 62, 64, 65, 68-70, 73,79-82, 87, 99, 104-106, 108,109, 118, 120, 122-125

Close up of stations around Montreal, Quebec and Trois-Rivieres in the province of Quebec can be found in Figure 6.4. Close up of stations in the area surrounding Moncton (NB), Halifax (NS) and Charlottetown (PE) are depicted in Figure 6.5. Close up of stations surrounding the city of St. John's (NL) are shown in Figure 6.7.

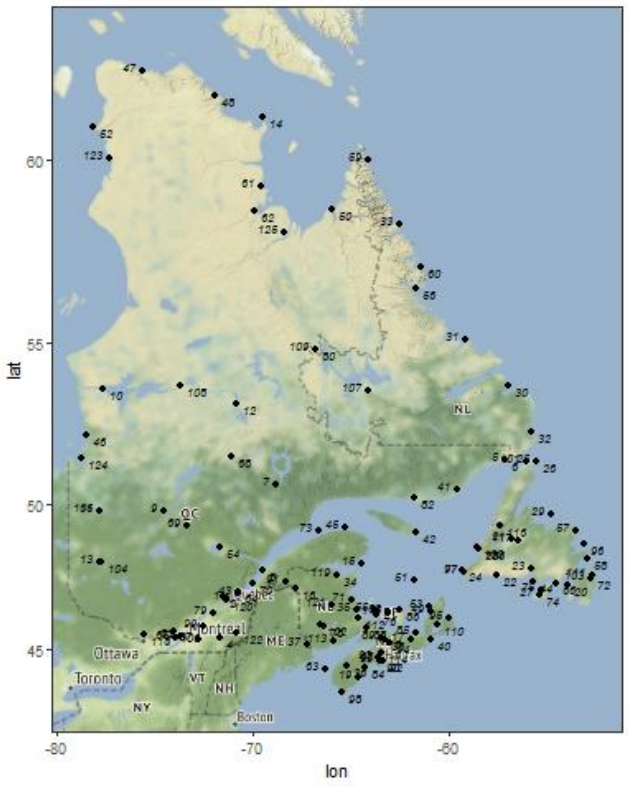

Figure 6.4 126 stations in Eastern Canada that passed the modified Mann-Kendall test [4]

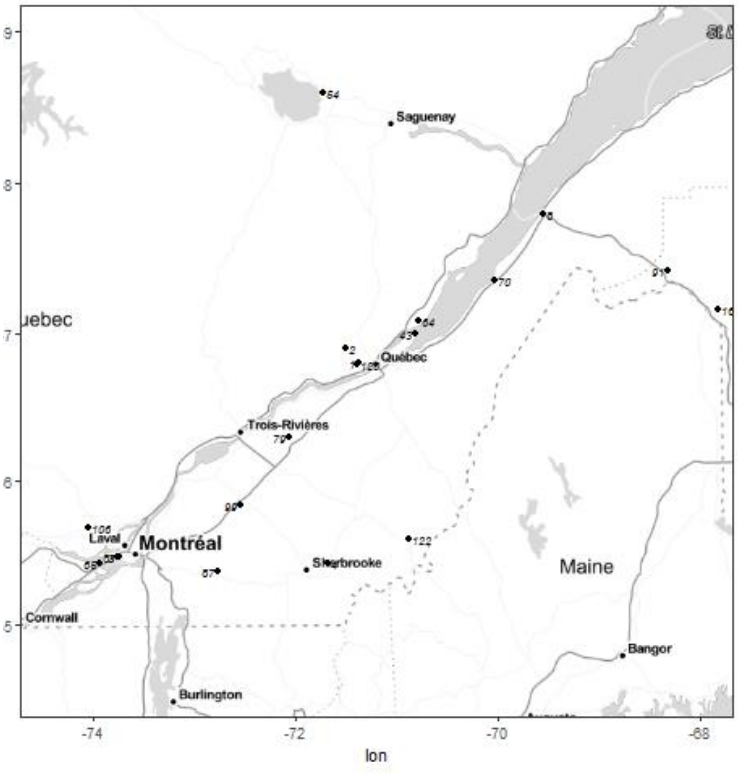

Figure 6.5 Close up of stations around Montreal, Quebec and Trois-Rivieres in the province of QC

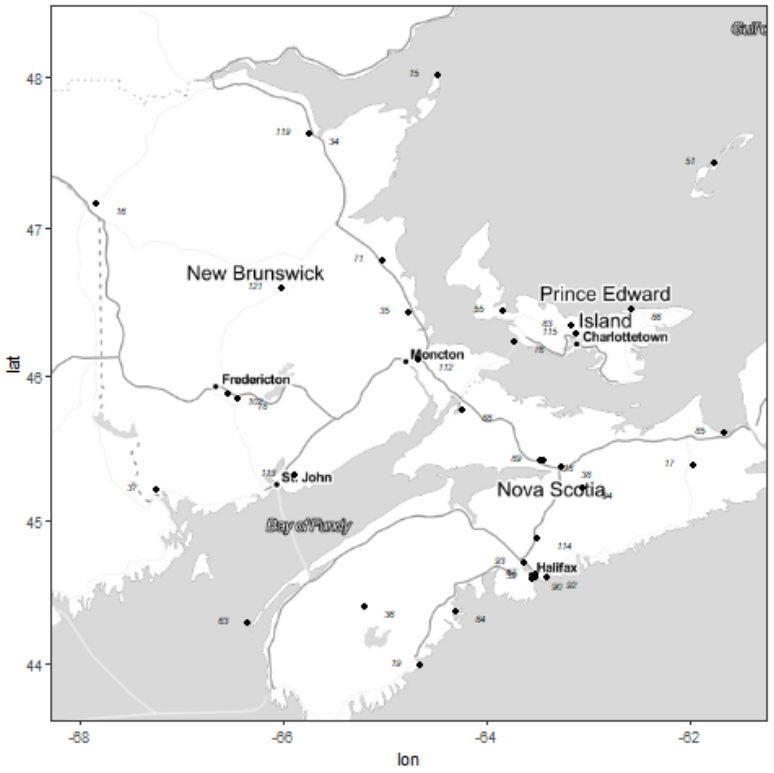

Figure 6.6 Close up of stations around Moncton (NB), Halifax (NS) and Charlottetown (PE)

All stations passed the modified Mann-Kendall (MMK) test for serially correlated data [5] using Hamed & Rao variance correction approach [6], so the samples can be considered stationary (i.e. there is no monotonic trend in the data). Moreover, the stations passed the Bayesian change point detection procedure of Seidou et al. [47] without detection of shifts. Details about the stations can be found in Appendix I. The values of sample statistics, i.e. minimum, maximum value, arithmetic, geometric, harmonic means, standard deviation, skewness, kurtosis, excess kurtosis, coefficient of variation and skewness for each station can be found in Appendix II, as well as summary of these values are given in Figure 6.8. The values of MMK test statistic and associated p-value can be found in Appendix III.

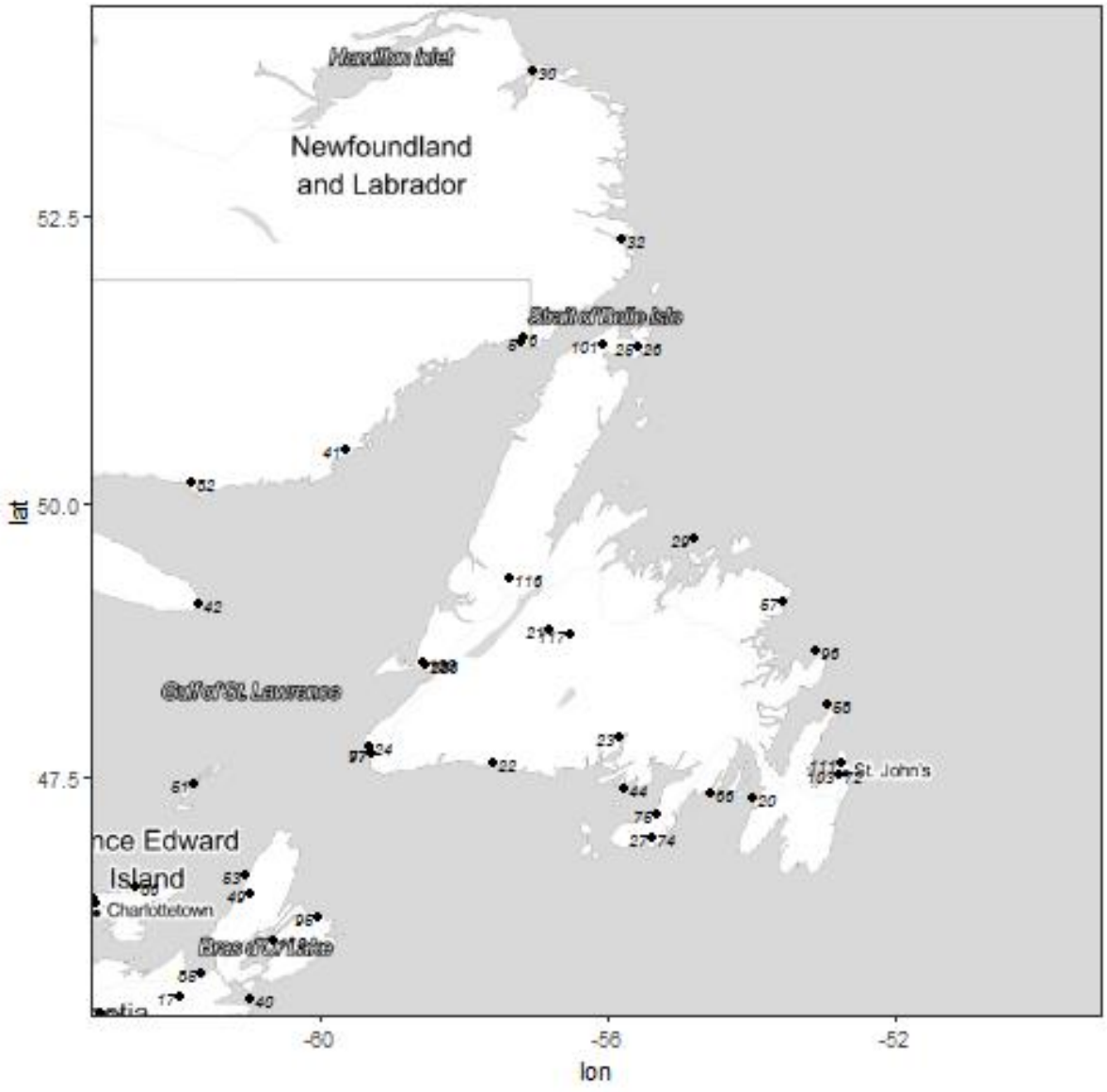

Figure 6.7 Close up of stations around St. John's (NL)

The goodness-of-fit metrics used in the case study are summarized below in Table 6.5.

Table 6.5 Goodness-of-fit metrics used in the Eastern Canada case study

GOFM	**Formula**	**Comment**
Likelihood	$L = \prod_{i=1}^{N} f_{\hat{\vartheta}}(x_i)$	$f_{\hat{\vartheta}}(x_i)$ is the PDF of the model with the estimated parameters $\hat{\vartheta}$
Akaike information criterion	$AIC = -2\ln\sum_{i=0}^{N} f(w_i) + 2n_{par}$	n_{par} is the number of parameters of a distribution

Bayesian information criterion	$BIC = -2\ln\sum_{i=0}^{N} f(x_i) + n_{par}\ln(N)$	*N* is the wind speed sample size
Kolmogorov-Smirnov statistic	$KS = \max_{0\le i\le N} \lvert F_i - \widehat{F_i}\rvert$	F_i is the empirical CDF and $\widehat{F_i}$ is the theoretical CDF
Anderson-Darling statistic	$AD = N\int_{-\infty}^{\infty} \frac{\left(F(x) - \widehat{F(x)}\right)^2}{\widehat{F(x)}(1 - \widehat{F(x)})} dF(x)$	*F* is the empirical CDF and $\widehat{F}$ is the theoretical CDF. AD places more weight on the tails of the distribution.
Root mean square error	$RMSE = \sqrt{\frac{\sum_{i=0}^{n}(x_i - \widehat{x_i})^2}{n}}$	x_i is the observed wind speed, $\widehat{x_i}$ is the predicted wind speed

The distributions used in the Eastern Canada case study with the respective acronyms, PDFs and references of use in similar studies are given in Table 6.6.

Table 6.6 Distributions used in the Eastern Canada case study

Distribution	**Acronym**	**PDF**	**Reference of use in similar WRE studies**
Generalized extreme value	GEV	$f_{GEV}(x,k,\lambda,u) = \frac{1}{\lambda}\left[1 - \frac{k}{\lambda}(x-u)\right]^{\frac{1}{k}-1} e^{-\left[1-\frac{k}{\lambda}(x-u)\right]^{\frac{1}{k}}}$, $\begin{cases} x > u + {}^{\alpha}/_{k} \ \ if\ k < 0 \\ x < u + {}^{\alpha}/_{k} \ \ if\ k > 0 \end{cases}$	[23] [41]-[44]
Two-parameter Weibull	W2	$f_{W2}(x,k,\lambda) = \frac{k}{\lambda}\left(\frac{x}{\lambda}\right)^{k-1} e^{-\left(\frac{x}{\lambda}\right)^{k}}, k>0, \lambda>0, x\ge 0$	[43]-[54]
Halphen type A	HA	$f_{HA}(x,m,\alpha,\nu) = \frac{1}{2m^{\nu}K_{\nu}(2\alpha)} x^{\nu-1} e^{-\alpha\left(\frac{x}{m}+\frac{m}{x}\right)}$, $m,\nu,x>0$	First time use for wind speed data
Halphen type B	HB	$f_{HB}(x,m,\alpha,\nu) = \frac{2}{m^{2\nu}ef_{\nu}(\alpha)} x^{2\nu-1} e^{-\alpha\left[-\left(\frac{x}{m}\right)^2+\alpha\frac{x}{m}\right]}$, $m,\nu,x>0$	First time use for wind speed data
Halphen inverse type B	HIB	$f_{HIB}(x,m,\alpha,\nu) = \frac{2}{m^{-2\nu}ef_{\nu}(\alpha)} w^{-2\nu-1} e^{-\alpha\left[-\left(\frac{w}{m}\right)^2+\alpha\frac{w}{m}\right]}$, $m,\nu,x>0$	First time use for wind speed data
Gaussian (Normal)	N	$f_N(x,\mu,\sigma) = \frac{1}{x\sigma\sqrt{2\pi}} e^{-\frac{(x-\mu)^2}{2\sigma^2}}$	[17][55]
Two-parameter Gamma	G2	$f_{G2}(x,\alpha,\beta) = \frac{1}{\Gamma(k)\theta^k} x^{k-1} e^{-\frac{x}{\theta}}, k,\theta,x>0$	[23] [41][43][44][47] [53][56]
Generalized Gamma	GG	$f_{GG}(x,a,d,p) = \frac{p}{\Gamma(d/p)a^d} x^{d-1} e^{-(\frac{x}{a})^p}, a,d,p,x>0$	[41]
Inverse Gamma	IG	$f_{IG}(x,\alpha,\beta) = \frac{\beta^{\alpha}}{\Gamma(\alpha)}\left(\frac{1}{x}\right)^{\alpha+1} e^{-\frac{\beta}{x}}, x>0$	[44][56]

The MLE is the most commonly used distribution parameter estimation technique for wind speed data [17]. MLE was used for parameter estimation of all models in the Eastern Canada case study.

6.6 Results and discussion

The descriptive statistics were calculated for the wind speed hourly data samples (Figure 6.8). It is worth mentioning that all stations except for Lac Beniot (CS ID 68) are heavy-tailed with positive excess kurtosis (See Appendix II).

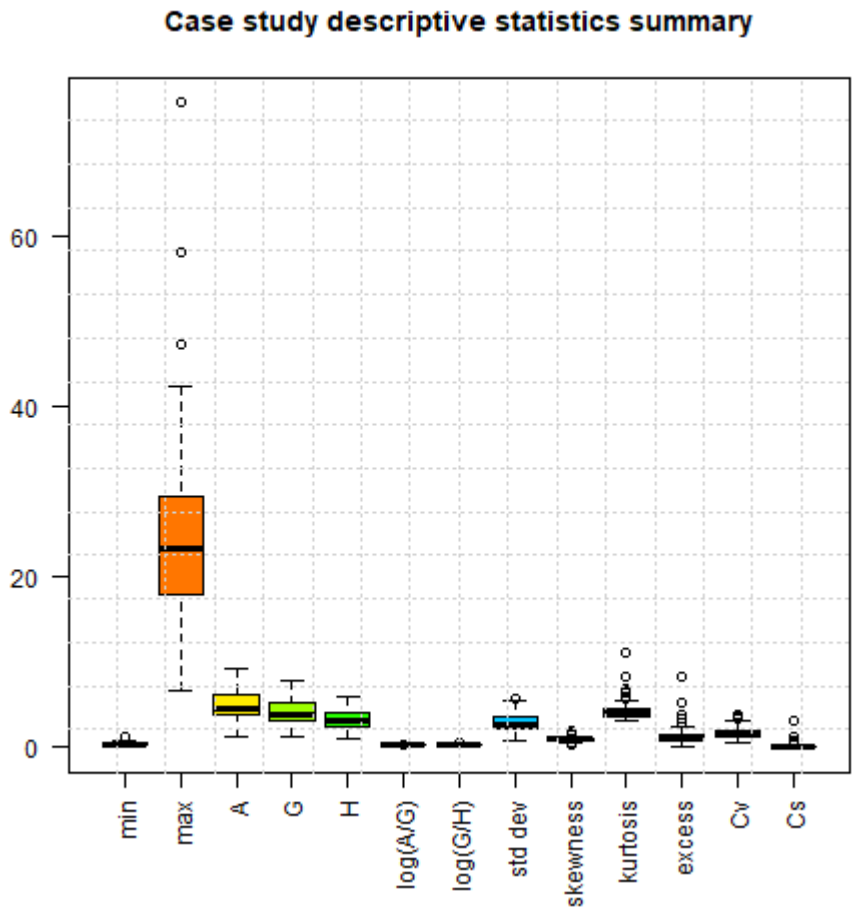

Figure 6.8 Descriptive statistics of the 126 stations summarized in a box plot

The best distribution fit results according to all metrics used in the case study are summarized in Table 6.7. The most common best-fit model is the HDF, found best on average in 76% of the stations (26% for HA and 38% for HB). The second to best-fit are the W2 (15% on average) and

GG (13% on average). What is significant is that no station data could be fitted to the HBI model. HDF (HA/HB) fit was found superior to the most commonly used model for the task of wind resource assessment, i.e. W2, 59%-100% of the time according to different GOF metrics (see Table 6). HDF showed better fit than the W2 on average 82% of the time and therefore is recommended for use.

Table 6.7 Best-fit distribution according to all GOF metrics for all stations of the Eastern Canada case study

	GEV/ML	W2/ML	HA/ML	HB/ML	HBI/ML	N/ML	G/ML	GG/ML	IG/ML	HDF superior to W2
LL	-	-	38%	46%	-	-	-	16%	-	100%
AIC	-	-	38%	46%	-	-	-	16%	-	100%
BIC	-	-	38%	46%	-	-	-	16%	-	99%
KS	1%	23%	19%	32%	-	2%	12%	10%	1%	61%
AD	-	25%	8%	42%	-	-	10%	15%	-	73%
RMSE	6.5%	40%	14%	16%	-	5%	8%	6.5%	4%	59%
Mean:	**1%**	**15%**	**26%**	**38%**	**0%**	**2%**	**5%**	**13%**	**1%**	**82%**

For simplicity of results assessment, GOF metrics for all stations are summarized in box plots in Figure 6.9 – Figure 6.14. AD boxplot can be found in Figure 6.13. A visually significantly better fit of HB and GG compared to the rest of candidate distributions can be observed for the right tail of the distribution (AD prioritizes the right tail fit).

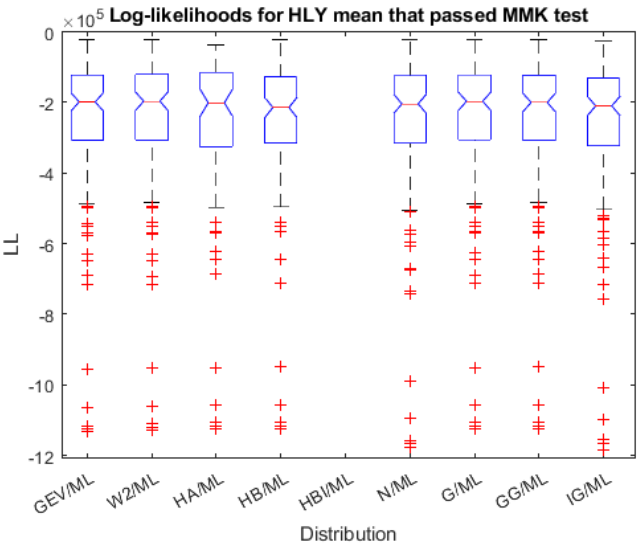

Figure 6.9 LL box plot

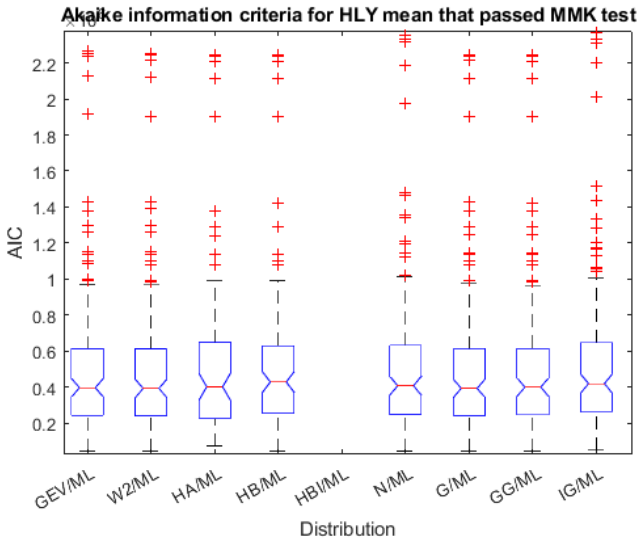

Figure 6.10 AIC box plot

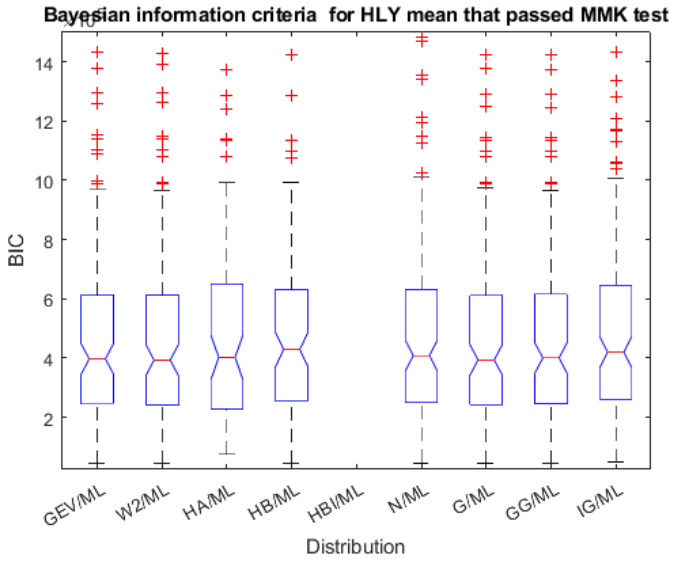

Figure 6.11 BIC statistic box plot

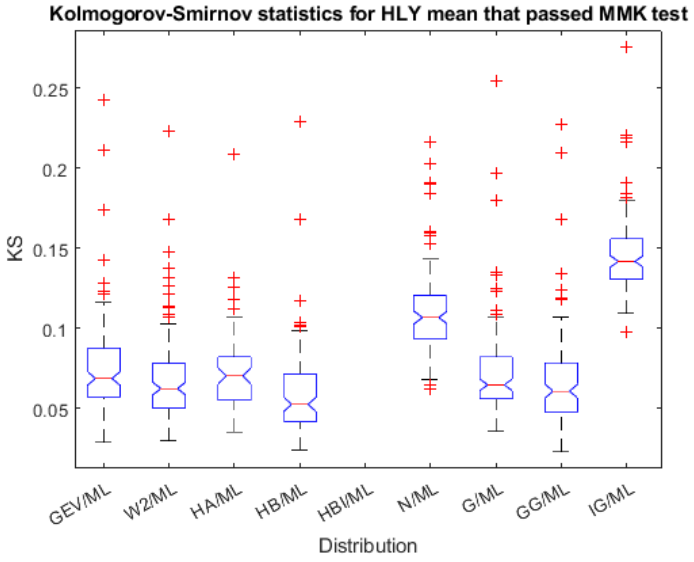

Figure 6.12 KS box plot

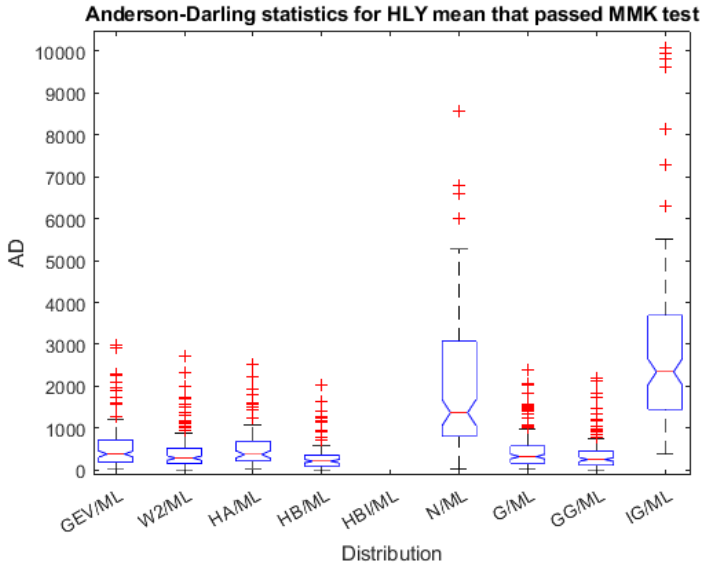

Figure 6.13 AD box plot

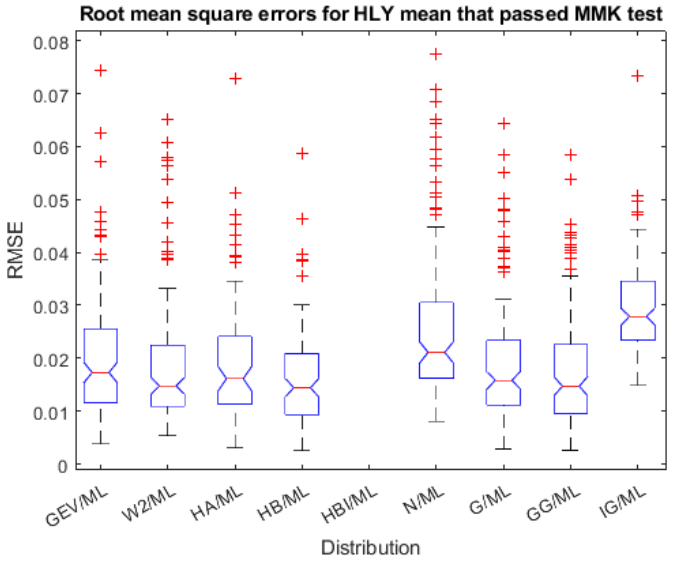

Figure 6.14 RMSE box plot

Best-fit model according to BIC and KS statistic listed by province are presented in Tables 6.8 and 6.9 respectively. No specific best-fit distributional pattern for onshore/offshore stations or short-term/long-term observation record was observed.

Table 6.8 Best-fit model according to BIC listed by province

NB	NL	NS	PE	QC
15: HB	20: GG	17: HA	55: GG	1: HA
16: HB	21: HB	18: HB	76: GG	2: HA
34: HA	22: HA	19: GG	83: GG	3: HB
35: HB	23: HA	36: HA	86: HB	4: HA
37: HA	24: HA	38: HA	115: GG	5: HB
71: HA	25: GG	39: HB		6: HA
78: HA	26: GG	40: HB		7: HA
91: HA	27: HB	49: HA		8: HB
102: HA	28: HB	53:HB		9: HB
112: GG	29:HB	63: HB		10: HA
113: GG	30: HA	67: HB		11: HB
119: HA	31: HB	84: HB		12:HB
121: HA	32: HB	85: HB		13: HB
	33: HA	88: HB		14: HB
	44: HB	90: GG		41: HA
	56: HA	92: HB		42: HB
	57: GG	95: HB		43: HB
	58: GG	98: HA		45: HB
	59: HA	110: GG		46: GG
	60: HA	114:GG		47: HB
	66: HA			48: HA
	72: HB			50: GG
	74: HB			51: GG
	75: HA			52: HB
	77: HA			54: HB
	96: HB			61: HB
	97: HA			62: HB
	100: HA			64: HA
	101: HB			65: HB
	103:HB			68: HB
	107: HA			69: HA
	111: GG			70: HA
	116: HA			73: HA
	117: HA			79: HB
	126: HA			80: GG
				81: HB
				82: HB
				87: HA
				99: HB
				104: HA
				105: HA
				106: HB
				108: HA
				109: HA
				118: W2
				120: HB
				122: HB
				123: HB
				124: HB
				125: GG

Perreault, et al. [9] showed that "*the Halphen type A distribution has the gamma (G) and the inverse gamma (IG) distributions as limiting forms*" [9]. This can be observed in the moment ratio diagrams of Figures 6.15 and 6.16. The (C_v,C_s) moment ratio diagram given in Figure 6.15 is not consistent with best-fit results according to any GOF measure (see Appendices V-X). All stations, except for station with CS ID = 23 (Station ID = 6708) fell into the area of the diagram that relates to HB.

Table 6.9 Best-fit model according to KS listed by province

NB	**NL**	**NS**	**PE**	**QC**
15: HA	20: HA	17: HB	55: HA	1: W2
16: HA	21: G	18: HA	76: HA	2: HB
34: HB	22: HB	19: HB	83: HA	3: GG
35: HA	23: W2	36: HB	86: HA	4: HB
37: HA	24: HB	38: HB	115: HA	5: HB
71: HB	25: HA	39: HA		6:
78: HB	26: HA	40: HA		7: HA
91: HA	27: HB	49: HB		8: HB
102: HB	28: W2	53: HA		9: HB
112: HA	29: W2	63: HA		10: HA
113: HA	30: W2	67: W2		11: HB
119: HB	31: W2	84: W2		12:HB
121: HB	32: HA	85: HA		13: HB
	33: W2	88: HA		14: HB
	44: HA	90: HA		41: HA
	56: HA	92: HA		42: HB
	57: HA	95: HA		43: HB
	58: HA	98: HA		45: HB
	59: HB	110: HB		46: GG
	60: HB	114: HA		47: HB
	66: HB			48: HA
	72: HA			50: GG
	74: HA			51: GG
	75: HB			52: HB
	77: HB			54: HB
	96: HA			61: HB
	97: HB			62: HB
	100: HB			64: HA
	101: GG			65: HB
	103: HA			68: HB
	107: HB			69: HA
	111: HA			70: HA
	116: HA			73: HA
	117: W2			79: HB
	126: HA			80: GG
				81: HB
				82: HB
				87: HA
				99: HB
				104: HA
				105: HA
				106: HB
				108: HA

				109: HA 118: W2 120: HB 122: HB 123: HB 124: HB 125: GG

The (δ_1, δ_2) moment ratio diagram is illustrated in Figure 6.16. According to the (δ_1, δ_2) moment ratio diagram, all stations are best characterized with a HA distribution with a positive υ scale parameter. While all the scale υ parameters, when their estimation was possible, were indeed found to be positive (See Appendix V), for some stations fitting to HA was not at all possible (the procedure of parameter estimation did not converge). This result is neither consistent with the (C_υ,C_s) moment ratio diagram given in Figure 6.15, nor with any of the GOF metrics). This aspect requires more investigation.

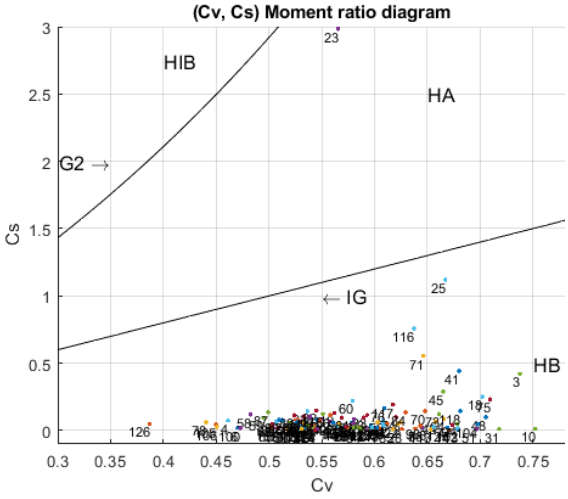

Figure 6.15 (C_v, C_s) Moment ratio diagram

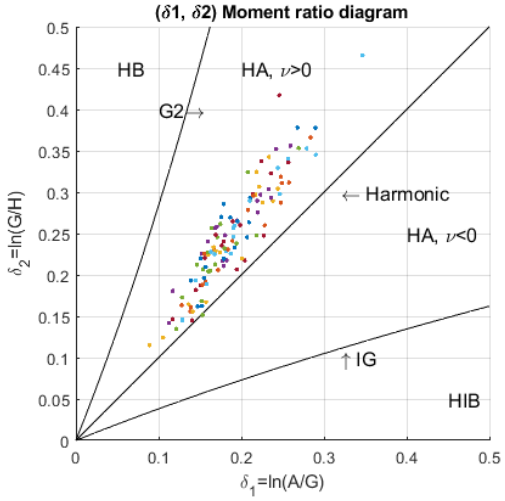

Figure 6.16 (δ_1, δ_2) Moment ratio diagram

6.6.1 Results for selected stations

We now look into the details of the cases of wind modelling for two stations for which W2 (station ID = 5251) and HA (station ID = 6501) have been determined to be best-fit according to KS. It's worth mentioning that according to log-likelihood related metrics (LL, AIC, and BIC) the top candidate in terms of fit for 5251 is HA, but for 6501 – GG. Both stations, 5251 and 6501, have a long observation record (60 and 59 years respectively). They are also quite close in terms of sample statistics (Table 6.11), but skewness-kurtosis plots, also sometimes called Cullen and Frey [64] graphs, given in Figures 6.21 - 6.22 for stations 5251 and 6501, exhibit a difference in sample point position and provide some insight into distribution model choice.

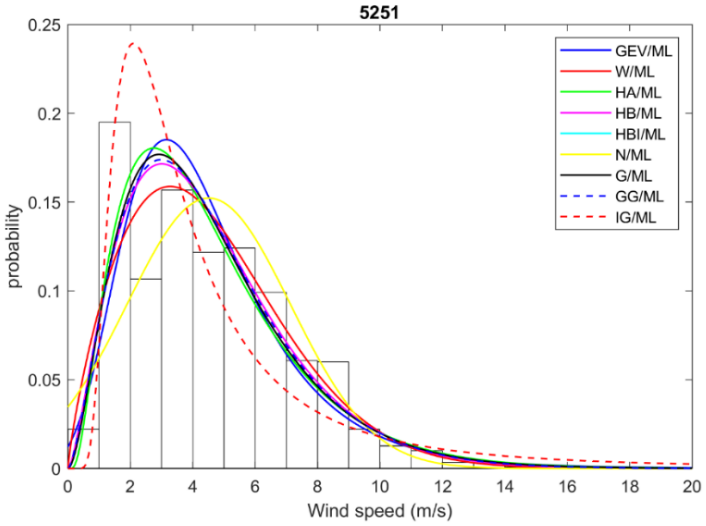

Figure 6.17 Histogram and fitted models for station ID = 5251 (W2 is best-fit according to KS)

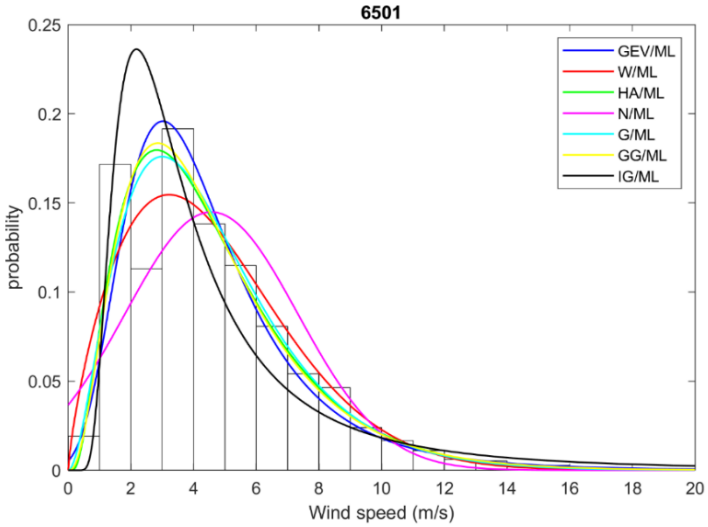

Figure 6.18 Histogram and fitted models for station ID = 6501 (HA is best-fit according to KS)

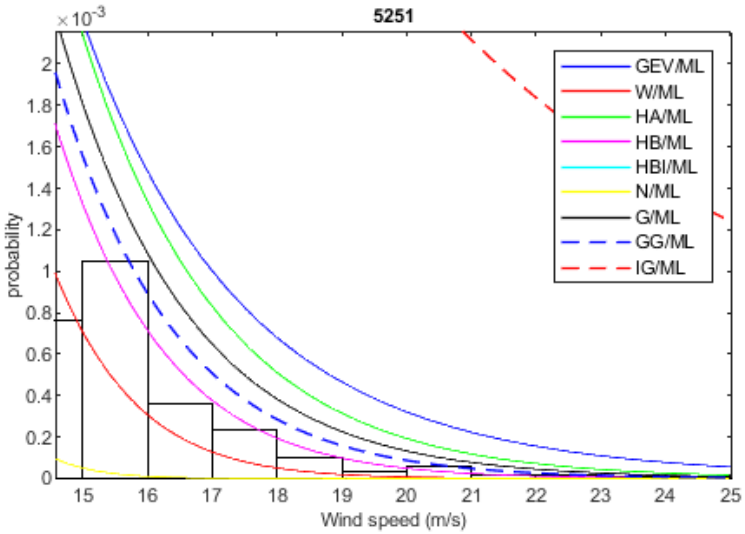

Figure 6.19 Tail zoom-in of histogram and fitted models for 5251

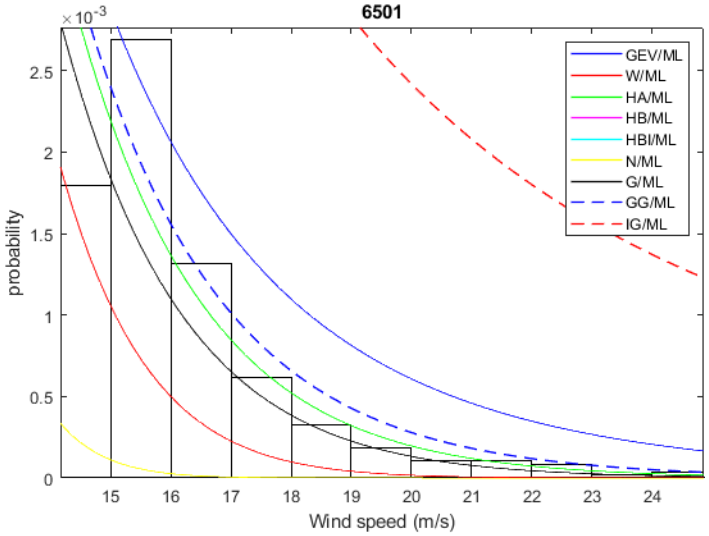

Figure 6.20 Tail zoom-in of histogram and fitted models for station 6501

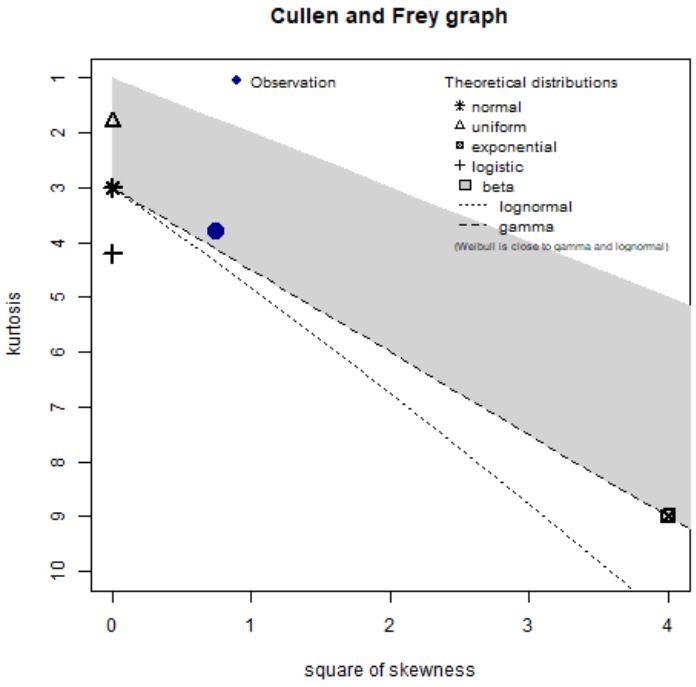

Figure 6.21 Skewness-kurtosis plot [64] for station 5251

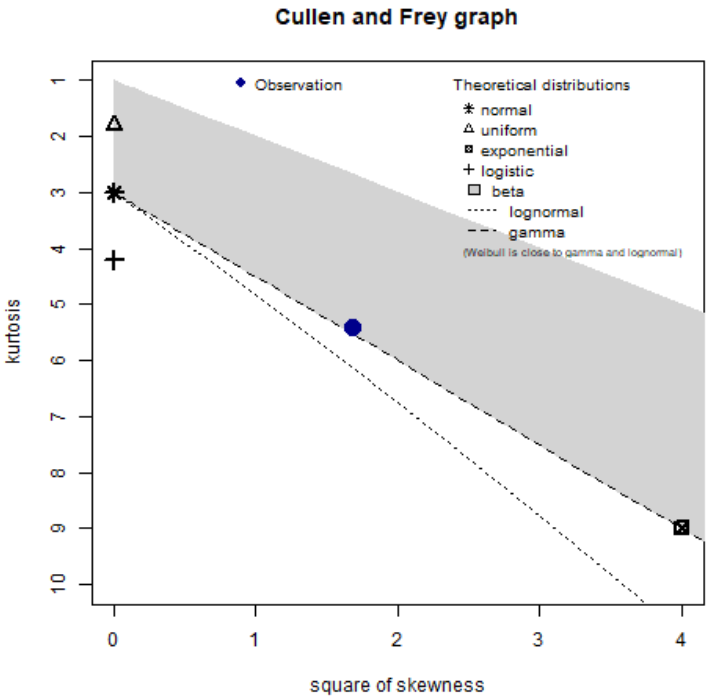

Figure 6.22 Skewness-kurtosis [64] for station 6501

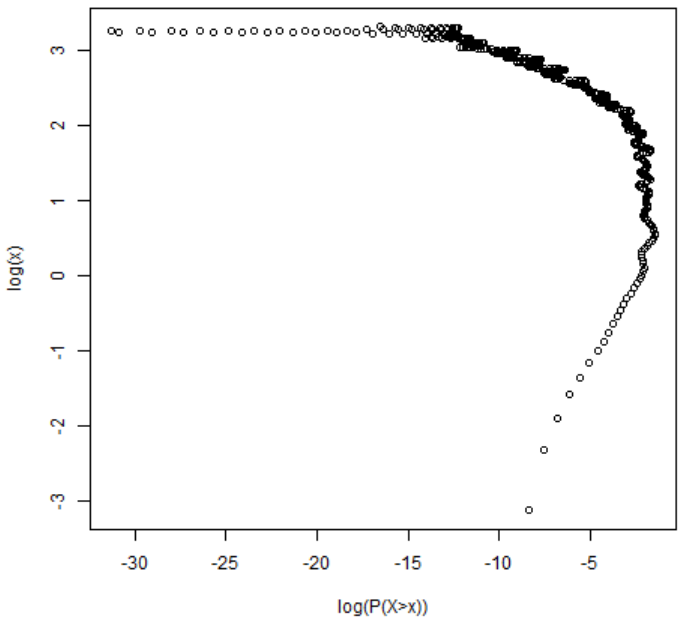

Figure 6.23: Log-log plot [36] for station ID = 5251 (W2 is best-fit according to KS)

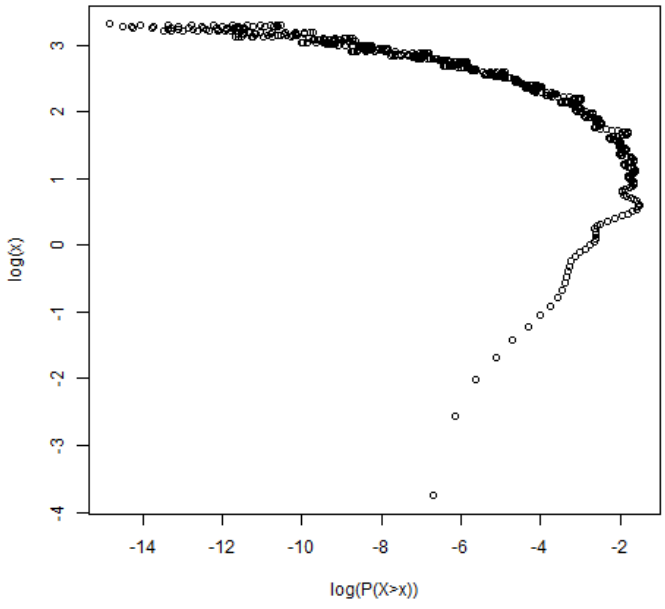

Figure 6.24: Log-log plot [36] for station ID = 6501 (HA is best-fit according to KS)

The log-log curve [36] in Figure 6.23 is not linear, hence we refer to mean excess plot (top right in Figure 6.25), the slope of which is positive. Hence, the tail behavior is classified as Class D, i.e. sub-exponential distributions (Table 6.10), according to the decision support system outlined in Figure 6.3 [40]. The top candidates to model tail behavior of such a sample are HA, HB, G2, P3, extreme value type 1 (EV1) or Gumbel distribution and lognormal (LN).

Table 6.10 Slope of mean excess plot, Shapiro-Wilk (SW) log-normality test, Modified Mann-Kendall (MMK) test, Jackson test statistics and p-values for selected stations (5251, 6501)

CS station ID	**Station ID**	**SW** (Shapiro and Wilk, 1965) **Log-normality test statistic**	**SW** (Shapiro and Wilk, 1965) **Log-normality test p-value**	**MMK** (Hamed and Ramachandra Rao, 1998) **statistic**	**MK** (Mann, 1945) **p-value**	**MMK** (Hamed and Ramachandra Rao, 1998) **p-value**	**Jackson`s test** (Jackson, 1967) **statistic**	**Jackson`s test** (Jackson, 1967) **p-value**	**Slope of mean excess plot**	**Tail behavior**
1	5251	0.93481231	2.28E-34	-0.2021858	0.02166128	0.12758335	1.56332114	1	2.68440656	Class D
19	6501	0.97841636	6.03E-21	-0.2513369	0.03794744	0.08424816	1.59586205	1	4.94858319	Class D

Keeping this in mind, we focus on how well HA and W2 model mean wind speed, which according to the sample is 4.51 m/s. The yellow curve represents the normal distribution with a mean of 4.51 and standard deviation of 2.62 (Table 6.11). Due to its symmetry, the mean of a normal distribution is also its median (that equally divides the area under the PDF is two) and its mode, i.e. most frequent or expected value. That is not the case for skewed distributions (all other candidate curves in the Figure 6.17). So, we are interested in the fifth bar from the left of the histogram in Figure 6.17, which corresponds to the bin from 4 to 5 m/s. The red curve corresponds to W2 and the green one – to HA. While Figure 6.17 does not answer the question which of the candidates is the best at modelling wind speed in all of its range, Figure 6.19 does. The fit in the right tail must be responsible for improved fit (Figure 6.19), where it is clear that the red W2 curve is closer to the histograms, rather than the green HA. The opposite is visible in Figure 6.20 (tail behavior for station 6501, where HA dominates).

Table 6.11 Sample statistics for selected stations (5251, 6501)

Station ID	**Sample minimum,** x_{min}	**Sample maximum,** x_{max}	δ_1	δ_2	**Sample mean,** μ	**Sample median**	**Sample mode,** x_M	**Sample standard deviation,** s	**Sample skewness,** $\sqrt{\beta_1}$	**Sample kurtosis,** β_2	**Sample excess kurtosis**	**Coefficient of variation,** C_v	**Coeffi of skewn** C_s
5251	0.56	26.94	0.19	0.23	4.51	4.17	1.67	2.62	0.86	3.79	0.79	1.52	0.0
6501	0.28	26.94	0.18	0.22	4.57	4.17	3.06	2.75	1.3	5.41	2.41	1.66	0.0

In the case of station 6501, the log-log curve [36] in Figure 6.24 is again not linear, and the slope of mean excess plot (top right in Figure 6.25) is again positive. Therefore, the tail behavior is also classified as Class D (6.Table 10) according to decision support system outlined

in Figure 6.3 [40]. HA is among the top candidates to model tail behavior, given that is the research question.

Table 6.12 Some sample statistics estimations based on estimated model parameters

Distribution	**Mean, μ**	**Mode, x_m**	**Standard deviation, σ**
N(μ, σ)	μ	μ	σ
HA(a, m, v)	$\frac{mK_{v+1}}{K_v}$	$m\left[\frac{v-1}{2a}+\sqrt{1+\frac{v-1^2}{2a}}\right]$	$\mathrm{m}/K_v\sqrt{K_vK_{v+2}-K_{v+1}^2}$
HB(a, m, v)	$\frac{mef_{v+1/2}(\alpha)}{ef_v(\alpha)}$	-	$\frac{m^2(ef_vef_{v+1}-ef_{v+1/2}^2)}{ef_v^2}$
W2(k, λ)	$\lambda\Gamma(1+1/k)$	$\lambda(k-1/k)^{1/k}$	$\lambda\sqrt{\Gamma\left(1-\frac{2}{k}\right)-\Gamma\left(1+\frac{1}{k}\right)^2}$

For a mindful comparison of PDFs in Figures 6.17 and 6.18, let's compute the mode, mean and standard deviation of some distributions of particular interest for the selected stations. A shortcut for the calculation is given in Table 6.12.

Table 6.13 Estimated parameters and moments for HA, HB, W2, GG, and N distributions for selected stations (5251, 6501)

CS station ID	**Station ID**	**Station name**	**Province**	**HA(α, *m, v)***	**HB(α, *m, v)***	**W2(k, λ)**	**GG(a, d, p)**	**N(μ, σ)**
1	5251	QUEBEC/JEAN LESAGE INTL A	QUEBEC	α = 0.5916372 m = 1.059223 v = 2.309711 $\widehat{x_M}$ = 3.404 μ = σ =	α = -5.276964 m = 11.20424 v = 1.279034 μ = σ =	λ = 5.091835 k = 1.81496 $\widehat{x_M}$ = μ = 4.53 σ =	a = 0.4458819 d = 2.264365 p = 1.134277 $\widehat{x_M}$ = μ =	μ = $\widehat{x_M}$ = 4.510853 σ = 2.620128
19	6501	WESTERN HEAD	NOVA SCOTIA	α = 0.6325211 m = 1.126856 v = 2.331912 μ = σ =	-	λ = 5.157046 k = 1.767681 μ = σ =	2.678728 5.599754 0.7021484 μ =	μ = $\widehat{x_M}$ = 4.568837 σ = 2.754406

The results of the calculation of the first and second non-central moments based on formulas given in Table 6.12 are presented among with the values of the estimated model parameters in Table 6.13.

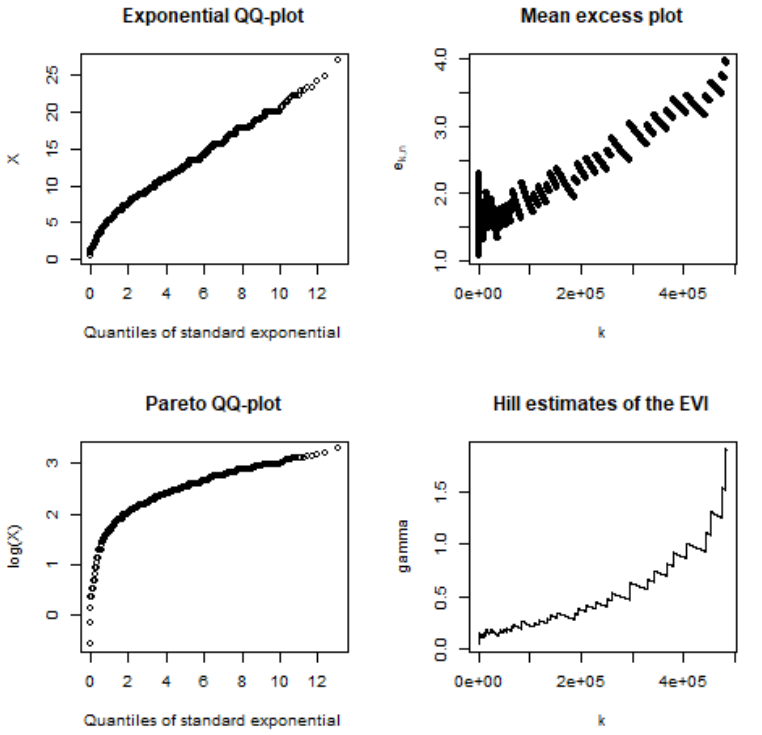

Figure 6.25 Exponential QQ plot, mean excess plot, Pareto QQ plot, Hill estimate of the extreme value indices (EVI) plot (Hill, 1975) for station ID = 5251 (W2 is best-fit according to KS)

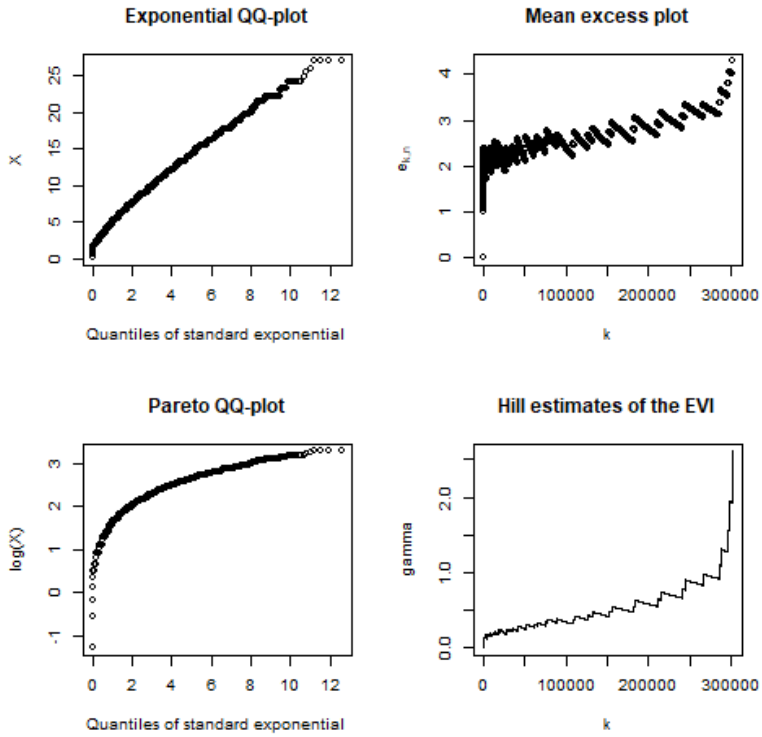

Figure 6.26 Exponential QQ plot, mean excess plot, Pareto QQ plot, Hill estimate of the EVI plot (Hill, 1975) for station ID = 6501 (HA is best-fit according to KS)

The exponential QQ-plots of Figures 6.24 and 6.25 (top left) are curves, but quite close to the line of slope 1, suggesting using the exponential distribution as a candidate model. The mean excess plots also support this argument, as they are not converging in both figures, while they are constant for exponential tail behavior [2]. On the other hand, Jackson's test [38] of exponentiality results with p-values of 1 for both stations suggests that there is not enough evidence to reject the null hypothesis of exponentiality. The Pareto-QQ plots of both figures confirm that the samples from selected stations do not exhibit Pareto type tail behavior (Class B). If they did, we would expect to see a line with a slope of 1 there instead of the curve. The Hill's ratio plots of both figures also do not converge to a constant, which suggests that Class C is not applicable for modelling tail behavior, because Hill's ratio is a consistent estimator of α in case when "*the tail is regularly varying (Class C) with tail index α*" [2]. The log-log plots support this as well, as they are linear for Class C, which is not the case for Figures 6.23 and 6.24. The Shapiro-Wilk [7] normality test of logarithm-transformed sample data rejects the null hypothesis of log normality (Class Lognormal) for any confidence level. This is the reason lognormal distributions were not originally considered among the candidates in the case study.

6.7 Conclusion and future work

In this research paper, the application of the HDF [65] was introduced to model mean wind speed. Long-term measured wind speed data sets of 126 stations in the East of Canada were examined in the case study. The effectiveness of the HDF was assessed against the W2 distribution, and 8 other distributions commonly used for mean wind speed modelling. The measures of effectiveness used in the case study included the LL, AIC, BIC, KS, AD statistics, and the RMSE. The goodness-of-fit results show very favorable results of the HDF performance for the task.

The most common best-fit model is the HDF, found best on average in 76% of the stations (26% for HA and 38% for HB). The second to best-fit are the W2 (15% on average) and GG (13% on average). What is significant is that no station data could be fitted to the HBI model. HDF (HA/HB) fit was found superior to the most commonly used model for the task of wind resource assessment, i.e. W2, 59%-100% of the time according to different GOF metric (see Table 6.5). HDF showed better fit than the W2 on average 82% of the time and therefore is recommended for use.

Modelling maximum wind speed for the extended case study with the HDF is planned to be carried out in subsequent study, as AD GOF favoring right tail fit showed improved fit for HB. The case study can also be extended by adding other distribution parameter estimation methods apart from the ML used in this case study. Dvorak et al. [8] points out that HDF does not seem to be "*as rich in a variety of forms and types as the Pearson system and they do not fulfill some particular requirements as ease of computation*" [8]. Future efforts should also focus on the continuation of this case study with the goal of comparing HDF with the Pearson distribution system.

6.8 Data availability

The data used in the case study are provided in the supplementary materials for reproducibility of results. Possible extension of this case study is encouraged.

6.9 Declaration of competing interest

There is no conflict of interest regarding this publication.

6.10 CRediT authorship contribution statement

Olga Tsvetkova: Methods, Writing - Original draft preparation.

Taha B.M.J. Ouarda: Idea & Conceptualization, Methods, Funding acquisition, Supervision, Writing - Reviewing and Editing.

6.11 Acknowledgements

This research was supported by the Canada Research Chair Program and the Natural Sciences and Engineering Research Council of Canada (NSERC).

7 BIBLIOGRAPHY

[1] F. Chebana, S. El Adlouni, and B. Bobée, “Mixed estimation methods for Halphen distributions with applications in extreme hydrologic events.”

[2] S. El Adlouni and B. Bobée, Halphen distribution family with application in hydrological frequency analysis. Water Resources Publications, LLC, 2017.

[3] National Bureau of Standards, Handbook of mathematical functions with formulas, graphs and mathematical tables, 10th Print. United States Department of Commerce, 1972.

[4] H. B. Mann, “Nonparametric Tests Against Trend,” Econometrica, vol. 13, no. 3, p. 245, Jul. 1945, doi: 10.2307/1907187.

[5] “Package ‘modifiedmk’ Title Modified Versions of Mann Kendall and Spearman’s Rho Trend Tests,” 2021, doi: 10.1017/CBO9781107415324.004.

[6] K. H. Hamed and A. Ramachandra Rao, “A modified Mann-Kendall trend test for autocorrelated data,” J. Hydrol., vol. 204, no. 1–4, pp. 182–196, Jan. 1998, doi: 10.1016/S0022-1694(97)00125-X.

[7] S. S. Shapiro and M. B. Wilk, “An analysis of variance test for normality (complete samples),” Biometrika, vol. 52, no. 3–4, pp. 591–611, Dec. 1965, doi: 10.1093/BIOMET/52.3-4.591.

[8] F. Dvorak, V., Bobée, B., Boucher, S., Ashkar, “Halphen distributions and related systems of frequency functions,” Quebec, 1988.

[9] L. Perreault, B. Bobée, and P. F. Rasmussen, “Halphen Distribution System. I: Mathematical and Statistical Properties,” J. Hydrol. Eng., vol. 4, no. 3, pp. 189–199, Jul. 1999, doi: 10.1061/(ASCE)1084-0699(1999)4:3(189).

[10] L. Perreault, B. Bobée, and P. F. Rasmussen, “Halphen Distribution System. II: Parameter and Quantile Estimation Estimation of extreme precipitations View project Statistical post-processing of ensemble weather forecasts View project,” Artic. J. Hydrol. Eng., 1999, doi: 10.1061/(ASCE)1084-0699(1999)4:3(200).

[11] F. Chebana, S. El Adlouni, and B. Bobée, “Method of moments of the Halphen distribution parameters,” Stoch. Environ. Res. Risk Assess., vol. 22, no. 6, pp. 749–757, 2008, doi: 10.1007/S00477-007-0184-4.

[12] S. El Adlouni and B. Bobée, “Sampling Techniques for Halphen Distributions,” J. Hydrol. Eng., vol. 12, no. 6, pp. 592–604, Nov. 2007, doi: 10.1061/(ASCE)1084-0699(2007)12:6(592).

[13] Y. Hundecha, A. St-Hilaire, T. B. M. J. Ouarda, S. El Adlouni, and P. Gachon, “A nonstationary extreme value analysis for the assessment of changes in extreme annual wind speed over the gulf of St. Lawrence Canada,” J. Appl. Meteorol. Climatol., vol. 47, no. 11, pp. 2745–2759, Nov. 2008, doi: 10.1175/2008JAMC1665.1.

[14] L. Zhang and V. P. Singh, “Revisiting the Application of Halphen Distributions in Flood Frequency Analysis,” J. Hydrol. Eng., vol. 26, no. 12, p. 04021042, Oct. 2021, doi: 10.1061/(ASCE)HE.1943-5584.0002133.

[15] S. El Adlouni, F. Chebana, and B. Bobée, “Generalized extreme value versus Halphen system: Exploratory study,” J. Hydrol. Eng., vol. 15, no. 2, pp. 79–89, 2010, doi: 10.1061/(ASCE)HE.1943-5584.0000152.

[16] R. Delhome, R. Billot, and N. E. El Faouzi, “Travel time statistical modeling with the Halphen distribution family,” J. Intell. Transp. Syst. Technol. Planning, Oper., vol. 21, no. 6, pp. 452–464, Nov. 2017, doi: 10.1080/15472450.2017.1326115.

[17] C. Jung and D. Schindler, “Wind speed distribution selection – A review of recent development and progress,” Renewable and Sustainable Energy Reviews, vol. 114. Elsevier Ltd, p. 109290, Oct. 01, 2019, doi: 10.1016/j.rser.2019.109290.

[18] J. A. A. Carta, P. Ramírez, and S. Velázquez, “A review of wind speed probability distributions used in wind energy analysis. Case studies in the Canary Islands,” Renew. Sustain. Energy Rev., vol. 13, no. 5, pp. 933–955, Jun. 2009, doi: 10.1016/j.rser.2008.05.005.

[19] T. B. M. J. Ouarda and C. Charron, “Distributions of wind speed in a northern environment,” in 2018 9th International Renewable Energy Congress, IREC 2018, May 2018, pp. 1–3, doi: 10.1109/IREC.2018.8362453.

[20] J. Zhou, E. Erdem, G. Li, and J. Shi, “Comprehensive evaluation of wind speed distribution models: A case study for North Dakota sites,” Energy Convers. Manag., vol. 51, no. 7, pp. 1449–1458, Jul. 2010, doi: 10.1016/j.enconman.2010.01.020.

[21] L. Wang, J. Liu, and F. Qian, “Wind speed frequency distribution modeling and wind energy resource assessment based on polynomial regression model,” Int. J. Electr. Power Energy Syst., vol. 130, p. 106964, Sep. 2021, doi: 10.1016/j.ijepes.2021.106964.

[22] H. Shi, Z. Dong, N. Xiao, and Q. Huang, “Wind Speed Distributions Used in Wind Energy Assessment: A Review,” Front. Energy Res., vol. 9, p. 790, Nov. 2021, doi: 10.3389/FENRG.2021.769920/BIBTEX.

[23] N. Aries, S. M. Boudia, and H. Ounis, “Deep assessment of wind speed distribution models: A case study of four sites in Algeria,” Energy Convers. Manag., vol. 155, pp. 78–90, Jan. 2018, doi: 10.1016/j.enconman.2017.10.082.

[24] I. Usta and Y. M. Kantar, “Analysis of some flexible families of distributions for estimation of wind speed distributions,” Appl. Energy, vol. 89, no. 1, pp. 355–367, Jan. 2012, doi: 10.1016/J.APENERGY.2011.07.045.

[25] J.-Y. Shin, T. B. M. J. Ouarda, and T. Lee, “Heterogeneous mixture distributions for modeling wind speed, application to the UAE,” Renew. Energy, vol. 91, pp. 40–52, Jun. 2016.

[26] S. El Adlouni, F. Chebana, and B. Bobée, “Generalized Extreme Value versus Halphen System: Exploratory Study,” J. Hydrol. Eng., vol. 15, no. 2, pp. 79–89, Feb. 2010, doi: 10.1061/(ASCE)HE.1943-5584.0000152.

[27] MathWorks, “Matlab R2018b.” [Online]. Available: https://www.mathworks.com/products/new_products/release2018b.html.

[28] “Package ‘GPBayes’ Title Tools for Gaussian Process Modeling in Uncertainty Quantification,” 2022, Accessed: Sep. 07, 2022. [Online]. Available: https://github.com/pulongma/GPBayes/issues.

[29] “R Core Team, R: A Language and Environment for Statistical Computing.” R Foundation for Statistical Computing, Vienna, Austria, 2020, [Online]. Available: https://www.r-project.org/.

[30] M. K. Robin S Hankin, “Package ‘hypergeo’ Title The Gauss Hypergeometric Function,” 2016.

[31] G. Morlat, “Les lois de probabilités de Halphen,” 1956. Accessed: Jul. 15, 2022. [Online]. Available: http://www.sfds.asso.fr/publicat/rsa.htm.

[32] L. Perreault, B. Bobée, and P. F. Rasmussen, “Halphen Distribution System. I: Mathematical and Statistical Properties,” J. Hydrol. Eng., vol. 4, no. 3, pp. 189–199, Jul. 1999, doi: 10.1061/(ASCE)1084-0699(1999)4:3(189).

[33] T. Werner and C. Upper, “Time Variation in the Tail Behavior of Bund Future Returns,” J. Futur. Mark., vol. 24, no. 4, pp. 387–398, 2004, doi: 10.1002/fut.10120.

[34] T. Werner and C. Upper, “Time Variation in the Tail Behaviour of Bunds Futures Returns,” SSRN Electron. J., Dec. 2002, doi: 10.2139/SSRN.362320.

[35] S. El Adlouni, B. Bobée, and T. B. M. J. Ouarda, “On the tails of extreme event distributions in hydrology,” J. Hydrol., vol. 355, no. 1–4, pp. 16–33, Jun. 2008, doi: 10.1016/J.JHYDROL.2008.02.011.

[36] J. Beirlant, T. De Wet, and Y. Goegebeur, “A goodness-of-fit statistic for Pareto-type behaviour,” J. Comput. Appl. Math., vol. 186, no. 1, pp. 99–116, Feb. 2006, doi: 10.1016/J.CAM.2005.01.036.

[37] P. Embrechts, C. Klüppelberg, and T. Mikosch, “Modelling Extremal Events,” Model. Extrem. Events, 1997, doi: 10.1007/978-3-642-33483-2.

[38] O. A. Y. Jackson, “An Analysis of Departures from the Exponential Distribution,” J. R. Stat. Soc. Ser. B, vol. 29, no. 3, pp. 540–549, Sep. 1967, doi: 10.1111/J.2517-6161.1967.TB00716.X.

[39] B. M. Hill, “A Simple General Approach to Inference About the Tail of a Distribution,” https://doi.org/10.1214/aos/1176343247, vol. 3, no. 5, pp. 1163–1174, Sep. 1975, doi: 10.1214/AOS/1176343247.

[40] E. Adlouni, B. Bobée, and O. Samoud, “GUIDE FOR THE USE OF THE DECISION SUPPORT SYSTEM,” no. C, pp. 1–13, 2018.

[41] B. Bobée and F. Ashkar, “The gamma family and derived distributions applied in hydrology,” p. 203, 1991.

[42] T. B. M. J. Ouarda, C. Charron, and F. Chebana, “Review of criteria for the selection of probability distributions for wind speed data and introduction of the moment and L-moment ratio diagram methods, with a case study,” Energy Convers. Manag., vol. 124, pp. 247–265, 2016.

[43] H. Akaike, “Statistical predictor identification,” Ann. Inst. Stat. Math. 1970 221, vol. 22, no. 1, pp. 203–217, Dec. 1970, doi: 10.1007/BF02506337.

[44] S. G, “Estimating the Dimension of a Model,” Ann. Stat., vol. 6, no. 2, pp. 461–464, 1978, doi: 10.2307/2958889.

[45] O. Tsvetkova, “Eastern Canada hourly wind speed dataset 126 stations,” 2022. https://data.mendeley.com/v1/datasets/pzpfg2fdcd/draft#folder-db4509c5-aef7-48da-a3d2-f65511050ee5.

[46] “Government of Canada,” Historic data. https://climat.meteo.gc.ca/historical_data/search_historic_data_e.html (accessed Oct. 02, 2019).

[47] O. Seidou, J. J. Asselin, and T. B. M. J. Ouarda, “Bayesian multivariate linear regression with application to change point models in hydrometeorological variables,” Water Resour. Res., vol. 43, no. 8, p. 8401, Aug. 2007, doi: 10.1029/2005WR004835.

[48] T. B. M. J. Ouarda et al., “Probability distributions of wind speed in the UAE,” Energy Convers. Manag., vol. 93, pp. 414–434, Mar. 2015.

[49] N. Ayuketang Arreyndip and E. Joseph, “Generalized Extreme Value Distribution Models for the Assessment of Seasonal Wind Energy Potential of Debuncha, Cameroon,” J. Renew. Energy, vol. 2016, pp. 1–9, 2016, doi: 10.1155/2016/9357812.

[50] T. B. M. J. Ouarda and C. Charron, “On the mixture of wind speed distribution in a Nordic region,” Energy Convers. Manag., vol. 174, no. August, pp. 33–44, 2018.

[51] H. Ounis and N. Aries, “On the wind resource in Algeria: Probability distributions evaluation:,” https://doi.org/10.1177/0957650920975883, vol. 235, no. 5, pp. 1187–1204, Nov. 2020, doi: 10.1177/0957650920975883.

[52] O. Tsvetkova and T. B. M. J. Ouarda, “A review of sensitivity analysis practices in wind resource assessment,” Energy Convers. Manag., vol. 238, p. 114112, Jun. 2021, doi: 10.1016/j.enconman.2021.114112.

[53] K. S. R. Murthy and O. P. Rahi, “A comprehensive review of wind resource assessment,” Renewable and Sustainable Energy Reviews, vol. 72. Elsevier Ltd, pp. 1320–1342, 2017.

[54] H. E. AKYUZ and H. GAMGAM, “Statistical Analysis of Wind Speed Data with Weibull, Lognormal and Gamma Distributions,” Cumhur. Sci. J., vol. 38, no. 4, pp. 68–76, Dec. 2017, doi: 10.17776/CSJ.358773.

[55] Z. H. Hulio, W. Jiang, and S. Rehman, “Techno-Economic assessment of wind power potential of Hawke’s Bay using Weibull parameter: A review,” Energy Strateg. Rev., vol. 26, p. 100375, Nov. 2019.

[56] M. Sumair, T. Aized, S. A. R. Gardezi, S. U. ur Rehman, and S. M. S. Rehman, “A novel method developed to estimate Weibull parameters,” Energy Reports, vol. 6, pp. 1715–1733, Nov. 2020, doi: 10.1016/j.egyr.2020.06.017.

[57] K. Azad, M. Rasul, P. Halder, and J. Sutariya, “Assessment of wind energy prospect by Weibull distribution for prospective wind sites in Australia,” in Energy Procedia, 2019, vol. 160, pp. 348–355.

[58] J. C. Aririguzo and E. B. Ekwe, “Weibull distribution analysis of wind energy prospect for Umudike, Nigeria for power generation,” Robot. Comput. Integr. Manuf., vol. 55, pp. 160–163, Feb. 2019, doi: 10.1016/J.RCIM.2018.01.001.

[59] F. Veronesi, S. Grassi, and M. Raubal, “Statistical learning approach for wind resource assessment,” Renew. Sustain. Energy Rev., vol. 56, pp. 836–850, Apr. 2016, doi: 10.1016/J.RSER.2015.11.099.

[60] I. Tizgui, F. El Guezar, H. Bouzahir, and B. Benaid, “Wind speed distribution modeling for wind power estimation: Case of Agadir in Morocco:,” https://doi.org/10.1177/0309524X18780391, vol. 43, no. 2, pp. 190–200, Jun. 2018, doi: 10.1177/0309524X18780391.

[61] D. Villanueva and A. Feijóo, “Wind power distributions: A review of their applications,” Renew. Sustain. Energy Rev., vol. 14, no. 5, pp. 1490–1495, 2010, doi: 10.1016/j.rser.2010.01.005.

[62] B. Safari, “Modeling wind speed and wind power distributions in Rwanda,” Renew. Sustain. Energy Rev., vol. 15, no. 2, pp. 925–935, Feb. 2011, doi: 10.1016/J.RSER.2010.11.001.

[63] N. Masseran, A. M. Razali, and K. Ibrahim, “An analysis of wind power density derived from several wind speed density functions: The regional assessment on wind power in Malaysia,” Renew. Sustain. Energy Rev., vol. 16, no. 8, pp. 6476–6487, Oct. 2012, doi: 10.1016/J.RSER.2012.03.073.

[64] A. Cullen and H. Frey, Probabilistic Techniques in Exposure Assessment. A Handbook for Dealing with Variability and Uncertainty. New York and London: Plenum Press, 1999.

[65] O. Tsvetkova and T. B. M. J. Ouarda, “Quasi-Monte Carlo technique in global sensitivity analysis of wind resource assessment with a study on UAE,” J. Renew. Sustain. Energy, vol. 11, no. 5, 2019, doi: 10.1063/1.5120035.

8 OFFSHORE WIND RESOURCE ASSESSMENT WITH QUICKSCAT DATA IN THE UAE

Titre de l'article :

ÉVALUATION DES RESSOURCES ÉOLIENNES OFFSHORE AVEC LES DONNÉES QUICKSCAT AUX ÉAU

Authors :

Olga Tsvetkova, INRS-ETE

Taha B.M.J. Ouarda, INRS-ETE

Titre of book or journal :

European Conference on Renewable Energy Systems (ECRES 2023)

Date of submission : 2022/09/16

DOI : -

Contribution of authors :

Olga Tsvetkova: Conceptualization, Methods, Writing - Original draft preparation.

Taha B.M.J. Ouarda: Funding acquisition, Supervision, Writing - Reviewing and Editing.

8.1 Abstract

SeaWinds/QuikSCAT wind speed data are used for offshore wind resource assessment of the Persian Gulf. The data were collected from 07.1999 to 11.2009. The wind speed is extrapolated to 112 m hub height. The two-parameter Weibull distribution is fitted to the extrapolated wind speed, and the Weibull shape and scale parameters are estimated with the maximum likelihood method. The region of interest is an 11 x 20 grid bounded to (51.8° E, 24° N; 56.3° E, 26.5° N) or 220 quadrants of size 25.45 km x 24 km. The annual energy production and wind electricity production cost were calculated for each quadrant. The annual energy production with a 3MW wind turbine are 1050 - 1265 W/m2 and 17.5 - 19 GWh/a. The average wind speed at 100 m height is 10.4 - 11 m/s. The most probable wind speed at 100 m height is 14.4 – 15.8 m/s, and the wind speed with maximum energy at 100 m height is 7.2 – 12.9 m/s. Offshore wind electricity can be delivered at the cost of 1.6 – 1.8 $ct/kWh with a 3 MW wind turbine.

8.2 Nomenclature

h_0	Roughness length
C_r	Maintenance cost
$D_{0.95}$	Critical value of Kolmogorov-Smirnov statistic at 5% significance level
EP_t	Theoretical wind energy production
$F_{n,0.95}(w)$	Confidence band for the empirical cumulative distribution function at 5% significance level
$F_n(w)$	Empirical cumulative distribution function of the wind speed
F_w	Cumulative distribution function of the two-parameter Weibull distribution
P_{curve}	Power curve of a wind turbine
w_{MP}	Most probable wind speed
w_{cut_in}	Cut in wind speed of a wind turbine
w_{cut_out}	Cut out wind speed of a wind turbine
w_{maxE}	Wind speed carrying maximum energy
A	Availability of a wind turbine
AEP	Annual energy production of a wind turbine
D	Kolmogorov-Smirnov statistic
EC	Offshore wind electricity cost
f(w)	Probability density function
h	height
I	Initial investment
i	Inflation rate
N	Wind speed time series sample size
r	Interest rate
SV	Scrap value
t	Lifetime of a wind turbine
w	Wind speed
Γ	Gamma function
λ	Scale parameter of the two-parameter Weibull distribution
μ	Mean value of wind speed
ρ	Air density
k	The shape parameter of the two-parameter Weibull distribution

8.3 Abbreviations

AEP	AEP
CDF	Cumulative distribution function
KS	Kolmogorov-Smirnov
MCP	Measure-correlate-predict
OWF	Offshore wind farm
W2	The two-parameter Weibull distribution
WRA	Wind resource assessment

8.4 Introduction

A rapid cost reduction over the last decade [1][2][3] was observed in the wind energy sector, making it a fast-growing industry. Offshore wind farms (OWFs) are being equipped with bigger turbines, and offshore wind is expected to continue to grow [1][3][4]. Offshore winds are more substantial and steadier compared to onshore winds. On the one hand, offshore wind resource is more promising than onshore, but on the other, it is more challenging. Mounting a wind turbine in an open sea requires more investment, effort and time. Higher investments have to do with the underwater tower, foundation and underwater cables [5]. Another challenge is collecting wind data at a planning stage. Often, there are no meteorological stations nearby and applying measure-correlate-predict (MCP) techniques using onshore data frequently provides results with too much uncertainty and other constraints. For instance, Manwell et al. [6] conclude that closer attention should be paid to the MCP method's ability to predict wind speed distributions. Measurement campaigns are usually expensive, and in situ measurements obtained show to be insufficient [7]. The question raised is whether wind speed data collected with remote sensing technology can be useful for offshore wind resource assessment (WRA)?

For instance, the QuikSCAT wind data have recently gained momentum in WRA with several case studies from over the world [8][9][10]. QuikSCAT data over the Persian Gulf was used to study the propagation of Makran swells [11] and nutrient salts' distribution in surface waters [12], but not for WRA per se. A world map of wind power density using QuikSCAT data (at 10 m height) was found in a study on wind power distribution over the ocean [13]. The use of satellite data over the Persian Gulf for WRA was suggested [14]. A more detailed WRA study of the Persian Gulf with QuikSCAT data has not yet been attempted in the literature. This research intends to fill this gap.

The present paper is organized into eight main sections. Section 8.4 introduces the problem with a brief literature review: Section 8.5 covers the methods and tools used in this work. Section 8.5.1 covers SeaWinds/QuikSCAT scatterometer. Section 8.5.2 describes techniques used for WRA, such as the distribution commonly used to describe wind behavior (Section 2.2.1), goodness-of-fit (Section 2.2.2), extrapolating wind speed data to hub height (Section 2.2.3) and the economic side of a wind project (Section 2.2.4). Section 8.6 describes the case study adopted in the present work. Section 8.6.1 describes the region of interest. Section. 8.6.2 lists the case study objectives. Section 8.6.3 lists the assumptions made in the case study. Section 8.6.4 gives a detailed description of QuikSCAT wind speed data. The results are discussed in Section 8.7 and the conclusions and potential directions for future work are presented in Section 8.8. Sources

of support and data are acknowledged in Section 8.9. Finally, the data availability statement and the declaration of interest statement can be found in Section 8.10 and Section 8.11 respectively.

8.5 Materials and methods

8.5.1 SeaWinds/QuickSCAT Scatterometer

The QuikSCAT (SeaWinds Scatterometer) is an earth-observing satellite providing estimates of wind speed and wind direction over Earth water bodies. SeaWinds is the main instrument with the QuikSCAT mission (1999 - 2018) aboard Titan II. It was initially intended to collect sea-surface wind speed and direction data independent of weather conditions [15]. QuikSCAT operates in a near-polar orbit at an altitude of 800 km with an 1800-kilometre swath. Such a configuration allows 90% coverage of Earth's oceans every day. It completes a full orbit in approximately 101 minutes, translating to a little more than 14 rotations per day [15]. It is an active radar scatterometer that operates by transmitting high-frequency microwave pulses to the water body surface and measuring the echoed radar pulses scattered back to the satellite. The instrument collects wind data over the water's body at 10 m height [15].

QuikSCAT data are superior to ships and buoys in terms of spatial resolution. It provides continuous, accurate and high-resolution measurements of wind speeds and direction regardless of weather conditions [15]. QuikSCAT wind data series ended in November 2009 when the SeaWinds antenna stopped rotating due to an unknown mechanical failure. Areas of use of QuikSCAT data are global climate research, operational weather forecasting, storm warning and WRA.

8.5.2 Wind resource assessment

8.5.2.1 The two-parameter Weibull distribution

Wind speed data are frequently fitted with the two-parameter Weibull (W2) [16]-[20]. Probability density function of the W2 is given in Eq. (81).

$$f(w) = \frac{k}{\lambda}\left(\frac{w}{\lambda}\right)^{k-1} e^{-\left(\frac{w}{\lambda}\right)^{k}}, \tag{81}$$

Where w is the wind speed data sample, k is the shape parameter, and λ is the scale parameter of the W2 distribution.

The mean of the W2 distribution can be calculated according to Eq. (82) [21].

$$\mu = \lambda\Gamma(1 + 1/k) \tag{82}$$

According to [22], the most probable wind speed w_{MP} and wind speed carrying most energy w_{maxE} are calculated with Eq. (83) and (84), respectively:

$$w_{MP} = \lambda(1 - 1/k)^{1/k} \tag{83}$$

$$w_{maxE} = \lambda(1 + 2/k)^{1/k} \tag{84}$$

8.5.2.2 Extrapolating wind speed to hub height

Given wind speed data at a reference height, $w(h_{ref})$, wind speed data at any height h can be obtained with the use of the log law [16]:

$$\frac{w(h)}{w(h_{ref})} = \frac{ln\left(\frac{h}{h_0}\right)}{ln\left(\frac{h_{ref}}{h_0}\right)}, \tag{85}$$

Where h_0 is the roughness length of the terrain under investigation.

8.5.2.3 Wind economics

If a considered wind regime is modelled with the W2 distribution, the wind theoretical energy production EP_t within a timeframe t in hours can be calculated according to Eq. (86):

$$EP_t(t) = pt = \frac{A}{2}\rho\lambda^3\Gamma\left(\frac{k+3}{k}\right)t, \tag{86}$$

Where *A* is the wind turbine's availability to generate electricity in percent of the timer available for electricity production (not down for maintenance), ρ is the air density, and Γ is the gamma function.

The annual energy production (AEP) of a specific wind turbine can be calculated according to Eq. (87):

$$AEP = 8760 \int_{w_{cut_in}}^{w_{cut_off}} P_{curve}(w) f(w) dw, \tag{87}$$

Where $P_{curve}(w)$ is the power curve of a specific wind turbine, w_{cut_in} is the cut-in speed, w_{cut_off} is the cut-off speed provided by the manufacturer and $f(w)$ is the probability density function of the W2.

According to [25], wind electricity cost EC can be calculated as the net present value of the expenses over energy generated over turbine lifetime *t*:

$$EC = \frac{I + C_r \left(\frac{1+i}{r-i}\right)\left[1 - \left(\frac{1+i}{1+r}\right)^t\right] - SV\left(\frac{1+i}{1+r}\right)^t}{t \times AEP}, \tag{88}$$

Where I is the initial investment cost (wind turbine price including installation costs), C_r is the maintenance or repair cost, SV is the scrap value, *r* is the interest rate, and *i* is the inflation rate. *AEP* is the wind turbine *AEP* (in kWh) defined by Eq. (87).

8.6 Description of the Persian Gulf case study

8.6.1 Region of interest

The region of interest is bounded to the box of (51.8° E, 24° N; 56.3° E, 26.5° N). It is an 11 x 20 grid of 25.45 x 25 km resolution. It covers mostly the Persian Gulf waters off the coast of the United Arab Emirates (UAE) (Figure 8.1). Recently, renewable energies received limited attention in the region due to the abundance of fossil fuel resources. However, increasing attention has been devoted to solar energy assessment over the past decade [26][27] and to WRA [28]-[31] to help meet the region's increasing demand for power. Nonetheless, most studies have focused on onshore renewable potential. The development of OWFs is presently receiving growing interest due to the ongoing oil crisis, the decreasing cost for the OWF development, and the excellent wind resource potential of the Persian Gulf.

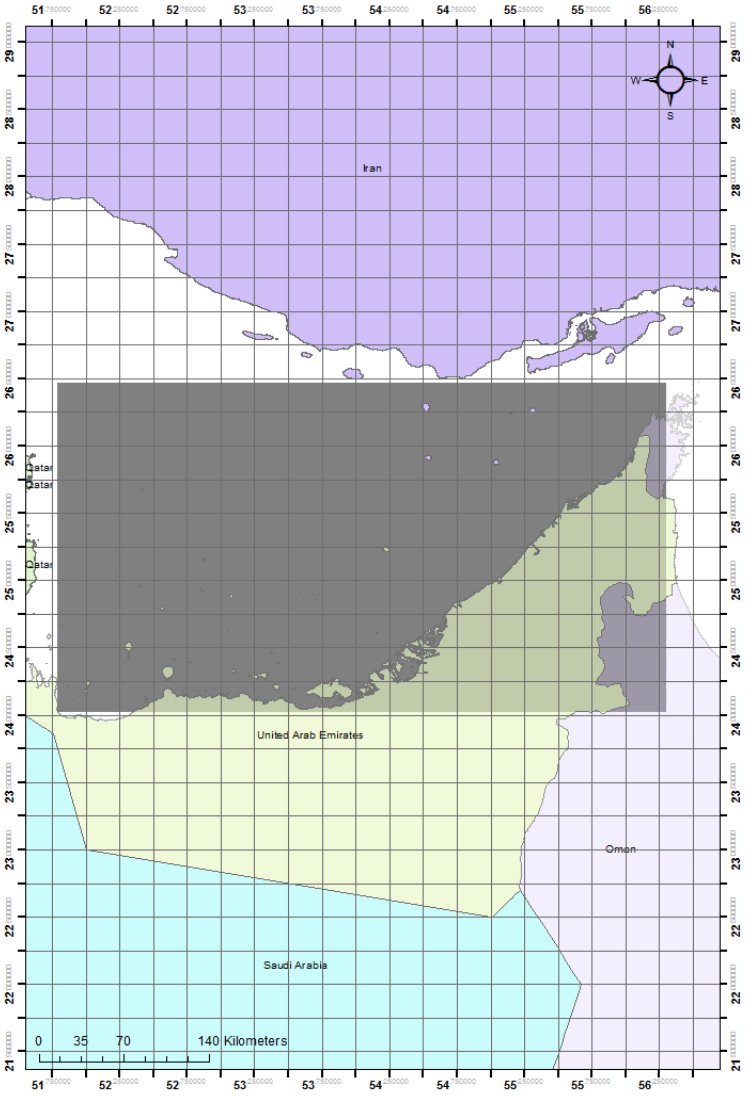

Figure 8.1 Region of interest

8.6.2 Objectives

The objectives of the Persian Gulf case study include accessing QuikSCAT wind speed data for 11 x 20 grid with 25 km resolution for the purpose of WRA, estimating AEP based on the W2 probability density function, estimating wind electricity cost and comparing results to results of similar calculations [16] but for onshore wind applications in Abu Dhabi.

8.6.3 Assumptions

The case study used the following assumptions:

1. Assumed turbine cost of 2250$/kW of rated power [16];

2. Assumed turbine lifetime of 20 years [16];

3. Maintenance or repair cost was assumed to be 25% of annual investment cost I, which is equal to I over the lifetime of a turbine [25];

4. Scrap value S was assumed to be 10% of investment cost I [25];

5. Roughness length 0.0002 [32];

6. 100% availability assumed according to the international standard IEC 61400-12-0 [33];

7. Interest rate r in UAE was assumed 1% [34];

8. Inflation rate i in UAE was assumed 1.39% [35];

9. The power curve of Vestas 112 (the specification is given in Table 8.1) was used for AEP assessment [36], wind speed data were extrapolated to a 100 m using the log law (Eq. 85) for the sake of comparing results to other studies;

10. Air density is considered constant and equal to 1.225 kg/m3.

Table 8.1 V112 specification [36]

Wind turbine	**Hub height, m**	**Rotor diameter, m**	**Rated power, kWh**	**Cut-in speed, m/s**	**Cut-off speed, m/s**
V 112	84, 94, 119	112	3000	3	25

8.6.4 QuickSCAT wind speed data

Ten-year long QuikSCAT wind speed data from 19.07.1999 to 19.11.2009 available online [37][38] are used in the case study. Wind measurements are independent of weather and time of day. The wind speed accuracy is 1 – 1.5 m/s [39]. The accuracy of measurements decreases with the rain as it contaminates the wind speed signal [32]. 3767 files (one file for each day, example is given in Figure 8.2) were collected and processed (10 days of data were missing). The spatial resolution of QuikSCAT is 25 km. The tools used to process the data and visualize results are Matlab [40], R [41], and ArcMap [42].

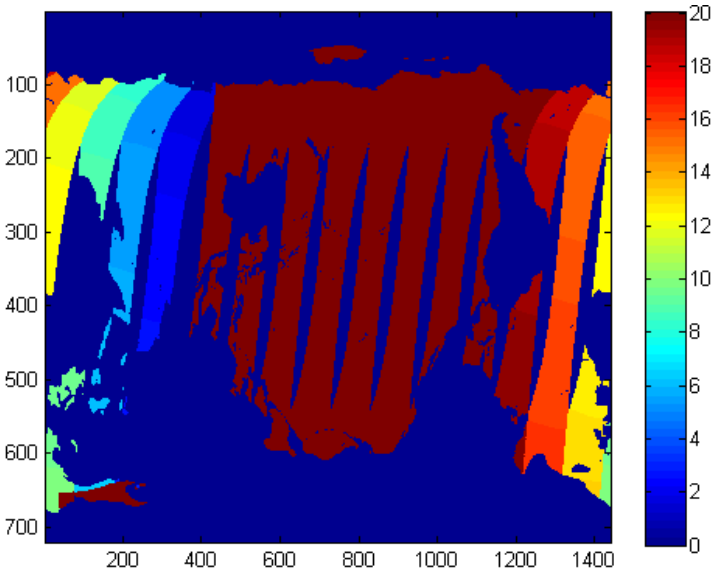

Figure 8.2 One-day QuickSCAT wind speed in m/s

8.7 Results and discussion

This section summarizes the results obtained in the case study.

8.7.1 Wind speed: mean, mode, maximum energy

Ten-year mean wind speed at 100 m height is calculated according to Eq. (82). The results for the 220 quadrants are given in Figure 8.3. The mean wind speed lies within 10 – 11 m/s.

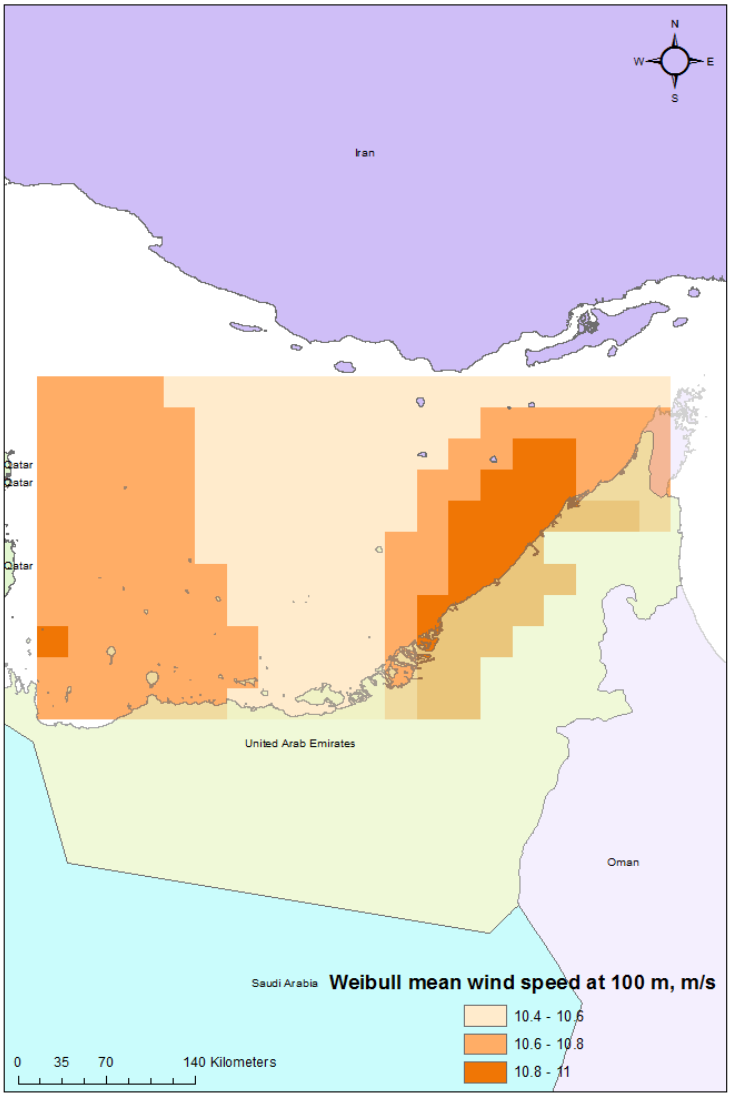

Figure 8.3 Weibull mean wind speed at 100 m map of the Persian Gulf

The most probable wind speed and wind speed with maximum energy at 100 m height are calculated with Eq. (83) and Eq. (84). The results are presented in Figure 8.4 and Figure 8.5, respectively. The most probable wind speed ranges from 14.4 to 15.8 m/s. The wind speed with maximum energy lies in the range of 7.2 – 12.9 m/s. This finding corresponds to those of [43].

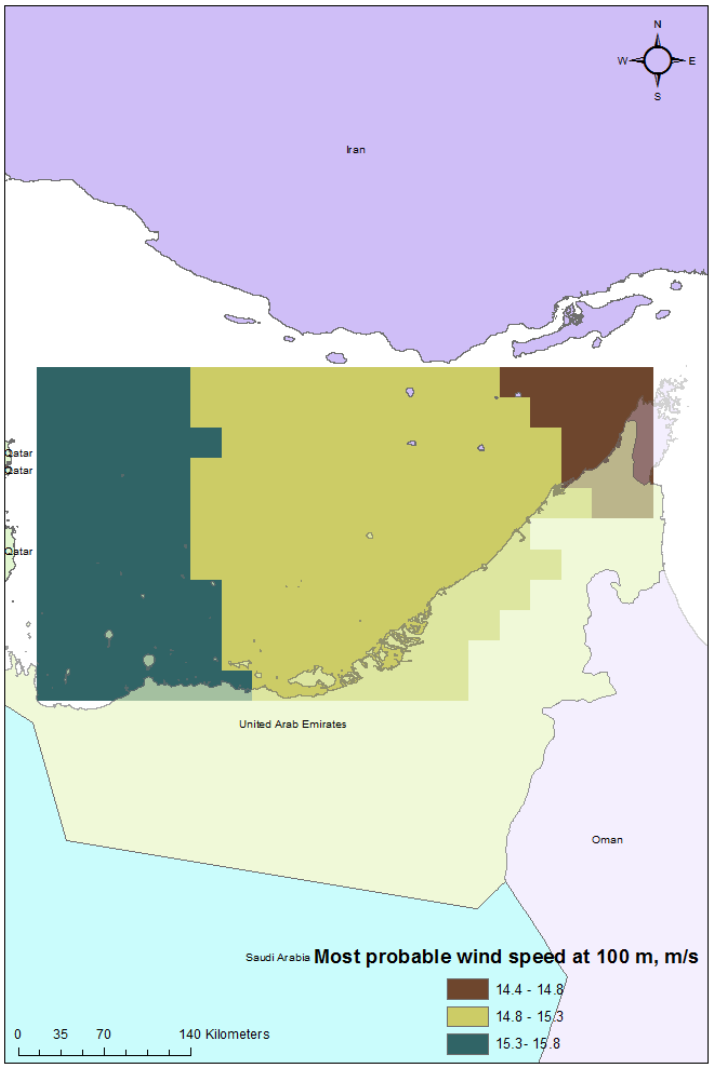

Figure 8.4 Most probable wind speed at 100 m map of the Persian Gulf

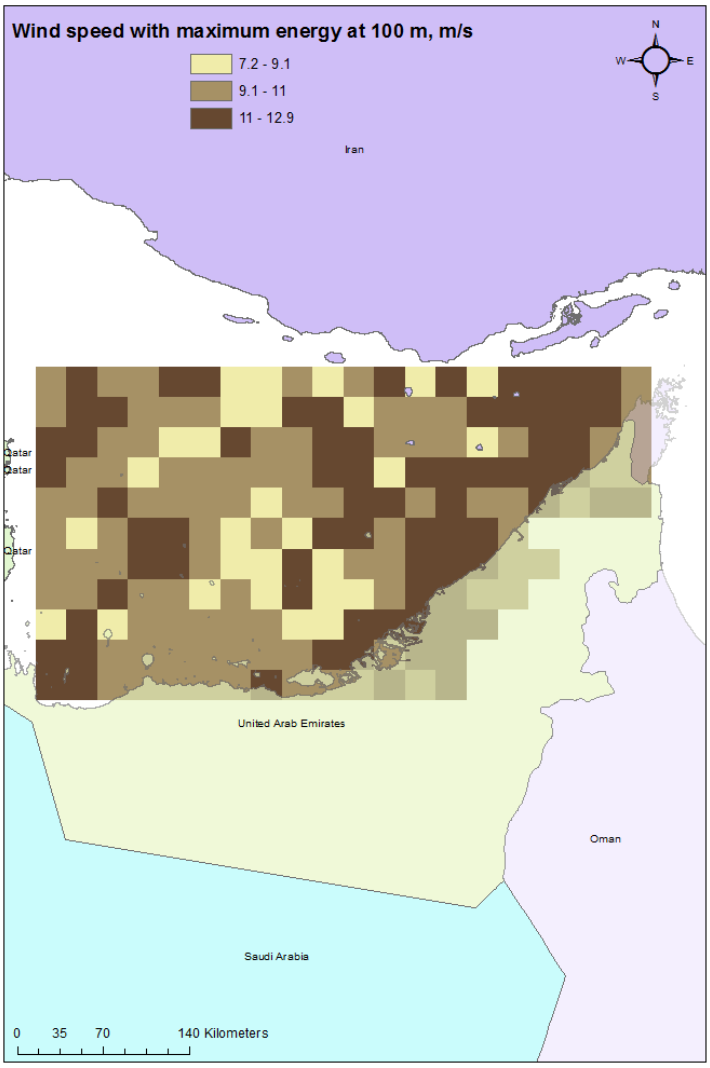

Figure 8.5 Maximum energy wind speed at 100 m map of the Persian Gulf

8.7.2 Annucal energy production

The annual energy production (AEP) with a three-blade horizontal axis wind turbine of the rated power of 3MW with the rated wind speed of 12 m/s (specification given in Table 8.1) was calculated according to Eq. (87). The AEP surface is shown in Figure 8.6 and on the map in Figure 8.7. A 3MW offshore wind turbine alone can supply from 17.5 – 19 GWh a year.

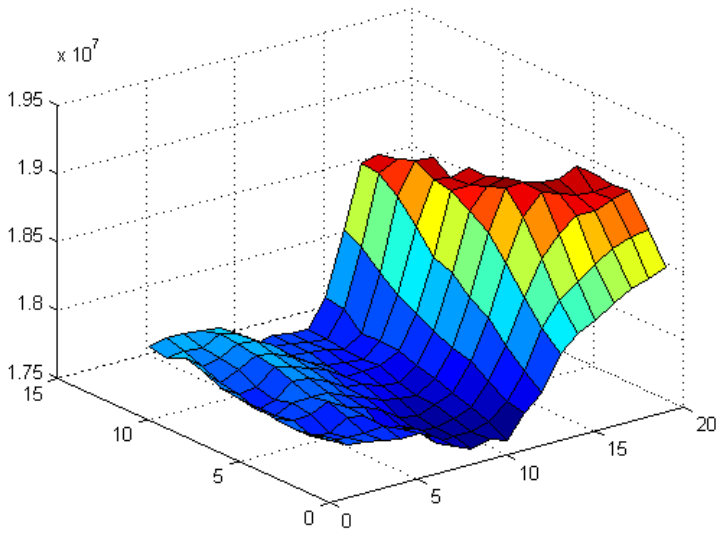

Figure 8.6 AEP surface of the region of interest

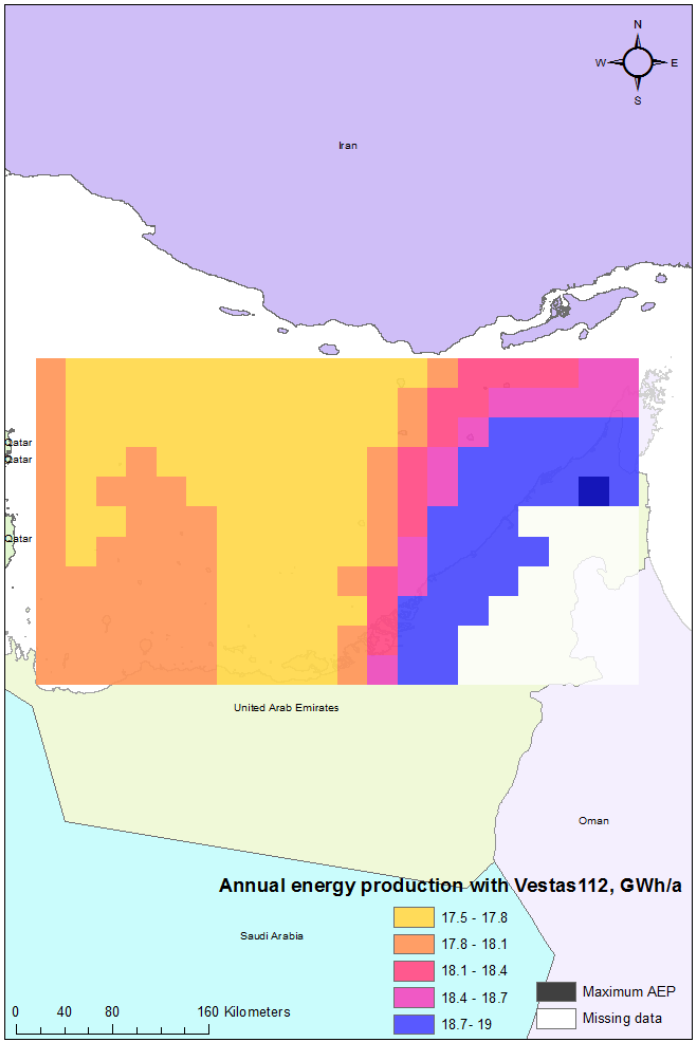

Figure 8.7 AEP with V112 map of the Persian Gulf

8.7.3 Electricity cost

Wind electricity production cost was calculated with Eq. (88) under the assumptions listed in the Description of the Persian Gulf case study section. A 3 MW turbine can supply wind electricity at the cost of 1.6 – 1.8 $ct/kWh (Figure 8.8). This finding corresponds to those of [14]. The three largest cities in the UAE, Dubai, Sharjah and Abu Dhabi (~60% of UAE population), are located on the Persian Gulf coastline. Therefore, offshore wind projects should be given closer consideration since the UAE government aims for sustainable development and strives to showcase it.

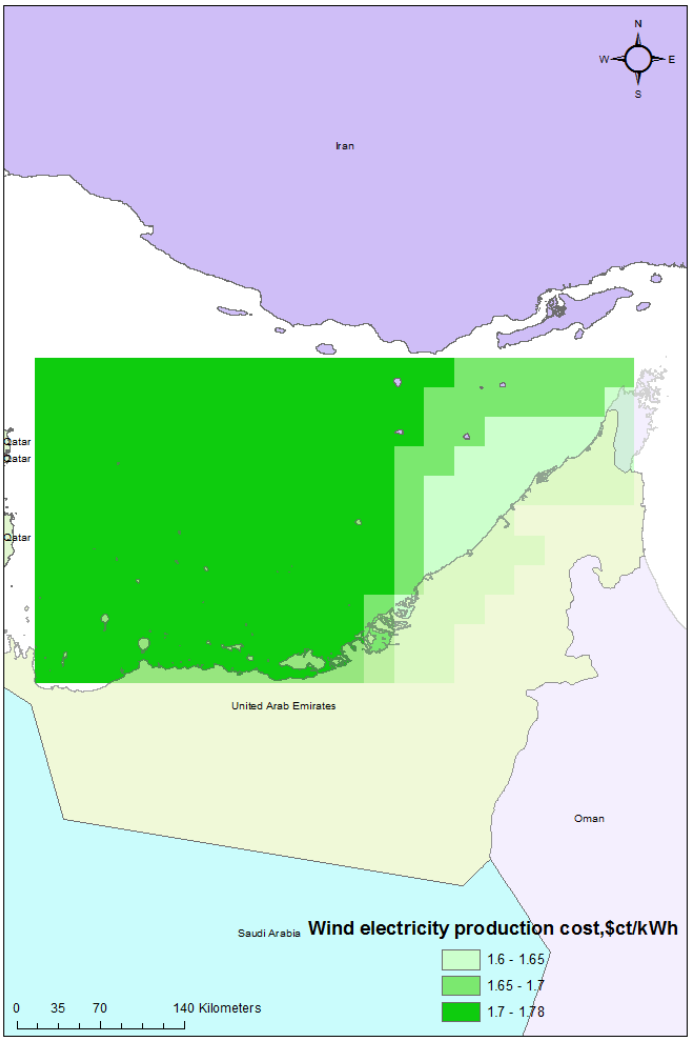

Figure 8.8 Wind electricity production cost map of the Persian Gulf

8.8 Conclusions and future work

In this study, QuikSCAT data were used for the purpose of nearshore wind resource assessment over the Persian Gulf. A consideration of nearshore offshore wind application development in the UAE is important because the three largest cities in UAE, home to approximately 60% of the population of the UAE, are located on the coastline. Wind speed time series were derived from the QuikSCAT dataset for 11 x 20 grid with 25 km resolution. Each of the time series were extrapolated to 94 m hub height using the log law, then fitted to the two-parameter Weibull distribution (shape and scale parameters were estimated using the maximum likelihood method). The Weibull mean, most probable and maximum energy wind speeds were calculated for each grid cells. The maps of the mean wind speed, most expected wind speed and maximum energy wind speed are given in Figure 3, Figure 4 and Figure 5 respectively. AEP and wind electricity price was estimated based on the W2 probability density function. The map of AEP and nearshore wind electricity cost with the Vestas V112 wind turbine are provided in Figure 8.6 and Figure 8.7 respectively. Offshore wind electricity was estimated at 1.6 – 1.8 $ct/khW.

Future work could explore topics such as combining QuikSCAT and onshore wind station records for application on islands close to Abu Dhabi, looking at other satellite wind data available (RADARSAT-2, AMI-SAR on ERS-2, ASAR on Envisat) [24]. Also, electricity demand side could be added to the case study, as well as spatial wind distribution could be studied.

8.9 Acknowledgements

Canada Research Chair Program and the Natural Sciences and Engineering Research Council of Canada (NSERC) supported the presented research.

The wind speed data used in the case study was part of the SeaWinds/QuikSCAT project run by the Jet Propulsion Laboratory (California Institute of Technology) for NASA's Earth Science Enterprise.

8.10 Data availability statement

The data that support the findings of this study are openly available in OPeNDAP Hyrax (1.16.0) [38].

8.11 Declaration of interest statement

There is no conflict of interest regarding this publication.

9 BIBLIOGRAPHY

[1] P. Veers, K. Dykes, E. Lantz, S. Barth, C.L. Bottasso, O. Carlson, A. Clifton, J. Green, P. Green, H. Holttinen, D. Laird, V. Lehtomäki, J.K. Lundquist, J. Manwell, M. Marquis, C. Meneveau, P. Moriarty, X. Munduate, M. Muskulus, J. Naughton, L. Pao, J. Paquette, J. Peinke, A. Robertson, J.S. Rodrigo, A.M. Sempreviva, J.C. Smith, A. Tuohy, R. Wiser, Grand challenges in the science of wind energy, Science (80-.). 366 (2019).

[2] T.J. Stehly, P.C. Beiter, 2018 Cost of Wind Energy Review, 2020.

[3] A. Cranmer, E. Baker, The global climate value of offshore wind energy, Environ. Res. Lett. 15 (2020) 54003.

[4] H. Díaz, C. Guedes Soares, Review of the current status, technology and future trends of offshore wind farms, Ocean Eng. 209 (2020) 107381.

[5] A. Mostafaeipour, Feasibility study of offshore wind turbine installation in Iran compared with the world, Renew. Sustain. Energy Rev. 14 (2010) 1722–1743.

[6] J.F. Manwell, A.L. Rogers, J.G. McGowan, B.H. Bailey, An offshore wind resource assessment study for New England, Renew. Energy. 27 (2002) 175–187.

[7] N. Fichaux, T. Poglio, T. Ranchin, Mapping offshore wind resources: Synergetic potential of SAR and scatterometer data, IEEE J. Ocean. Eng. 30 (2005) 516–525.

[8] S.V.V. Arun Kumar, G. Nagababu, R. Sharma, R. Kumar, Synergetic use of multiple scatterometers for offshore wind energy potential assessment, Ocean Eng. 196 (2020) 106745.

[9] M. Cáceres-Soto, H.H. Sepúlveda, K. Muñoz-Mellado, O. Artal, Comparison of QuikSCAT, WRF and buoy ocean surface wind data off Valparaiso Bay, Chile, J. Mar. Syst. 203 (2020) 103263.

[10] H.K. Jani, G. Nagababu, R.P. Patel, S.S. Kachhwaha, A Comparative Analysis of LiDAR and Wind Mast Measured Wind Data with the Reanalysis Datasets for an Offshore Location of Gujarat, in: Lect. Notes Mech. Eng., Springer, 2020: pp. 627–634.

[11] T.R. Anoop, P.R. Shanas, V.M. Aboobacker, V.S. Kumar, L.S. Nair, R. Prasad, S. Reji, On the generation and propagation of Makran swells in the Arabian Sea, Int. J. Climatol. 40 (2020) 585–593.

[12] I. A. Al-Akhaly, N. A. Al-Shwafi, S. A. Al-Kabsh, Distribution of Nutrient Salts and Chlorophyll-a in Surface Water along the Gulf of Aden and Arabian Sea Coast, Yemen, Sultan Qaboos Univ. J. Sci. [SQUJS]. 25 (2020) 17.

[13] E.C. Morgan, M. Lackner, R.M. Vogel, L.G. Baise, Probability distributions for offshore wind speeds, Energy Convers. Manag. 52 (2011) 15–26.

[14] G. Amirinia, S. Mafi, S. Mazaheri, Offshore wind resource assessment of Persian Gulf using uncertainty analysis and GIS, Renew. Energy. 113 (2017) 915–929.

[15] QuikSCAT, (n.d.). https://winds.jpl.nasa.gov/missions/quikscat/ (accessed August 19, 2020).

[16] J.F. Manwell, J.G. McGowan, A.L. Rogers, Wind energy explained : theory, design and application, Wiley, 2009.

[17] K. Azad, M. Rasul, P. Halder, J. Sutariya, Assessment of wind energy prospect by Weibull distribution for prospective wind sites in Australia, in: Energy Procedia, Elsevier Ltd, 2019: pp. 348–355.

[18] Z.H. Hulio, W. Jiang, S. Rehman, Techno-Economic assessment of wind power potential of Hawke's Bay using Weibull parameter: A review, Energy Strateg. Rev. 26 (2019) 100375.

[19] O. Tsvetkova, T.B.M.J. Ouarda, Quasi-Monte Carlo technique in global sensitivity analysis of wind resource assessment with a study on UAE, J. Renew. Sustain. Energy. 11 (2019).

[20] T.B.M.J. Ouarda, C. Charron, On the mixture of wind speed distribution in a Nordic region, Energy Convers. Manag. 174 (2018) 33–44.

[21] M. Evans, N. Hastings, B. Peacock, Statistical Distributions, 3rd ed., John Wiley & Sons, Ltd, 2000.

[22] O.S. Ohunakin, O.O. Akinnawonu, Assessment of wind energy potential and the economics of wind power generation in Jos, Plateau State, Nigeria, Energy Sustain. Dev. 16 (2012) 78–83.

[23] T.B.M.J. Ouarda, C. Charron, F. Chebana, Review of criteria for the selection of probability distributions for wind speed data and introduction of the moment and L-moment ratio diagram methods, with a case study, Energy Convers. Manag. 124 (2016) 247–265.

[24] T.P. Chang, Performance comparison of six numerical methods in estimating Weibull parameters for wind energy application, Appl. Energy. 88 (2011) 272–282.

[25] L.D.A. Lima, C.R.B. Filho, Wind resource evaluation in São João do Cariri (SJC) - Paraiba, Brazil, Renew. Sustain. Energy Rev. 16 (2012) 474–480.

[26] IRENA, Masdar Institute, Renewable Energy Prospects: United Arab Emirates, REmap 2030 analysis, (2015). https://www.irena.org/remap (accessed January 10, 2020).

[27] T.B.M.J. Ouarda, C. Charron, P.R. Marpu, F. Chebana, The Generalized Additive Model for the Assessment of the Direct, Diffuse, and Global Solar Irradiances Using SEVIRI Images, With Application to the UAE, IEEE J. Sel. Top. Appl. Earth Obs. Remote Sens. 9 (2016) 1553–1566.

[28] S. Loutatidou, N. Liosis, R. Pohl, T.B.M.J. Ouarda, H.A. Arafat, Wind-powered desalination for strategic water storage: Techno-economic assessment of concept, Desalination. 408 (2017) 36–51.

[29] M.S. Naizghi, T.B.M.J.M.J. Ouarda, Teleconnections and analysis of long-term wind speed variability in the UAE, Int. J. Climatol. 37 (2017) 230–248.

[30] J.-Y. Shin, T.B.M.J. Ouarda, T. Lee, Heterogeneous mixture distributions for modeling wind speed, application to the UAE, Renew. Energy. 91 (2016) 40–52.

[31] T.B.M.J. Ouarda, C. Charron, J.-Y. Shin, P.R. Marpu, A.H. Al-Mandoos, M.H. Al-Tamimi, H. Ghedira, T.N. Al Hosary, Probability distributions of wind speed in the UAE, Energy Convers. Manag. 93 (2015) 414–434.

[32] P. Beaucage, G. Lafrance, J. Lafrance, J. Choisnard, M. Bernier, Synthetic aperture radar satellite data for offshore wind assessment: A strategic sampling approach, J. Wind Eng. Ind. Aerodyn. 99 (2011) 27–36.

[33] IEC, Iec 61400-12-1, 2005.

[34] UAE interest rate, (n.d.). https://tradingeconomics.com/united-arab-emirates/interest-rate (accessed August 18, 2020).

[35] UAE inflation rate, (n.d.). https://tradingeconomics.com/united-arab-emirates/inflation-cpi (accessed August 18, 2020).

[36] Vestas V112 Offshore, (n.d.). https://en.wind-turbine-models.com/turbines/667-vestas-v112-offshore (accessed August 18, 2020).

[37] FTP Access to SeaWinds/QuikSCAT images, (n.d.). ftp://ftp.ssmi.com/qscat/bmaps_v04/ (accessed August 18, 2020).

[38] OPeNDAP Hyrax (1.16.0), Contents of /OceanWinds/quikscat/, (2020). https://opendap.jpl.nasa.gov/opendap/OceanWinds/quikscat/contents.html (accessed August 10, 2020).

[39] N. Ebuchi, H.C. Graber, M.J. Caruso, Evaluation of wind vectors observed by QuikSCAT/SeaWinds using ocean buoy data, J. Atmos. Ocean. Technol. 19 (2002) 2049–2062.

[40] MathWorks, Matlab R2018b, (n.d.). https://www.mathworks.com/products/new_products/release2018b.html.

[41] R Core Team, R: A Language and Environment for Statistical Computing, (2020). https://www.r-project.org/.

[42] ArcGIS, ArcMap, (n.d.). https://desktop.arcgis.com/en/arcmap/.

[43] T. Ouarda, Modeling and integration of information about inter-annual variability in renewables, Keynote Presentation. 3rd International Workshop on Data Analytics for Renewable Energy Integration, ECML-PKDD 2015 conference, Porto, Portugal, September 7-11, 2015., Porto, Portugal, 2015.

10 GENERAL CONCLUSION AND DISCUSSION

This dissertation consisted of four articles (Tsvetkova and Ouarda, 2019)(Tsvetkova and Ouarda, 2021)(Tsvetkova and Ouarda, 2022)(Tsvetkova and Ouarda, 2023b). The first two focused on sensitivity analysis. (Tsvetkova and Ouarda, 2019) is a research into the sampling used for the quasi-monte Carlo experiment of the "*golden standard of global sensitivity analysis*", the Sobol method. (Tsvetkova and Ouarda, 2021) is a comprehensive review of the sensitivity analysis practices in the field of wind resource assessment. (Tsvetkova and Ouarda, 2023b) introduced the Halphen distribution family, used in flood frequency analysis, to model mean wind. (Tsvetkova and Ouarda, 2022) is an application paper for offshore wind resource assessment. The first and fourth papers used wind speed data from the United Arab Emirates. The third paper used wind speed data from 126 historical meteorological datasets in Eastern Canada (Tsvetkova, 2022). The second paper (Tsvetkova and Ouarda, 2021) was dedicated purely to a review of sensitivity and somewhat uncertainty analyses in wind resource assessment.

The research paper (Tsvetkova and Ouarda, 2019) focused on the aspects of the application of the Sobol method as a variance-based global sensitivity analysis method for wind resource assessment and some aspects of its application. (Tsvetkova and Ouarda, 2019) conducted two case studies (one on a test model, another – on a wind energy model at Masdar City, United Arab Emirates) and concluded that, first, sampling based on Sobol sequences outperformed Latin hypercube sampling and pseudo-random sampling. Second, it was concluded that brute force calculation of the first-order and total effect sensitivity indices offers high accuracy and is recommended for use in most wind resource assessment models. When the number of variables does not allow it, estimation of these indices can be used. Third, the United Arab Emirates case study on the estimation of annual energy production in Masdar City suggests that "*the influence of variance in Weibull parameters on the variance of annual energy production might be overestimated, while the influence of variance in air density might be overlooked. These results are specific to the case study and should not be generalized without further effort*."

The annual energy production case study (Tsvetkova and Ouarda, 2019) illustrated how the Sobol method of global sensitivity analysis (which offers uncertainty analysis results alongside) can be set up with the means of a quasi-Monte Carlo experiment and at no extra cost ('R Core Team, R: A Language and Environment for Statistical Computing', 2020). The wind community could benefit from adopting the Sobol method, due to the fact, that it provides credible sensitivity results for annual energy production models nonlinear in their nature. The second reason for speaking in favour of Quasi-Monte Carlo use is that by setting up a global sensitivity

analysis study with quasi-Monte Carlo, a probability density function of the output model (uncertainty analysis results) is obtained with the same experiment. Finally, a quasi-Monte Carlo experiment allows for miscellaneous data and information about a site of interest to be incorporated into an uncertainty study, including both uncertainty and sensitivity analyses.

Moving on to the findings of the comprehensive review (Tsvetkova and Ouarda, 2021), it was discovered that the common sensitivity analysis practices in the field of wind potential estimation greatly correspond with those of (Mora, Spelling and Weijde, 2021) in offshore wind and (Menberg, Heo and Choudhary, 2016) but in application to building energy models. In both wind energy and building energy, the models are nonlinear (Menberg, Heo and Choudhary, 2016). The difference is that in building simulation global sensitivity analysis is computationally expensive (Burhenne *et al.*, 2013), while it provides stable results (Menberg, Heo and Choudhary, 2016). In wind energy models in the scope of the review (Tsvetkova and Ouarda, 2021), a computational burden is not an issue (except for the offshore cost model of (Mora, Spelling and Weijde, 2021)), although it is one for weather research and forecast models computational fluid dynamics models (Tsvetkova and Ouarda, 2019).

It was also observed in the review (Tsvetkova and Ouarda, 2021), that the definition and purpose of sensitivity analysis in wind energy potential estimation are often misconstrued in several ways. A universal definition of sensitivity analysis in this field is currently absent. (Tsvetkova and Ouarda, 2021) concluded that this discrepancy in terminology causes a discrepancy in motivation, misunderstanding in the research questions sensitivity analysis addresses and goals sensitivity analysis could help achieve (Section 4.11 for details). The finding corresponds with (Saltelli *et al.*, 2008)(Razavi and Gupta, 2015).

(Tsvetkova and Ouarda, 2021) found that the most common sensitivity analysis outputs among variables of interest used in wind energy potential estimation have been identified as goodness-of-fit metrics, wind power, wind energy or annual energy production, net present value, internal rate of return, levelized cost of energy, capital and operational expenses of wind turbines or farms. All of the mentioned were also shown to be nonlinear. Convenience is what lies at the root of the popularity of one-at-a-time sensitivity analysis, yet not its credibility. On top of this, one-at-a-time sensitivity analysis has been previously shown to be unsuitable for nonlinear models by some scholars (Harenberg *et al.*, 2018)(Saltelli and Annoni, 2010)(Douglas-Smith *et al.*, 2020). Nevertheless, one-at-a-time sensitivity analysis is still flourishing by dominating other sensitivity analysis methods in the field of wind energy potential estimation with prevailing nonlinear models. 53-100% of articles reviewed in each category (82% on average, see Table

4.10) used the local method (Tsvetkova and Ouarda, 2021). Despite its unreliability, policy implications were made based on the results of sensitivity analyses of levelized cost of energy (Carmichael, Lea and Balatbat, 2016)(Sliz-Szkliniarz *et al.*, 2019), this in itself is a call for some serious concern. Moreover, professional software designed for the assessment of renewable energy projects, for instance, RETScreen (*Natural Resources Canada: RETScreen*, 2020), is promoting the use of unreliable analysis as a means of assessing risks associated with investing in wind project development.

Section 2.8 Geography (Tsvetkova and Ouarda, 2021) found that Great Britain, the United States and China are the most studied countries in this regard. In addition, the levelized cost of energy was found the most popular model in wind project assessment. (Tsvetkova and Ouarda, 2021) reported that "*offshore wind is of special significance to the UK and Spain*". The offshore wind energy sector has shown significant cost reduction in the last decade, making the more abundant potential of offshore wind energy feasible for making it part of the grid. Assessment of possible profits of the next generation of offshore floating wind farms calls for complex nonlinear techno-economic models "*that capture the new relationships formed due to rapid technological advancement and policy incentives*" (Mora, Spelling and Weijde, 2021). They report that relationships between inputs and outputs in complex cost models of the offshore wind sector are poorly understood, therefore, global sensitivity analysis was deemed necessary to study these such models (Mora, Spelling and Weijde, 2021).

(Pianosi and Wagener, 2018) emphasized the significance of global sensitivity analysis for decision support in the policy. Yet this voice remains unheard, although the abundance of software tools for global sensitivity analysis was shown (Tsvetkova and Ouarda, 2021). "*When GSA was found to be used in wind resource assessment*" (Tsvetkova and Ouarda, 2021), the most common method was the Sobol method, and the least common was Shapley effects (Song, Nelson and Staum, 2015) and PAWN (Pianosi and Wagener, 2018).

(Tsvetkova and Ouarda, 2021) focused on the specifics of the application and discussed three examples illustrating that one-at-a-time sensitivity analysis cannot only be misleading for nonlinear models but also – for linear models under some circumstances (See Section 4.10.1). (Tsvetkova and Ouarda, 2021) warn that if local sensitivity analysis was chosen to be used at all, it "*should be used with extreme caution, as SA results are sensitive to the distributions of the inputs*".

The third article of this dissertation (Tsvetkova and Ouarda, 2023b) introduced the application of the Halphen distribution family (Zhang and Singh, 2021) to model mean wind speed.

(Tsvetkova and Ouarda, 2023b) assessed the effectiveness of the Halphen distribution family against some distributions, such as the two-parameter Weibull distribution, and some other distributions commonly called for the task (Table 6.6). The goodness-of-fit metrics used in the case study included the log-likelihood, Akaike information criterion, Bayesian information criterion, Kolmogorov-Smirnov statistic, Anderson-Darling statistic, and the root mean square error (Table 6.5). The goodness-of-fit results show very favourable results of the Halphen distribution family performance for the task.

(Tsvetkova and Ouarda, 2023b) found the most common best-fit model to belong to the Halphen distribution family (26% for Halphen type A and 38% for Halphen type B). The second to best-fit were reported by (Tsvetkova and Ouarda, 2023b) to be the two-parameter Weibull (15%) and generalized Gamma distribution (13%). (Tsvetkova and Ouarda, 2023b) found that none of the hourly wind speed data at the 126 stations in Eastern Canada could be fitted to the Halphen inverse type B distribution. Halphen-A and Halphen-B fit was found superior to the most commonly used model for the task of wind resource assessment (two-parameter Weibull), 59%-100% of the time (Tsvetkova and Ouarda, 2023b) according to different goodness-of-fit metrics (Table 6.5). (Tsvetkova and Ouarda, 2023b) recommended the Halphen distribution family for mean wind speed modelling, which is closely related to wind energy potential estimation.

In an application study (Tsvetkova and Ouarda, 2022), QuikSCAT satellite data were used for nearshore wind resource assessment of the Persian Gulf. Consideration of a possible nearshore offshore wind application development in the United Arab Emirates is important because the three largest cities are located on the coastline. Wind speed time series were derived from the QuikSCAT dataset for 11 x 20 grid with 25 km resolution. Then, each of the time series was extrapolated to 94 m hub height using the log law, after which they were fitted to the two-parameter Weibull distribution (shape and scale parameters were estimated using the maximum likelihood method). The Weibull mean, most probable and maximum energy wind speeds were calculated for each grid cell. The maps of the mean wind speed, most expected wind speed and maximum energy wind speed were given in Figure 8.3, Figure 8.4 and Figure 8.5. The map of annual wind energy and nearshore wind electricity cost (with the Vestas V112 wind turbine) was provided in Figure 8.6 and Figure 8.7 respectively. Offshore wind electricity was estimated to be at 1.6 – 1.8 $ct/khW.

(Tsvetkova and Ouarda, 2021) suggest for future research to be focused on global sensitivity analysis in wind resource assessment. (Tsvetkova and Ouarda, 2021) found that not one global sensitivity analysis study of goodness-of-fit metrics and payback period was spotted.

Another gap in the literature according to (Tsvetkova & Ouarda, 2021) is the limited amount of studies dealing with sensitivity analysis of goodness-of-fit measures. Calculating Shapley effects (Song, Nelson and Staum, 2015) for factors contributing to net present value and/or levelized cost of energy (as most popular outputs (Tsvetkova and Ouarda, 2021)) for both onshore and offshore applications (especially for floating offshore wind farms as it is one the hot topics in wind energy (Tsvetkova and Ouarda, 2021)) would be novel for the industry (Tsvetkova and Ouarda, 2021). (Martin *et al.*, 2016) defined the most influential factors for the operation and maintenance cost of a floating offshore wind farm and suggested refining their distributions and running a "*more sophisticated global sensitivity analysis in order to quantify the amount of sensitivity*" (Martin *et al.*, 2016). So applying Sobol, Shapley or PAWN to this experimental design is of justified importance (Tsvetkova and Ouarda, 2021).(Mytilinou and Kolios, 2019) suggest increasing the sample size of Monte Carlo simulation to study the higher order interdependencies, this can be done with total effect Sobol SI's. Finally, (Guedes Soares, 2021) suggested studying "*sensitivity of LCOE of OFFWFs to the years in which each of the different costs occur*" (Guedes Soares, 2021).

(Tsvetkova and Ouarda, 2023b) suggest modelling maximum wind speed with the Halphen distribution family (L. Perreault, Bobée and Rasmussen, 1999a), because Anderson-Darling statistic favouring the right tail fit showed improved fit for Halphen type B (Tsvetkova and Ouarda, 2023b). Dvorak et al.(Dvorak, V., Bobée, B., Boucher, S., Ashkar, 1988) pointed out that the Halphen distribution system does not seem to be "*as rich in a variety of forms and types as the Pearson system and they do not fulfill some particular requirements as ease of computation*". Therefore, future efforts could also focus on the continuation of this case study with the goal of comparing the Halphen distribution system with the Pearson distribution system (Tsvetkova and Ouarda, 2023b).

Wind direction was not part of this research, incorporating wind direction data into the uncertainty and sensitivity analyses in wind resource assessment could be of potential interest.

11 BIBLIOGRAPHY

El Adlouni, Salaheddine ; Bobée, B. (2014) *Delta diagram based test for the Halphen (A and B) and the Gamma distributions - NASA/ADS*. Available at: https://ui.adsabs.harvard.edu/abs/2014EGUGA..1616580E/abstract (Accessed: 29 July 2022).

El Adlouni, S. and Bobée, B. (2007) 'Sampling Techniques for Halphen Distributions', *Journal of Hydrologic Engineering*, 12(6), pp. 592–604. doi: 10.1061/(ASCE)1084-0699(2007)12:6(592).

El Adlouni, S. and Bobée, B. (2017) *Halphen distribution family with application in hydrological frequency analysis*. Water Resources Publications, LLC.

El Adlouni, S., Chebana, F. and Bobée, B. (2010) 'Generalized extreme value versus Halphen system: Exploratory study', *Journal of Hydrologic Engineering*, 15(2), pp. 79–89. doi: 10.1061/(ASCE)HE.1943-5584.0000152.

Akaike, H. (1970) 'Statistical predictor identification', *Annals of the Institute of Statistical Mathematics 1970 22:1*, 22(1), pp. 203–217. doi: 10.1007/BF02506337.

Amirinia, G., Mafi, S. and Mazaheri, S. (2017) 'Offshore wind resource assessment of Persian Gulf using uncertainty analysis and GIS', *Renewable Energy*, 113, pp. 915–929.

Aries, N., Boudia, S. M. and Ounis, H. (2018) 'Deep assessment of wind speed distribution models: A case study of four sites in Algeria', *Energy Conversion and Management*, 155, pp. 78–90. doi: 10.1016/j.enconman.2017.10.082.

Ayodele, T. R. (2015) 'Wind Turbines : Uncertainty Analysis Approaches', *Encyclopedia of Energy Engineering and Technology, Second Edition*. Second. Taylor and Francis: New York. Available at: https://www.taylorfrancis.com/books/e/9781351237734/chapters/10.1081/E-EEE2-120051392.

Babuska, I., Nobile, F. and Tempone, R. (2010) 'A Stochastic Collocation Method for Elliptic Partial Differential Equations with Random Input Data on JSTOR', *SIAM Review*, 52(2). Available at: https://www.jstor.org/stable/20780147#metadata_info_tab_contents (Accessed: 21 September 2022).

Burhenne, S. *et al.* (2013) 'Uncertainty quantification for combined building performance and cost-benefit analyses', *Building and Environment*, 62, pp. 143–154. doi: 10.1016/j.buildenv.2013.01.013.

Campolongo, F., Cariboni, J. and Saltelli, A. (2007) 'An effective screening design for sensitivity

analysis of large models', *Environmental Modelling and Software*, 22(10), pp. 1509–1518. doi: 10.1016/j.envsoft.2006.10.004.

Carmichael, D. G., Lea, K. A. and Balatbat, M. C. A. (2016) 'The financial additionality and viability of CDM projects allowing for uncertainty', *Environment, Development and Sustainability*, 18(1), pp. 129–141.

Carta, J. A. A., Ramírez, P. and Velázquez, S. (2009) 'A review of wind speed probability distributions used in wind energy analysis. Case studies in the Canary Islands', *Renewable and Sustainable Energy Reviews*, 13(5), pp. 933–955. doi: 10.1016/j.rser.2008.05.005.

Carta, J. A., Díaz, S. and Castañeda, A. (2020) 'A global sensitivity analysis method applied to wind farm power output estimation models', *Applied Energy*, 280, p. 115968. doi: 10.1016/j.apenergy.2020.115968.

Chebana, F., El Adlouni, S. and Bobée, B. (2008) 'Method of moments of the Halphen distribution parameters', *Stochastic Environmental Research and Risk Assessment*, 22(6), pp. 749–757. doi: 10.1007/S00477-007-0184-4.

Chebana, F., Adlouni, S. El and Bobée, B. (2010) 'Mixed estimation methods for Halphen distributions with applications in extreme hydrologic events', *Stochastic Environmental Research and Risk Assessment*, 24(3), pp. 359–376. doi: 10.1007/S00477-009-0325-Z/FIGURES/8.

Cukier, R. I., Levine, H. B. and Shuler, K. E. (1978) 'Nonlinear sensitivity analysis of multiparameter model systems', *Journal of Computational Physics*. Academic Press, pp. 1–42.

Delhome, R., Billot, R. and El Faouzi, N. E. (2017) 'Travel time statistical modeling with the Halphen distribution family', *Journal of Intelligent Transportation Systems: Technology, Planning, and Operations*, 21(6), pp. 452–464. doi: 10.1080/15472450.2017.1326115.

Douglas-Smith, D. *et al.* (2020) 'Certain trends in uncertainty and sensitivity analysis: An overview of software tools and techniques', *Environmental Modelling and Software*. Elsevier Ltd, p. 104588.

Dvorak, V., Bobée, B., Boucher, S., Ashkar, F. (1988) *Halphen distributions and related systems of frequency functions*. Quebec.

Dykes, K. *et al.* (2014) 'Sensitivity analysis of wind plant performance to key turbine design parameters: A systems engineering approach', *32nd ASME Wind Energy Symposium*, (February).

Ferretti, F., Saltelli, A. and Tarantola, S. (2016) 'Trends in sensitivity analysis practice in the last decade', *Science of The Total Environment*, 568, pp. 666–670.

Funtowicz, S. O. and Ravetz, J. R. (1990) ‘Uncertainty and Quality in Science for Policy’, *Uncertainty and Quality in Science for Policy*. doi: 10.1007/978-94-009-0621-1.

Goda, T. (2021) *A simple algorithm for global sensitivity analysis with Shapley effects*.

Guedes Soares, C. (ed.) (2021) *Developments in Renewable Energies Offshore*. Marine Tec. CRC Press, Taylor & Francis Group. Available at: https://books.google.ca/books?hl=en&lr=&id=ORn9DwAAQBAJ&oi=fnd&pg=PA315&dq=sensitivity+analysis+LCOE+offshore+wind+&ots=PUMJ0QrAcR&sig=TGmEau2qwXMEhLggOdfYAC_Jsg8&redir_esc=y#v=onepage&q=sensitivity analysis LCOE offshore wind&f=false (Accessed: 15 October 2020).

Hadi, F. A., Oudah, S. S. and Al-baldawi, R. A. (2020) ‘An Economic Study of a Wind Energy Project Using Different Sources of Wind Data’, *Iraqi Journal of Science*, 61(2), pp. 322–332. doi: 10.24996/ijs.2020.61.2.10.

Hamed, K. H. and Ramachandra Rao, A. (1998) ‘A modified Mann-Kendall trend test for autocorrelated data’, *Journal of Hydrology*, 204(1–4), pp. 182–196. doi: 10.1016/S0022-1694(97)00125-X.

Harenberg, D. *et al.* (2018) ‘Uncertainty quantification and global sensitivity analysis for economic models’, *Quantitative Economics*, 10(1), pp. 1–41.

Heck, N., Smith, C. and Hittinger, E. (2016) ‘A Monte Carlo approach to integrating uncertainty into the levelized cost of electricity’, *Electricity Journal*, 29(3), pp. 21–30. doi: 10.1016/j.tej.2016.04.001.

Hill, B. M. (1975) ‘A Simple General Approach to Inference About the Tail of a Distribution’, *https://doi.org/10.1214/aos/1176343247*, 3(5), pp. 1163–1174. doi: 10.1214/AOS/1176343247.

Iooss, A. B. *et al.* (2021) *Package ‘ sensitivity ’*. Available at: https://cran.r-project.org/web/packages/sensitivity/sensitivity.pdf (Accessed: 2 August 2021).

Jackson, O. A. Y. (1967) ‘An Analysis of Departures from the Exponential Distribution’, *Journal of the Royal Statistical Society: Series B (Methodological)*, 29(3), pp. 540–549. doi: 10.1111/J.2517-6161.1967.TB00716.X.

Jansen, M. J. W. (1999) ‘Analysis of variance designs for model output’, *Computer Physics Communications*, 117(1), pp. 35–43.

Jung, C. and Schindler, D. (2017) ‘Global comparison of the goodness-of-fit of wind speed distributions’, *Energy Conversion and Management*, 133, pp. 216–234. doi:

10.1016/J.ENCONMAN.2016.12.006.

Jung, C. and Schindler, D. (2019) 'Wind speed distribution selection – A review of recent development and progress', *Renewable and Sustainable Energy Reviews*. Elsevier Ltd, p. 109290. doi: 10.1016/j.rser.2019.109290.

Kwon, S. D. (2010) 'Uncertainty analysis of wind energy potential assessment', *Applied Energy*, 87(3), pp. 856–865. doi: 10.1016/j.apenergy.2009.08.038.

Lackner, M. A., Rogers, A. L. and Manwell, J. F. (2007) 'Uncertainty Analysis in Wind Resource Assessment and Wind Energy Production Estimation', in *45th AIAA Aerospace Sciences Meeting and Exhibit 08 January 2007 - 1*. Reno, Nevada, pp. 1–16. doi: 10.2514/6.2007-1222.

Lee, J. C. Y. and Jason Fields, M. (2021) 'An overview of wind-energy-production prediction bias, losses, and uncertainties', *Wind Energy Science*, 6(2), pp. 311–365. doi: 10.5194/WES-6-311-2021.

Leinfellner, W. *et al.* (1990) 'UNCERTAINTY AND QUALITY IN SCIENCE FOR POLICY', *THEORY AND DECISION LIBRARY General Editors: W. Leinfellner and G. Eberlein Series A: Philosophy and Methodology of the Social Sciences Editors: W. Leinfellner*. Available at: http://www.andreasaltelli.eu/file/repository/UQSP.pdf (Accessed: 20 September 2022).

Madariaga, A. *et al.* (2017) 'Electrical losses in multi-MW wind energy conversion systems', *Renewable Energy and Power Quality Journal*, pp. 322–327. doi: 10.24084/repqj10.305.

Mann, H. B. (1945) 'Nonparametric Tests Against Trend', *Econometrica*, 13(3), p. 245. doi: 10.2307/1907187.

Manwell, J. F., McGowan, J. G. and Rogers, A. L. (2009) *Wind energy explained : theory, design and application*. Wiley.

Martin, R. *et al.* (2016) 'Sensitivity analysis of offshore wind farm operation and maintenance cost and availability', *Renewable Energy*, 85, pp. 1226–1236.

Mate, G. (2008) *In the realm of hunrgy ghosts: Close Encounters with addiction*. Vintage. Penguin Random House Vintage Canada. Available at: https://drgabormate.com/book/in-the-realm-of-hungry-ghosts/.

MathWorks (no date) 'Matlab R2018b'. Available at: https://www.mathworks.com/products/new_products/release2018b.html.

Menberg, K., Heo, Y. and Choudhary, R. (2016) 'Sensitivity analysis methods for building energy

models: Comparing computational costs and extractable information', *Energy and Buildings*, 133, pp. 433–445. doi: 10.1016/j.enbuild.2016.10.005.

Mora, E. B. *et al.* (2019) 'The effects of mean wind speed uncertainty on project finance debt sizing for offshore wind farms', *Applied Energy*, 252, p. 113419. doi: 10.1016/j.apenergy.2019.113419.

Mora, E. B., Spelling, J. and Weijde, A. H. (2021) 'Global sensitivity analysis for offshore wind cost modelling', *Wind Energy*, p. we.2612. doi: 10.1002/we.2612.

Mora, E. B., Spelling, J. and van der Weijde, A. H. (2019) 'Benchmarking the PAWN distribution-based method against the variance-based method in global sensitivity analysis: Empirical results', *Environmental Modelling and Software*, 122. doi: 10.1016/j.envsoft.2019.104556.

Morlat, G. (1956) *Les lois de probabilités de Halphen*, *Elecrtricite de France, Service des Études et Recherches Hydrauliques*. Available at: http://www.sfds.asso.fr/publicat/rsa.htm (Accessed: 15 July 2022).

Morris, M. D. (1991) 'Factorial sampling plans for preliminary computational experiments', *Technometrics*, 33(2), pp. 161–174. doi: 10.1080/00401706.1991.10484804.

Murthy, K. S. R. and Rahi, O. P. (2017) 'A comprehensive review of wind resource assessment', *Renewable and Sustainable Energy Reviews*. Elsevier Ltd, pp. 1320–1342.

Mytilinou, V. and Kolios, A. J. (2019) 'Techno-economic optimisation of offshore wind farms based on life cycle cost analysis on the UK', *Renewable Energy*, 132, pp. 439–454. doi: 10.1016/j.renene.2018.07.146.

National Bureau of Standards (1972) *Handbook of mathematical functions with formulas, graphs and mathematical tables*. 10th Print. Edited by M. Abromovitz and I. Stegun. United States Department of Commerce. Available at: https://personal.math.ubc.ca/~cbm/aands/abramowitz_and_stegun.pdf.

Natural Resources Canada: RETScreen (2020). Available at: https://www.nrcan.gc.ca/maps-tools-publications/tools/data-analysis-software-modelling/retscreen/7465 (Accessed: 13 August 2020).

Nikishova, A. *et al.* (2017) 'Uncertainty quantification and sensitivity analysis applied to the wind wave model SWAN', *Environmental Modelling & Software*, 95, pp. 344–357. doi: 10.1016/J.ENVSOFT.2017.06.030.

Ouarda, T. B. M. J. and Charron, C. (2018) 'Distributions of wind speed in a northern environment',

in *2018 9th International Renewable Energy Congress, IREC 2018*. Institute of Electrical and Electronics Engineers Inc., pp. 1–3. doi: 10.1109/IREC.2018.8362453.

Ouarda, T. B. M. J., Charron, C. and Chebana, F. (2016) 'Review of criteria for the selection of probability distributions for wind speed data and introduction of the moment and L-moment ratio diagram methods, with a case study', *Energy Conversion and Management*, 124, pp. 247–265.

Owen, A. B. (2014) 'Sobol' indices and Shapley value', *SIAM/ASA Journal on Uncertainty Quantification*, 2(1), pp. 245–251.

'Paris Agreement' (2015) *International Legal Materials*, 55. Available at: https://heinonline.org/HOL/Page?handle=hein.journals/intlm55&id=803&div=&collection= (Accessed: 13 July 2022).

Perreault, L., Bobée, B. and Rasmussen, P. F. (1999a) 'Halphen Distribution System. I: Mathematical and Statistical Properties', *Journal of Hydrologic Engineering*, 4(3), pp. 189–199. doi: 10.1061/(ASCE)1084-0699(1999)4:3(189).

Perreault, L., Bobée, B. and Rasmussen, P. F. (1999b) 'Halphen Distribution System. I: Mathematical and Statistical Properties', *Journal of Hydrologic Engineering*, 4(3), pp. 189–199. doi: 10.1061/(ASCE)1084-0699(1999)4:3(189).

Perreault, L, Bobée, B. and Rasmussen, P. F. (1999) 'Halphen Distribution System. II: Parameter and Quantile Estimation Estimation of extreme precipitations View project Statistical post-processing of ensemble weather forecasts View project', *Article in Journal of Hydrologic Engineering*. doi: 10.1061/(ASCE)1084-0699(1999)4:3(200).

Phil Gibbs (1997) *What is Occam's Razor?* Available at: https://math.ucr.edu/home/baez/physics/General/occam.html.

Pianosi, F. and Wagener, T. (2018) 'Distribution-based sensitivity analysis from a generic input-output sample', *Environmental Modelling and Software*, 108, pp. 197–207.

Puy, A. *et al.* (2020) 'The battle of total-order sensitivity estimators'. Available at: http://arxiv.org/abs/2009.01147 (Accessed: 20 October 2020).

Puy, A. *et al.* (2021) 'sensobol : an R package to compute variance-based sensitivity indices', *arXiv preprint arXiv:2101.10103*.

Quan, H. *et al.* (2020) 'A Survey of Computational Intelligence Techniques for Wind Power Uncertainty Quantification in Smart Grids', *IEEE Transactions on Neural Networks and Learning Systems*, 31(11), pp. 4582–4599. doi: 10.1109/TNNLS.2019.2956195.

‘R Core Team, R: A Language and Environment for Statistical Computing’ (2020). Vienna, Austria: R Foundation for Statistical Computing. Available at: https://www.r-project.org/.

Razavi, S. *et al.* (2020) ‘The Future of Sensitivity Analysis: An Essential Discipline for Systems Modeling and Policy Support’, *Environmental Modelling & Software*, p. 104954. doi: 10.1016/j.envsoft.2020.104954.

Razavi, S. and Gupta, H. V. (2015) ‘What do we mean by sensitivity analysis? the need for comprehensive characterization of “global” sensitivity in Earth and Environmental systems models’, *Water Resources Research*, 51(5), pp. 3070–3092. Available at: https://agupubs.onlinelibrary.wiley.com/doi/full/10.1002/2014WR016527 (Accessed: 14 July 2020).

Razavi, S. and Gupta, H. V. (2019) ‘A multi-method Generalized Global Sensitivity Matrix approach to accounting for the dynamical nature of earth and environmental systems models’, *Environmental Modelling and Software*, pp. 1–11. doi: 10.1016/j.envsoft.2018.12.002.

Richter, P. (2020) ‘Uncertainty Quantification of Offshore Wind Farms Using Monte Carlo and Sparse Grid’, *Applied Energy*.

Richter, P., Wolters, P. R. J. and Frank, R. Ç. A. V. M. (2019) ‘Uncertainty Quantification of Offshore Wind Farms’, *Wind Energy*.

Salehin, S. *et al.* (2016) ‘Assessment of renewable energy systems combining techno-economic optimization with energy scenario analysis’, *Energy*, 112, pp. 729–741.

Saltelli, A. *et al.* (2008) *Global Sensitivity Analysis: The Primer*. John Wiley & Sons, Ltd.

Saltelli, A. *et al.* (2010) ‘Variance based sensitivity analysis of model output. Design and estimator for the total sensitivity index’, *Computer Physics Communications*, 181(2), pp. 259–270.

Saltelli, A. *et al.* (2019) ‘Why so many published sensitivity analyses are false: A systematic review of sensitivity analysis practices’, *Environmental Modelling & Software*, 114, pp. 29–39.

Saltelli, A. *et al.* (2020) ‘Five ways to ensure that models serve society: a manifesto’, *Nature 2021 582:7813*, 582(7813), pp. 482–484. doi: 10.1038/d41586-020-01812-9.

Saltelli, A. *et al.* (2021) ‘Sensitivity analysis: A discipline coming of age editorial for the special issue “Sensitivity analysis for environmental modelling”, Environmental Modelling & Software’, *Environmental Modelling & Software*, p. 105226. doi: 10.1016/J.ENVSOFT.2021.105226.

Saltelli, A. (2022) ‘RECKONING WITH UNCERTAINTY SOCIAL SCIENCES LESSONS FOR

MATHEMATICAL MODELING', *Mathematics for action supporting science-based decision making*, (UNESCO). Available at: http://www.andreasaltelli.eu/file/repository/MfA_Toolkit_Saltelli.pdf (Accessed: 20 September 2022).

Saltelli, A. *et al.* (2022) 'Science, the endless frontier of regulatory capture', *Futures*, 135, p. 102860. doi: 10.1016/J.FUTURES.2021.102860.

Saltelli, A. and Annoni, P. (2010) 'How to avoid a perfunctory sensitivity analysis', *Environmental Modelling & Software*, 25(12), pp. 1508–1517.

Saltelli, A., Giampietro, M. and Ravetz, J. (2016) 'Decalogue of the diligent quantifier. A Pledge VERSION 2'. doi: 10.1161/CIRCRESAHA.114.303819.

Saltelli, A. and Sarewitz, D. (2022) *Reformation in the Church of Science — The New Atlantis*, *The New Antantis*. Available at: https://www.thenewatlantis.com/publications/reformation-in-the-church-of-science (Accessed: 20 September 2022).

Saltelli, A., Tarantola, S. and Chan, K. P. S. (1999) 'A quantitative model-independent method for global sensitivity analysis of model output', *Technometrics*, 41(1), pp. 39–56. doi: 10.1080/00401706.1999.10485594.

Shapiro, S. S. and Wilk, M. B. (1965) 'An analysis of variance test for normality (complete samples)', *Biometrika*, 52(3–4), pp. 591–611. doi: 10.1093/BIOMET/52.3-4.591.

Shapley, L. S. (1951) *Notes on the n-Pearson game -- II: the value of the n-Pearson game*. Santa Monica, California.

Shi, H. *et al.* (2021) 'Wind Speed Distributions Used in Wind Energy Assessment: A Review', *Frontiers in Energy Research*, 9, p. 790. doi: 10.3389/FENRG.2021.769920/BIBTEX.

Shin, J.-Y., Ouarda, T. B. M. J. and Lee, T. (2016) 'Heterogeneous mixture distributions for modeling wind speed, application to the UAE', *Renewable Energy*, 91, pp. 40–52.

Sliz-Szkliniarz, B. *et al.* (2019) 'Assessing the cost of onshore wind development scenarios: Modelling of spatial and temporal distribution of wind power for the case of Poland', *Renewable and Sustainable Energy Reviews*, 109, pp. 514–531. doi: 10.1016/J.RSER.2019.04.039.

Sobol′, I. . (1990) 'ОБ ОЦЕНКЕ ЧУВСТВИТЕЛЬНОСТИ НЕЛИНЕЙНЫХ МАТЕМАТИЧЕСКИХ МОДЕЛЕЙ (On sensitivity estimation for nonlinear mathematical models)', *Математическое моделирование (Matem. Model.)*, 2(1), pp. 12–18.

Soe, T. T., Zheng, M. and Aung, Z. N. (2015) 'Assessment of economic feasibility on promising wind energy sites in Myanmar', *International Journal of Renewable Energy Research*, 5(3), pp. 699–707.

Song, E., Nelson, B. L. and Staum, J. (2015) *Shapley Effects for Global Sensitivity Analysis: Theory and Computation*.

Tran, T. T. D. and Smith, A. D. (2018) 'Incorporating performance-based global sensitivity and uncertainty analysis into LCOE calculations for emerging renewable energy technologies', *Applied Energy*, 216, pp. 157–171.

Tsvetkova, O. (2022) *Eastern Canada hourly wind speed dataset 126 stations*. doi: 10.17632/pzpfg2fdcd.1.

Tsvetkova, O. and Ouarda, T. B. M. J. (2019) 'Quasi-Monte Carlo technique in global sensitivity analysis of wind resource assessment with a study on UAE', *Journal of Renewable and Sustainable Energy*, 11(5). doi: 10.1063/1.5120035.

Tsvetkova, O. and Ouarda, T. B. M. J. (2020) 'Erratum: "Quasi-Monte Carlo technique in global sensitivity analysis of wind resource assessment with a study on UAE" [J. Renewable Sustainable Energy **11** , 053303 (2019)]', *Journal of Renewable and Sustainable Energy*, 12(6), p. 069901. doi: 10.1063/5.0007143.

Tsvetkova, O. and Ouarda, T. B. M. J. (2021) 'A review of sensitivity analysis practices in wind resource assessment', *Energy Conversion and Management*, 238, p. 114112. doi: 10.1016/j.enconman.2021.114112.

Tsvetkova, O. and Ouarda, T. B. M. J. (2022) 'Offshore wind resource assessment with QuickSCAT data in the UAE', in *European Conference on Renewable Energy Systems*. Riga. Available at: https://ecres.net/index.html.

Tsvetkova, O. and Ouarda, T. B. M. J. (2023a) 'Use of the Halphen distribution family for mean wind speed estimation with application to Eastern Canada', *Energy Conversion and Management*, 276, p. 116502. doi: http://doi.org/10.1016/J.ENCONMAN.2022.116502.

Tsvetkova, O. and Ouarda, T. B. M. J. (2023b) 'Use of the Halphen distribution family for mean wind speed estimation with application to Eastern Canada', *Energy Conversion and Management*, 276, p. 116502. doi: 10.1016/J.ENCONMAN.2022.116502.

Ulker, F., Allaire, D. and Willcox, K. (2017) 'Sensitivity-guided decision-making for wind farm micro-siting', *International Journal for Numerical Methods in Fluids*, 83(1), pp. 52–72.

UNFCCC guidelines on the assessment of investment analysis (no date).

Usta, I. and Kantar, Y. M. (2012) 'Analysis of some flexible families of distributions for estimation of wind speed distributions', *Applied Energy*, 89(1), pp. 355–367. doi: 10.1016/J.APENERGY.2011.07.045.

Vargas, S. A. *et al.* (2019) 'Wind power generation: A review and a research agenda', *Journal of Cleaner Production*, 218, pp. 850–870.

Velarde, J., Kramhøft, C. and Sørensen, J. D. (2019) 'Global sensitivity analysis of offshore wind turbine foundation fatigue loads', *Renewable Energy*, 140, pp. 177–189. doi: 10.1016/J.RENENE.2019.03.055.

Wang, L., Liu, J. and Qian, F. (2021) 'Wind speed frequency distribution modeling and wind energy resource assessment based on polynomial regression model', *International Journal of Electrical Power & Energy Systems*, 130, p. 106964. doi: 10.1016/j.ijepes.2021.106964.

Xu, X. and Yan, Z. (2017) 'Probabilistic load flow calculation with quasi-Monte Carlo and multiple linear regression', *International Journal of Electrical Power & Energy Systems*, 88, pp. 1–12. doi: 10.1016/J.IJEPES.2016.11.013.

Zhang, L. and Singh, V. P. (2021) 'Revisiting the Application of Halphen Distributions in Flood Frequency Analysis', *Journal of Hydrologic Engineering*, 26(12), p. 04021042. doi: 10.1061/(ASCE)HE.1943-5584.0002133.

Zhou, J. *et al.* (2010) 'Comprehensive evaluation of wind speed distribution models: A case study for North Dakota sites', *Energy Conversion and Management*, 51(7), pp. 1449–1458. doi: 10.1016/j.enconman.2010.01.020.

12 APPENDIX I : R SCRIPT FOR EXAMPLE IN SECTION 2.11.1

```
library(sensobol)
library(sensitivity)
setwd("C:/Users/tsvetkol/Documents/WIND RELATED RESEARCH/submitted/A2 SA review/revision/example/")
linear <- function(X) {
        Y <- X[,1] + X[,2] + X[,3] + X[,4] + X[,5]
        return(Y)
}
# Define settings
N <- 1000; params <- paste("X", 1:5, sep = ""); R <- 10
# Create sample matrix
mat <- sobol_matrices(N = N, params = params)
Y <- linear(mat)
# Compute and bootstrap Sobol' indices
ind <- sobol_indices(Y = Y, N = N, params = params, boot = TRUE, R = R)
plot_multiscatter(data = mat, N = N, Y = Y, params = params)
plot_scatter(data = mat, Y = Y, N = N, params = params)
plot_sobol(data = ind)
plot_uncertainty(Y = Y, N = N)

sa <- morris(model = morris.fun, factors = 20, levels = 4, r = 4)
print(sa)
plot(sa)
```

13 APPENDIX II : EASTERN CANADA CASE STUDY STATIONS OVERVIEW

Table 13.1 Eastern Canada case study stations overview

CS station ID	Station ID	Station name	Province	Latitude	Longitude	Elevation, m.	First Year	Last Year	Years collected	Number of data points
1	5251	QUEBEC/JEAN LESAGE INTL A	QUEBEC	46.8	-71.38	74.4	1953	2013	60	485707
2	5293	VALCARTIER A	QUEBEC	46.9	-71.5	167.6	1978	2018	40	72439
3	5415	MONTREAL/PIERRE ELLIOTT TRUDEAU INTL A	QUEBEC	45.47	-73.75	35.97	1953	2013	60	502624
4	5530	SHERBROOKE A	QUEBEC	45.43	-71.68	241.4	1962	2005	43	320292
5	5668	BLANC SABLON	QUEBEC	51.42	-57.22	19.2	1967	1982	15	78840
6	5669	LOURDES DE BLANC SABLON A	QUEBEC	51.45	-57.18	37.18	1970	2014	44	220175
7	5707	MANICOUAGAN A	QUEBEC	50.65	-68.83	406.3	1961	1971	10	29826
8	5839	RIVIERE DU LOUP	QUEBEC	47.8	-69.55	148.4	1965	1980	15	121201
9	6029	CHIBOUGAMAU CHAPAIS A	QUEBEC	49.77	-74.53	387.1	1982	2014	32	199814
10	6047	LA GRANDE RIVIERE A	QUEBEC	53.63	-77.7	195.1	1976	2012	36	304160
11	6053	MATAGAMI A	QUEBEC	49.77	-77.82	281.3	1973	1991	18	112387
12	6058	NITCHEQUON	QUEBEC	53.2	-70.9	536.1	1953	1985	32	235079
13	6081	VAL-D'OR A	QUEBEC	48.06	-77.79	337.4	1955	2012	57	463422
14	6089	CAPE HOPES ADVANCE	QUEBEC	61.08	-69.55	73.2	1953	1971	18	46645
15	6205	MISCOU ISLAND (AUT)	NEW BRUNSWICK	48.01	-64.49	4	1964	2018	54	291390
16	6256	ST LEONARD A	NEW BRUNSWICK	47.16	-67.83	242.2	1985	2014	29	153857
17	6330	COPPER LAKE	NOVA SCOTIA	45.38	-61.97	96.9	1953	1974	21	97014
18	6335	DEBERT A	NOVA SCOTIA	45.42	-63.45	44.2	1953	1960	7	65086
19	6501	WESTERN HEAD	NOVA SCOTIA	43.99	-64.66	10.06	1959	2018	59	301754
20	6557	ARGENTIA A	NEWFOUNDLAND	47.3	-54	15.5	1976	1986	10	49995
21	6581	BUCHANS A	NEWFOUNDLAND	48.85	-56.83	276.1	1953	1965	12	55225
22	6584	BURGEO 2	NEWFOUNDLAND	47.62	-57.62	10.6	1994	2006	12	94017
23	6708	ST ALBANS	NEWFOUNDLAND	47.87	-55.85	13.4	1968	1983	15	79823
24	6709	ST ANDREWS	NEWFOUNDLAND	47.77	-59.33	10.7	1953	1966	13	60136
25	6710	ST ANTHONY	NEWFOUNDLAND	51.37	-55.58	17.4	1953	1965	12	54653
26	6711	ST ANTHONY	NEWFOUNDLAND	51.37	-55.6	11.5	1970	1996	26	128993
27	6723	ST LAWRENCE	NEWFOUNDLAND	46.92	-55.38	48.5	1966	1996	30	180363

28	6740	STEPHENVILLE A	NEWFOUNDLAND	48.53	-58.55	24.7	1953	2014	61	439895
29	6756	TWILLINGATE	NEWFOUNDLAND	49.68	-54.82	4.9	1953	1967	14	68357
30	6773	CARTWRIGHT	NEWFOUNDLAND	53.71	-57.04	14.3	1953	2015	62	442305
31	6778	MAKKOVIK A	NEWFOUNDLAND	55.08	-59.19	70.4	1985	2015	30	119736
32	6783	MARY'S HARBOUR A	NEWFOUNDLAND	52.3	-55.83	10.6	1983	2013	30	116606
33	6797	SAGLEK	NEWFOUNDLAND	58.33	-62.59	516	1989	2018	29	145767
34	6916	BATHURST A	NEW BRUNSWICK	47.63	-65.75	58.8	1994	2013	19	110852
35	6918	BUCTOUCHE CDA CS	NEW BRUNSWICK	46.43	-64.77	35.9	2005	2018	13	110505
36	6923	KEJIMKUJIK 1	NOVA SCOTIA	44.4	-65.2	125	1994	2018	24	157471
37	7026	ST STEPHEN (AUT)	NEW BRUNSWICK	45.22	-67.25	26.1	1977	2006	29	121782
38	7162	TRURO (AUT)	NOVA SCOTIA	45.37	-63.27	39.9	1994	2005	11	75524
39	7169	MCNABS ISLAND (AUT)	NOVA SCOTIA	44.6	-63.53	15.4	1999	2018	19	151731
40	7173	HART ISLAND (AUT)	NOVA SCOTIA	45.35	-60.98	8.2	1994	2018	24	129896
41	8456	CHEVERY	QUEBEC	50.47	-59.64	7.7	1994	2018	24	142423
42	8675	HEATH POINT	QUEBEC	49.09	-61.7	7	1994	2018	24	95265
43	8989	ILE D'ORLEANS	QUEBEC	47	-70.81	3.6	1994	2018	24	17078
44	8991	SAGONA ISLAND	NEWFOUNDLAND	47.37	-55.79	59.7	1994	2017	23	94300
45	8999	CAP-MADELEINE	QUEBEC	49.25	-65.32	29	1994	2018	24	132126
46	9002	EASTMAIN A	QUEBEC	52.23	-78.52	7.32	1992	2014	22	39448
47	10226	SALLUIT A	QUEBEC	62.18	-75.67	227.08	1969	2015	46	61606
48	10252	KANGIQSUJUAQ A	QUEBEC	61.59	-71.93	157.58	1992	2015	23	55420
49	10661	NORTHEAST MARGAREE (AUT)	NOVA SCOTIA	46.37	-60.98	54	1994	2018	24	40984
50	10684	KANGIQSUALUJJUAQ A	QUEBEC	58.71	-65.99	66.14	1992	2015	23	63006
51	10763	ILES DE LA MADELEINE	QUEBEC	47.43	-61.77	7.6	1993	2018	25	140456
52	10789	AKULIVIK A	QUEBEC	60.82	-78.15	23.16	1992	2015	23	64075
53	10792	GRAND ETANG	NOVA SCOTIA	46.55	-61.05	12.8	1994	2018	24	206943
54	10797	MISTOOK	QUEBEC	48.6	-71.72	112.5	1994	2018	24	68093
55	10800	SUMMERSIDE	PRINCE EDWARD ISLAND	46.44	-63.84	12.2	1994	2018	24	193635
56	10813	NAIN	NEWFOUNDLAND	56.55	-61.68	7.6	1994	2018	24	104903
57	10817	POOLS ISLAND	NEWFOUNDLAND	49.11	-53.58	19.3	1994	2018	24	188737
58	10818	GRATES COVE	NEWFOUNDLAND	48.17	-52.94	46.2	1994	2017	23	174062
59	10836	CAPE KAKKIVIAK	NEWFOUNDLAND	59.99	-64.17	551.1	1994	2018	24	94188
60	10841	CAPE KIGLAPAIT	NEWFOUNDLAND	57.14	-61.48	834.1	1994	2017	23	119333
61	10855	AUPALUK A	QUEBEC	59.3	-69.6	36.9	1992	2015	23	40788
62	10856	TASIUJAQ A	QUEBEC	58.67	-69.95	36.9	1993	2015	22	49777
63	10859	BRIER ISLAND	NOVA SCOTIA	44.29	-66.35	15.8	1969	2018	49	206693

64	10869	CAP-TOURMENTE	QUEBEC	47.08	-70.78	6	1994	2018	24	146543
65	10873	STE-ANNE-DE-BELLEVUE 1	QUEBEC	45.43	-73.93	39	1994	2018	24	57376
66	10909	MARTICOT ISLAND	NEWFOUNDLAND	47.33	-54.59	21.8	1994	2018	24	57922
67	10945	SHEARWATER JETTY	NOVA SCOTIA	44.63	-63.52	5.5	1994	2018	24	166933
68	26778	LAC BENOIT	QUEBEC	51.53	-71.11	549	1994	2018	24	90186
69	26797	CHAMOUCHOUANE	QUEBEC	49.28	-73.36	303.8	1994	2018	24	39032
70	26893	LA POCATIERE	QUEBEC	47.36	-70.03	31	1996	2018	22	48800
71	26968	KOUCHIBOUGUAC CS	NEW BRUNSWICK	46.78	-65.02	21	2005	2018	13	56252
72	27115	ST JOHN'S WEST CDA CS	NEWFOUNDLAND	47.52	-52.78	114	1999	2013	14	115310
73	27195	CAP-CHAT	QUEBEC	49.11	-66.65	5	1996	2018	22	135316
74	27621	ST LAWRENCE	NEWFOUNDLAND	46.92	-55.38	48.5	1998	2006	8	66884
75	27712	WINTERLAND	NEWFOUNDLAND	47.14	-55.33	29.26	1999	2018	19	135268
76	27846	CONFEDERATION BRIDGE	PRINCE EDWARD ISLAND	46.23	-63.73	54.1	1999	2006	7	37758
77	29471	WRECKHOUSE	NEWFOUNDLAND	47.71	-59.31	31.7	2000	2006	6	55810
78	29493	GAGETOWN AWOS A	NEW BRUNSWICK	45.84	-66.45	50.6	2000	2018	18	94953
79	29714	LEMIEUX	QUEBEC	46.3	-72.06	97.2	1999	2018	19	136144
80	30164	SCHEFFERVILLE	QUEBEC	54.8	-66.8	517.2	2005	2018	13	64342
81	30165	MONTREAL/PIERRE ELLIOTT TRUDEAU INTL	QUEBEC	45.47	-73.74	32.1	2008	2018	10	66528
82	30168	NATASHQUAN A	QUEBEC	50.19	-61.81	11.7	2008	2018	10	68794
83	30308	HARRINGTON CDA CS	PRINCE EDWARD ISLAND	46.34	-63.17	53	2004	2018	14	119609
84	31829	LUNENBURG	NOVA SCOTIA	44.36	-64.3	3.8	2002	2018	16	131817
85	41575	TRACADIE	NOVA SCOTIA	45.61	-61.68	66.67	2003	2018	15	132171
86	41903	ST. PETERS	PRINCE EDWARD ISLAND	46.45	-62.58	29.7	2003	2018	15	128039
87	42013	GRANBY	QUEBEC	45.37	-72.77	86	2003	2018	15	50637
88	42083	NAPPAN AUTO	NOVA SCOTIA	45.76	-64.24	19.8	2003	2018	15	124848
89	42243	DEBERT	NOVA SCOTIA	45.42	-63.47	37.5	2003	2018	15	122873
90	43124	HALIFAX KOOTENAY	NOVA SCOTIA	44.59	-63.55	52	2004	2018	14	101129
91	43323	EDMUNDSTON	NEW BRUNSWICK	47.42	-68.32	154.2	2004	2018	14	103677
92	43404	OSBORNE HEAD DND	NOVA SCOTIA	44.61	-63.42	30	2004	2018	14	85804
93	43406	BEDFORD BASIN	NOVA SCOTIA	44.71	-63.63	3.5	2004	2018	14	97665
94	44363	UPPER STEWIACKE RCS	NOVA SCOTIA	45.23	-63.06	23.5	2005	2018	13	103267
95	44503	SYDNEY CS	NOVA SCOTIA	46.16	-60.04	62.5	2006	2018	12	106826
96	45047	BONAVISTA	NEWFOUNDLAND	48.67	-53.11	25.6	2006	2018	12	98733
97	45307	WRECKHOUSE	NEWFOUNDLAND	47.71	-59.31	31.7	2006	2018	12	101878
98	46007	BACCARO PT	NOVA SCOTIA	43.45	-65.47	4.6	2007	2018	11	95696

99	47587	SAINT-GERMAIN-DE-GRANTHAM	QUEBEC	45.83	-72.54	85	2008	2018	10	80411
100	47607	STEPHENVILLE RCS	NEWFOUNDLAND	48.56	-58.57	58	2008	2018	10	85459
101	48348	ST. ANTHONY	NEWFOUNDLAND	51.39	-56.07	32.9	2009	2018	9	74927
102	48568	FREDERICTON	NEW BRUNSWICK	45.87	-66.54	20.7	2010	2018	8	67566
103	48871	ST JOHNS WEST CLIMATE	NEWFOUNDLAND	47.51	-52.78	110	2010	2018	8	67305
104	49390	VAL D'OR A	QUEBEC	48.05	-77.78	337.4	2011	2018	7	53798
105	49491	MATAGAMI A	QUEBEC	49.76	-77.8	279.8	2011	2018	7	52561
106	49608	MONTREAL MIRABEL INTL A	QUEBEC	45.68	-74.04	82.3	2012	2018	6	49372
107	49629	CHURCHILL FALLS A	NEWFOUNDLAND	53.56	-64.11	439.5	2011	2018	7	52052
108	49648	LA GRANDE 4 A	QUEBEC	53.75	-73.68	306.3	2011	2018	7	48417
109	49649	SCHEFFERVILLE A	QUEBEC	54.81	-66.81	520.9	2012	2018	6	50055
110	49748	ESKASONI FIRST NATION AUTOMATIC WEATHER STATION	NOVA SCOTIA	45.92	-60.65	28	2011	2018	7	55871
111	50089	ST. JOHN'S INTL A	NEWFOUNDLAND	47.62	-52.75	140.5	2012	2018	6	54126
112	50309	MONCTON INTL A	NEW BRUNSWICK	46.11	-64.68	70.7	2012	2018	6	52220
113	50310	SAINT JOHN A	NEW BRUNSWICK	45.32	-65.89	108.8	2012	2018	6	51561
114	50620	HALIFAX INTL A	NOVA SCOTIA	44.88	-63.51	145.4	2012	2018	6	49913
115	50621	CHARLOTTETOWN A	PRINCE EDWARD ISLAND	46.29	-63.12	48.5	2012	2018	6	49891
116	50677	CORMACK RCS	NEWFOUNDLAND	49.32	-57.39	165.8	2012	2018	6	44830
117	50678	MILLERTOWN RCS	NEWFOUNDLAND	48.82	-56.54	203.6	2013	2018	5	41723
118	50719	OTTAWA GATINEAU A	QUEBEC	45.52	-75.56	64.3	2012	2018	6	30377
119	51418	BATHURST A	NEW BRUNSWICK	47.63	-65.74	58.8	2013	2018	5	40616
120	51457	QUEBEC INTL A	QUEBEC	46.79	-71.39	74.4	2013	2018	5	40628
121	51537	DOAKTOWN AUTO RCS	NEW BRUNSWICK	46.59	-66.01	43	2013	2018	5	40682
122	51638	LAC MEGANTIC	QUEBEC	45.6	-70.88	460.3	2013	2018	5	40458
123	52038	PUVIRNITUQ A	QUEBEC	60.05	-77.29	25.3	2014	2018	4	36621
124	52081	WASKAGANISH A	QUEBEC	51.47	-78.76	24.08	2014	2018	4	10602
125	52179	KUUJJUAQ A	QUEBEC	58.09	-68.42	39.9	2014	2018	4	37136
126	52759	STEPHENVILLE A	NEWFOUNDLAND	48.54	-58.55	24.7	2014	2018	4	32042

14 **APPENDIX III:** DESCRIPTIVE STATISTICS OF THE WIND SPEED DATA FOR STATIONS OF EASTERN CANADA CASE STUDY

Table 14.1 Descriptive statistics of the wind speed data for the examined stations

CS station ID	Station ID	Sample minimum	Sample maximum	Arithmetic mean, A	Geometric mean, G	Harmonic mean, H	δ_1	δ_2	Sample standard deviation, s	Sample skewness	Sample kurtosis	Sample excess kurtosis	Coefficient of variation, C_v	Coeffi of skewn C_s
1	5251	0.56	26.94	4.51	3.74	2.99	0.19	0.23	2.62	0.86	3.79	0.79	1.52	0.0
2	5293	0.56	15	3.28	2.81	2.39	0.15	0.16	1.78	0.85	3.33	0.33	0.97	0.1
3	5415	0.56	25	4.36	3.62	2.88	0.18	0.23	2.52	0.98	4.24	1.24	1.46	0.0
4	5530	0.56	18.61	3.18	2.6	2.09	0.2	0.22	2	1.08	4.05	1.05	1.26	0.1
5	5668	0.56	38.33	7.22	5.8	4.34	0.22	0.29	4.46	0.93	4.1	1.1	2.76	0.0
6	5669	0.56	30.83	5.9	4.74	3.7	0.22	0.25	3.81	1.11	4.38	1.38	2.46	0.0
7	5707	0.56	17.78	3.84	3.38	2.92	0.13	0.15	1.92	0.97	4.4	1.4	0.96	0.1
8	5839	0.56	20	4.22	3.65	3.04	0.15	0.18	2.14	0.65	3.31	0.31	1.08	0.0
9	6029	0.56	15.56	3.51	3	2.47	0.15	0.2	1.84	0.71	3.33	0.33	0.96	0.1
10	6047	0.56	25.83	4.29	3.73	3.18	0.14	0.16	2.19	0.83	3.86	0.86	1.11	0.0
11	6053	0.56	16.94	3.9	3.28	2.61	0.17	0.23	2.14	0.71	3.32	0.32	1.17	0.0
12	6058	0.56	26.94	4.67	3.91	3.15	0.18	0.22	2.64	0.86	3.91	0.91	1.49	0.0
13	6081	0.56	17.5	3.78	3.22	2.62	0.16	0.2	2.04	0.8	3.6	0.6	1.1	0.0
14	6089	0.56	33.61	7.97	6.58	5.08	0.19	0.26	4.68	1	4.2	1.2	2.74	0.0
15	6205	0.28	33.06	5.45	4.57	3.61	0.18	0.24	3.08	0.98	4.36	1.36	1.74	0.0
16	6256	0.56	19.44	3.61	3.02	2.43	0.18	0.22	2.06	0.84	3.82	0.82	1.17	0.1
17	6330	0.56	20	4.34	3.66	2.98	0.17	0.21	2.44	0.86	3.68	0.68	1.37	0.0
18	6335	0.56	31.39	4.41	3.45	2.55	0.24	0.3	2.83	0.83	3.75	0.75	1.82	0.0
19	6501	0.28	26.94	4.57	3.81	3.06	0.18	0.22	2.75	1.3	5.41	2.41	1.66	0.0
20	6557	0.56	30	7.4	6.51	5.48	0.13	0.17	3.5	0.81	4.59	1.59	1.65	0.0
21	6581	0.83	29.17	6.15	5.08	3.98	0.19	0.25	3.57	0.86	3.63	0.63	2.07	0.0
22	6584	0.56	33.06	5.85	4.52	3.23	0.26	0.34	3.97	1.08	4.2	1.2	2.69	0.0
23	6708	0.56	27.22	3.68	3.04	2.41	0.19	0.23	2.17	1	4.67	1.67	1.28	0.1
24	6709	0.83	40.28	5.03	4	3.09	0.23	0.26	3.51	2.03	11.16	8.16	2.45	0.0
25	6710	0.83	25	6.23	5.6	4.95	0.11	0.12	2.8	1	5.13	2.13	1.26	0.0
26	6711	0.56	26.94	6.84	6.12	5.31	0.11	0.14	3.08	0.8	4.48	1.48	1.39	0.0
27	6723	0.56	40.28	7.56	6.39	5.16	0.17	0.21	4.12	0.77	3.51	0.51	2.25	0.0
28	6740	0.56	25.83	5.43	4.63	3.84	0.16	0.19	2.91	0.87	4.28	1.28	1.56	0.0
29	6756	0.83	32.22	7.72	6.64	5.5	0.15	0.19	4.09	0.96	4.25	1.25	2.17	0.0
30	6773	0.56	32.5	5.88	4.92	3.95	0.18	0.22	3.37	1.01	4.66	1.66	1.93	0.0
31	6778	0.56	33.33	6.38	5.47	4.53	0.15	0.19	3.38	0.94	4.5	1.5	1.79	0.0
32	6783	0.56	25.83	5.44	4.59	3.65	0.17	0.23	2.95	0.86	4.2	1.2	1.6	0.0
33	6797	0.56	75.56	7.73	6.1	4.55	0.24	0.29	5.05	1.08	4.56	1.56	3.3	0.0
34	6916	0.56	18.06	3.74	3.21	2.71	0.15	0.17	2.01	0.86	3.67	0.67	1.09	0.1

35	6918	0.28	16.11	3.59	3.04	2.43	0.17	0.23	1.98	0.96	4.25	1.25	1.09	0.1
36	6923	0.28	11.94	1.94	1.6	1.3	0.19	0.21	1.24	1.43	5.77	2.77	0.79	0.7
37	7026	0.56	15	2.77	2.25	1.76	0.21	0.25	1.71	0.97	3.81	0.81	1.06	0.1
38	7162	0.56	15	2.9	2.26	1.7	0.25	0.29	1.98	1.12	4.31	1.31	1.35	0.1
39	7169	0.28	39.72	5.81	4.67	3.38	0.22	0.32	3.51	0.85	3.73	0.73	2.12	0.0
40	7173	0.28	26.67	6.68	5.63	4.35	0.17	0.26	3.55	0.68	3.4	0.4	1.89	0.0
41	8456	0.28	22.78	4.66	3.89	3.09	0.18	0.23	2.7	1.07	4.45	1.45	1.57	0.0
42	8675	0.28	26.94	7.03	5.97	4.75	0.16	0.23	3.81	0.89	3.72	0.72	2.07	0.0
43	8989	0.56	23.61	5.6	4.59	3.54	0.2	0.26	3.34	0.96	4.03	1.03	2	0.0
44	8991	0.28	35.56	9.29	7.79	5.95	0.18	0.27	5.05	0.75	3.45	0.45	2.75	0.0
45	8999	0.28	27.78	5.47	4.41	3.28	0.21	0.3	3.29	0.8	3.42	0.42	1.99	0.0
46	9002	0.56	20.56	4.69	4.29	3.83	0.09	0.11	1.81	0.3	3.74	0.74	0.7	0.0
47	10226	0.56	27.78	6.15	5.06	3.88	0.2	0.27	3.6	1	4.49	1.49	2.11	0.0
48	10252	0.56	33.33	6.58	5.42	4.27	0.19	0.24	3.89	0.93	4.03	1.03	2.3	0.0
49	10661	0.28	12.22	1.99	1.49	1.05	0.29	0.35	1.47	1.33	5.37	2.37	1.08	0.4
50	10684	0.56	27.78	4.94	4.4	3.8	0.12	0.15	2.28	0.89	5.14	2.14	1.05	0.0
51	10763	0.28	24.17	6.4	5.5	4.41	0.15	0.22	3.25	0.74	3.7	0.7	1.65	0.0
52	10789	0.56	23.06	6.61	5.82	4.94	0.13	0.16	3.11	0.62	3.59	0.59	1.46	0.0
53	10792	0.28	35	6.78	5.43	4	0.22	0.31	4.33	1.18	4.84	1.84	2.77	0.0
54	10797	0.28	18.61	3.91	3.13	2.33	0.22	0.3	2.44	0.91	3.68	0.68	1.53	0.0
55	10800	0.28	26.67	5.32	4.48	3.51	0.17	0.25	2.88	0.83	3.93	0.93	1.56	0.0
56	10813	0.28	27.22	5.36	3.79	2.38	0.35	0.47	4.03	0.97	3.56	0.56	3.03	0.0
57	10817	0.28	28.89	6.78	5.8	4.65	0.16	0.22	3.54	0.81	3.74	0.74	1.85	0.0
58	10818	0.28	42.22	7.72	6.46	4.85	0.18	0.29	4.08	0.59	3.38	0.38	2.16	0.0
59	10836	0.56	38.06	8.16	6.31	4.62	0.26	0.31	5.54	0.98	3.67	0.67	3.76	0.0
60	10841	1.11	58.06	8.6	6.78	5.07	0.24	0.29	5.77	1.22	4.84	1.84	3.87	0.0
61	10855	0.56	23.06	6.26	5.37	4.29	0.15	0.23	3.14	0.64	3.57	0.57	1.57	0.0
62	10856	0.56	26.39	6.72	5.77	4.69	0.15	0.21	3.46	0.69	3.44	0.44	1.78	0.0
63	10859	0.28	29.72	6.58	5.44	4.21	0.19	0.26	3.88	1	3.92	0.92	2.29	0.0
64	10869	0.28	17.5	2.64	2.1	1.64	0.23	0.25	1.85	1.6	6.31	3.31	1.3	0.2
65	10873	0.28	16.94	3.22	2.68	2.04	0.19	0.27	1.81	0.78	3.61	0.61	1.02	0.1
66	10909	0.28	26.39	5.19	4.3	3.37	0.19	0.24	3.1	1.12	4.64	1.64	1.85	0.0
67	10945	0.28	47.22	4.42	3.58	2.68	0.21	0.29	2.7	1.17	6.69	3.69	1.65	0.0
68	26778	0.28	17.5	3.96	3.11	2.19	0.24	0.35	2.46	0.68	2.99	-0.01	1.53	0.0
69	26797	0.28	6.67	1.32	1.14	0.98	0.15	0.15	0.75	1.25	5.42	2.42	0.42	2.9
70	26893	0.28	22.78	4.1	3.17	2.26	0.26	0.34	2.78	1.07	4.11	1.11	1.89	0.0
71	26968	0.28	15	1.74	1.42	1.14	0.2	0.22	1.16	1.74	8.16	5.16	0.77	1.1
72	27115	0.56	19.17	4.38	3.6	2.77	0.2	0.26	2.53	0.82	3.68	0.68	1.46	0.0
73	27195	0.28	22.78	5.36	4.19	3.04	0.25	0.32	3.59	1.01	3.66	0.66	2.4	0.0
74	27621	0.56	35	6.97	5.52	3.92	0.23	0.34	4.36	0.94	3.99	0.99	2.73	0.0
75	27712	1.11	28.89	6.15	5.15	4.17	0.18	0.21	3.54	0.91	3.73	0.73	2.04	0.0

76	27846	0.56	33.33	8.64	7.34	5.68	0.16	0.26	4.49	0.7	3.55	0.55	2.33	0.0
77	29471	0.56	35.56	6.72	5.08	3.57	0.28	0.35	4.82	1.29	5.18	2.18	3.46	0.0
78	29493	1.11	15.56	3.65	3.17	2.74	0.14	0.15	1.96	1.08	4.25	1.25	1.05	0.1
79	29714	0.28	15.56	3.2	2.59	1.93	0.21	0.29	1.9	0.79	3.58	0.58	1.12	0.1
80	30164	0.28	41.67	4.27	3.61	2.87	0.17	0.23	2.33	1.03	6.89	3.89	1.27	0.0
81	30165	0.28	15.56	4	3.41	2.72	0.16	0.22	2.11	0.74	3.48	0.48	1.11	0.0
82	30168	0.28	20	4.88	4.07	3.18	0.18	0.25	2.77	0.9	3.86	0.86	1.57	0.0
83	30308	0.28	18.61	4.37	3.72	2.97	0.16	0.23	2.32	0.88	4.11	1.11	1.23	0.0
84	31829	0.28	33.89	5.04	4.08	3.05	0.21	0.29	3.06	0.97	4.13	1.13	1.86	0.0
85	41575	0.28	18.06	4.5	3.8	2.97	0.17	0.25	2.38	0.68	3.49	0.49	1.26	0.0
86	41903	0.28	18.61	4.4	3.76	3.05	0.16	0.21	2.33	0.83	3.71	0.71	1.24	0.0
87	42013	0.28	11.94	2.07	1.61	1.18	0.25	0.31	1.41	1.23	4.94	1.94	0.96	0.4
88	42083	0.28	19.17	4.26	3.43	2.55	0.22	0.3	2.61	0.87	3.61	0.61	1.59	0.0
89	42243	0.28	18.61	3.59	2.77	1.94	0.26	0.36	2.36	0.91	3.81	0.81	1.55	0.0
90	43124	0.28	24.72	4.79	4.08	3.33	0.16	0.2	2.67	1.23	5.41	2.41	1.49	0.0
91	43323	0.28	10.28	2.22	1.74	1.29	0.25	0.3	1.48	0.94	3.46	0.46	0.98	0.2
92	43404	0.28	29.44	5.9	4.94	3.88	0.18	0.24	3.37	1.02	4.46	1.46	1.92	0.0
93	43406	0.28	22.22	4.23	3.24	2.22	0.27	0.38	2.85	1.01	4.06	1.06	1.92	0.0
94	44363	0.28	19.44	3.16	2.38	1.65	0.28	0.37	2.23	1.11	4.53	1.53	1.57	0.1
95	44503	0.28	21.11	5.09	4.31	3.41	0.17	0.23	2.75	0.83	3.73	0.73	1.49	0.0
96	45047	0.28	33.89	8.55	7.29	5.73	0.16	0.24	4.42	0.66	3.26	0.26	2.29	0.0
97	45307	0.28	39.17	6.99	5.34	3.75	0.27	0.35	4.87	1.21	4.99	1.99	3.39	0.0
98	46007	0.28	28.33	6.12	5.1	4.06	0.18	0.23	3.57	1.01	4.09	1.09	2.08	0.0
99	47587	0.28	21.67	3.76	3.03	2.25	0.21	0.3	2.29	0.93	4.07	1.07	1.39	0.0
100	47607	0.28	18.06	3.53	2.86	2.2	0.21	0.26	2.19	1.05	4.33	1.33	1.36	0.1
101	48348	1.11	28.89	6.42	5.49	4.53	0.16	0.19	3.43	0.83	3.71	0.71	1.83	0.0
102	48568	1.11	18.89	3.7	3.16	2.68	0.16	0.17	2.07	1.02	4.11	1.11	1.15	0.1
103	48871	0.28	18.61	4.29	3.63	2.81	0.17	0.26	2.28	0.71	3.42	0.42	1.21	0.0
104	49390	1.11	15.28	3.95	3.5	3.06	0.12	0.13	1.91	0.83	3.63	0.63	0.92	0.1
105	49491	1.11	15.28	4.16	3.66	3.17	0.13	0.14	2.06	0.83	3.63	0.63	1.02	0.0
106	49608	0.28	13.89	2.81	2.32	1.78	0.19	0.26	1.63	0.96	4.16	1.16	0.94	0.2
107	49629	1.11	15	3.85	3.32	2.83	0.15	0.16	2.05	0.92	3.78	0.78	1.1	0.1
108	49648	1.11	18.06	4.29	3.74	3.2	0.14	0.16	2.2	0.85	3.7	0.7	1.13	0.0
109	49649	1.11	21.11	4.42	3.84	3.28	0.14	0.16	2.32	0.98	4.1	1.1	1.22	0.0
110	49748	0.28	26.39	4.02	3.23	2.45	0.22	0.28	2.68	1.68	8.16	5.16	1.78	0.0
111	50089	0.28	29.72	6.93	5.99	4.84	0.15	0.21	3.49	0.74	3.63	0.63	1.76	0.0
112	50309	0.28	23.33	4.89	4.23	3.49	0.14	0.19	2.54	0.98	4.22	1.22	1.32	0.0
113	50310	0.28	20.28	4.47	3.5	2.31	0.25	0.42	2.72	0.74	3.64	0.64	1.66	0.0
114	50620	0.28	22.5	5.14	4.48	3.69	0.14	0.19	2.59	0.88	4.03	1.03	1.3	0.0
115	50621	0.28	25.83	4.75	4.07	3.25	0.16	0.23	2.5	1	5.09	2.09	1.32	0.0
116	50677	0.28	14.44	3.04	2.42	1.82	0.23	0.29	1.97	1.1	4.21	1.21	1.27	0.1

117	50678	0.28	10.83	1.96	1.55	1.15	0.23	0.3	1.27	1.12	4.64	1.64	0.82	0.5
118	50719	0.28	16.94	3.64	2.96	2.14	0.21	0.32	2.11	0.77	3.62	0.62	1.23	0.0
119	51418	0.28	15	3.11	2.43	1.75	0.24	0.33	2.05	1.07	4.14	1.14	1.36	0.1
120	51457	0.28	36.11	4.11	3.29	2.35	0.22	0.34	2.5	0.86	4.25	1.25	1.52	0.0
121	51537	0.28	10.83	2.34	1.75	1.2	0.29	0.38	1.66	1.06	4.01	1.01	1.18	0.2
122	51638	0.28	12.5	2.94	2.39	1.81	0.21	0.28	1.79	0.95	3.79	0.79	1.09	0.1
123	52038	1.11	21.67	6.38	5.57	4.73	0.14	0.16	3.21	0.8	3.55	0.55	1.61	0.0
124	52081	0.28	13.89	4.52	4.02	3.36	0.12	0.18	1.99	0.48	3.27	0.27	0.87	0.0
125	52179	0.28	16.11	4.01	3.36	2.59	0.17	0.26	2.2	0.88	4	1	1.21	0.0
126	52759	0.28	25.83	5.42	4.28	3.1	0.24	0.32	3.55	1.23	5.33	2.33	2.33	0.0

15 APPENDIX IV: TEST STATISTICS FOR THE WIND SPEED DATA OF STATIONS IN EASTERN CANADA CASE STUDY

Table 15.1 Slope of mean excess plot, Shapiro-Wilk (SW) log-normality test, Modified Mann-Kendall (MMK) test, Jackson test statistics and p-values for all stations

CS station ID	**Station ID**	**SW** (Shapiro and Wilk, 1965) **Log-normality test statistic**	**SW** (Shapiro and Wilk, 1965) **Log-normality test p-value**	**MMK** (Hamed and Ramachandra Rao, 1998) **statistic**	**MK** (Mann, 1945) **p-value**	**MMK** (Hamed and Ramachandra Rao, 1998) **p-value**	**Jackson`s test** (Jackson, 1967) **statistic**	**Jackson`s test** (Jackson, 1967) **p-value**	**Slope of mean excess plot**	**Tail behavior**
1	5251	0.93481231	2.28E-34	-0.2021858	0.02166128	0.12758335	1.56332114	1	2.68440656	Class D
2	5293	0.95892703	2.48E-28	-0.0829268	0.45172647	0.2764187	1.52610075	1	-6.4991479	Class E
3	5415	0.95711197	7.16E-29	-0.1289617	0.14363575	0.20440144	1.56498987	1	-0.8616302	Class E
4	5530	0.9639304	9.56E-27	-0.1818182	0.0837127	0.06806273	1.61709338	1	1.35168316	Class D
5	5668	0.97638483	6.59E-22	-0.15	0.44404364	0.22268739	1.60151372	1	6.61710348	Class D
6	5669	0.96658447	7.79E-26	-0.0909091	0.45855875	0.28144999	1.63432095	1	8.33372025	Class D
7	5707	0.97584232	3.74E-22	-0.1272727	0.64042879	0.30672146	1.48347736	1	0.29553217	Class D
8	5839	0.96953715	9.38E-25	0.18333333	0.34441752	0.26813169	1.48320724	1	7.23863026	Class D
9	6029	0.93444108	1.91E-34	-0.0080645	0.96119873	0.95898441	1.50195529	1	10.7414845	Class D
10	6047	0.91188302	1.23E-38	-0.2192192	0.05790218	0.07938472	1.49275953	1	-6.7049647	Class E
11	6053	0.96111328	1.17E-27	-0.1461988	0.40110257	0.19297135	1.52632486	1	15.2726748	Class D
12	6058	0.96599302	4.83E-26	0.10606061	0.39410715	0.05112528	1.54777502	1	-7.8198381	Class E
13	6081	0.94150267	6.74E-33	0.07320024	0.42084374	0.14686764	1.52128921	1	-15.157217	Class E
14	6089	0.94865349	3.58E-31	0.04093567	0.83373524	0.64818442	1.5723862	1	5.85079177	Class D
15	6205	0.96736848	1.48E-25	0.02651515	0.84036442	0.74330691	1.55056855	1	0.80017988	Class D
16	6256	0.97336741	3.14E-23	-0.1895425	0.2888828	0.12257836	1.54894854	1	2.58657075	Class D
17	6330	0.95072477	1.23E-30	-0.0181818	1	1	1.54234048	1	-2.1288076	Class E
18	6335	0.94607421	8.15E-32	0.23809524	0.54800557	0.19931025	1.62006894	1	-1.0474461	Class E
19	6501	0.97841636	6.03E-21	-0.2513369	0.03794744	0.08424816	1.59586205	1	4.94858319	Class D
20	6557	0.98029839	5.39E-20	-0.3333333	0.45237036	0.21211346	1.45321575	1	6.63357691	Class D

21	6581	0.95384202	8.45E-30	-0.2	0.70711423	0.40509468	1.56308889	1	-9.9139578	Class E
22	6584	0.9736668	4.20E-23	-0.2	0.43627493	0.06472304	1.66649257	1	-8.5922124	Class E
23	6708	0.92647291	4.85E-36	0.22222222	0.46551217	0.16110606	1.57339242	1	-4.8109461	Class E
24	6709	0.97112435	3.85E-24	-0.1428571	0.76389059	0.41234628	1.6898481	1	1.74757555	Class D
25	6710	0.96755682	1.73E-25	0.06666667	1	1	1.43417475	1	3.41664655	Class D
26	6711	0.96167589	1.76E-27	-0.047619	0.84308523	0.81161818	1.43286562	1	8.93068579	Class D
27	6723	0.97842407	6.08E-21	-0.1809524	0.26387201	0.17409393	1.52634236	1	0.41597246	Class D
28	6740	0.95685804	6.04E-29	0.18530612	0.05869675	0.19090927	1.51811884	1	3.78472722	Class D
29	6756	0.9709129	3.18E-24	0	1	1	1.51564016	1	8.27069864	Class D
30	6773	0.9602558	6.31E-28	-0.0579592	0.55818465	0.44638122	1.55907095	1	-1.8456878	Class E
31	6778	0.97805488	4.02E-21	0.20879121	0.32442369	0.10657076	1.5150236	1	-3.5942856	Class E
32	6783	0.95959034	3.94E-28	-0.1538462	0.50215825	0.27939239	1.52503252	1	4.94084834	Class D
33	6797	0.97202713	8.83E-24	-0.0735294	0.71083593	0.6069561	1.64122849	1	-0.5934565	Class E
34	6916	0.96473836	1.79E-26	-0.1025641	0.66933401	0.38640725	1.52089551	1	10.2497783	Class D
35	6918	0.96337438	6.26E-27	-0.1025641	0.66933401	0.38907499	1.53675444	1	20.9562541	Class D
36	6923	0.95603741	3.50E-29	0.04575163	0.82021675	0.8066977	1.62969963	1	14.8891822	Class D
37	7026	0.94834736	2.99E-31	-0.1428571	0.51122035	0.06206496	1.60121212	1	-8.5639959	Class E
38	7162	0.94109217	5.43E-33	0.16666667	0.60216753	0.17375311	1.66850983	1	11.1839127	Class D
39	7169	0.94480077	4.00E-32	-0.2794118	0.12747693	0.18862426	1.58583059	1	-3.1506054	Class E
40	7173	0.93831946	1.30E-33	0.12380952	0.55261513	0.13194898	1.50947487	1	1.54263405	Class D
41	8456	0.95502865	1.81E-29	-0.0631579	0.72117631	0.72336297	1.56864683	1	12.2161765	Class D
42	8675	0.9377185	9.59E-34	0.20588235	0.26605176	0.05655811	1.52756212	1	11.5777406	Class D
43	8989	0.96600834	4.89E-26	0.4	0.46243273	0.2660457	1.58244215	1	11.5506313	Class D
44	8991	0.95604772	3.52E-29	0.16363636	0.53341651	0.2554553	1.5240639	1	4.90611012	Class D
45	8999	0.96159223	1.66E-27	0.14619883	0.40110257	0.39801429	1.58267489	1	-10.461789	Class E
46	9002	0.89741883	6.91E-41	0.09090909	0.57278231	0.46190887	1.34676725	1	0.40353873	Class D
47	10226	0.93861073	1.51E-33	-0.2066667	0.15425751	0.13930185	1.56984582	1	10.4143809	Class D
48	10252	0.97070993	2.65E-24	-0.0289855	0.86215561	0.74540156	1.5745926	1	2.43050786	Class D

49	10661	0.9366207	5.55E-34	-0.2	0.80649594	0.71409977	1.72997772	1	-2.5015868	Class E
50	10684	0.91253666	1.58E-38	0.16666667	0.26433733	0.13824615	1.43996805	1	-6.2704313	Class E
51	10763	0.94440289	3.22E-32	0.05882353	0.7618734	0.52398724	1.489577	1	11.0177912	Class D
52	10789	0.95888706	2.41E-28	0.02898551	0.86215561	0.72994085	1.44821935	1	11.5631234	Class D
53	10792	0.97838935	5.85E-21	-0.057971	0.70984368	0.51589066	1.62919164	1	12.4044824	Class D
54	10797	0.96144078	1.48E-27	0.12727273	0.64042879	0.22179148	1.60736136	1	0.43519723	Class D
55	10800	0.95481011	1.57E-29	0.01298701	0.95502646	0.89164261	1.52453336	1	-0.3561772	Class E
56	10813	0.94242542	1.10E-32	-0.030303	0.94532987	0.88324926	1.73424363	1	6.90223172	Class D
57	10817	0.94627557	9.12E-32	0.03030303	0.8656491	0.69245629	1.50555291	1	9.41346406	Class D
58	10818	0.93784318	1.02E-33	-0.1052632	0.53760324	0.20811161	1.50378922	1	2.40317922	Class D
59	10836	0.97289302	2.00E-23	0.01818182	1	1	1.6635247	1	10.688216	Class D
60	10841	0.97383519	4.95E-23	-0.3186813	0.12531111	0.05495594	1.66216111	1	1.16627959	Class D
61	10855	0.9284077	1.15E-35	-0.1304348	0.38530998	0.27006424	1.47728004	1	-6.3970974	Class E
62	10856	0.954859	1.62E-29	0.08225108	0.61176003	0.13112966	1.49265256	1	2.07979197	Class D
63	10859	0.95917041	2.93E-28	-0.0217391	0.90129784	0.8386627	1.57591341	1	11.141533	Class D
64	10869	0.96832087	3.29E-25	-0.2526316	0.12728869	0.10749857	1.69799329	1	-3.9318051	Class E
65	10873	0.95704567	6.85E-29	0.21428571	0.53618677	0.2126473	1.54223966	1	-12.28814	Class E
66	10909	0.97110481	3.78E-24	0.04761905	1	1	1.58636234	1	0.84644596	Class D
67	10945	0.95331019	6.03E-30	0.05263158	0.77956607	0.65972822	1.59589914	1	-1.1814594	Class E
68	26778	0.96347796	6.77E-27	-0.2761905	0.16585666	0.06412279	1.59602339	1	-2.9646804	Class E
69	26797	0.89400236	2.21E-41	-0.2857143	0.38647623	0.10706378	1.54789949	1	9.32743581	Class D
70	26893	0.96193969	2.14E-27	-0.047619	1	1	1.66582712	1	-10.380662	Class E
71	26968	0.8974126	6.89E-41	0.06666667	1	1	1.65950249	1	6.13878741	Class D
72	27115	0.96106509	1.13E-27	-0.1794872	0.42771051	0.09447317	1.55867945	1	17.0724157	Class D
73	27195	0.94275486	1.31E-32	0.01052632	0.97411775	0.97099606	1.65428844	1	1.02836412	Class D
74	27621	0.95464	1.41E-29	-0.3571429	0.26551039	0.07362676	1.61023359	1	7.10547151	Class D
75	27712	0.95806841	1.37E-28	-0.0666667	0.7665253	0.53407036	1.55972186	1	10.6881494	Class D
76	27846	0.95209676	2.83E-30	0	1	1	1.4986696	1	6.06753571	Class D

77	29471	0.9794812	2.04E-20	-0.0666667	1	1	1.71007256	1	8.86518404	Class D
78	29493	0.97570922	3.25E-22	0.09090909	0.75549688	0.52960709	1.52563149	1	14.4016511	Class D
79	29714	0.95068113	1.19E-30	0.05263158	0.77956607	0.50888243	1.57181801	1	11.1652229	Class D
80	30164	0.97266038	1.60E-23	0.02564103	0.95135213	0.93011753	1.52752719	1	0.75446435	Class D
81	30165	0.95574029	2.88E-29	0.15555556	0.59150504	0.11270953	1.50735904	1	19.0980643	Class D
82	30168	0.96913896	6.64E-25	-0.1111111	0.72051479	0.49646544	1.55164422	1	14.8035902	Class D
83	30308	0.95142679	1.88E-30	-0.010989	1	1	1.51485875	1	18.0578582	Class D
84	31829	0.98062706	8.02E-20	0.12380952	0.55261513	0.25693653	1.59392287	1	-4.8610456	Class E
85	41575	0.94137046	6.29E-33	-0.0666667	0.7665253	0.301116	1.50743351	1	17.2246441	Class D
86	41903	0.97759499	2.42E-21	-0.0095238	1	1	1.51289751	1	-8.9899278	Class E
87	42013	0.94118096	5.69E-33	-0.3333333	0.36752074	0.05295609	1.67075836	1	19.7744645	Class D
88	42083	0.94991966	7.56E-31	-0.1208791	0.58407037	0.07955597	1.59434405	1	17.7210905	Class D
89	42243	0.94230537	1.03E-32	-0.1208791	0.58407037	0.24056589	1.63991705	1	13.181518	Class D
90	43124	0.97768012	2.66E-21	0.03030303	0.94532987	0.90212139	1.54922473	1	-1.2272778	Class E
91	43323	0.93673974	5.88E-34	0	1	1	1.64618544	1	-15.868101	Class E
92	43404	0.9658352	4.26E-26	-0.1111111	0.72051479	0.57063966	1.55846282	1	10.2306174	Class D
93	43406	0.96171733	1.82E-27	-0.0545455	0.87626966	0.67052487	1.65899371	1	18.7592327	Class D
94	44363	0.94327203	1.74E-32	-0.2121212	0.37269149	0.06233324	1.69247158	1	-3.5261599	Class E
95	44503	0.95386022	8.55E-30	-0.0606061	0.83701148	0.68830643	1.52327199	1	12.9337324	Class D
96	45047	0.9636125	7.50E-27	0.05454546	0.87626966	0.74296076	1.49550741	1	-2.5480518	Class E
97	45307	0.95529246	2.15E-29	0.15151515	0.53713386	0.14139297	1.68700806	1	11.8812594	Class D
98	46007	0.97885514	9.92E-21	0.16363636	0.53341651	0.19059469	1.57092374	1	11.9156812	Class D
99	47587	0.95270444	4.13E-30	-0.0181818	1	1	1.59203912	1	-2.1523862	Class E
100	47607	0.95827514	1.58E-28	-0.0222222	1	1	1.60771755	1	5.40230921	Class D
101	48348	0.9588749	2.39E-28	0.11111111	0.75445418	0.43293719	1.51750012	1	10.0336228	Class D
102	48568	0.96175385	1.87E-27	0.21428571	0.53618677	0.05421063	1.54519674	1	-4.3571003	Class E
103	48871	0.96641287	6.78E-26	-0.3571429	0.26551039	0.08046745	1.51063435	1	10.9554423	Class D
104	49390	0.96717869	1.27E-25	0.07142857	0.90153863	0.85286992	1.46614106	1	-3.576914	Class E

105	49491	0.97142313	5.06E-24	0.14285714	0.71052302	0.37979686	1.47820763	1	17.8292863	Class D
106	49608	0.97964629	2.48E-20	-0.3333333	0.36752074	0.10222829	1.56477759	1	14.1662494	Class D
107	49629	0.96710891	1.20E-25	0.2	0.70711423	0.24216476	1.51836126	1	11.1672923	Class D
108	49648	0.96127137	1.31E-27	-0.0714286	0.90153863	0.72134696	1.49585029	1	-4.5533548	Class E
109	49649	0.972995	2.20E-23	0.33333333	0.36752074	0.0801209	1.51245995	1	-5.559103	Class E
110	49748	0.97478645	1.27E-22	-0.2	0.70711423	0.40641853	1.6603877	1	7.70248528	Class D
111	50089	0.9649493	2.11E-26	-0.2	0.70711423	0.38202473	1.48559667	1	5.29683996	Class D
112	50309	0.98712011	7.08E-16	-0.0666667	1	1	1.50755097	1	6.98969019	Class D
113	50310	0.97000601	1.41E-24	-0.0666667	1	1	1.58608973	1	-6.9961901	Class E
114	50620	0.98561749	6.77E-17	-0.0666667	1	1	1.48851245	1	9.56242402	Class D
115	50621	0.98000869	3.81E-20	0.06666667	1	1	1.51236611	1	1.38414564	Class D
116	50677	0.96281358	4.10E-27	-0.4	0.46243273	0.07480954	1.63645409	1	21.4041495	Class D
117	50678	0.95280991	4.41E-30	-0.2	0.80649594	0.62319154	1.63456231	1	-24.350595	Class E
118	50719	0.98259763	9.71E-19	0.04761905	1	1	1.55997813	1	-20.143569	Class E
119	51418	0.96771933	1.99E-25	0.2	0.80649594	0.57419188	1.6488314	1	6.21708212	Class D
120	51457	0.94780528	2.19E-31	-0.0666667	1	1	1.58867705	1	-1.1715843	Class E
121	51537	0.94138976	6.35E-33	0	1	1	1.69568491	1	26.9418209	Class D
122	51638	0.96686503	9.80E-26	-0.3333333	0.45237036	0.27651246	1.59400317	1	27.8832854	Class D
123	52038	0.98072059	8.99E-20	-0.2	0.80649594	0.58267765	1.4854465	1	15.0241735	Class D
124	52081	0.94354083	2.01E-32	0.4	0.46243273	0.05889361	1.41541359	1	12.4844673	Class D
125	52179	0.93580971	3.72E-34	0.2	0.80649594	0.59460175	1.53313478	1	13.9734908	Class D
126	52759	0.96215025	2.50E-27	0	1	1	1.6463994	1	9.84037738	Class D

16 APPENDIX V: ESTIMATED PARAMETERS FOR HALPHEN DISTRIBUTION FAMILY FOR ALL STATIONS IN EASTERN CANADA CASE STUDY

Table 16.1 Estimated parameters for HDF for all stations

CS station ID	Station ID	Station name	Province	HA, α, *m*, *v*	HB, α, *m*, *v*	Years collected	Elevation, m
1	5251	QUEBEC/JEAN LESAGE INTL A	QUEBEC	4.0960920e-02 6.3681010e-02 2.3506790e-01	4.7960350e-02 7.2552360e-02 2.9643370e-01	60	74.4
2	5293	VALCARTIER A	QUEBEC	1.4083120e+03 2.5896970e+05 1.6308770e+10	-	40	167.6
3	5415	MONTREAL/PIERRE ELLIOTT TRUDEAU INTL A	QUEBEC	1.9568490e-02 1.8002560e-02 7.5457070e-02	4.4917490e-02 6.5283050e-02 2.3025260e-01	60	35.97
4	5530	SHERBROOKE A	QUEBEC	2.0408160e-01 5.7322030e-01 5.7978410e+00	-	43	241.4
5	5668	BLANC SABLON	QUEBEC	1.9942760e-01 3.8956660e-01 1.9516860e+00	6.0390000e-02 7.9205730e-02 1.0590340e-01	15	19.2
6	5669	LOURDES DE BLANC SABLON A	QUEBEC	1.5193530e-01 2.6545630e-01 1.0074200e+00	-	44	37.18
7	5707	MANICOUAGAN A	QUEBEC	9.0528080e-02 1.0671120e-01 2.0347530e-01	-	10	406.3
8	5839	RIVIERE DU LOUP	QUEBEC	-	2.6114340e-02 3.4029430e-02 3.6034810e-02	15	148.4
9	6029	CHIBOUGAMAU CHAPAIS A	QUEBEC	-	3.6233620e-02 4.8820970e-02 1.4597630e-01	32	387.1
10	6047	LA GRANDE RIVIERE A	QUEBEC	4.1366030e-02 6.0564330e-02 3.1796050e-01	4.2471850e-02 5.6963900e-02 1.5588030e-01	36	195.1
11	6053	MATAGAMI A	QUEBEC	-	6.5000840e-02 9.8906660e-02 4.5366790e-01	18	281.3
12	6058	NITCHEQUON	QUEBEC	4.7310970e-02 6.5793580e-02 2.1147270e-01	6.1495790e-02 8.7638250e-02 2.9964400e-01	32	536.1
13	6081	VAL-D'OR A	QUEBEC	1.6289890e-02 1.6425830e-02 1.1574300e-01	2.9143840e-02 3.9855350e-02 1.2232030e-01	57	337.4
14	6089	CAPE HOPES ADVANCE	QUEBEC	-	2.8961960e-01 4.6447660e-01 2.3146830e+00	18	73.2
15	6205	MISCOU ISLAND (AUT)	NEW BRUNSWICK	-	1.0506120e-02 1.4077980e-02 1.1850240e-02	54	4
16	6256	ST LEONARD A	NEW BRUNSWICK	5.0397450e-02 7.2231860e-02 2.4157440e-01	6.0780910e-02 8.7571420e-02 3.1082730e-01	29	242.2

17	6330	COPPER LAKE	NOVA SCOTIA	9.4928350e-02 1.6058780e-01 7.7389680e-01	9.0600560e-02 1.2593830e-01 3.8563690e-01	21	96.9
18	6335	DEBERT A	NOVA SCOTIA	6.6416980e-02 7.3866250e-02 1.6801170e-01	4.3468270e-02 6.0002750e-02 1.0505590e-01	7	44.2
19	6501	WESTERN HEAD	NOVA SCOTIA	6.0899960e-02 1.0333150e-01 4.6217380e-01	-	59	10.06
20	6557	ARGENTIA A	NEWFOUNDLAND	-	5.1652060e-02 4.9957610e-02 1.6348540e-02	10	15.5
21	6581	BUCHANS A	NEWFOUNDLAND	9.8128220e-02 1.6974770e-01 1.0225960e+00	2.0359160e-01 3.4979720e-01 2.1773120e+00	12	276.1
22	6584	BURGEO 2	NEWFOUNDLAND	1.9485020e-01 3.4525260e-01 1.3358240e+00	2.1237790e-02 2.2771710e-02 2.6282380e-03	12	10.6
23	6708	ST ALBANS	NEWFOUNDLAND	7.3097140e-02 1.0174130e-01 2.9703730e-01	1.0764730e-01 1.6788190e-01 7.4284420e-01	15	13.4
24	6709	ST ANDREWS	NEWFOUNDLAND	2.0733220e-01 3.1900530e-01 9.2826400e-01	-	13	10.7
25	6710	ST ANTHONY	NEWFOUNDLAND	-	1.0617630e-01 1.3109820e-01 2.6263750e-01	12	17.4
26	6711	ST ANTHONY	NEWFOUNDLAND	-	6.0964460e-02 7.4327660e-02 1.5275310e-01	26	11.5
27	6723	ST LAWRENCE	NEWFOUNDLAND	5.2101160e-02 6.1000000e-02 4.0934150e-01	9.1132390e-02 1.2524660e-01 4.0448120e-01	30	48.5
28	6740	STEPHENVILLE A	NEWFOUNDLAND	5.0756620e-02 8.5084640e-02 4.5651790e-01	3.7315100e-02 4.7019120e-02 1.1464010e-01	61	24.7
29	6756	TWILLINGATE	NEWFOUNDLAND	8.9163510e-02 8.6294390e-02 3.3388190e-01	1.6516440e-01 2.1440220e-01 5.1498540e-01	14	4.9
30	6773	CARTWRIGHT	NEWFOUNDLAND	4.2631060e-02 6.0121290e-02 1.9755930e-01	6.1624990e-02 8.6846570e-02 2.7613620e-01	62	14.3
31	6778	MAKKOVIK A	NEWFOUNDLAND	7.0028460e-02 8.3931190e-02 1.8291390e-01	9.8111770e-02 1.2920470e-01 3.3670190e-01	30	70.4
32	6783	MARY'S HARBOUR A	NEWFOUNDLAND	-	8.0414140e-02 1.1510530e-01 4.3412210e-01	30	10.6
33	6797	SAGLEK	NEWFOUNDLAND	7.5023690e-02 7.8497970e-02 9.3288110e-02	5.6007030e-02 7.6859330e-02 1.0948200e-01	29	516
34	6916	BATHURST A	NEW BRUNSWICK	5.3963780e+01 2.3839240e+03 1.2748220e+07	-	19	58.8
35	6918	BUCTOUCHE CDA CS	NEW BRUNSWICK	-	6.3235090e-02 8.7303700e-02 2.6990200e-01	13	35.9
36	6923	KEJIMKUJIK 1	NOVA SCOTIA	7.4863250e-01 3.7263480e+00 1.1017300e+02	-	24	125

37	7026	ST STEPHEN (AUT)	NEW BRUNSWICK	5.8236170e-02 8.2554880e-02 2.2745240e-01	1.3563500e-01 3.0551030e-01 3.3881700e+00	29	26.1
38	7162	TRURO (AUT)	NOVA SCOTIA	7.2455650e-02 8.6015680e-02 1.4225030e-01	-	11	39.9
39	7169	MCNABS ISLAND (AUT)	NOVA SCOTIA	-	3.1817540e-02 4.1257120e-02 5.6448160e-02	19	15.4
40	7173	HART ISLAND (AUT)	NOVA SCOTIA	-	1.1394260e-01 2.4255710e-01 3.2220440e+00	24	8.2
41	8456	CHEVERY	QUEBEC	4.7561900e-02 9.1084110e-02 6.3204570e-01	9.2562520e-02 1.3295450e-01 4.4309490e-01	24	7.7
42	8675	HEATH POINT	QUEBEC	-	1.0280760e-01 1.2829140e-01 3.0476460e-01	24	7
43	8989	ILE D'ORLEANS	QUEBEC	2.4087090e-01 4.8699960e-01 2.8558840e+00	4.2226710e-01 7.7992660e-01 5.5383090e+00	24	3.6
44	8991	SAGONA ISLAND	NEWFOUNDLAND	-	1.6937920e-01 3.2045400e-01 3.1878980e+00	23	59.7
45	8999	CAP-MADELEINE	QUEBEC	3.4217110e-01 9.3983060e-01 9.2857910e+00	3.2439990e-02 4.1981350e-02 5.6105120e-02	24	29
46	9002	EASTMAIN A	QUEBEC	-	4.0105760e-02 4.7795100e-02 9.9738660e-02	22	7.32
47	10226	SALLUIT A	QUEBEC	-	2.5343350e-01 5.6593630e-01 6.8099010e+00	46	227.08
48	10252	KANGIQSUJUAQ A	QUEBEC	1.3464490e-01 1.8665440e-01 5.4410810e-01	2.3512000e-01 3.8990390e-01 2.1041580e+00	23	157.58
49	10661	NORTHEAST MARGAREE (AUT)	NOVA SCOTIA	4.5098350e-02 4.7617820e-02 7.9448980e-02	-	24	54
50	10684	KANGIQSUALUJJUAQ A	QUEBEC	-	7.1638320e-02 9.0782320e-02 2.1745460e-01	23	66.14
51	10763	ILES DE LA MADELEINE	QUEBEC	-	.4195460e-02 8.5880040e-02 2.6946900e-01	25	7.6
52	10789	AKULIVIK A	QUEBEC	-	8.1641210e-02 1.0324310e-01 2.5721770e-01	23	23.16
53	10792	GRAND ETANG	NOVA SCOTIA	4.5953530e-01 1.3570260e+00 1.5559980e+01	.9787620e-02 5.3995740e-02 7.4100400e-02	24	12.8
54	10797	MISTOOK	QUEBEC	1.4625750e-01 3.0110140e-01 1.6000780e+00	3.6381880e-02 4.8389110e-02 6.6623540e-02	24	112.5
55	10800	SUMMERSIDE	PRINCE EDWARD ISLAND	-	6.2252310e-02 9.3792990e-02 4.2790690e-01	24	12.2
56	10813	NAIN	NEWFOUNDLAND	4.2808770e-02 6.5045280e-02 1.3302980e-01	2.6383230e-02 3.8135840e-02 9.6604520e-02	24	7.6

57	10817	POOLS ISLAND	NEWFOUNDLAND	-	.7350330e-02 8.9581830e-02 2.6298180e-01	24	19.3
58	10818	GRATES COVE	NEWFOUNDLAND	-	2.7670880e-02 3.3744840e-02 4.2178880e-02	23	46.2
59	10836	CAPE KAKKIVIAK	NEWFOUNDLAND	1.1199000e-01 1.2052040e-01 1.5219240e-01	2.9628150e-02 3.1755050e-02 5.6517800e-04	24	551.1
60	10841	CAPE KIGLAPAIT	NEWFOUNDLAND	1.0767390e-01 1.2662320e-01 2.2653820e-01	-	23	834.1
61	10855	AUPALUK A	QUEBEC	-	1.1519660e-01 1.7196820e-01 8.6338450e-01	23	36.9
62	10856	TASIUJAQ A	QUEBEC	-	1.1821040e-01 1.5896810e-01 5.0575100e-01	22	36.9
63	10859	BRIER ISLAND	NOVA SCOTIA	-	1.1492390e-01 1.7364740e-01 6.9299050e-01	49	15.8
64	10869	CAP-TOURMENTE	QUEBEC	1.3062060e-01 2.2009230e-01 7.5090910e-01	-	24	6
65	10873	STE-ANNE-DE-BELLEVUE 1	QUEBEC	-	2.5135820e-02 3.1585770e-02 3.9765420e-02	24	39
66	10909	MARTICOT ISLAND	NEWFOUNDLAND	6.8048080e-02 9.1046800e-02 5.4671480e-01	1.8937340e-01 2.9404290e-01 1.2399300e+00	24	21.8
67	10945	SHEARWATER JETTY	NOVA SCOTIA	2.1620050e-01 5.7837510e-01 5.4367130e+00	2.5488450e-02 3.3506560e-02 4.4302850e-02	24	5.5
68	26778	LAC BENOIT	QUEBEC	3.2953370e-02 4.3649650e-02 7.5927250e-02	2.0281760e-02 2.9433860e-02 4.1651020e-02	24	549
69	26797	CHAMOUCHOUANE	QUEBEC	1.8443680e+01 5.8005400e+02 2.8594490e+06	-	24	303.8
70	26893	LA POCATIERE	QUEBEC	2.6710360e-01 5.2497890e-01 2.4396690e+00	2.0652060e-02 2.2147830e-02 3.4377600e-03	22	31
71	26968	KOUCHIBOUGUAC CS	NEW BRUNSWICK	5.0148400e-01 1.5510880e+00 1.7979680e+01	-	13	21
72	27115	ST JOHN'S WEST CDA CS	NEWFOUNDLAND	-	2.5922010e-02 3.2959530e-02 4.2014980e-02	14	114
73	27195	CAP-CHAT	QUEBEC	9.0591850e-02 1.4349490e-01 4.8872480e-01	1.5937370e-02 1.7009780e-02 2.8356910e-03	22	5
74	27621	ST LAWRENCE	NEWFOUNDLAND	-	6.2602310e-02 8.3104840e-02 1.2260700e-01	8	48.5
75	27712	WINTERLAND	NEWFOUNDLAND	1.5389370e-01 2.9904850e-01 1.8002790e+00	1.1960630e-01 1.6809050e-01 5.2405130e-01	19	29.26
76	27846	CONFEDERATION BRIDGE	PRINCE EDWARD ISLAND	-	2.0165460e-01 3.5875890e-01 3.2526660e+00	7	54.1

77	29471	WRECKHOUSE	NEWFOUNDLAND	2.0815790e-01 3.0329920e-01 8.2013740e-01	-	6	31.7
78	29493	GAGETOWN AWOS A	NEW BRUNSWICK	6.0863220e-02 1.1976980e-01 1.4269900e+00	-	18	50.6
79	29714	LEMIEUX	QUEBEC	-	1.7830050e-02 2.3033880e-02 3.1168190e-02	19	97.2
80	30164	SCHEFFERVILLE	QUEBEC	-	8.9883800e-02 1.2495890e-01 4.0907370e-01	13	517.2
81	30165	MONTREAL/PIERRE ELLIOTT TRUDEAU INTL	QUEBEC	-	6.9968600e-02 9.7299770e-02 3.3081130e-01	10	32.1
82	30168	NATASHQUAN A	QUEBEC	-	1.1930340e-01 1.7649670e-01 6.9723780e-01	10	11.7
83	30308	HARRINGTON CDA CS	PRINCE EDWARD ISLAND	-	5.9855970e-02 8.1505220e-02 2.5346880e-01	14	53
84	31829	LUNENBURG	NOVA SCOTIA	2.6765990e-01 7.1111800e-01 6.5767320e+00	3.2191100e-02 4.2152670e-02 5.5504440e-02	16	3.8
85	41575	TRACADIE	NOVA SCOTIA	-	7.3717410e-02 1.3817520e-01 1.2569610e+00	15	66.67
86	41903	ST. PETERS	PRINCE EDWARD ISLAND	-	6.0274290e-02 8.1297270e-02 2.3972800e-01	15	29.7
87	42013	GRANBY	QUEBEC	3.7682400e-02 4.8197470e-02 1.5346340e-01	1.0280830e-02 1.1044290e-02 2.1161120e-03	15	86
88	42083	NAPPAN AUTO	NOVA SCOTIA	2.3258880e-01 5.9324750e-01 4.9474520e+00	2.7582740e-02 3.6151370e-02 4.8714100e-02	15	19.8
89	42243	DEBERT	NOVA SCOTIA	2.7141240e-02 3.3959900e-02 5.3349220e-02	1.7931920e-02 2.7213110e-02 4.0480980e-02	15	37.5
90	43124	HALIFAX KOOTENAY	NOVA SCOTIA	-	-	14	52
91	43323	EDMUNDSTON	NEW BRUNSWICK	3.0331570e-02 2.9419280e-02 4.1579050e-02	7.4831210e-03 7.9743930e-03 1.6850940e-03	14	154.2
92	43404	OSBORNE HEAD DND	NOVA SCOTIA	-	1.3610130e-01 1.9229310e-01 6.2518580e-01	14	30
93	43406	BEDFORD BASIN	NOVA SCOTIA	3.7319470e-02 5.1363000e-02 1.0364510e-01	2.4961400e-02 3.8602090e-02 5.9095880e-02	14	3.5
94	44363	UPPER STEWIACKE RCS	NOVA SCOTIA	1.2466300e-01 2.1552030e-01 7.5816780e-01	9.3288150e-03 1.1555020e-02 1.2565860e-02	13	23.5
95	44503	SYDNEY CS	NOVA SCOTIA	-	7.7940080e-02 1.0883370e-01 3.7136230e-01	12	62.5
96	45047	BONAVISTA	NEWFOUNDLAND	-	1.0772400e-01 1.5754540e-01 7.3780870e-01	12	25.6
97	45307	WRECKHOUSE	NEWFOUNDLAND	3.1334760e-01 5.8419080e-01 2.4541570e+00	2.0496150e-02 2.5279170e-02 2.7322820e-02	12	31.7

98	46007	BACCARO PT	NOVA SCOTIA	6.0310040e-02 5.9165220e-02 2.7357570e-01	1.5001800e-01 2.1623730e-01 7.3076240e-01	11	4.6
99	47587	SAINT-GERMAIN-DE-GRANTHAM	QUEBEC	3.5627790e-01 1.0371180e+00 1.1801460e+01	2.9970360e-02 3.9169160e-02 5.2411690e-02	10	85
100	47607	STEPHENVILLE RCS	NEWFOUNDLAND	3.9949440e-02 4.1251370e-02 1.6661300e-01	4.2540630e-01 1.5659820e+00 4.7005250e+01	10	58
101	48348	ST. ANTHONY	NEWFOUNDLAND	9.6758680e-02 1.2495770e-01 3.6566980e-01	1.2402560e-01 1.6421780e-01 4.4036730e-01	9	32.9
102	48568	FREDERICTON	NEW BRUNSWICK	6.3667670e+02 7.7284290e+04 1.7483850e+09	-	8	20.7
103	48871	ST JOHNS WEST CLIMATE	NEWFOUNDLAND	-	8.8774960e-02 1.4874570e-01 9.6980650e-01	8	110
104	49390	VAL D'OR A	QUEBEC	5.9515210e-02 6.9012130e-02 4.2156090e-01	8.4149140e-02 1.1193710e-01 3.0121460e-01	7	337.4
105	49491	MATAGAMI A	QUEBEC	7.2468250e-02 8.3266230e-02 3.7040140e-01	9.3736960e-02 1.2503180e-01 3.3799660e-01	7	279.8
106	49608	MONTREAL MIRABEL INTL A	QUEBEC	-	9.8981210e-02 1.6023650e-01 8.4302300e-01	6	82.3
107	49629	CHURCHILL FALLS A	NEWFOUNDLAND	8.7181020e+02 1.2191880e+05 7.6333290e+09	-	7	439.5
108	49648	LA GRANDE 4 A	QUEBEC	1.0289170e-01 1.1800690e-01 1.3496150e-01	1.0755790e-01 1.4433860e-01 3.9548500e-01	7	306.3
109	49649	SCHEFFERVILLE A	QUEBEC	1.1729280e-01 2.2447840e-01 3.0861460e+00	-	6	520.9
110	49748	ESKASONI FIRST NATION AUTOMATIC WEATHER STATION	NOVA SCOTIA	5.8718810e-02 6.0554950e-02 1.7704330e-01	-	7	28
111	50089	ST. JOHN'S INTL A	NEWFOUNDLAND		1.1107110e-01 1.4442320e-01 3.9981690e-01	6	140.5
112	50309	MONCTON INTL A	NEW BRUNSWICK	-	1.2010750e-01 1.6040150e-01 4.3046650e-01	6	70.7
113	50310	SAINT JOHN A	NEW BRUNSWICK	-	2.8202850e-02 4.1131630e-02 6.6148290e-02	6	108.8
114	50620	HALIFAX INTL A	NOVA SCOTIA	-	1.0418130e-01 1.3600670e-01 3.5507620e-01	6	145.4
115	50621	CHARLOTTETOWN A	PRINCE EDWARD ISLAND	-	1.0185580e-01 1.3648550e-01 3.9451140e-01	6	48.5
116	50677	CORMACK RCS	NEWFOUNDLAND	5.6303600e-02 8.0829840e-02 3.3088270e-01	3.9351990e-02 5.4126660e-02 7.7038110e-02	6	165.8
117	50678	MILLERTOWN RCS	NEWFOUNDLAND	6.3281930e-02 1.1580540e-01 5.0185220e-01	2.5830250e-02 3.5466360e-02 5.1339110e-02	5	203.6

118	50719	OTTAWA GATINEAU A	QUEBEC	-	3.9753410e-02 5.1038120e-02 7.0524010e-02	6	64.3
119	51418	BATHURST A	NEW BRUNSWICK	3.0862500e-01 7.0188710e-01 4.4385730e+00	1.6565970e-02 1.7611680e-02 3.5378290e-03	5	58.8
120	51457	QUEBEC INTL A	QUEBEC	-	4.3770700e-02 5.7719070e-02 8.5419130e-02	5	74.4
121	51537	DOAKTOWN AUTO RCS	NEW BRUNSWICK	2.8056040e-01 5.7873330e-01 2.8825240e+00	1.3739000e-02 1.4979260e-02 0.0000000e+00	5	43
122	51638	LAC MEGANTIC	QUEBEC	1.4304330e-01 3.1780230e-01 1.9973630e+00	3.4685200e-02 4.5715020e-02 6.0319740e-02	5	460.3
123	52038	PUVIRNITUQ A	QUEBEC	1.2918360e-01 1.6595800e-01 4.5664300e-01	1.6029300e-01 2.0614570e-01 4.9477990e-01	4	25.3
124	52081	WASKAGANISH A	QUEBEC	-	1.0165530e-01 1.2832630e-01 3.4127470e-01	4	24.08
125	52179	KUUJJUAQ A	QUEBEC	-	1.1703200e-01 1.7912550e-01 8.3719680e-01	4	39.9
126	52759	STEPHENVILLE A	NEWFOUNDLAND	1.0359370e+00 2.9547970e+00 3.1000970e+01	8.4928170e-02 1.1746310e-01 1.7004910e-01	4	24.7